Delineation of Coalbed Methane Prospects Using High-Resolution Seismic Reflections at Fort Yukon, Alaska

Richard D. Miller
John C. Davis
Ricardo Olea
Christian Tapie
David R. Laflen
Mitchell Fiedler

Kansas Geological Survey
1930 Constant Avenue
Lawrence, Kansas 66047

Final Report to

Jim Clough
Alaska Division of Geological & Geophysical Surveys
Fairbanks, Alaska

Open-file Report No. 2002-16

December 2002

This project was funded by State of Alaska funds and through a grant (Program/Project Identification No. DE-FC26-00NT40271) from the U.S. Department of Energy, National Energy technology Laboratory.

Delineation of Coalbed Methane Prospects Using High-Resolution Seismic Reflections at Fort Yukon, Alaska

by

Richard D. Miller
John C. Davis
Ricardo Olea
Christian Tapie
David Laflen
Mitchell Fiedler

Kansas Geological Survey
Lawrence, Kansas

for

James G. Clough

Alaska Division of Geological & Geophysical Surveys
Fairbanks, Alaska

December 2002

Open-file Report 2002-16

Table of Contents

Executive Summary 1

Introduction 2

Geologic Setting 5

High Resolution Seismic Profiling: Concepts 7

Data Acquisition 10
- Survey Design 10
- Severe Limitations 11
- Equipment and Recording Parameters 12
- Quality Control 15
- Walkaway Noise Testing 16
- Field Geometry—Source/Receiver 17
- Recording Parameters 18
- Shot Gathers 18
- Data Resolution 19

Data Processing 20

Interpretation 22
- Line 1 24
- Line 2 27
- Line 3 30
- Line 4 31
- Line 5 32
- Line 6 34
- Line 7 35
- Horizon Contours 36
- Structures 38

Conclusions 39
- Goals and Accomplishments 40

Acknowledgements 42

Appendix A: Summary of Processing Parameters 43

References 47

List of Tables and Figures

Figures 1-28 and 81-83 are on the page listed.
Figures 29-80 follow the page listed.

Table 1. Processing flow for data collected at Fort Yukon....21

Figure 1. Site map....3
Figure 2. Characteristics of methane production from coal....4
Figure 3. General geologic setting....5
Figure 4. General geologic column from 1994 USGS core....6
Figure 5. Possible scenarios beneath Fort Yukon....8
Figure 6. Seismic raypaths from source to receiver....9
Figure 7. Three seismic lines originally proposed....10
Figure 8. Seven seismic lines acquired....11
Figure 9. L-382 Hercules transport plane....11
Figure 10. Pallet of cables and geophones being loaded on plane....12
Figure 11. Buggy-style vibrator....12
Figure 12. Entire load transported....12
Figure 13. Seismograph and supporting equipment....12
Figure 14. Winterized recording vehicle....13
Figure 15. Drilling geophone pilot holes....13
Figure 16. Drilling geophone pilot holes....13
Figure 17. Three-geophone array in snow trench....14
Figure 18. Several receiver stations active throughout acquisition....14
Figure 19. IVI minivib moving down seismic line....15
Figure 20. Vibrator traversing path cleared by loader....15
Figure 21. GPS surveying....15
Figure 22. Fixed 240-channel spread with shooting geometry....17
Figure 23. 240-trace symmetric split-spread shot gather from line 7....18
Figure 24. Spectra for reflections from the potential coal interval....18
Figure 25. 240-trace symmetric split-spread shot gather from line 4....19
Figure 26. Asymmetric split-spread shot gather from line 5....19
Figure 27. Site map with the seven seismic profiles located....23
Figure 28. Site map overlain on an aerial photograph of Fort Yukon, Alaska....24
Figure 29. Line 1 CMP stacked section uninterpreted....24
Figure 30. Line 1 CMP stacked section interpreted....25
Figure 31. Line 1 CMP stacked section interpreted....26
Figure 32. Line 1 CMP stacked section with instantaneous frequency....26
Figure 33. Zoomed-in portion of line 1 focusing on the “coal interval”....27
Figure 34. Zoomed-in version of line 1 focusing on the “coal interval”....27
Figure 35. Line 2 CMP stacked section uninterpreted....27
Figure 36. Line 2 CMP stacked section interpreted....28
Figure 37. Line 2 CMP stacked section interpreted....28
Figure 38. Line 2 CMP stacked section with instantaneous frequency....28
Figure 39. Zoomed-in portion of line 2 focusing on the “coal interval”....29

Figure 40. Line 3 CMP stacked seismic reflection section uninterpreted 30
Figure 41. Line 3 CMP stacked seismic reflection section interpreted 30
Figure 42. Line 3 CMP stacked section interpreted.....30
Figure 43. Line 3 CMP stacked section with instantaneous frequency 31
Figure 44. Zoomed-in portion of line 3 focusing on the “coal interval” 31
Figure 45. Line 4 CMP stacked section uninterpreted.....31
Figure 46. Line 4 CMP stacked section interpreted 31
Figure 47. Line 4 CMP stacked section interpreted.....31
Figure 48. Line 4 CMP stacked section with instantaneous frequency 32
Figure 49. Zoomed-in portion of line 4 focusing on the “coal interval” 32
Figure 50. Southeast portion of line 5 CMP stacked section uninterpreted.....32
Figure 51. Northwest portion of line 5 CMP stacked section uninterpreted 32
Figure 52. Southeast portion of line 5 CMP stacked section interpreted.....33
Figure 53. Southeast portion of line 5 CMP stacked section interpreted.....33
Figure 54. Line 5 CMP stacked section interpreted.....33
Figure 55. Line 5 CMP stacked section with instantaneous frequency 33
Figure 56. Zoomed-in portion of line 5 focusing on the “coal interval” 33
Figure 57. Line 6 CMP stacked section uninterpreted.....34
Figure 58. Line 6 CMP stacked section interpreted.....34
Figure 59. Line 6 CMP stacked section interpreted.....34
Figure 60. Line 6 CMP stacked section with instantaneous frequency 34
Figure 61. Zoomed-in portion of line 6 focusing on the “coal interval” 35
Figure 62. Line 7 CMP stacked section uninterpreted.....35
Figure 63. Line 7 CMP stacked section interpreted.....35
Figure 64. Line 7 CMP stacked section interpreted.....35
Figure 65. Line 7 CMP stacked section with instantaneous frequency 36
Figure 66. Zoomed-in portion of line 7 focusing on the “coal interval” 36
Figure 67. Reflection time to the top of the 365 m coal seam 37
Figure 68. Reflection time to the top of the 391 m coal seam 37
Figure 69. Reflection time to the top of the shallowest of the possible coal interfaces.....37
Figure 70. Reflection time to the top of the intermediate of the possible coal interfaces 37
Figure 71. Reflection time to the top of the deepest of the possible coal interfaces 37
Figure 72. Reflection time to bedrock 37
Figure 73. Isopach map for the interval from the 391 m coal to bedrock.....37
Figure 74. Standard error map for the 365 m coal seam (Figure 67).....37
Figure 75. Standard error map for the 391 m coal seam (Figure 68).....37
Figure 76. Standard error map for the shallowest possible coal interface (Figure 69).....37
Figure 77. Standard error map for the intermediate possible coal interface (Figure 70).....73
Figure 78. Standard error map for the deepest possible coal interface (Figure 71).....37
Figure 79. Standard error map for the bedrock (Figure 72).....37
Figure 80. Standard error map for the interval from the 391 m coal to bedrock (Figure 73).....37
Figure 81. Seismic profiles overlain by a possible interpretation of the structural features.....38
Figure 82. Geologic cross-section that fits the data.....40
Figure 83. Aerial photo of Fort Yukon, Alaska.....42

EXECUTIVE SUMMARY

High-resolution seismic reflection methods were effective characterizing a coalbed methane prospect that has the potential to satisfy the municipal needs of rural Fort Yukon, located in central Alaska. A cooperative research effort between the Alaska Division of Geological & Geophysical Surveys (ADGGS) and the Kansas Geological Survey (KGS) set out to:

1) generate high resolution (>120 Hz P-wave) signals with sufficient sitewide coherency, resolution, and signal-to-noise ratio to allow the top and basal contact of the lignitic coal encountered at around 391 m in a nearby borehole to be confidently mapped;

2) optimize acquisition for 2½-D imaging such that the reliability of line-to-line extrapolation of reflections can be based on geostatistical estimations; and

3) use geostatistical correlations of seismic attributes to extend interpretations between survey lines.

Secondary goals of this project included: determining equipment configurations and parameters that maximize signal-to-noise and resolution potential; correlating reflections with known geology based on drill data; insuring offset distributions are sufficient to measure and correct for non-vertical incidence based on a velocity function determined from NMO curves and semblance analysis yet maintain close-offset trace concentration; adapting acquisition and processing as necessary to maximize dominant and bandwidth frequency while maintaining optimum and consistent penetration depths along profile lines; tailoring processing flows to optimize the accuracy of the velocity function and minimize contribution from longer offset traces; optimizing source and receiver coupling; developing a velocity function to allow accurate time-to-depth conversions; determining and compensating for near-surface static and coupling variability on recorded data directly related to differential permafrost thickness; identification and avoidance of pitfalls and artifacts resulting from applying conventional processes to high resolution data.

Reflections with upper corner frequencies over 200 Hz and dominant frequencies over 150 Hz were generated and recorded sitewide. These seismic reflection data permit delineation and line-to-line correlation of any bed thicker than 5 m within this 150 m thick interval of interest 350 to 500 m below ground surface (BGS). Reflection wavelets are consistent and unique enough to correlate individual events between survey lines separated by as much as 2 km in some places. Horizontal resolution of these data allowed the mapping of subtle stratigraphic features observed to vary over 100s of meters. Drilling will be a critical component in extending the interpretations of these data to fully describe, in detail, the geology of this site. This permafrost setting presented unique challenges to achieving and maintaining optimum acquisition parameters. A series of very small offset faults (< 10 m) trending to the southwest and synforms with northeast/southwest axis are inferred throughout the reflection section. These features are evident and can be correlated from the basement reflector through the multitude of high amplitude reflectors interpreted below the base of ice bonding. It will be possible, once additional ground truth is established, to undertake detailed sitewide mapping of the top and bottom of any coal seam thicker than 5 m and characterize the many subtle depositional geometries evident on the seismic sections.

A group of high amplitude reflections from 350 ms to 500 ms are evident on all seismic data acquired in the Fort Yukon survey. Based on the calculated average velocity, these reflections are from reflectors between 350 m and 500 m deep. Descriptions of core recovered from the 400 m deep 1994 USGS boring indicate the shallowest coal (lignite) encountered along seismic line 1 was a thin stringer about 350 m below ground surface. Another thin coal seam at 370 m was followed by a coal unit of unknown thickness (9+ m) encountered about 391 m BGS. The 391 m deep coal is the primary target of this high-resolution seismic reflection survey. Based on reflection wavelet analysis alone, the 391 m deep coal seam is probably between 10 and 15 m thick. If high-amplitude reflections on seismic data correlate to coal (lignite) layers seen in core, as they appear to, it is also reasonable to suggest high amplitude reflections returning from within this 150 m thick interval are sensitive to and indicative of coal-rich portions of the geologic column.

Reflectors between 350 m and 500 m BGS (the "coal interval") are proposed to be a series of coal seams ranging in thickness from stringers (a few centimeters) to over 15 m in places. With the variable lithology and depositionally controlled geometries of this lacustrine environment it is not possible to confidently map individual coal layer thickness around the site without the aid of strategically placed drill holes. From reflection characteristics, the coal interval encountered at 391 m is continuous and appears to vary in thickness across the site from as thin as a few meters to maybe as thick as 20 to 25 m.

Minor fractures, faults, and folds present on most lines can be traced vertically throughout the seismically-imaged portion of the stratigraphic column. All coherent sitewide reflectors above basement possess a gentle southwesterly dip averaging from a little more than 1° on the 391 m deep coal to about 2° on 600 m plus deep basement reflector. A good deal of the variability in reflection character and coherency around this site is a result of scatter from out of the plane segments of faults and fractures. These small-scale fractures and faults do not provide a particularly good setting for high-resolution seismic reflection imaging, but they do provide an excellent scenario for elevated fracture permeability and water saturation, both necessary for efficient production of methane from coal.

A carefully designed drilling program will enhance interpretation of these seismic data. Estimates of layer thickness and descriptions of lithology at a sub-ten meter scale will be possible with control across most of this site between the basement and 300 m BGS. It might even be possible to equate specific seismic attributes to gas concentrations and fracture permeability near faults or folds as well as possibly within the seams themselves.

INTRODUCTION

Only in the last century has coalbed methane been recognized as a significant potential energy source rather than a mining hazard (Rightmire, 1984). While successful production of coalbed gas in the lower 48 states has continued to grow for nearly two decades, Alaska's coalbed methane resources still remain unexploited. However, within the next decade coalbed and shalebed methane will likely become significant sources of energy for urban and rural citizens throughout Alaska as well as many other parts of North America where the economics have only recently stimulated exploration and production.

State and federal agencies, municipal and tribal governments, regional Native corporations, and industry are combining their efforts to evaluate coalbed methane (CBM) and shalebed gas potential in rural Alaska. Gas produced using shallow well fields and short pipelines could have considerable impact in remote villages, currently isolated from the power grid, by dramatically lowering the cost of survival in these communities. Pollution from existing diesel generators would be substantially reduced while industrial development (and thereby jobs) could be enhanced in areas where energy is currently subsidized and/or imported. A medium-sized community of 700 people uses ~250,000 gallons of diesel fuel per year, roughly half for electrical power generation and half for heating. This liquid fuel volume translates to ~34.5 million cubic feet of gas per year. At least 25 remote communities are situated on or near Alaska coal fields that could supply that need.

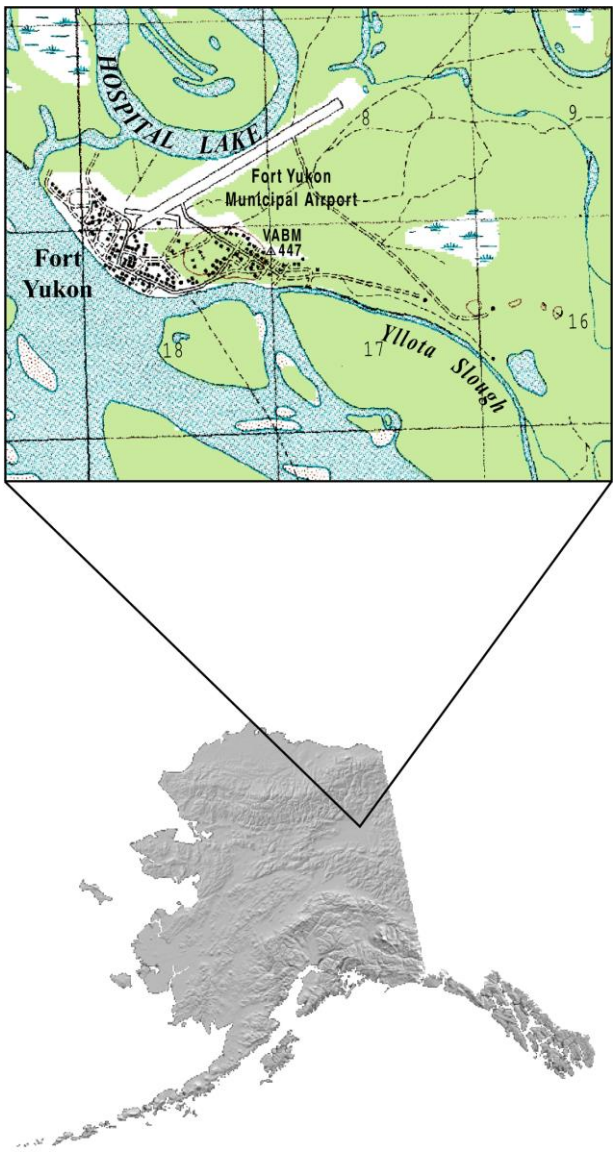

Figure 1. Site map.

Fort Yukon, Alaska, has been classified a priority site based on village demographics, geologic setting, presence of potentially gassy coal, and the likelihood of bringing a CBM production unit on line (Figure 1) (Tyler et al., 2000). The component of the Fort Yukon study described here was designed to delineate potential coalbed methane resources directly under and in close proximity to Fort Yukon. The people of Fort Yukon pay for fuel oil (diesel) at between 2 to 4 times the price in Anchorage or Fairbanks, so rural electric costs could rise to 4 times equivalent kWh rates paid in any of the three major cities of Alaska. This is the case not only for Fort Yukon, but for most of the more than 150 “roadless” rural communities in Alaska. Without passable roads into or out of Fort Yukon, unemployment can exceed 80 percent at times. Lacking a consistent commercial tax base for making capital improvements or sustaining social programs, the cost of living is considerably higher in Fort Yukon than either the state or national averages.

Several key factors are critical for a coal layer to be considered a viable methane source: net coal thickness, coal rank (low coal rank suggests biogenic gas whereas higher coal rank infers a thermogenic gas source), gas content, permeability (very low and very high are detrimental), hydrodynamics (water production is necessary for gas production), structure, and depth to target beds (Murray, 1991). Several of these key coalbed characteristics (net coal thickness,

structure, depth, and gas content) need to be determined and evaluated before methane reserves can be estimated and appraised for resource development. Seismic reflection imaging can provide valuable information on thickness of potential coalbed gas zones and subsurface structures that may enhance or impede production. High-resolution seismic reflection has proven effective for imaging coal seams less than 3 m thick (Gochioco, 1992) at depths in excess of 300 m for exploration and hazard evaluation (Miller et al., 1992).

Methane from Coal

Production of methane from coal beds is based on several coal specific characteristics and the geologic setting (Kaiser et al., 1994).

- coal is both the source and reservoir rock
- coal is a microporous solid with an enormous internal surface area
- coal permeability comes from fractures (cleats)
- coal can sorb > 600 cubic feet of gas per ton

The process of sorption is critical to CBM reservoir behavior (Figure 2). Sorption is the physical process whereby gas is held by weak bonds on the surfaces of pores, cleats, and fractures. Burial depth is an important factor in determining coal reservoir characteristics, since increased pressure increases the amount of gas trapped in pores. Gas moves through the coal matrix by diffusion toward fractures. Permeability is completely dependent on fractures and cleats.

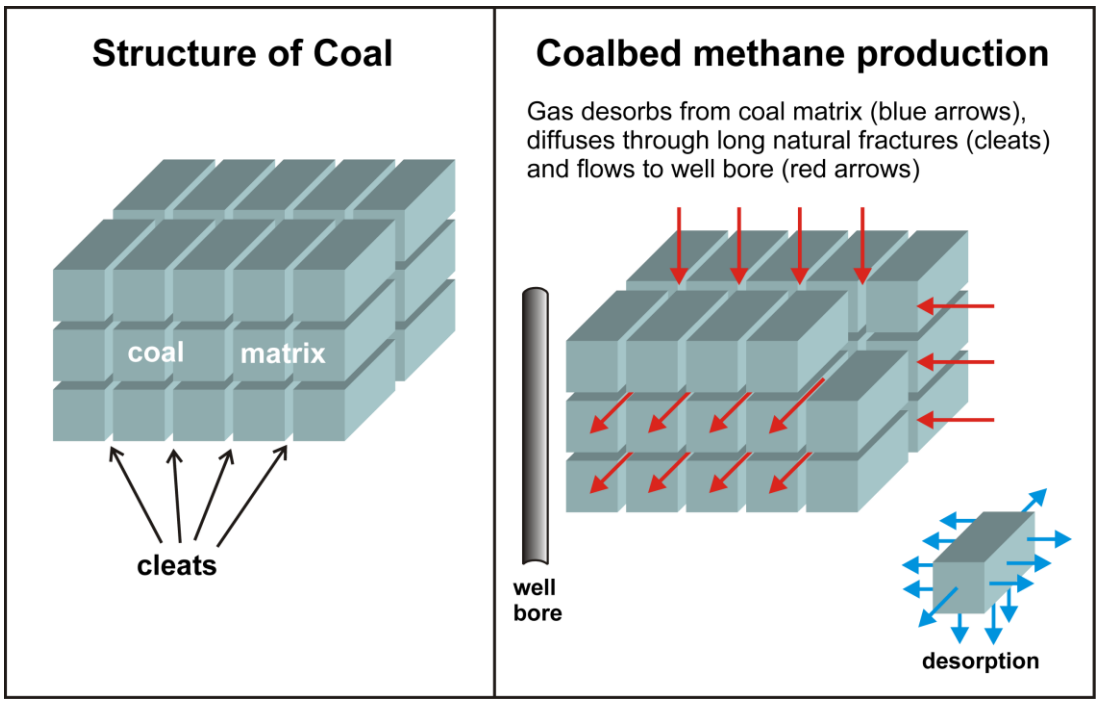

Figure 2. Characteristics of methane production from coal (based on Zuber, 1996).

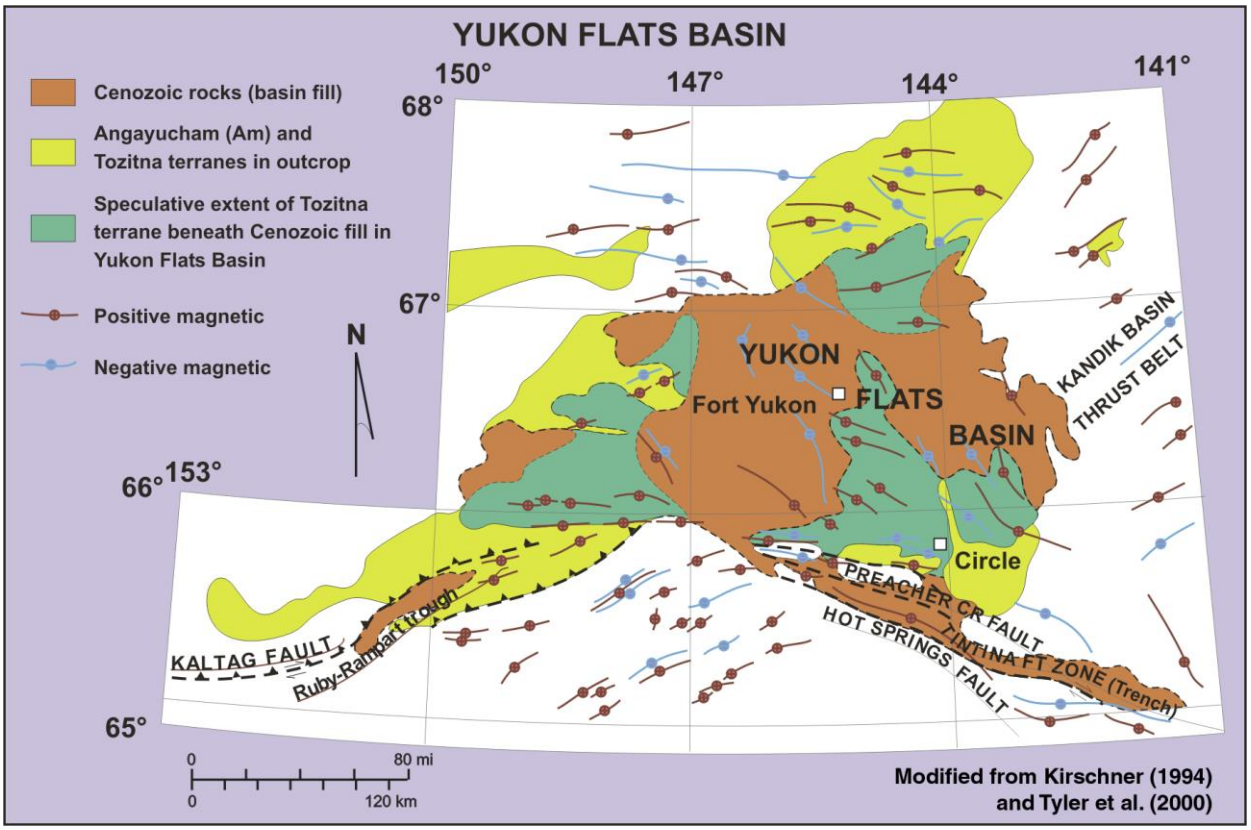

Figure 3. General geologic setting of Alaska and Yukon Flats Basin in particular.

GEOLOGIC SETTING

The Yukon Flats Basin of east-central Alaska is an alluvial and marshy, lake-dotted lowland area of more than 13,800 km^2, located south of the Brooks Range and north of the Yukon-Tanana Uplands (Kirschner, 1994) (Figure 3). Tectonically, the Yukon Flats Basin is interpreted as a pull-apart basin or rhombus graben; however, some evidence supports the notion that the basin formed as a result of crustal rotation (Kirschner, 1994). Regardless of the mechanism responsible for the basin's conception, it is commonly accepted that the process is still active today. The lowland that characterizes this basin extends upstream into other parts of the Yukon River and Porcupine River drainage basin. Based on gravity modeling, the Yukon Flats Basin may have as much as 3000 m of Cenozoic fill, while interpretation of seismic data acquired along the Yukon River pushes that estimate to over 4000 m (Hite and Nakayama, 1980). On average, the sediment load (thickness) regionally across the basin is thought to be less than 1000 m. The upper 100 m of sediments in the basin is predominantly Tertiary lacustrine silts and clays. Covering most of Yukon Flats is an anomalously flat layer of Quaternary river deposits leaving the ground surface more closely resembling a coastal plain setting than an inland basin. The surface elevation is around 200 m above sea level.

Based on a 1994 corehole commissioned by the U.S. Geological Survey (USGS) for climate studies, a coal zone encountered at 391 m is known to be gassy and contain several individual coal beds that are of ligite rank (0.3% mean random vitrinite reflectance) (Figure 4).

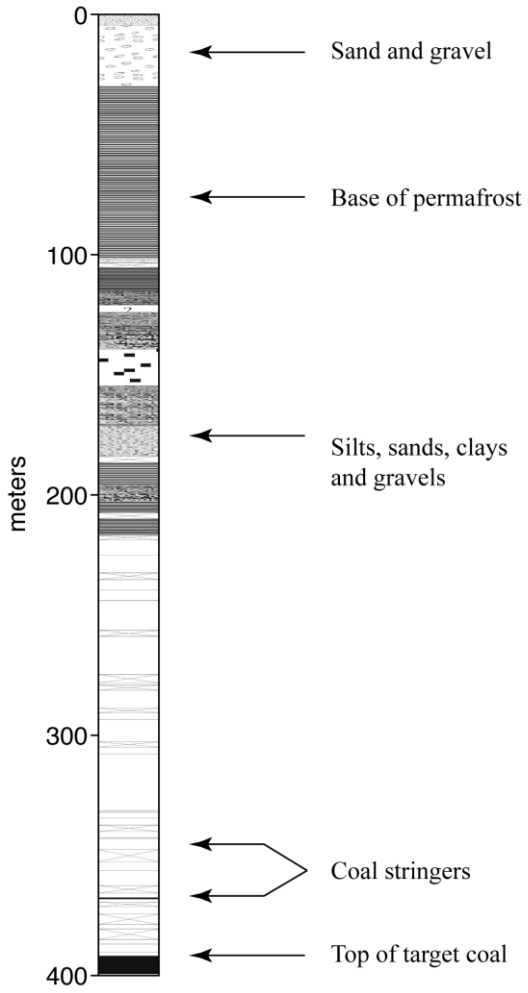

Figure 4. General geologic column describing the core retrieved by the USGS in 1994 near the U.S. Air Force radar station at Fort Yukon, Alaska.

Petrographic studies show that the coal is composed mostly of detrital vitrinite and appears to be of lacustrine origin (Barker, 2001). Adsorption isotherm studies indicate a gas-saturated storage capacity of about 40 scf/ton (as received basis) at 400 m depth.

Historically, coal has not been considered an economic resource in the Yukon Flats Basin (Wahrhaftig et al., 1994) with only minor occurrences of coal reported throughout the basin (Barnes, 1967). These previously discovered scattered coal reserves are Tertiary subbituminous to lignite in rank and have not been of commercial thickness or quality. Improvements in technology and economics associated with gas development have made low-grade coals a target of resource development in other parts of North America, particularly within the Power River Basin (Montgomery, 1999). Within the last 20 years, coal beds within the Yukon Flats Basin, previously characterized as noncommercial because of poor grade, have become the focus of detailed evaluations. Efficient development of any CBM resource requires a good understanding of a coal seam's lateral extent, structural anomalies, and thickness.

In the Fort Yukon area, permafrost is around 75 m thick with unconsolidated, probably saturated, sediments present from the base of ice bonding to at least 400 m BGS where the primary target of this study (a lignitic coal bed) was recovered in cores. Permafrost environments present unique challenges to the acquisition, processing, and interpretation of seismic reflection data regardless of target or resolution requirements (Palmore, 1984). Seismic reflection profiling in a permafrost setting, especially high-resolution profiling, is complicated by the near-surface high velocity layer defined by the base of the ice-bonded zone (Poley and Lawton, 1991). This frozen earth setting is made even more troublesome when a significant portion of the sediments between the target and the base of the permafrost are unconsolidated, resulting in a pronounced velocity inversion. Near-surface sediment velocities measured from first arrivals on seismograms in the Fort Yukon area range from around 3750 to 4000 m/s for the ice bonded portion and 1600 to 1750 m/s for the unconsolidated, saturated sediments above the coal interval, as estimated from the NMO velocity measurements.

Variable permafrost thickness and material properties and the presence of free gas within frozen sediments cause extreme lateral velocity changes and adversely affect the transmission of seismic energy. Based on the type and configuration of surface heat sources (such as lakes and

rivers), the permafrost thickness can vary by tens of meters and therefore result in substantial static irregularities on CMP stacked seismic sections. As well, velocity can vary by 50% laterally with changes in permafrost lithology. Success using high-resolution seismic reflection to delineate relatively shallow (<1000 m) and thin (~3 to 10 m) methane hydrate lenses below a thick sequence (~600 m) of ice-bonded unconsolidated sediments in the Mackenzie Delta, Northwest Territory, provided several key insights into this study of coal beds beneath Fort Yukon (Hunter et al., 1999). Enhancements to resolution and signal-to-noise ratio came as a result of rigidly coupling receivers and direct contact of the source with frozen ground, a lesson learned at the Mallik site. Most significant of the insights gained from previous high-resolution seismic studies in permafrost settings relate to distribution and constraint of source-to-receiver offsets to optimize normal moveout corrections while retaining sufficient offsets to study AVO effects.

What If ????

Why is the resolution and delineation potential and expense of high resolution seismic reflection necessary at Fort Yukon? Nine meters of gassy lignite were recovered in core from the base of the 1994 USGS climate drill hole at Fort Yukon. However, the gas content and quality (methane or CO_2) of the lignite was not determined and its total thickness and lateral continuity remain unknown as well. In this geologic setting the continuity of the coal, its structural characteristics (faults, fractures, and dip), and thickness cannot be adequately appraised from a single borehole. Lithologic or structural complexities possible at this site can make conclusive hole-to-hole correlations across distances as short as several hundred meters difficult. Dozens of boreholes across this approximately 5 km^2 area may not provide sufficient data for sitewide mapping and resource appraisal. As well, the site selected for a detailed drilling and sampling program and production test must reasonably represent the "norm" or appraisals of sitewide methane production potential could be in error.

For example, it is not outside the realm of possibility that the 1994 USGS corehole encountered the coal seam on the down-thrown side of a large fault block (Figure 5). In such a setting there would be a significant risk in assuming that the coal is continuous and uniformly thick beneath and around the town. Changes in coal seam characteristics could affect the design and location of a well field intended to feed a multi-million dollar municipal electrical power generating facility. It is also possible in this depositional environment that the lacustrine coal observed in the core was from a small channel no larger than the slough bounding the south side of the village or the edge of larger deposits only present south of the village. A variety of other fault and depositional scenarios could be imagined that would dramatically reduce the producible volume and yield.

HIGH RESOLUTION SEISMIC PROFILING: CONCEPTS

Seismic reflection is a geophysical technique that relies on sound waves to travel through the earth and interact with discrete changes in seismic velocity and/or mass density in a predictable way (Garland, 1979) (Figure 6). These changes in velocity and/or density are known as acoustic impedance contrasts. Acoustic impedance contrasts commonly occur at natural boundaries, such as changes in lithology. To detect or image a lithologic contact using seismic

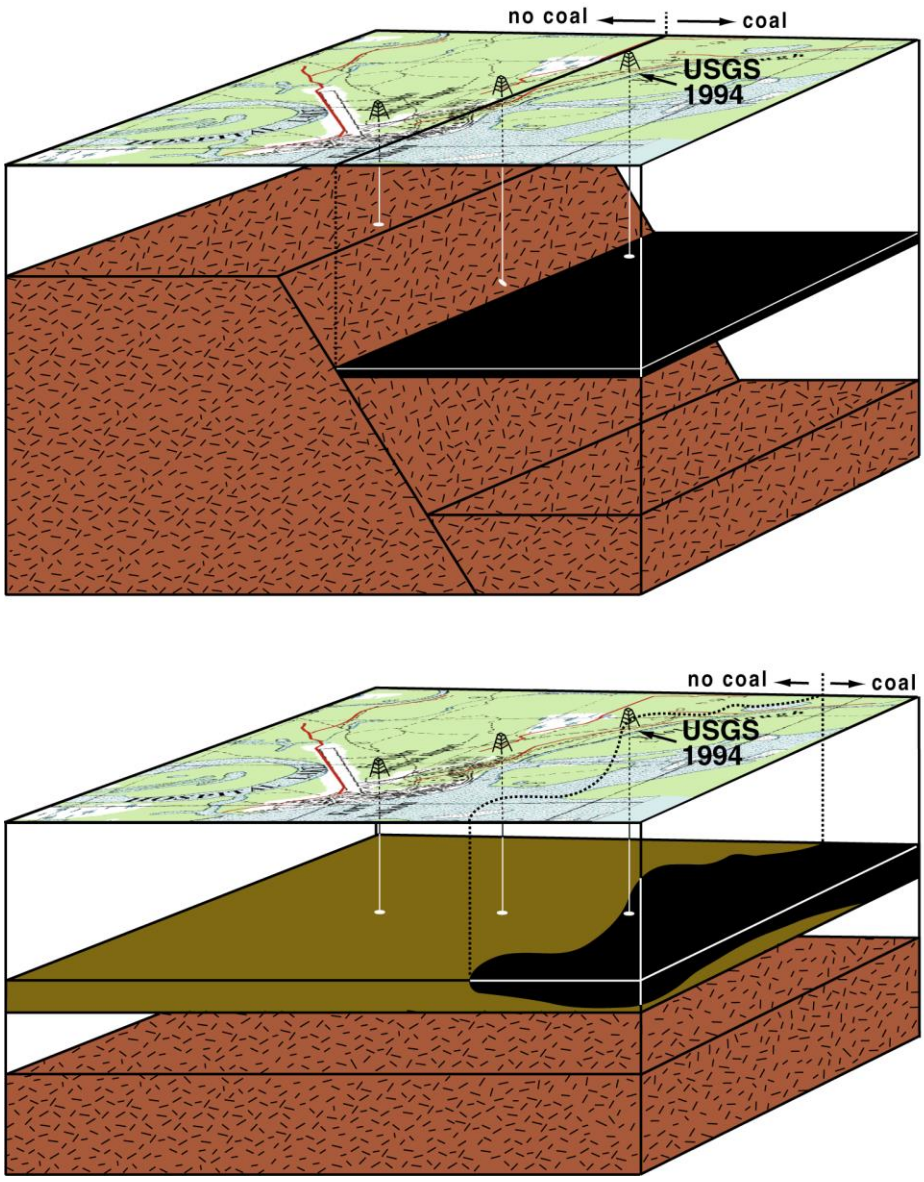

Figure 5. Possible scenarios beneath Fort Yukon that would have been disastrous if present and the coal was assumed continuous beneath the village. Based on the 1994 USGS corehole.

reflection only requires an acoustic impedance contrast. Delineating or resolving a layer (top and bottom), and therefore providing an estimate of bed thickness, requires an acoustic impedance contrast, as with detecting, and also high frequencies. Dominant frequency and upper corner frequency within the reflection bandwidth are key to the resolving power of a seismic reflection data set.

Effective high-resolution seismic reflection surveys require both redundancy in subsurface sampling within the optimum source-to-receiver offsets (Hunter et al., 1999) and high energy and high frequency seismic signals (Steeples and Miller, 1990). By definition, high-frequency seismic signals are greater than 80 Hz (Sheriff, 2002). It was known going into the

Fort Yukon seismic study that to successfully meet the program objectives frequencies at least twice this defined high-frequency threshold would be necessary.

Competing with the need for more traces (i.e., greater fold) to boost the signal-to-noise ratio is the need to minimize the number of wavelets summed together to maximize the resolution. Summing or stacking generally reduces higher frequency components of the signal through destructive interference while increasing the signal-to-noise ratio. Throughout acquisition and processing a balance must be found and maintained between these two critical characteristics of the data.

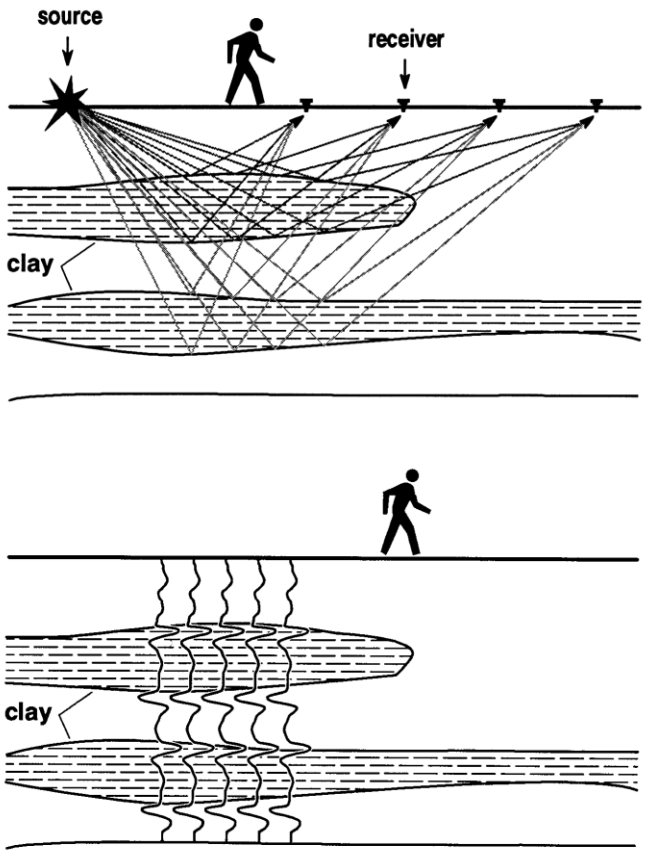

Figure 6. Seismic raypaths from source to receiver for two coal layers and interpretation.

Resolution

Imaging and resolving as they relate to interpreting seismic reflection sections are quite different objectives. To image an acoustic impedance contrast (assuming the contrast is more than one wavelength deep) requires only sufficient energy be imparted to the ground for a wavelet to travel from source to reflector to receiver (considering transmission losses in the earth) and an appropriate source-to-receiver offset for the depth and overburden velocity (Figure 6). Resolving the top and bottom of the layer (defined as a uniform material with acoustic impedance contrasts on top and bottom), on the other hand, requires not only sufficient energy and appropriate source-to-receiver offsets but also high enough reflection frequencies to permit energy returning from the top of the layer to be separated from energy reflecting off the bottom. Realizing the full theoretical resolving potential of high-resolution seismic reflection data is not realistic. However, quantifying the resolving potential of a data set using practical criteria provides realistic objectives and reasonable expectations for geologic interpretations.

The vertical resolution limit of a reflection data set can be estimated using either the theoretical maximum defined by the ¼λ axiom (Widess, 1973), or a more practical limit of ½λ (Miller et al., 1995). Since wavelength is a function of velocity and frequency, improving vertical resolution can only be accomplished by increasing the bandwidth and dominant frequency of the seismic signal. Using 180 Hz and a velocity of 1800 m/s, the practical vertical resolution is around 5 m with a theoretical limit of around 2.5 m. From the 1994 USGS core data, the acoustic impedance contrast between the coal and overlying clay should be sufficient to provide a high amplitude reflection. Considering 9 m of coal was penetrated before drilling operations ended at 400 m, 180 Hz seismic reflection data should resolve the top and bottom of the 391 m coal.

Resolving variations in geometry and/or stratigraphy in the horizontal dimension is more challenging, and estimating the horizontal resolving potential of reflection data is not nearly as straightforward. Horizontal resolution has been described for broadband, zero-phase seismic data as a zone of influence (Brühl et al., 1996) with Rayleigh's criteria suggested as the basis to quantify the minimum distance two objects can be separated and still be distinguishable (Kallweit and Wood, 1982). This distance can be calculated using the relationship $F = \sqrt{LVZ/2}$, where F is the broadband Fresnel zone, L is the trough-to-trough zero phase wavelet duration, V is the velocity, and Z is the depth to the reflector (Ebrom et al., 1996).

Gradual changes in geometry and lithology can be interpreted well below the horizontal resolution limits of the data. Bed truncations from faulting, fracturing, or pinch outs can be indirectly dectectable if bed offsets or separations are smaller than the zone of influence or Fresnel zone. The horizontal resolution limit, as defined by the Fresnel zone, of the two major targets beds of this study is 46 m for the 391 m coal and 76 m for the 650 m basement. Even though separations in a bed cannot be uniquely distinguishable or quantified beneath the Fresnel zone, the presence of diffractions can be used as indicative of interruptions in bedding or layers where separations are less than resolvable.

DATA ACQUISITION

Survey Design

The primary goal of this study was to detect, delineate, and evaluate local stratigraphic, structural, and topographic features at or near the coal bed contacts using the highest signal-to-noise ratio and resolution reflection data possible with state-of-the-art high resolution methodologies and equipment. Survey design focused on optimally and confidently interpolating the coal reflection between all the 2-D lines, specifically under the town and in the area immediately east of town. Environmental concerns and cultural features restricted line placements. Geostatistical analysis of interpolation error based on line spacing and orientation provided qualitative constraints on extrapolation confidence for three lines originally proposed to surround the town (Figure 7). This idealized line deployment scheme was modified during initial site visits due to vegetation, cultural obstacles, and spring thaw.

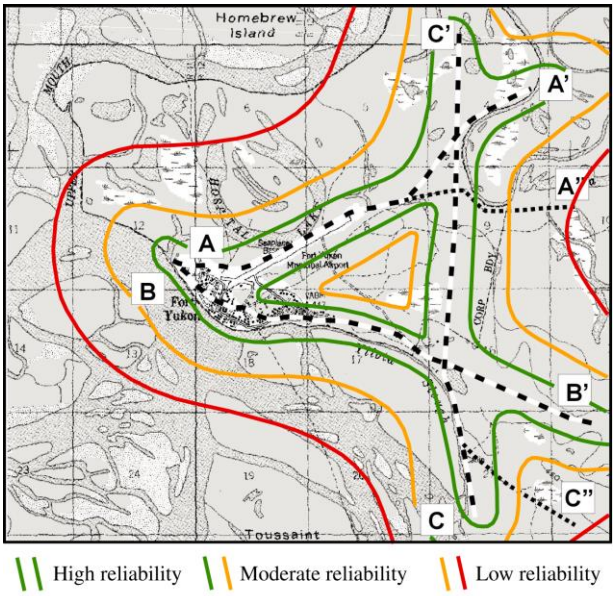

Figure 7. Location of shallow seismic lines A-A', B-B', and C-C'. Lines A-A" and C-C" are potential alternatives to proposed lines depending on logistical considerations. The location of the 1994 USGS climate drill hole site is at the intersection of lines B-B' and C-C'.

After considering access constraints and obstacles, seven lines were acquired in and around the town of Fort Yukon and the U.S. Air Force radar station immediately east of town (Figure 8). Snow removal was necessary for the vibrator to navigate the paths and

ATVs to move equipment and personnel along the lines. A short test survey line (line 1) acquired within a few meters of the 1994 USGS climate corehole provided critical ground truth. The Yukon River and Hospital Lake represent significant surface heat sources that influence the subsurface variability of the permafrost in the Fort Yukon area, adversely affected data quality, and further constrained locations of seismic lines.

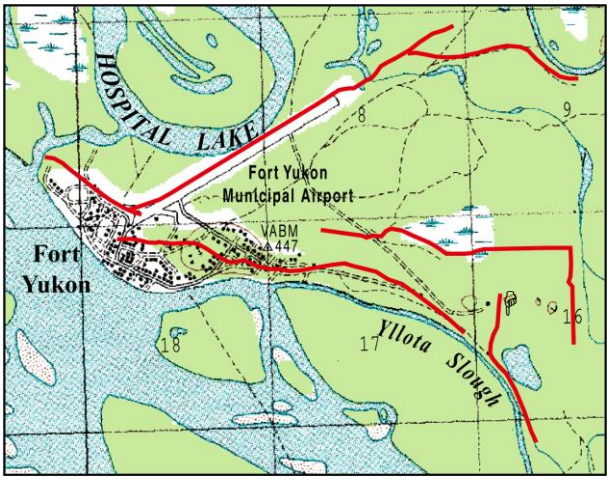

Figure 8. Seven seismic lines displayed using GPS data acquired along each line with ±2 cm accuracy. The USGS corehole (★) is immediately adjacent to line 1.

Severe Limitations: "Small Footprint" and Airlift Portable (weight and size)

Transporting equipment to rural areas is expensive and constrained by airfield limitations, proximity to navigable waterways, and vehicle capacities. Without roads to transport seismic gear, most conventional equipment and field exploration methods could not be considered for Fort Yukon, as would be the case for many rural villages. Considering the limited transport size and weight restrictions, even equipment modifications for operating in this cold climate had to be made efficiently.

Adding to these problems is the need for "small footprint" exploration methods. Traversing wooded and high-relief areas in this delicate environment needed to conform with strict federal, state, municipal, tribal government and village and regional Native corporation guidelines and constraints. Off-road travel could not involve destruction of vegetation or scarring of the ground surface.

An L-382 Hercules transport with a 24,000 kg payload and 16 m long by 2.5 m high cargo hold transported the seismic equipment from Fairbanks to Fort Yukon and back (~580 km roundtrip) (Figure 9). This aircraft landed on the 1.5 km, ice/snow packed, gravel runway

Figure 9. L-382 Hercules transport operated by Lynden Air Cargo. The 400 mile round trip to Fort Yukon from Fairbanks cost $32,000.

Figure 10. A single pallet of cables and geophones on the rear ramp of the transport.

Figure 11. Buggy-style vibrator was driven onto the aircraft.

operated by the Alaska Department of Transportation. Cargo included six pallets of cables and geophones (Figure 10), two 6 x 6 ATVs, one 4 x 6 seismograph ATV, one snowmobile, an IVI minivib (Figure 11), one pallet of computers, and one pallet of personal gear (Figure 12). Loading and unloading the aircraft took about 30 minutes.

Equipment and Recording Parameters

Data were recorded to optimize reflection events between about 300 and 700 m BGS. Equipment and recording parameters were selected based on experience at similar sites and preliminary tests along line 1 (intersecting the corehole site). Due to transportation issues and the obvious need to minimize equipment moved to the site, most adjustments to the acquisition procedures, parameters, and equipment were simply on-site fine tuning activities.

A 240-channel Geometrics Strataview seismic recording system shock mounted in a customized steel frame on a 4-wheel drive, 6-wheel John Deere Gator recorded the 12,000-sample-per-trace, uncorrelated data (Figure 13). Data were digitally sampled at 1 ms intervals for each of the three sweeps run at every station. Each of the three shot records recorded at each station was digitally saved as a unique file on the seismograph's hard drives. The final data set included seven lines, which included source occupation of more than 2600 stations. Storing

Figure 12. The entire load transported by the aircraft.

Figure 13. The seismograph and supporting equipment.

Figure 14. Winterized self-propelled recording vehicle.

Figure 15. Pilot holes drilled and geophone spikes frozen into place.

these data required in excess of 60 gigabytes (100 CDs) of digital space. To maintain as quiet a recording environment as possible, the entire recording system (including all support systems) was operated on 12 V battery power.

Seismograph

With temperatures dipping below -30º C, the seismograph, supporting equipment, and operator had to be protected from the cold. A customized, double-lined vinyl cover with operator boot was installed to enclose the ATV's seismograph area (Figure 14). A thermostatically controlled propane heater was also added to the vehicle to maintain an inside temperature of around 60º F. Cables connecting the seismograph to the geophones entered the seismograph compartment through velcro sealable slits. Several radio frequencies were used to maintain contact with crew and transmitted the vibrator operating data (source signal–ground force). A 110 V generator was used when backing up data from seismograph hard drives to external hard drives. External hard drives were the host for transporting data to the mobile processing center set up at the lodge where the data were burned to CD.

Receivers

Based on testing at several other permafrost sites, conventional ice plates do not provide sufficient coupling for high-frequency recording. All snow and ice was removed and pilot holes drilled (melted) into the frozen ground to optimize the high frequency recording potential of the three 10 Hz Mark Products digital grade geophones planted at each station (Figure 15). Hammer drills with 20 cm long carbide bits, powered by small electric generators, bored through the frozen gravelly surface material (Figure 16).

Figure 16. Drilling geophone pilot holes.

Figure 17. Three-geophone array in 1 m long snow/ice trench.

Figure 18. Several receiver stations were active throughout acquisition.

Geophones were then inserted into the holes (still wet from frictional melting) and frozen into place at the bottom of trenches dug through snow and ice up to 1 m deep (Figure 17). This process dramatically increased the time and effort necessary to deploy geophone spreads, but the rewards were evident as upper corner frequencies of stacked reflections exceeded 180 Hz in some places.

Up to four drills were working simultaneously to plant geophones into the road bed, edge of the runway, dirt paths, through sloughs, and into organic-rich soil in wooded areas (Figure 18). A sufficient buffer was maintained between geophone planting and live recording stations to allow continuous data recording.

Source

Considering the near-surface conditions, target depth, resolution requirements, environmental limitations, and transportation constraints, an IVI minivib outfitted with a prototype high output valve (3 to 4 × normal power above 150 Hz) was the optimum source configuration for this site and project (Figure 19). This center-articulating buggy-mount, high-frequency vibrator (15 to 500 Hz, 8000 lb peak force) provided the necessary mobility and coupling (Figure 20). With the "small footprint" and minimal ground compression, the source did not leave an impression that would survive the summer, even along the trails and open areas where some thawing had occurred. The vibrator was winterized to allow operation in temperatures well below -40º C.

Snow was removed from roads and trails using a front-end loader owned and operated by the Native Village of Fort Yukon. The vibrator pad was seated onto thin (< 5 cm) frozen snow, ice, or frozen ground, but never onto loose, lightly compacted, or deep snow. Three 10 second

Figure 19. IVI minivib moving down the seismic line past the recording vehicle and snow machine used to move equipment.

Figure 20. Vibrator traversing path cleared by loader.

upsweeps from 25 to 250 Hz were recorded at each shot station. Shot stations were on 10 m intervals. Ground force, mass accelerometer, and base plate accelerometer were recorded and saved for each shot. Software used to control the vibrator's power output maintained the maximum force without overdriving the valve and/or decoupling the baseplate.

Figure 21. GPS surveying using differential Trimble system with an accuracy of ±2 cm.

Surveying

Accurate station surveying is essential for any high-resolution seismic reflection program. All stations necessary for elevation corrections and absolute location of the 2-D profiles were surveyed with a Trimble 4800 and 4700 differential GPS at a ±2 cm accuracy in x, y, and z. Initially, each station was located using a measuring chain or takeouts (5 m spacing) on the seismic cables (Figure 21).

Quality Control

Quality Control (QC) was critical and continuously practiced throughout acquisition. Near-surface inconsistencies, topography, an extremely wide and changing optimum recording window, and poor source/receiver coupling conditions necessitated strict compliance with QC guidelines and meticulous monitoring of data, an absolutely essential aspect of the data acquisition. The seismograph CRT display, nearly real-time digital filtering, on-board correlation software, and real-time graphical display of noise levels permitted instantaneous monitoring of cultural, air traffic, vehicle traffic noise, power-line noise, cable-to-ground leakage, and geophone plant quality.

After each geophone was planted, it was tested to insure a cable-to-ground resistance greater than 2000K ohms and individual geophone continuity within 5% of nominal string

impedance (adjusted for cable lengths). In addition, each geophone underwent a modified "tap and twist" test. Any sweep with background noise levels on active geophones greater than 0.05 mV was restarted. The ability of the seismograph to monitor real-time noise levels, signal quality (through digital filtering), and unacceptable geophone plants as well as measurements by line testing equipment of earth leakage and continuity minimized the number of recorded shots not maximized for this site and equipment configuration.

Each vibrator sweep was monitored at the vibrator for uniformity in energy levels using force curves produced by the vibrator computer. The sweeps were also studied on the seismograph by the seismograph operator, looking for consistency in ground force frequency and amplitude. Pad coupling problems due to surface conditions and frequency dependent decoupling due to overdriving the mass were identified and appropriate compensatory adjustments made.

Walkaway Noise Testing

The unique characteristics of this site were evident during walkaway testing performed along line 1 prior to collecting the CMP data along that profile. Each high-resolution seismic reflection program must be tuned for the acoustic and logistical conditions of the particular site. As previously stated, identification and confirmation of reflection hyperbola on walkaway noise tests are essential and best accomplished through mathematical curve fitting using a borehole-derived velocity structure (when available) and observation of file-to-file consistency. Walkaway noise tests were designed so the subsurface was oversampled horizontally and the source-to-farthest-receiver offset was at least equivalent to the maximum depth of interest. All aspects of the complete wavefield, especially the reflections, were appropriately appraised on the walkaway data.

The walkaway noise test allowed comparison of the signal-to-noise ratio and frequency content of various source parameters, receiver coupling, and instrument configurations. Walkaway tests performed on this survey were significantly condensed but still allowed the necessary identification of individual events within the full wavefield. Phase velocity and wave type are the most important pieces of information obtained from walkaways. The relationship of velocity and wave type to spread geometries and offsets must be completely analyzed and understood for acquisition parameters and equipment to be optimized for any shallow reflection survey (Pullan and Hunter, 1990).

Walkaways consisted of source-to-receiver offsets ranging from about 3 m to almost 500 m. Consistent with experience at similar permafrost sites, the IVI Minivib outfitted with a high output valve (3 to 4 times the power above 150 Hz) was the optimum source configuration for the near-surface conditions, target depth, resolution requirements, and environmental limitations.

Receivers available for testing included both triple 10 Hz 2Uw and dual 40 Hz L-28E geophones, both manufactured by Mark Products and wired in series. The 10 Hz geophones were tested first and, consistent with previous experience with targets of this type and depth range, produced a response good enough to forego testing of the 40 Hz phones. The need for a strong signal and flat response from geophones with a high spurious noise threshold is paramount for high frequency reflection profiling.

In summary, the walkaway noise testing as designed and executed to allow evaluation of acoustic signature, optimum acquisition equipment and parameters, near-surface velocity structure, horizontal consistency in reflection character, general resolution potential, signal-to-noise ratio, and impact of cultural noise.

Field Geometry—Source/Receiver

The emphasis of any high-resolution reflection survey is maximization of the resolution potential, data interpretability, and signal-to-noise ratio. Continuous CMP profile lines (Mayne, 1962) were acquired using a 240-channel fixed spread, incrementally rolled to maintain a full complement of optimum offsets within the primary 120-channel recording window (50-300 m) for each recorded shot (Hunter et al., 1984) (Figure 22). A fixed 240-station spread with a rolling source resulted in 40 to 60-fold CMP redundancy with an asymmetric split-spread source/receiver geometry. The source-to-nearest receiver offset ranged from a minimum of 2 m to 20 m while the maximum source-to-receiver offset was from 600 m to around 900 m. The seismic source, geophone type, spread geometry, shots/point, and acquisition philosophy used to acquire the CMP profile lines were based on project logistics, results of walkaway noise tests, and survey objectives.

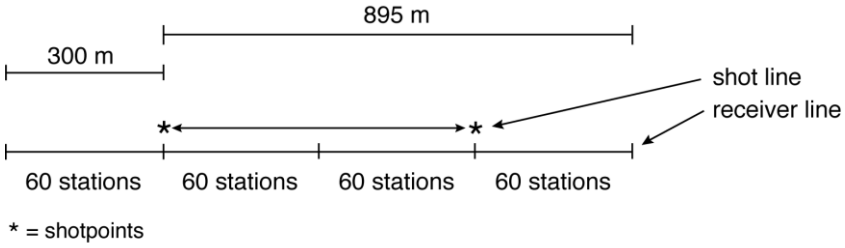

Figure 22. Fixed 240-channel spread with shooting geometry for asymmetric split spread.

Relative orientation of source and receivers is critical for recording reflections from the optimum source offset distance. For targets that are relatively shallow and thin (by conventional standards) it is important to record reflections returning from reflectors at a specific set of incident angles or reflection angles. In this setting, the problem is complicated by the base of the high-velocity permafrost, which defines a velocity inversion. This high-velocity layer dramatically alters reflection raypaths during their travel from source to reflector and then to receivers. To insure that the ever-changing optimum source offset was always recorded, 240 receivers were deployed in a fixed spread 1.2 km long. By recording geophones over this wide range of offsets, if the geology did change unexpectedly, the optimum reflection window would still be recorded.

The receivers were spaced on 5 m intervals with sweeps recorded at shot stations located at every other receiver station. The source was offline from 2 to 10 m, as dictated by surface limitations. These data possessed a nominal fold of around 60, but since only the optimum offsets were used, the stacked sections are around 12 to 18 fold. By avoiding long offset effects (wide angle, high velocity layer distortion, etc.), traces used in the stacked sections have the highest signal-to-noise ratio, lowest wavelet distortion (from NMO stretching), and highest frequency.

Recording Parameters

Parameters such as sampling interval and record length were determined after examination of the dominant frequency and usable bandwidth of reflection energy recorded during the walkaway noise tests. The sampling interval was chosen to insure at least 4 samples/wavelength of the upper corner frequency and 7-10 samples/wavelength of the dominant reflection energy were recorded. The total number of samples recorded was based on maximum time (depth) of interest (basement at ~700 m), which was determined using the depth interval of interest and average velocity estimations.

Oversampling of the Fresnel zone was restricted to 15 times for the deepest imageable reflection events (Steeples and Miller, 1990) while a minimum of 5 times was maintained for the shallowest events.

Shot Gathers

More than a dozen high quality (high signal-to-noise ratio and dominant frequency) reflections are prominent from 300 m to the basement at over 600 m (Figure 23). Correlating to the USGS corehole, these reflections fully sample the depth of known coal and extend into the

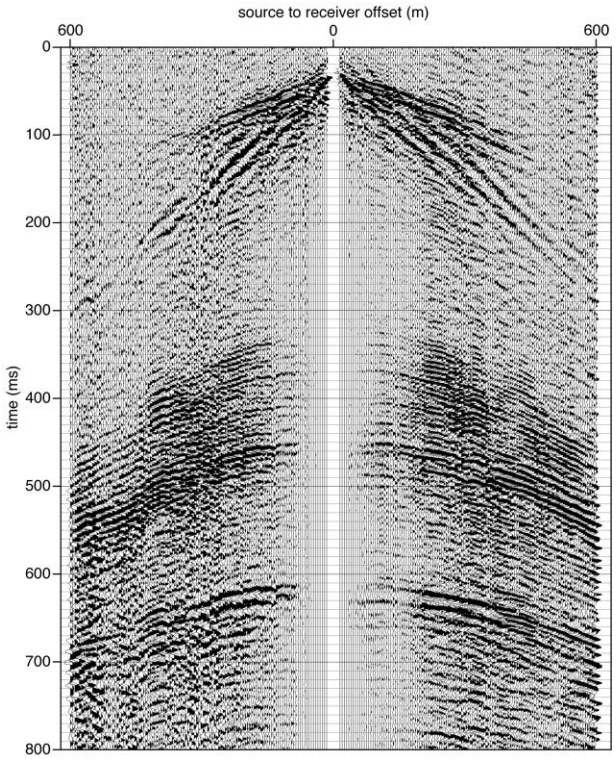

Figure 23. 240-trace symmetric split-spread shot gather from along line 7. Reflections from basement are easily distinguishable by their characteristically lower dominant frequency. Reflections from the potential coal interval exceed 180 Hz in some places.

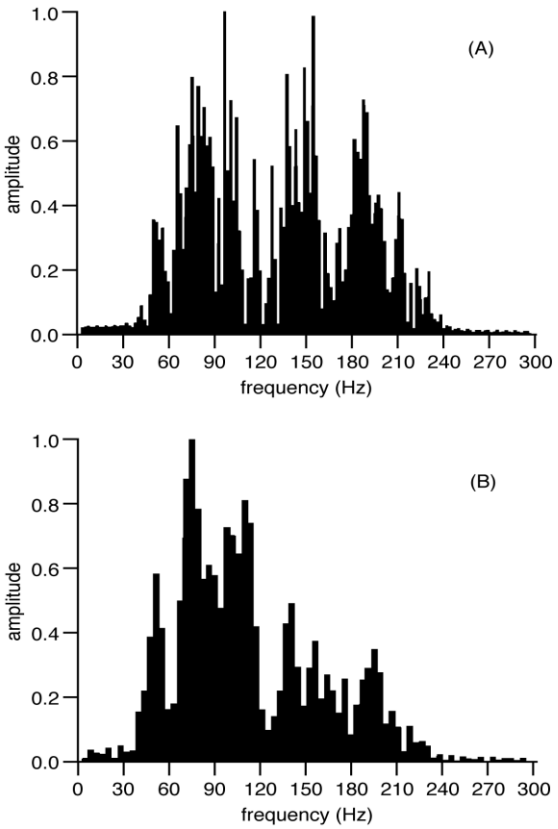

Figure 24. Spectra for reflections from the potential coal interval (A) have double the bandwidth and dominant frequency of the basement reflections (B).

interval having a high possibility of coal. Reflections fill the time-depth interval where coal is known to exist. Considering the unique and abrupt transition from very limited reflection returns (above 300 m where no coal was encountered) to the zone of abundant reflection arrivals (300 to 650 m where three reflections were encountered in the first 100 m), it is reasonable to suggest that the highly reflective zones are indicative of coal seams. The basement reflection is easily identified by its characteristic lower frequency and less coherent reflecting nature.

Data Resolution

Reflections above basement have a dominant frequency around 150 Hz with a usable upper corner frequency slightly greater than 200 Hz (Figure 24A). Reflections from the basement have a characteristically lower dominant frequency at around 90 Hz (Figure 24B) and a much more diffuse, less trace-to-trace coherent appearance.

There are clearly three different groups of reflection arrivals present on shot gathers from across the site (northernmost, Figure 25; southernmost, Figure 26). One set is about 50 ms in length and arrives between 350 and 400 ms. A second set comes in consistent with a high amplitude event at about 450 ms. The second reflecting "packet" is followed by about 100 ms of

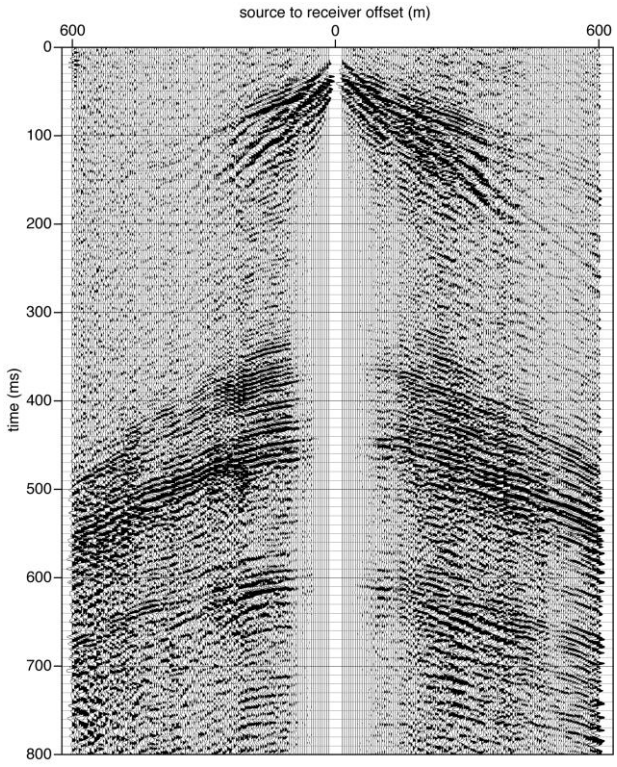

Figure 25. 240-trace symmetric split-spread shot gather from along line 4, the northern- and eastern-most profile. Correlation with the drive signal (synthetic) provided the best results.

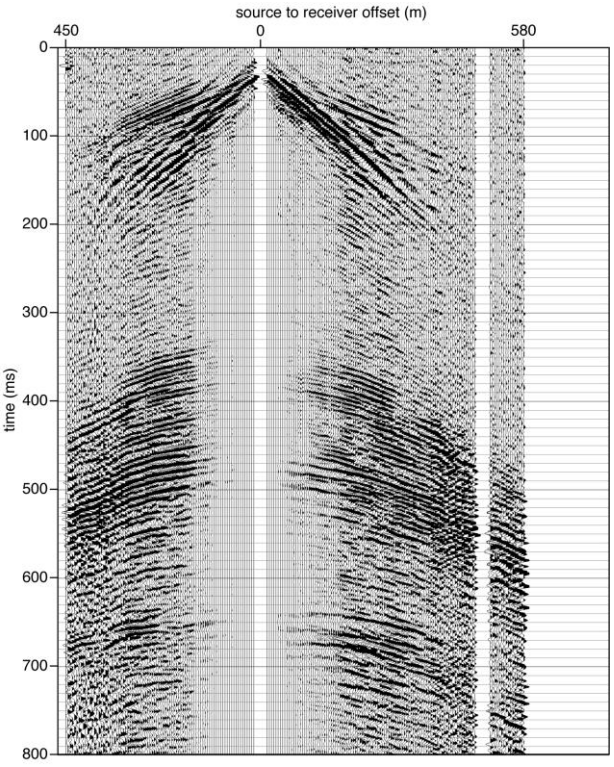

Figure 26. High-amplitude reflections are easily interpreted from around 320 ms to basement at 640 ms on line 5, the southernmost profile. Very subtle reflections can be seen between the base of permafrost at about 70 ms and the top of the high amplitude reflection interval.

relative quiet, likely indicative of sand, gravel, clay, and silt units similar to those observed in the core between the base of the permafrost and the top of the 350 m coal unit. A final reflection packet is interpreted as the top of basement, with a weathered, diffuse appearance. Since the data possess a practical vertical bed resolution potential of around 5 m, the top and bottom of the 9+ m coal layer encountered 400 m BGS in the drill hole should be resolvable. These data are estimated to have a 45 m horizontal resolution, which in the case of a coal layer terminated by faulting or depositional forces, would allow identification of the truncation within 9 receiver stations or 18 traces on CMP sections.

DATA PROCESSING

Precorrelation operations were instrumental in broadening the bandwidth and flattening the spectra, therefore increasing data resolution and improving source wavelet characteristics. Testing the effectiveness of deconvolution and correlation with the ground force and synthetic drive signals demonstrated that scaling followed by correlation with the synthetic drive signal produced the best bandwidth and upper corner frequency reflections. All data were recorded uncorrelated to allow evaluation of this full range of post-acquisition, pre-correlation processing possibilities (Doll and Çoruh, 1995).

Noise reduction was critical. Noise included: 60 Hz powerline and higher modes (removed by the hum filter), cultural noise (snow machines, automobiles, people walking, etc., removed by trace editing before the three sweeps/station were vertically stacked), and cable/ geophone crew noise (walking, drilling geophone holes, moving cables, etc., removed after correlation, but before vertical stacking of three sweeps/station).

Concern for improperly stacked reflections decreasing the signal-to-noise and the resolution potential as a result of the pronounced velocity inversion at the base of the permafrost required careful velocity and statics analysis. Obviously, velocity plays a role in NMO corrections, but as critical is velocity's role in many statics operations. Maintaining a focused and narrow window of source offsets was key to avoiding NMO artifacts in the presence of the extreme velocity inversion at the base of the permafrost. To insure the accuracy of the stacked sections and interpretations based on the stacked sections, special emphasis was placed on velocity irregularities near the 390 ms reflection that might originate from within the permafrost.

CMP lines were processed into a final stacked format using WinSeis, a commercial processing software package. The basic architecture and sequence of steps followed during the generation of the final stacked sections were similar to conventional petroleum exploration processing flows (Table 1). Specific processing parameters were determined based on experience and individual analysis (Appendix A). Step-by-step QC helped insure the stacked sections were at the limits of the data potential. These data were fk migrated, however comparing sections from before and after, little was accomplished through migration except a 5 to 10% drop in dominant frequency and a bit more coherency. The main distinctions between high-resolution and conventional data processing relate to the emphasis placed on velocity analysis, optimum offset window (especially for near-vertical raypaths), extending the upper corner frequency while broadening the bandwidth, minimizing extensive wavelet processing, care and precision of muting operations, constraining statics operations (maximum shifts no greater than ¼ wavelength

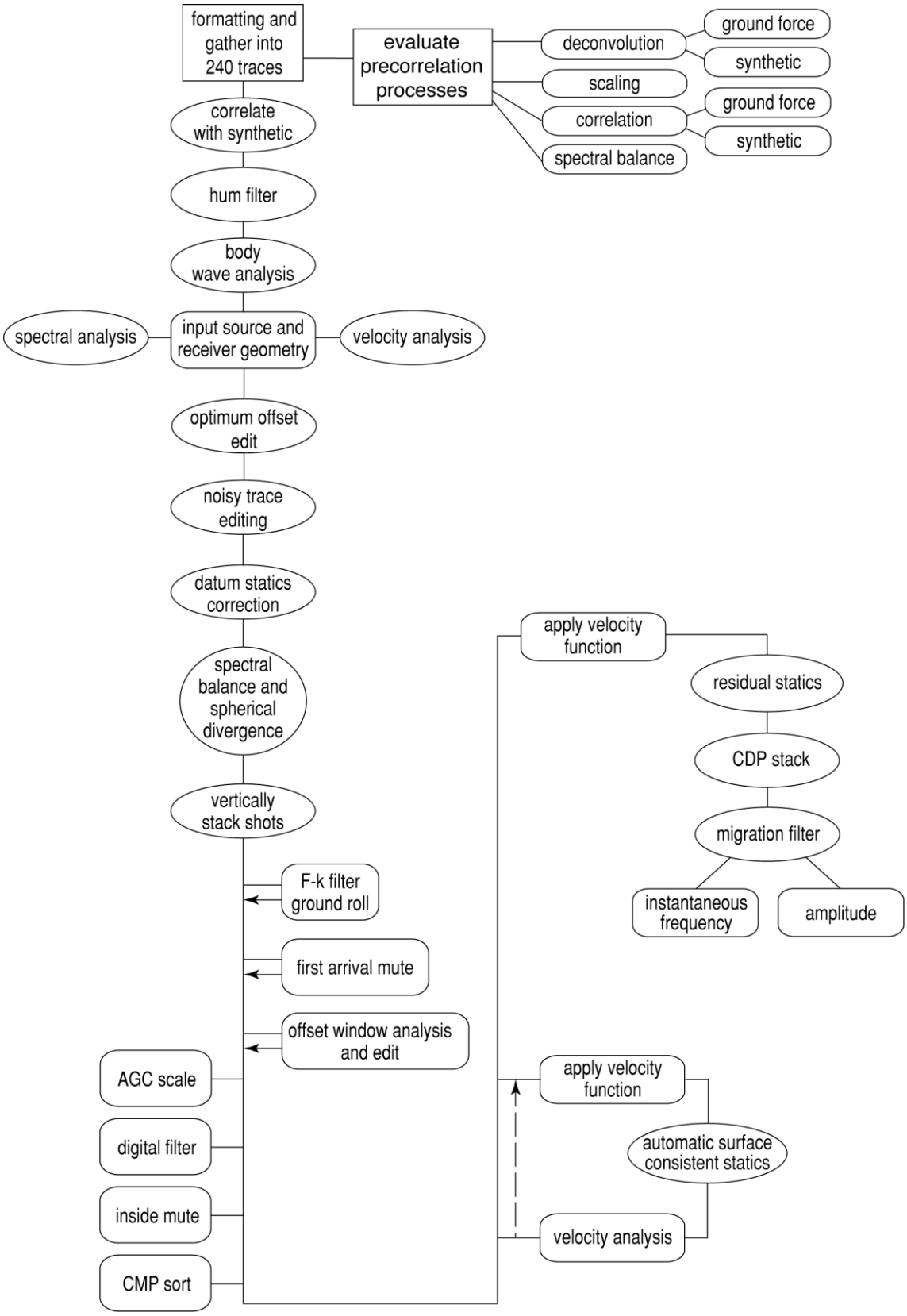

Table 1. Processing flow for data collected at Fort Yukon. See Appendix A for specific parameters used.

of the dominant reflection energy with correlation windows at least 10 times the dominant wavelength), and coincident iterative velocity and statics analysis.

INTERPRETATION

Geologic control is necessary to insure geophysical interpretations are correctly correlated to subsurface layers. Ground truth established from borehole samples and lithologic descriptions were matched with reflections after estimating time-to-depth conversions based on NMO velocities. This mating of the borehole and seismic data provided the groundwork for geologic interpretations in this report. Details about and properties of the subsurface observed on high resolution reflection data from sub-wavelength bed interference, bed tuning, and irregularities from interbedding makes interpreting some high-resolution data overwhelming. Time-to-depth conversions and ground truth ties are key to interpreting the very subtle and sometimes highly variable events observed on seismic sections.

Seismic sections from this study possess far more detail about the structure and stratigraphy of the subsurface than can be confidently interpreted with the very limited supporting data available at this time. Once a thorough drilling program has been implemented and a variety of geophysical logs run, these data could be extended to provide details about the most subtle (from a conventional seismic sense) of geologic features. Information obtained from strategically placed boreholes could provide sufficient insight to justify re-processing portions of these data. Interpretations presented here focus on the primary objectives of this study: sitewide 391 m coal layer continuity and potential for more coal below the 400 m TD of the corehole.

Seismic attributes extracted from reflection waveforms relate to unique geologic characteristics of earth materials. Along line 1 where borehole data (however limited) does exist, amplitude and frequency analysis was used to enhance and support interpretations of the coals encountered in the corehole. Based on seismic correlations to the borehole geology, inferences were made into the geology between 400 m and the basement.

Horizons mapped using automatic trace-to-trace correlation routines required only minor manual adjustments for excessive data variability. Reflections from the basement surface, the 480 ms (~480 m) high amplitude reflection, the 390 ms (391 m deep) coal seam, the 370 ms coal stringer, and two reflectors between the 391 m coal and the 480 m reflector appear continuous across most of the site. With no control data, contours of these horizons are based purely on seismic data. Line-to-line correlations in time and waveform are quite good considering no lines overlap sufficiently to tie.

Interpretations of fault planes—location, displacement, strike, and dip—were somewhat speculative. Preference was given to interpretations that resulted in normal hanging-wall footwall orientations. As well, strike-slip movement was considered and suggested on several faults based on changes in seismic characteristics across what appeared to be disturbed zones. On several profiles reverse faulting appears to fit the data best, but the fault plane was interpreted normal to be more consistent with the probable stress regime. Minor modifications to the interpreted fault zone would easily accommodate reverse or thrust faulting if consistent with the current and past tectonic setting. Several strong hyperbolic diffraction arrivals, normally indicative of faulting, become prominent at specific frequencies on wiggle trace amplitude displays.

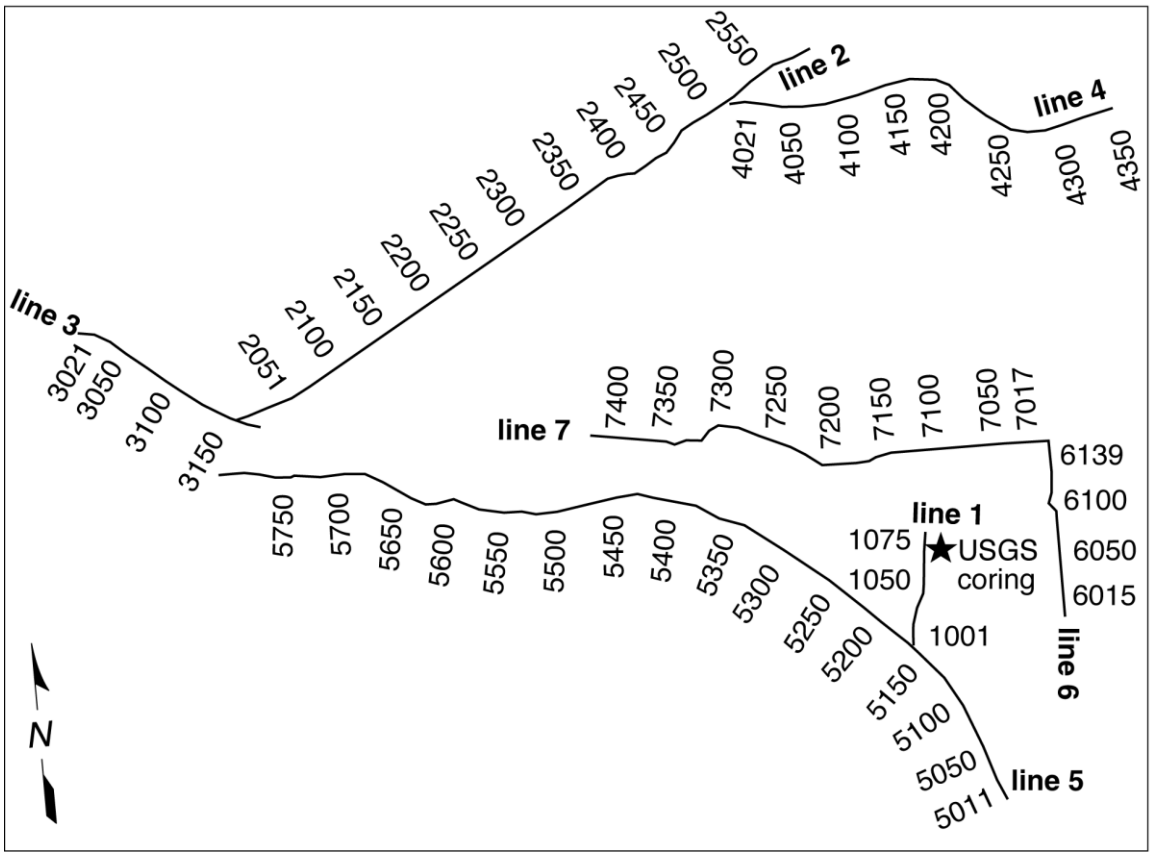

Figure 27. Site map with the seven seismic profiles located using DGPS. The 1994 USGS core-hole is located on line 1.

Coincident sign frequency and wiggle trace amplitude analysis was instrumental in delineating faults and fracture zones. The maximum displacement observed on any fault interpreted on these data is just under 10 m. Distinguishing faults that are mappable across the site from fracture zones having only localized bed distortions is an important distinction for future production tests. Diffraction patterns seem diagnostic of the larger faults with pronounced offset. The strongest diffractions are associated with where major faults intersect the basement surface with measurable and abrupt bed offset. Amplitude and frequency variations in the 400 m coal seam are related to changes in physical properties of the coal (thickness, velocity, attenuation, etc.). These data could contribute significantly to future characterization of the coal seam, including volume, gas concentrations, fracture density, and other properties that influence production estimates.

Line deployments considered subsurface coverage, proximity to other lines, and surface limitations or restrictions (Figures 27 and 28). Line and station numbers are chronologically assigned based on acquisition order and direction the source progressed down the line. Lines were sequentially acquired based on geography, clearances (runway), and snow removal.

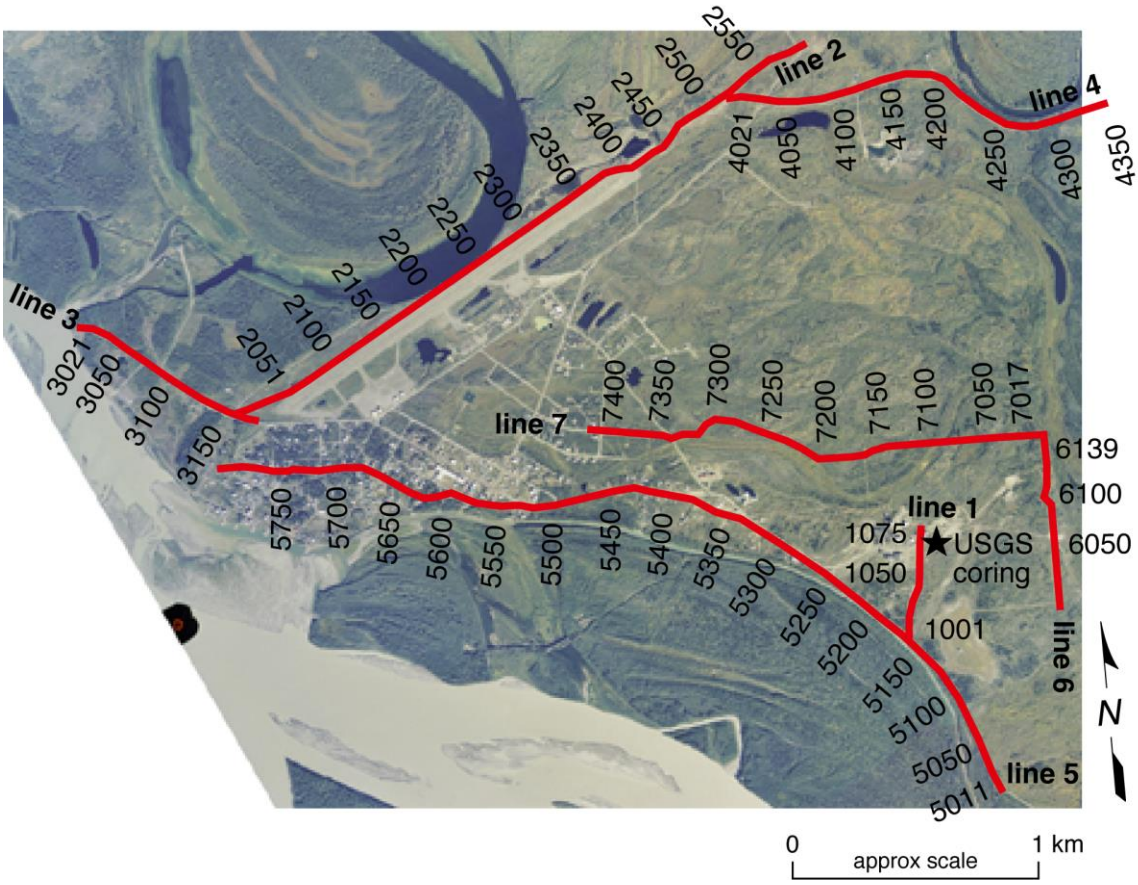

Figure 28. Site map overlain on an aerial photograph of the Fort Yukon, Alaska area. The seismic line followed established roads in town and paths used for local travel by snow machines and ATVs. Snow was partially cleared from roads and paths to improve source and receiver coupling.

Line 1

Coherent reflection events arriving from 300 to over 600 ms on line 1 are returning from an interval containing the drill-confirmed target coal seam(s) and represent the zone possessing the greatest potential for yet undiscovered coal in this area (Figure 29). Time-to-depth estimations are based on the NMO velocity, which was calculated during an iterative series of statics and velocity analysis (Table 1). Within this 300 ms interval of interest the average velocity ranges from around 1800 m/s to 2000 m/s (Appendix A). For practical purposes time-to-depth conversion can be approximated using a one-to-one relationship (e.g., 400 ms ~ 400 m). As will be obvious during discussion later in this report, this conversion equation is not exact, but it will provide quick and easy depth information sufficient to meet the objectives of this report.

Variable area wiggle trace CMP stacked sections provide a measure of reflection amplitude and frequency (Figure 29). Key to interpreting the seven stacked sections from this project was the tie between seismic station 1070 and the 1994 USGS corehole. Changes in lithology within the upper 300 m of this borehole were not sufficient to produce an acoustic impedance contrast large enough to result in a high amplitude reflection event. Acoustic impedance

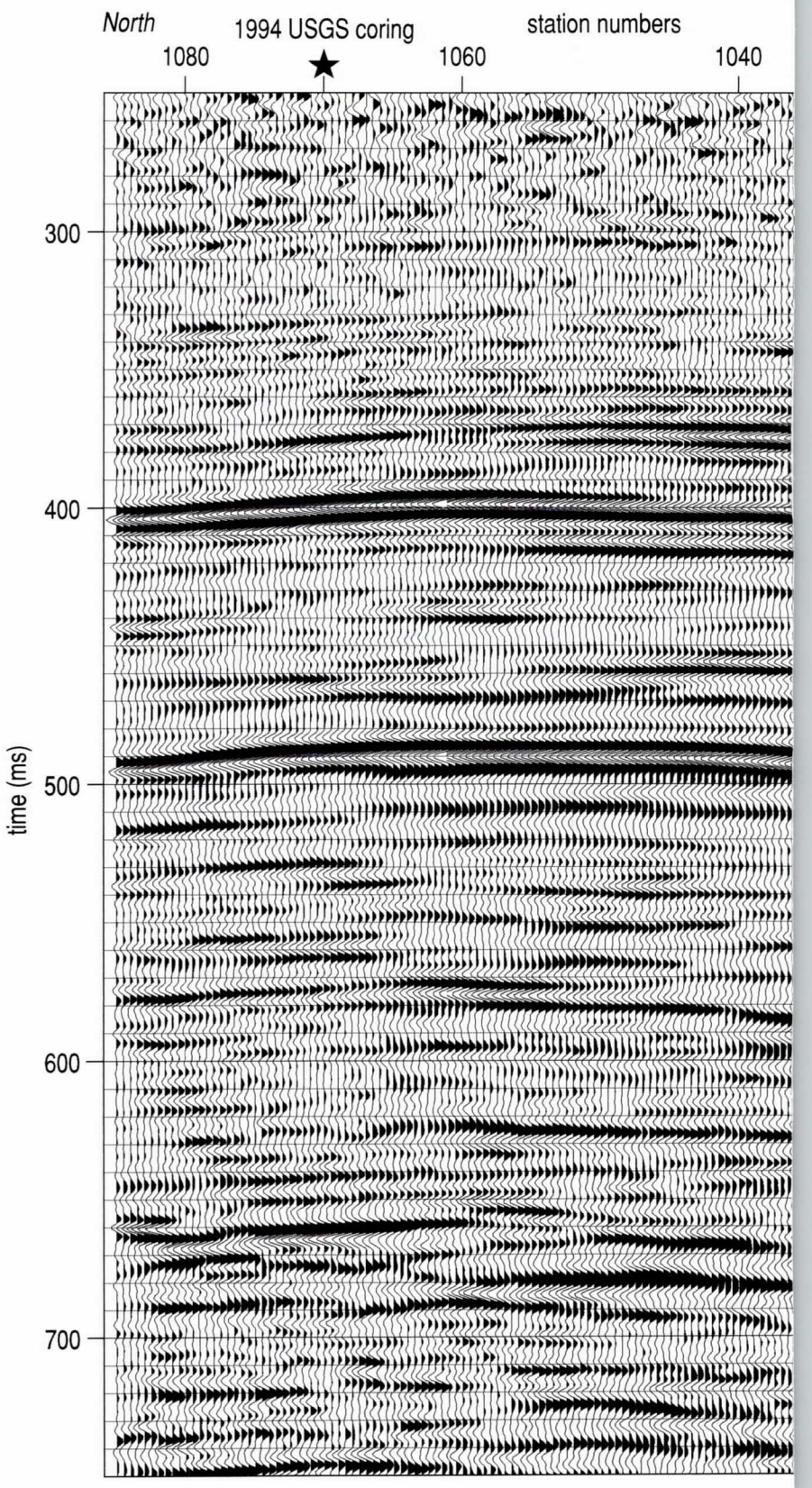

Figure 29.

29a

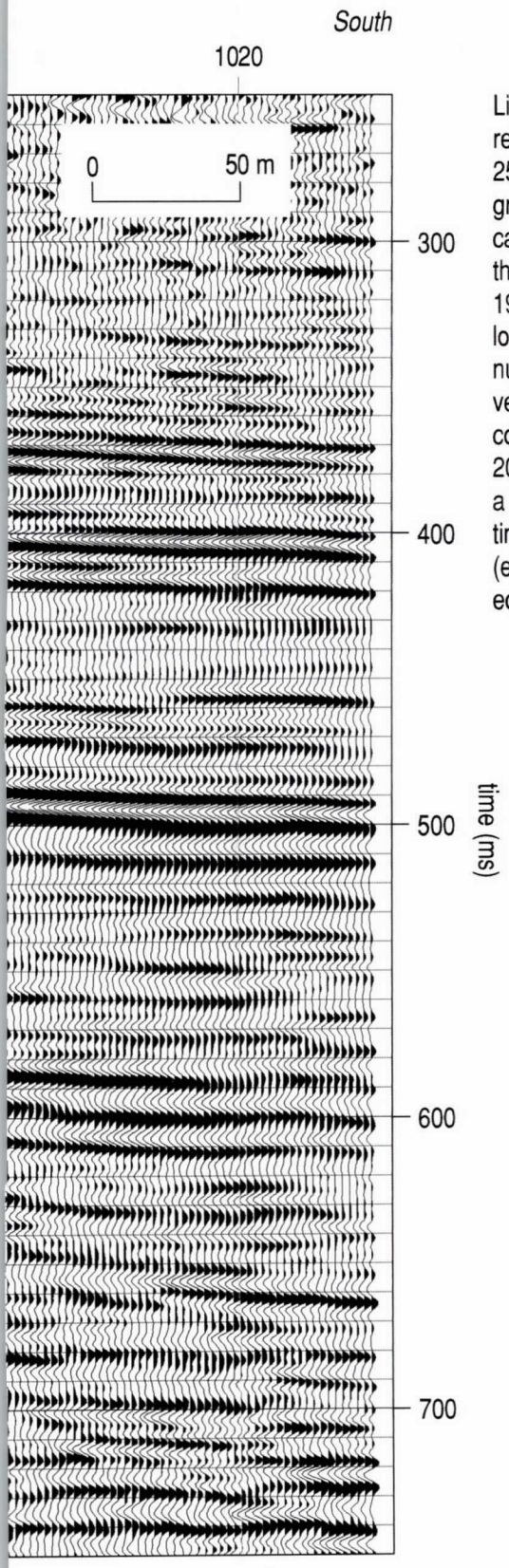

Line 1 CMP stacked seismic reflection section with upper 250 ms cropped. Several groups of coherent reflections can be interpreted across the length of this section. The 1994 USGS corehole was located at approximately station number 1070. With the average velocity to the high amplitude coherent reflections around 2000 m/s, depth estimates are a 1-to-1 correlation between time (ms) and depth (meters) (e.g., 400 msec is approximately equal to 400 m).

contrasts at contacts between silt, clay, or sand sequences in this saturated setting are little more than a few percent and produce extremely subtle reflections. Below 300 m coal seams and stringers, some less than a meter thick, were observed in core. Coincident with the depths coals were identified in the core, reflectivity increases and distinguishable reflections can be interpreted that are coherent and possess consistent wavelet characteristics across the length of the seismic profile. The contact between the 391 m coal and its overclay is responsible for the high amplitude reflection at around 390 ms. This reflection event is the anchor or "marker" that will be used to interpret seismic reflections from this area.

Interpretations in this report will focus on coherent reflection events arriving between around 300 ms and the basement, which at times is at a time depth in excess of 650 ms (Figure 29). The 391 m coal reflector arrives at around 390 ms. A reflection from around 370 ms is interpreted to be the coal seam encountered at about 365 m in the corehole. The event at about 480 ms is almost 100 m below the TD of the corehole and appears to be the highest amplitude event on most of the stacked sections. With only minimal ground truth it is extremely tempting to interpret this 480 ms reflection as another thick coal seam. Between the high amplitude event at 390 ms—identified as the target coal of this survey—and the 480 ms reflection is a series of reflections that correlate to continuous reflections on shot gathers. This group of reflections possesses wavelet characteristics consistent with drill-confirmed coal reflections above 400 m. Several of these high frequency reflections interpretable across the section between the 390 ms and 480 ms events also vary laterally in phase, amplitude, and frequency. Reflection characteristics observed within this interval, when contrasted to known coal reflections, are strongly suggestive of coal layers. It is therefore reasonable at this point to suggest repetitive coal layers may be responsible for at least some of these sitewide coherent reflection events between 350 and 500 ms. The basement reflection arrives at around 650 ms and is characterized by its lower frequency and more chaotic appearance of the reflected wavelet. This unique characteristic of the basement reflection was also noted on shot gathers. A series of events with very limited lateral extent and relatively lower amplitudes between the basement and high amplitude reflection at around 480 ms are likely returning from a lithologic sequence similar to that above 300 ms.

Since these data are zero phase, reflection peaks are selected as the center of the reflection peak (Figure 30). Polarity of reflection events is retained from recording through processing to be consistent with SEG convention (i.e., positive reflection is the zero peak of a zero phase wavelet) (Sheriff, 2002). Reflection events likely to be significant to any future CBM production analysis are interpreted on seismic sections across the site in six different colors (annotated on each figure). Only the 390 ms reflection event can be confidently tied to a reflector (391 m coal). Lateral variability in the reflection waveforms is indicative of changes in geology. For example, between stations 1050 and 1030 the 390 ms reflection undergoes a change in wavelet characteristics possibly representative of a channel, changes in lithology, or may indicate bed geometry variations (thickening or thinning) within the coal seam. As well, the event at around 375 ms beneath station 1063 appears to thicken to the south from less than a few meters to over 5 m in about 20 to 30 m. This could be the seismic image of an ancient river or lake bank, analogous to many modern settings in this area. A similar pinch-out feature below station 1050 at 470 ms might be some kind of erosional feature similar to those seen in modern lake and stream depositional setting. These are just a few examples of many small-scale geologic features that are within the resolving power of these data. Once lithology and layer properties are established

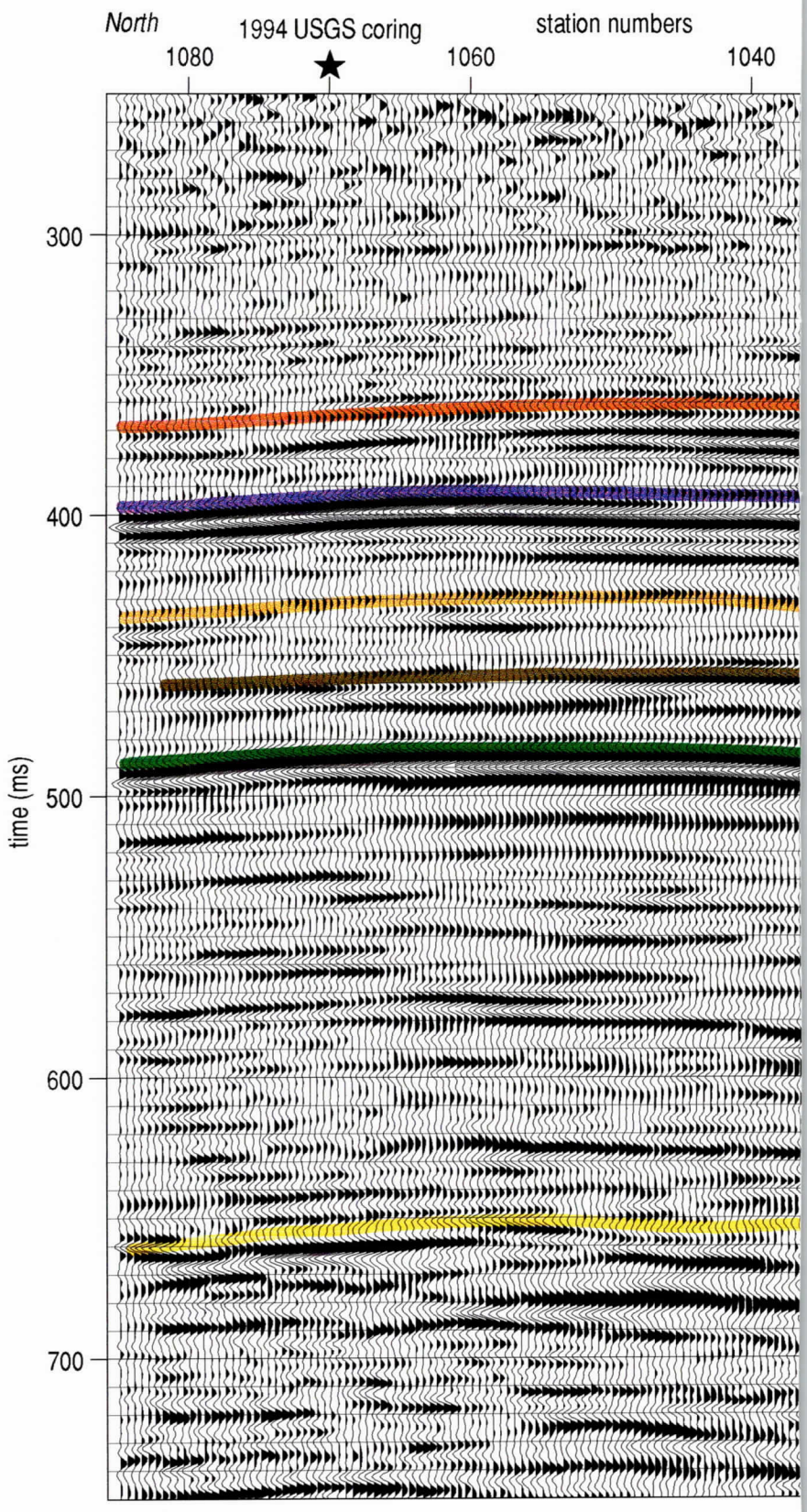

Figure 30.

30a

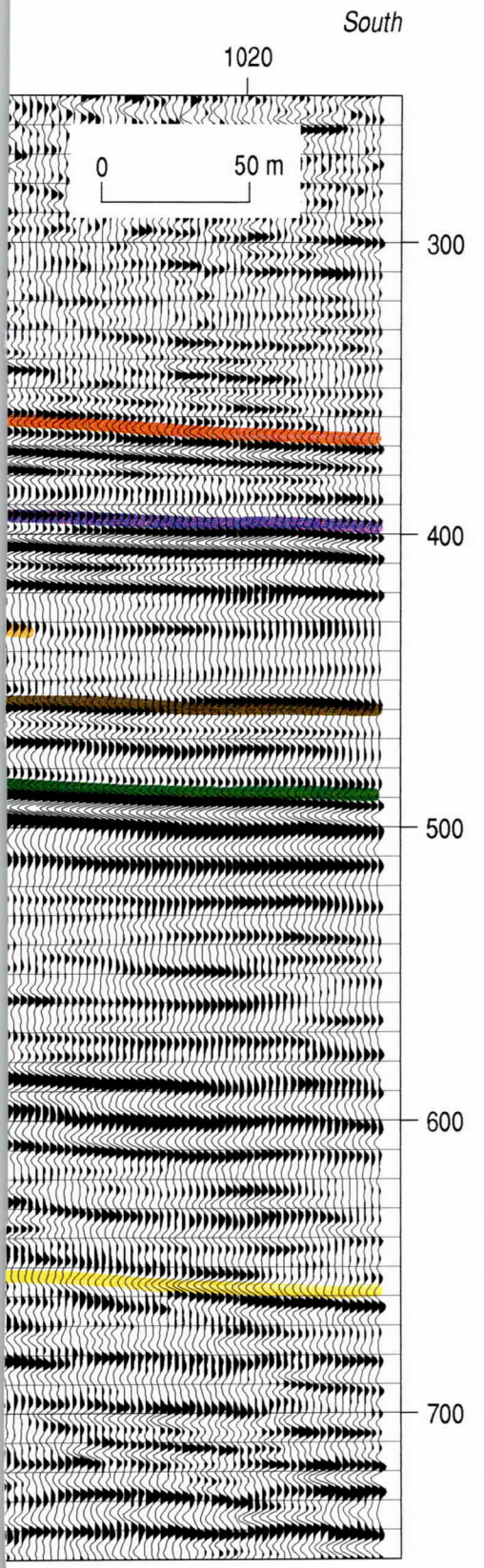

Line 1 CMP stacked seismic reflection section with upper 250 ms cropped and sitewide coherent and correlatable reflections interpreted with a sitewide consistent color sequence. The highest amplitude events are within the interval interpreted to be coal rich. Based on the only drill hole in the area, the orange event is the 365 m coal encountered in the corehole and the purple event is the 391 m coal that was penetrated about 9 m before drilling was curtailed. Several reflections with similar character are interpreted between the 391 m coal and about 500 ms, where the "coal interval" seems to either end or change its seismic character. The yellow reflection possesses a broken, less trace-to-trace coherent appearance and is at a depth consistent with the top of the Mesozoic section.

- 365 m coal seam
- interpreted 391 m coal
- possible coal interface
- possible coal interface
- possible coal interface
- bedrock

through drilling, many more details about the geology can be interpreted and the significance of those details to the CBM resource question established.

Seismic sections from this site can be divided into four unique intervals based on event coherency, amplitudes, frequency, and geometry. The first, from a seismic reflectivity perspective, is a relatively quiet zone extending from the surface down to about 280 ms (Figure 31). This zone includes the permafrost above a thick sequence of likely saturated silt, sand, gravel, and clay layers separated by lithologic boundaries with very small percent changes in acoustic impedance. Reflections that can be confidently identified within this interval are predominantly low amplitude with minimal to no sitewide coherency. This observation is consistent with reflections interpreted on shot gathers (Figures 23, 25, and 26). Reflections above 300 ms are present on shot gathers but processing focused on the lower 400 m of basin sediments.

A second packet of reflections characterized by high amplitude sitewide coherent reflections possesses overall wavelet properties consistent with the 390 ms coal reflections. The acoustic impedance contrast of the three coal seams encountered in the borehole between 300 and 400 m coals would produce the highest amplitude reflections of any contact sampled by the borehole. Consistent with this observation is the suggestion that high amplitude events below the 400 m coal are from coal seams. Considering the depositional environment and age of the sediments in this basin, the chances are good coal layers are present below the drill-confirmed 400 m coal layer.

Interpretable reflections, prevalent throughout the interval from 500 ms to the basement at 650 ms, do not possess the same wavelet characteristics as either the “coal interval” or the shallow reflection zone. The upper three unique seismic intervals will be easily separable once a detailed lithologic log can be generated that includes the entire Cenozoic section.

The diffuse nature of the basement reflection evident on the stacked section is consistent with the character of the same basement reflection on shot gathers. Energy observed below the basement reflection is the result of scatter and multiple reflections from the overlying sediments. This interval contains the large diffraction events used on other lines to map and correlate faulting.

Color instantaneous frequency plots overlaid by the variable area wiggle trace display of the seismic data allow fault and fracture characteristics to be easily distinguished from static and folding (Figure 32). No faulting or fracturing is particularly evident on line 1, but this display format was an excellent tool on the longer profiles where line separations are over 2 km.

Changes in instantaneous frequency characteristics of individual reflecting events can be indicative of changes in physical properties of that unit (Figure 32). Relative changes in frequency along a reflecting horizon can be the result of tuning effects from reflectors separated by less than a wavelength, or changes in lithology can produce marked changes in frequency characteristics. With the upper frequency color band selected at around 150 Hz, frequency plots provide an enhanced image of diffraction patterns, especially when they originate from the basement reflector. Frequency can also be used to highlight any unique reflecting horizon (Figure 34). Undulations in the coal seam suggest the thickest part of the seam is approximately where

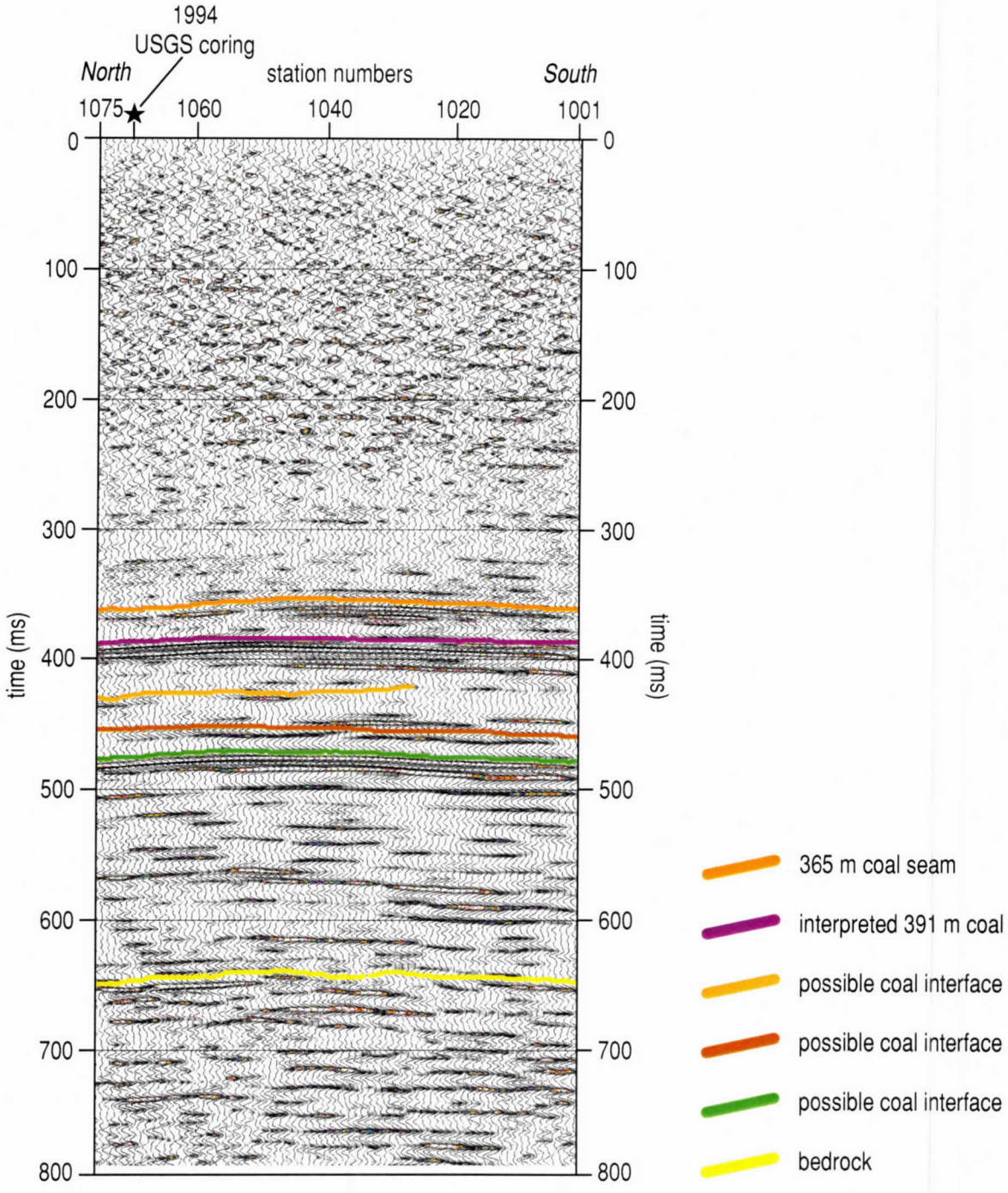

Figure 31. Line 1 CMP stacked seismic reflection section with wiggle traces overlain by color amplitude enhancement of the frequency mid-range (140 Hz to 180 Hz) and key sitewide coherent reflection events interpreted using a color scheme consistent throughout this report. The lack of coherent events within the permafrost and what is identified as the sub-permafrost is very evident on this display format. Reflections within the coal and sub-coal interval, extending from just above the 365 m coal down to the top of the Mesozoic section, which begins at about 650 m, possess excellent frequency content (useable in excess of 200 Hz in some places) and sitewide coherency. This consistency across the site is especially noteworthy considering these lignite coal reflections are within a portion of the Tertiary section that possesses a large percentage of lucustrine sediments, which are usually characterized by significant lateral variability over short distances.

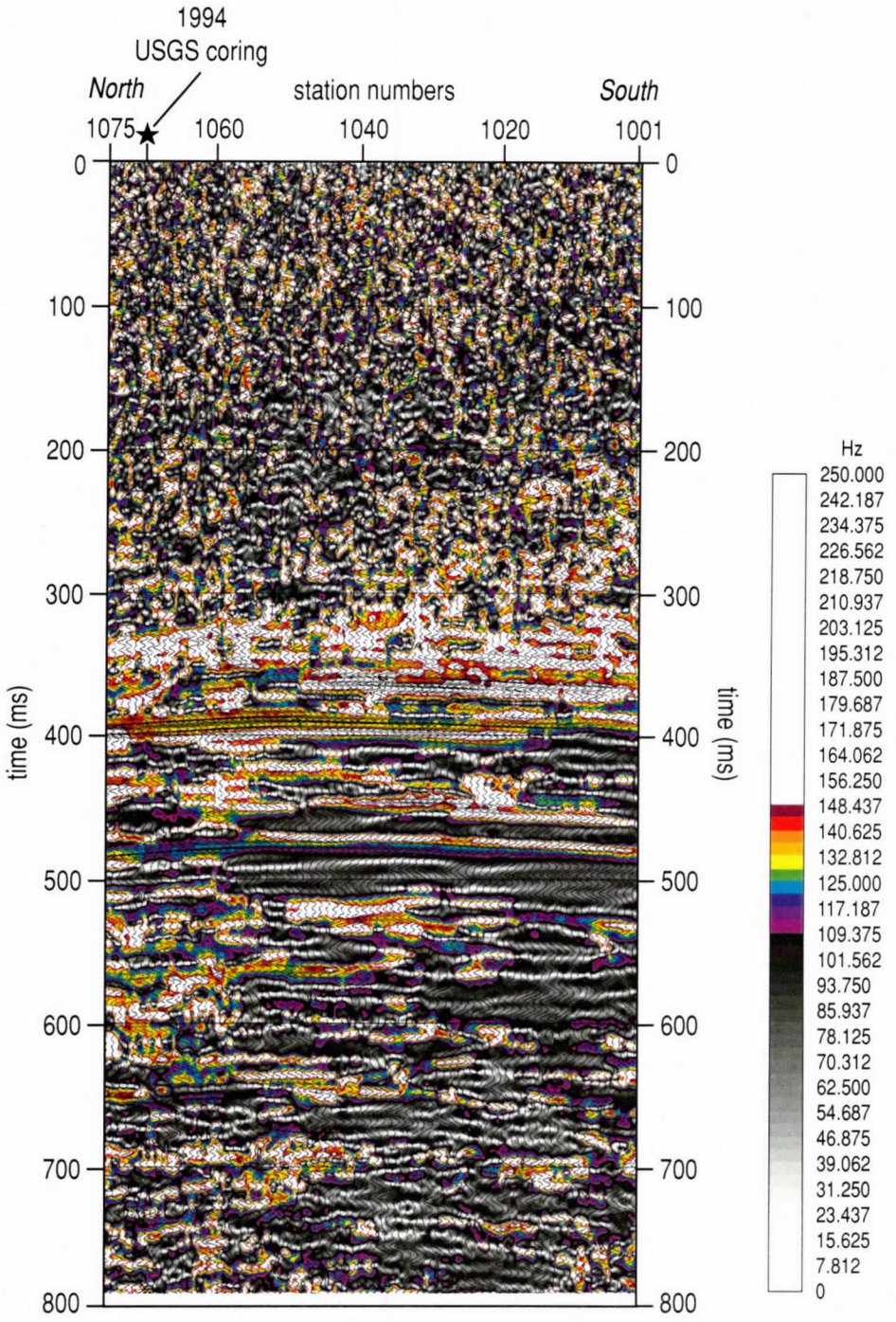

Figure 32. Line 1 CMP stacked section with instantaneous frequency overlain by wiggle trace data focusing on the frequency range between 100 Hz and 150 Hz. This frequency range seems most sensitive to bed terminations and the resulting diffracted energy interpreted to be associated with faulting. Changes in reflection character, and therefore geology, can be easily identified on frequency plots.

the corehole was drilled and the seam thins to the south. Without good ground truth it is very difficult to determine which data attribute provides the most diagnostic insight into specific physical properties and characteristics. Frequency plots seem to best emphasize diffraction patterns that are interpreted to be diagnostic of faulting in this area.

The high amplitude reflection correlated to the 391 m coal seam is used as the "type section" for in this study (Figure 33). Color amplitude plots improve the contrast and allow subtle changes in amplitude to become discernible. Without ground truth to confidently pin the base of the 391 m coal on the seismic section, the basal coal contact is interpreted from wavelet properties (i.e., frequency and amplitude). The coal seam identified at about 365 ms thickens to the south beyond about station 1050. The 390 ms coal seam and/or the clay that overlays that coal changes in thickness at around station 1040. The 480 ms coal thickens to the south. Between the two high amplitude events (390 and 480 ms) that are likely coals several stringers less than 5 m thick are present with variable changes in thickness and that change in either physical characteristics or the sediments that overlay them.

Expanding the depth and offset scales and focusing the frequency analysis into the 150 to 250 Hz range, wiggle trace overlays can be correlated with the lithology log to estimate the thickness of the 391 m deep coal layer (Figure 34). It is necessary to use waveform interference to estimate the thickness of sub-wavelength bedding. Even though the bed resolution is less than 5 m (which is the half-wavelength criteria) if the bandwidth is not sufficiently large and balanced it is possible for two reflectors separated by more than 15 m to have reflection waveforms that interfere with each other. By selecting the positive peak of the zero phase wavelet associated with the top of the coal (as matched with the borehole) and the negative peak of the zero phase wavelet representing the bottom of the coal, an estimate of coal thickness is between 10 m and 15 m. This should be considered an extremely conservative estimate considering the wavelet properties that were used to designate reflection time. If a more liberal approach is used based on wavelet interference effects, the base of the coal can be interpreted at about 410 to maybe as much as 415 m, making the coal upwards of 20 m thick (Figure 31). Without drill data to correlate these reflection arrivals to reflectors it is not possible to make definitive stratigraphic depth interpretations.

Line 2

The CMP stacked section from line 2 has several structural and stratigraphic features and characteristics that are representative and consistent with observations on stacked sections from around the site (Figure 35). Fractures, folds, and synforms have all been interpreted beneath line 2. It is difficult to find a single reflection event with uniform waveform coherence across the entire line. Breaks in coherency within groups of reflections are a consistent characteristic on other high-resolution data from this kind of unconsolidated permafrost setting. High frequency components of the signal are well preserved and seem to be most prevalent in places where layers are thin. Stacked reflection wavelets with dominant frequencies over 200 Hz are scattered throughout the "coal reflection interval." Breaks in coherency of individual reflecting events interpreted to be related to minor structural features are scattered beneath this site and intersect these seven 2-D profiles at a variety of angles.

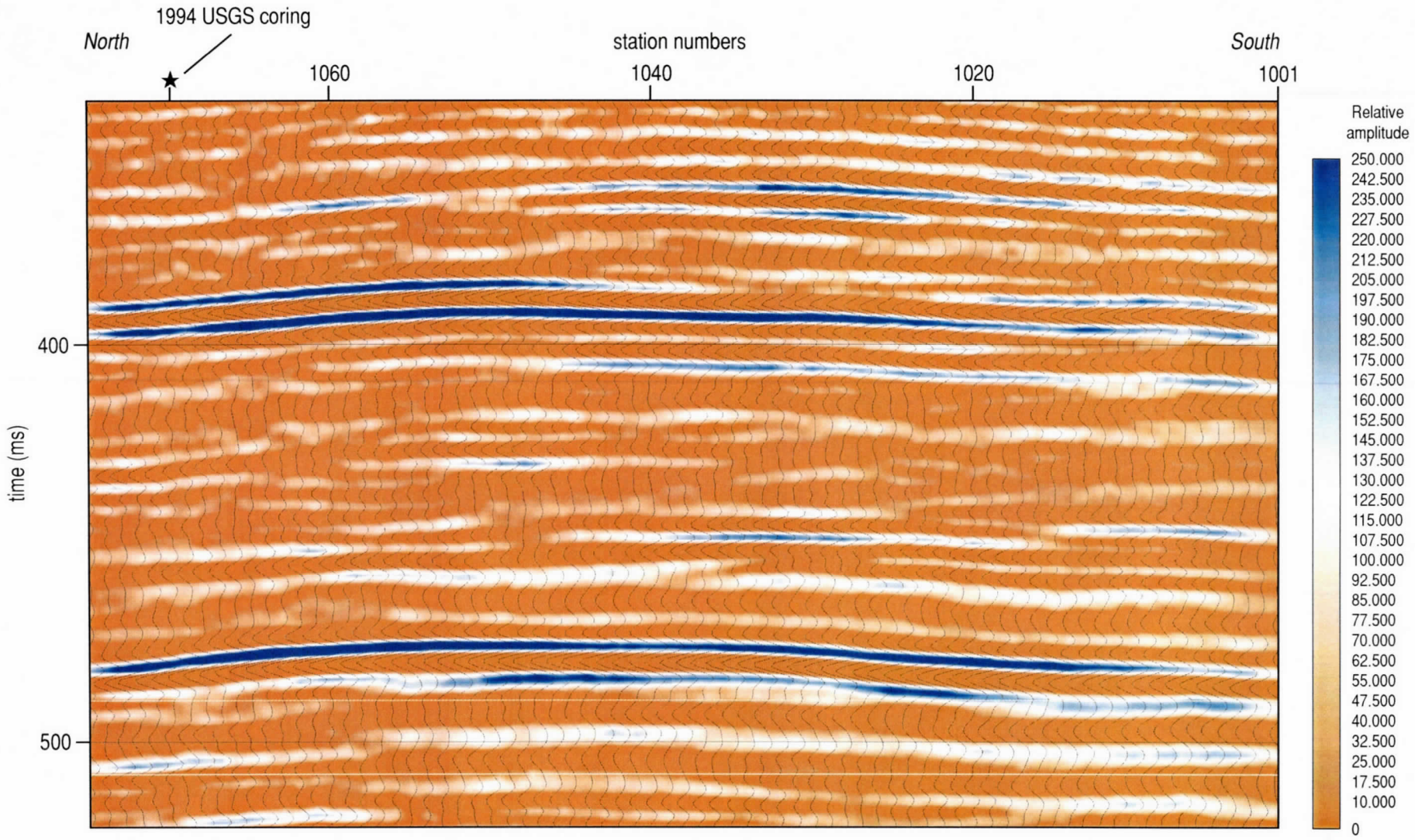

Figure 33. A zoomed-in portion of line 1 CMP stacked section focusing on the "coal interval" using color amplitude overlain by wiggle trace representation of the seismic reflection data. This display format highlights lateral amplitude variations. Once the coal interval has been completely cored and analyzed for gas content, amplitude variations (also referred to as bright spots) along a single reflecting unit might correlate to increased gas concentration indicative of increased cleating, fractures, or fault surfaces.

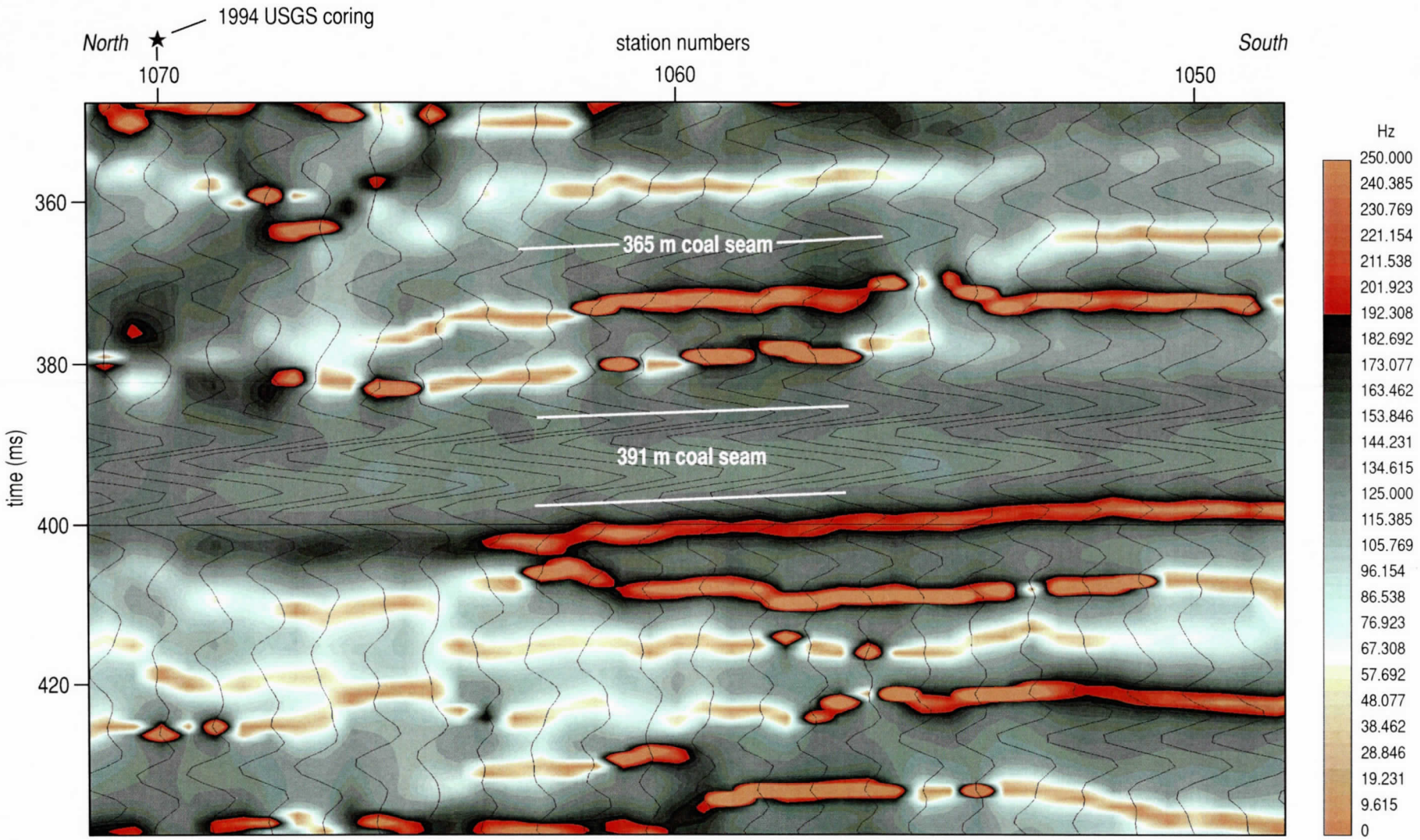

Figure 34. A zoomed-in version of line 1 CMP stacked section focusing on the "coal interval" and the cored interval between 350 and 410 m in particular. This wiggle trace over instantaneous frequency plot likely maps the top and bottom of the 391 m coal. Once drill data to 500 m or more is available, correlation of this entire suite of reflections to lithology should produce an extremely detailed stratigraphic model for the Fort Yukon area.

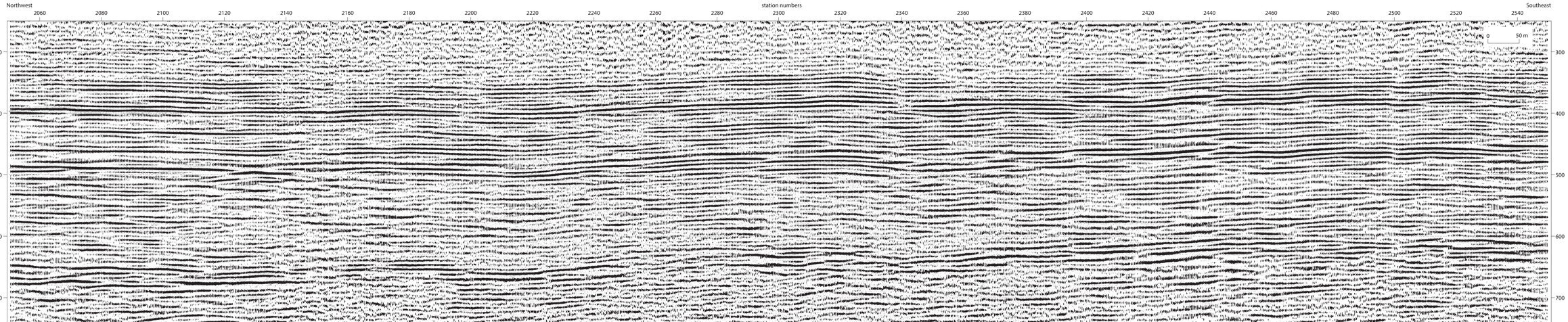

Figure 35.

Line 2 CMP stacked seismic reflection section with upper 250 ms cropped. Several groups of coherent reflections can be interpreted across the length of this section and from line to line around the site. With the average velocity to the high amplitude coherent reflections around 2000 m/s, depth estimates are a 1-to-1 correlation between time (ms) and depth (meters) (e.g., 400 ms is approximately equal to 400 m).

Minor faulting with a variety of displacements and dips are prevalent on the interpreted section (Figure 36). Diffractions can be observed where the largest faults penetrate basement. These diffraction events are much more pronounced on unmigrated sections, as expected, since a primary function of migration is to collapse diffractions. With the variety of fault orientations and displacements (both amount and relative movement), correlating individual structures from line to line requires that each characteristic of a structure be interpolated consistently. For example, the diffraction pattern at the basement intersection of the fault interpreted at station 2320 could be diagnostic of this particular fault plane and used to support correlations with other lines. In fact, this is the case and the diffraction pattern noted here on line 2 is also evident on line 7. With no true line ties between the stacked sections, matching events based on character from line to line required simultaneous interpretation of characteristics 100% consistent between lines.

Reflection, fault, and synform boundaries are color coded to be consistent between all lines. Matching reflector with reflection interpretation of the stacked sections employed time, attributes, and waveform correlation techniques. Overlaying the amplitude plots with the standard variable area wiggle traces plots improves the consistency in structural interpretations (Figure 37). The coal reflection interpreted at around 390 ms on line 1 is also present at about the same time on line 2 and is clearly a major reflection observable across the entire length of this profile. Bed offset is considered diagnostic of faulting. Matching the vertical consistency in the shape of synforms and relative location in the subsurface was the basis for determining the sitewide orientations of these structures. Interference from fractures are likely responsible for some of the drops in coherency and intermittent changes in waveform characteristics that do not necessarily extend vertically throughout the section. Fractures might also be responsible for some of the out-of-the-plane scatter that manifests itself as both coherent and non-coherent noise on stacked sections.

Localized changes in the frequency response of key reflecting horizons is probably indicative of changes in physical properties of the reflector or changes in the near-surface velocity (Figure 38). Of particular interest, frequency analysis along line 2 seems to indicate that discriminating diffraction patterns can be improved by using the lower frequency portion of the signal; this is especially evident beneath station 2350. Meaningful changes in the dominant frequency of the coal seam reflection are almost as dramatic as changes observed in the amplitude spectra. Correlating amplitude and frequency changes with specific changes in rock properties, including gas concentrations, bed thickness changes, lithologic changes, etc. should be possible once each specific attribute can be calibrated with a very directed drilling program. Rock properties, especially the lateral variability, will be instrumental in optimizing the design of methane production programs.

Reflectors imaged on line 2 have excellent lateral continuity and appear to have experienced small scale (< 10 m) faulting and folding (Figures 37 and 38). Coincident interpretation of amplitude and instantaneous frequency overlaid by wiggle trace displays allows reflection characteristics likely indicative of rock properties to be discriminated from near-surface influences. On both amplitude and instantaneous frequency sections the fault at 2350 is pronounced. On the frequency display, diffraction events and drops in dominant frequency of the seismic waveform is consistent with the fault trace. On the amplitude plot a marked drop in coherency makes this fault the most pronounced feature on the line. Several explanations exist for the

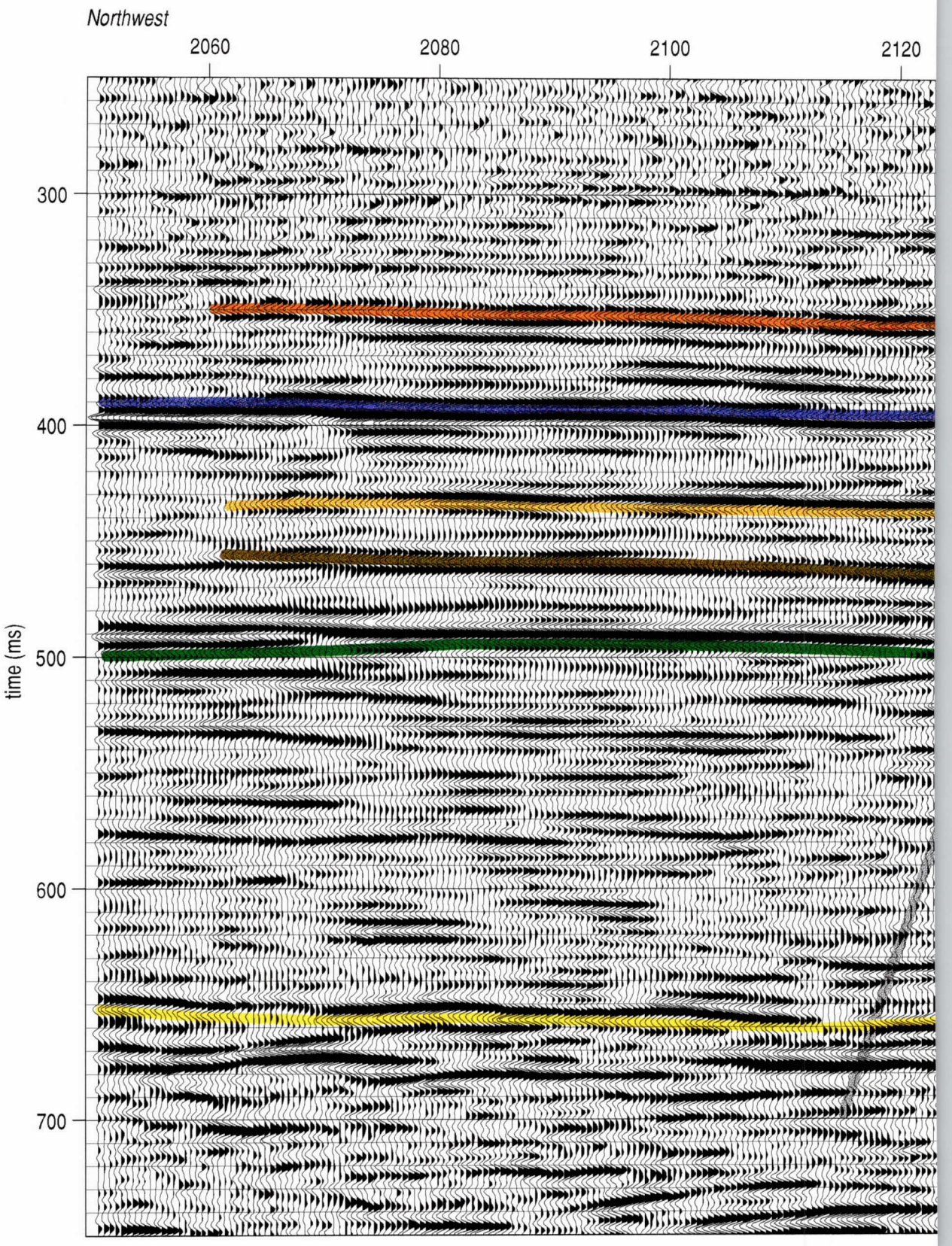

Figure 36.

36a

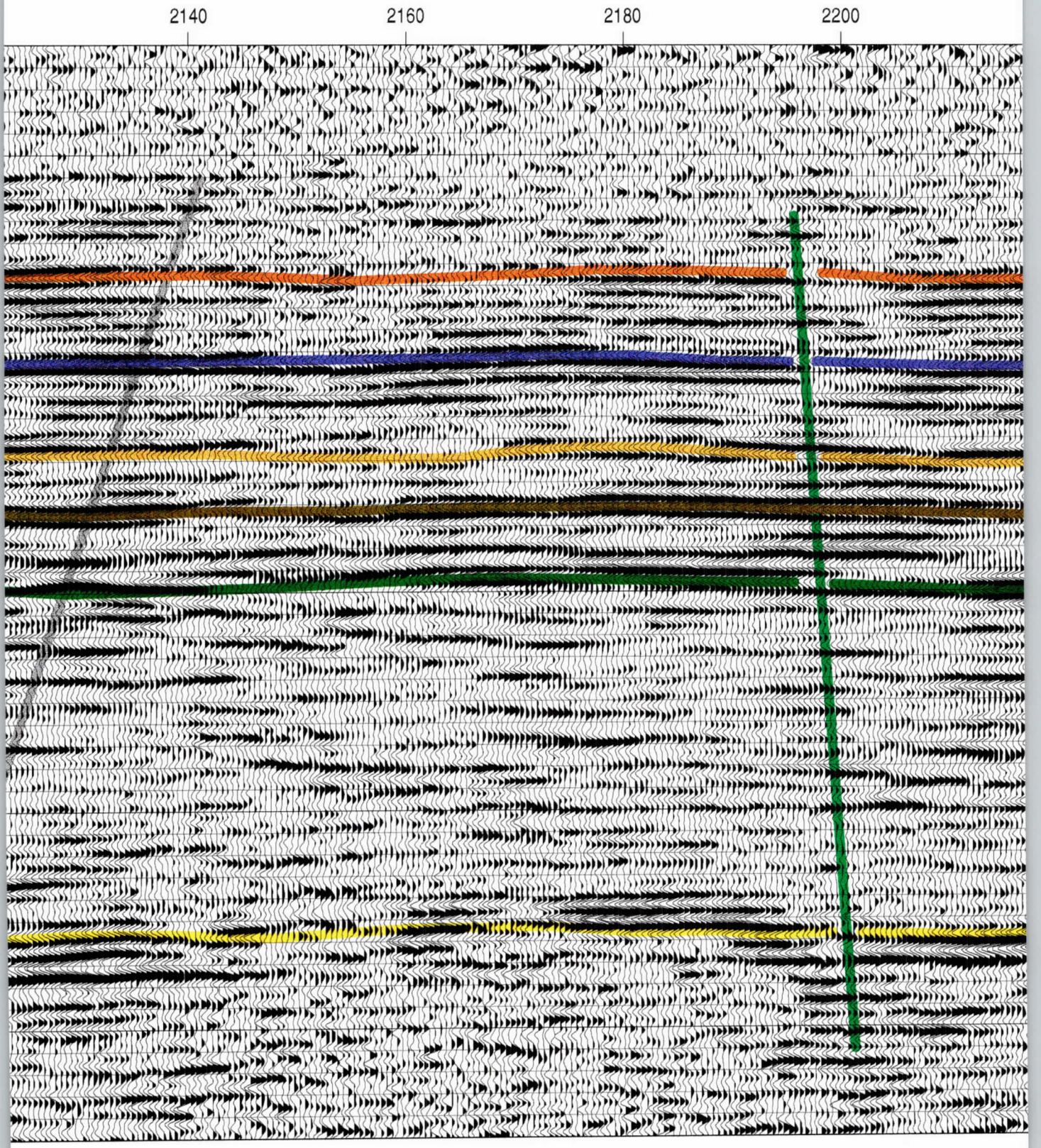

36b

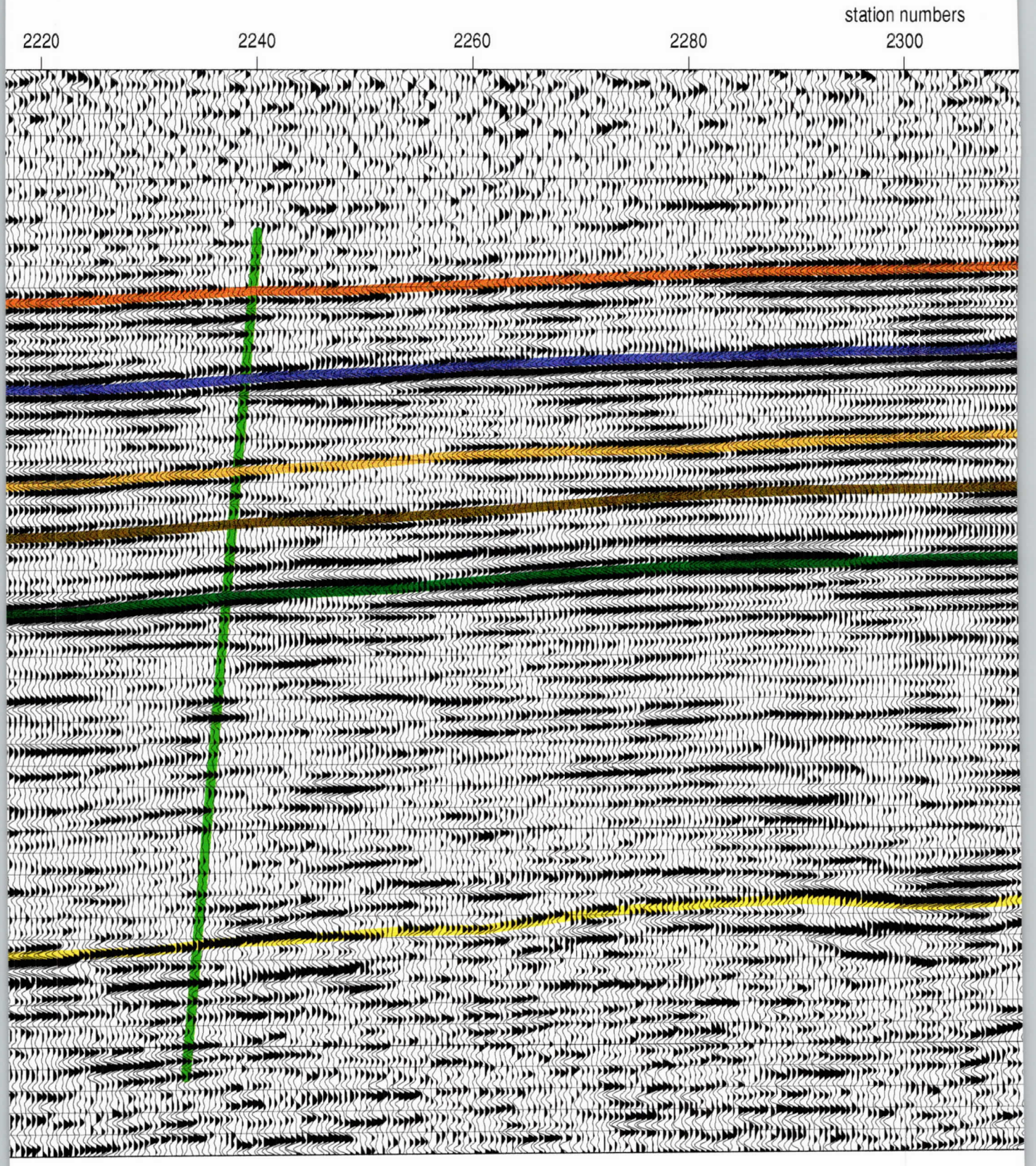

36c

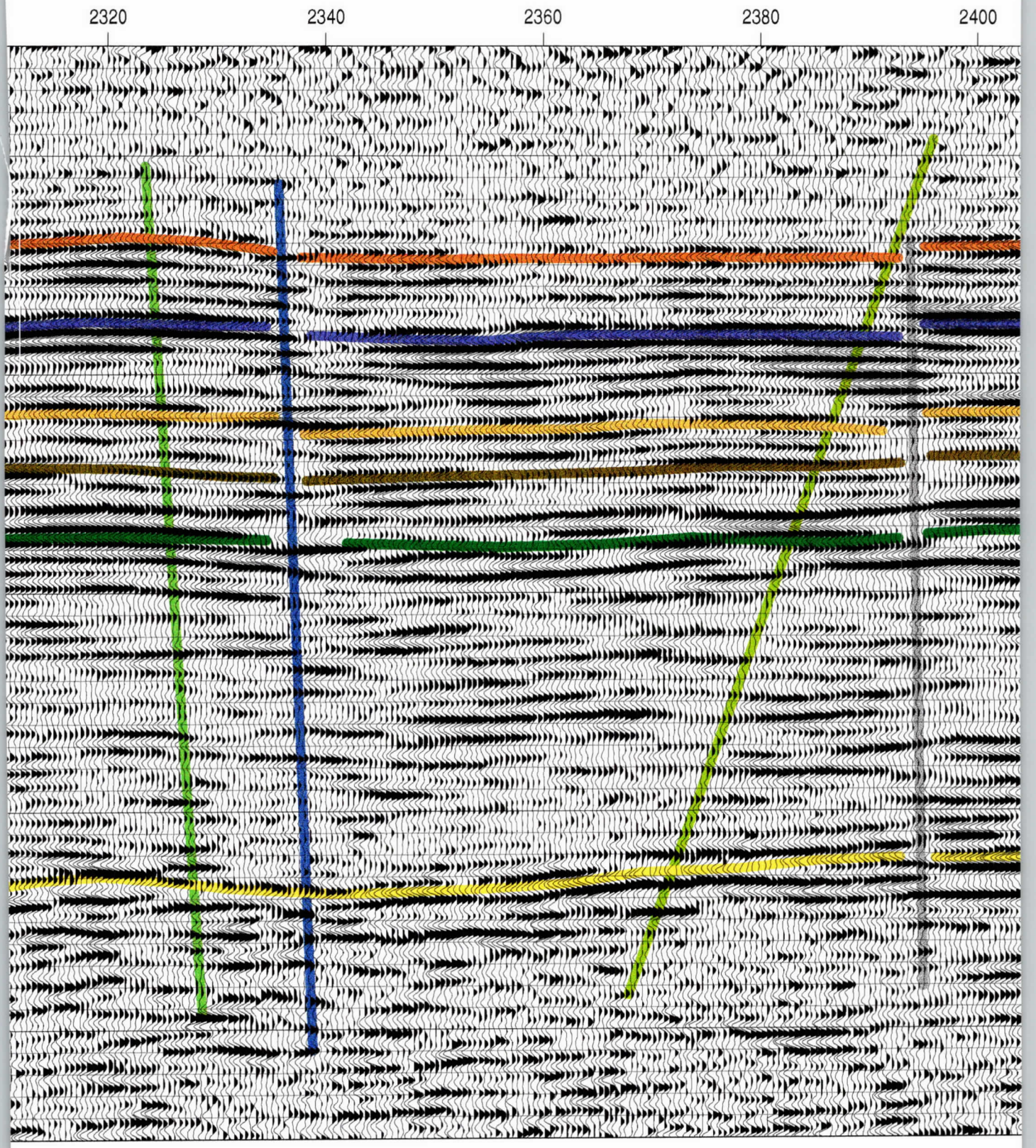

36d

36e

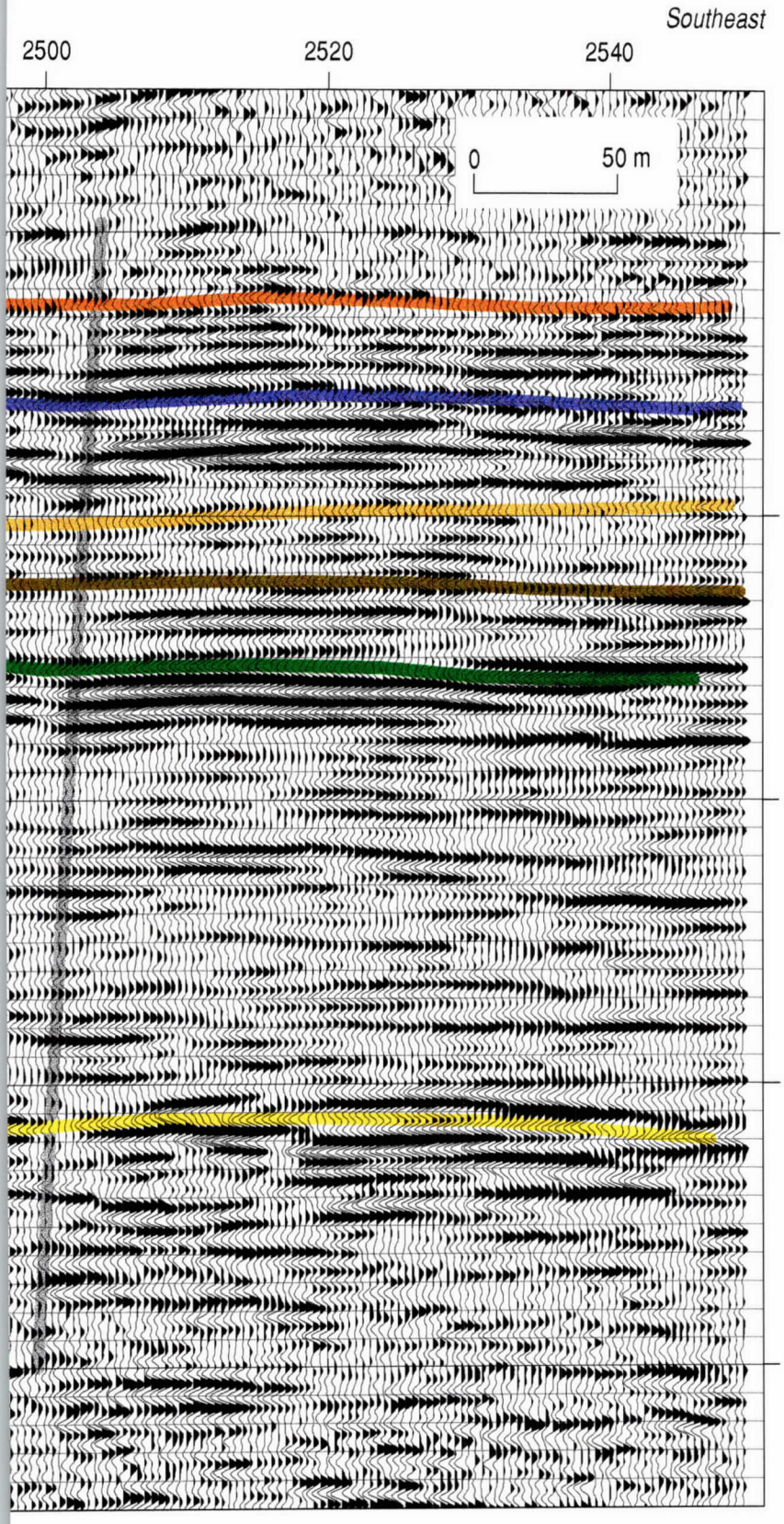

Line 2 CMP stacked seismic reflection section with upper 250 ms cropped and sitewide coherent and correlatable reflections interpreted with a sitewide consistent color sequence. The highest amplitude events are within the interval interpreted to be coal rich. Based on the only drill hole in the area, the orange event is the 365 m coal encountered in the corehole and the purple event is the 391 m coal that was penetrated about 9 m before drilling was curtailed. Several reflections with similar character are interpreted between the 391 m coal and about 500 ms where the "coal interval" seems to either end or change its seismic character. The yellow reflection possesses a broken, less trace-to-trace coherent appearance and is at a depth consistent with the top of the Mesozoic section. Fault and fold features are interpreted across the profile. Non-vertical change from reflection to reflection in ever-deepening succession was the main criteria for interpreting a vertical change in a reflection as a fault or fold and not near-surface static.

- 365 m coal seam
- interpreted 391 m coal
- possible coal interface
- possible coal interface
- possible coal interface
- bedrock

36f

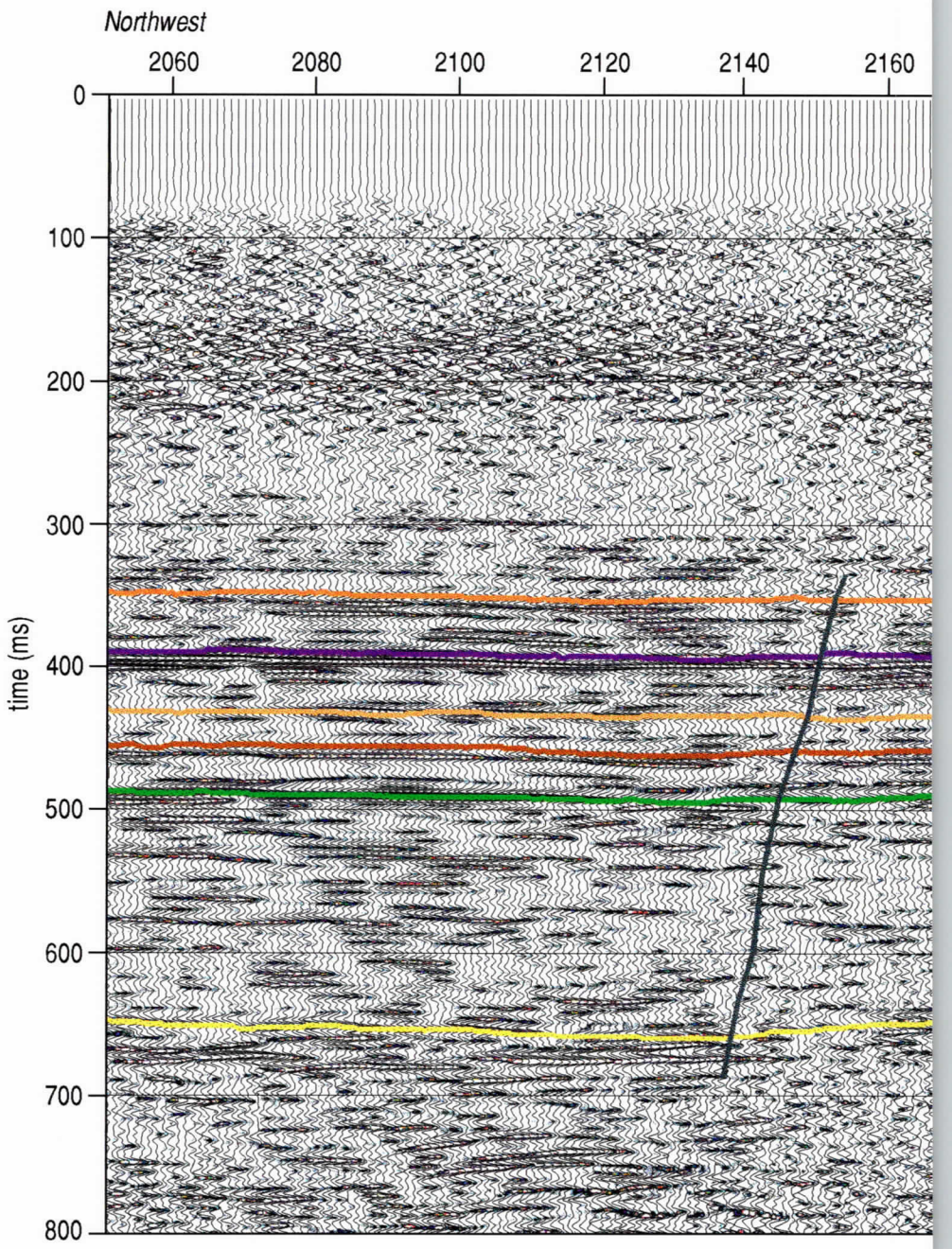

Figure 37. Line 2 CMP stacked seismic reflection section with wiggle traces overlain by color
throughout this report. The lack of coherent events within the permafrost and what is identifie
down to the top of the Mesozoic section, which begins at about 650 m, possess excellent freq
fault lines correlate from line to line. Variability in the reflection packet (about 20 to 30 ms) of

37a

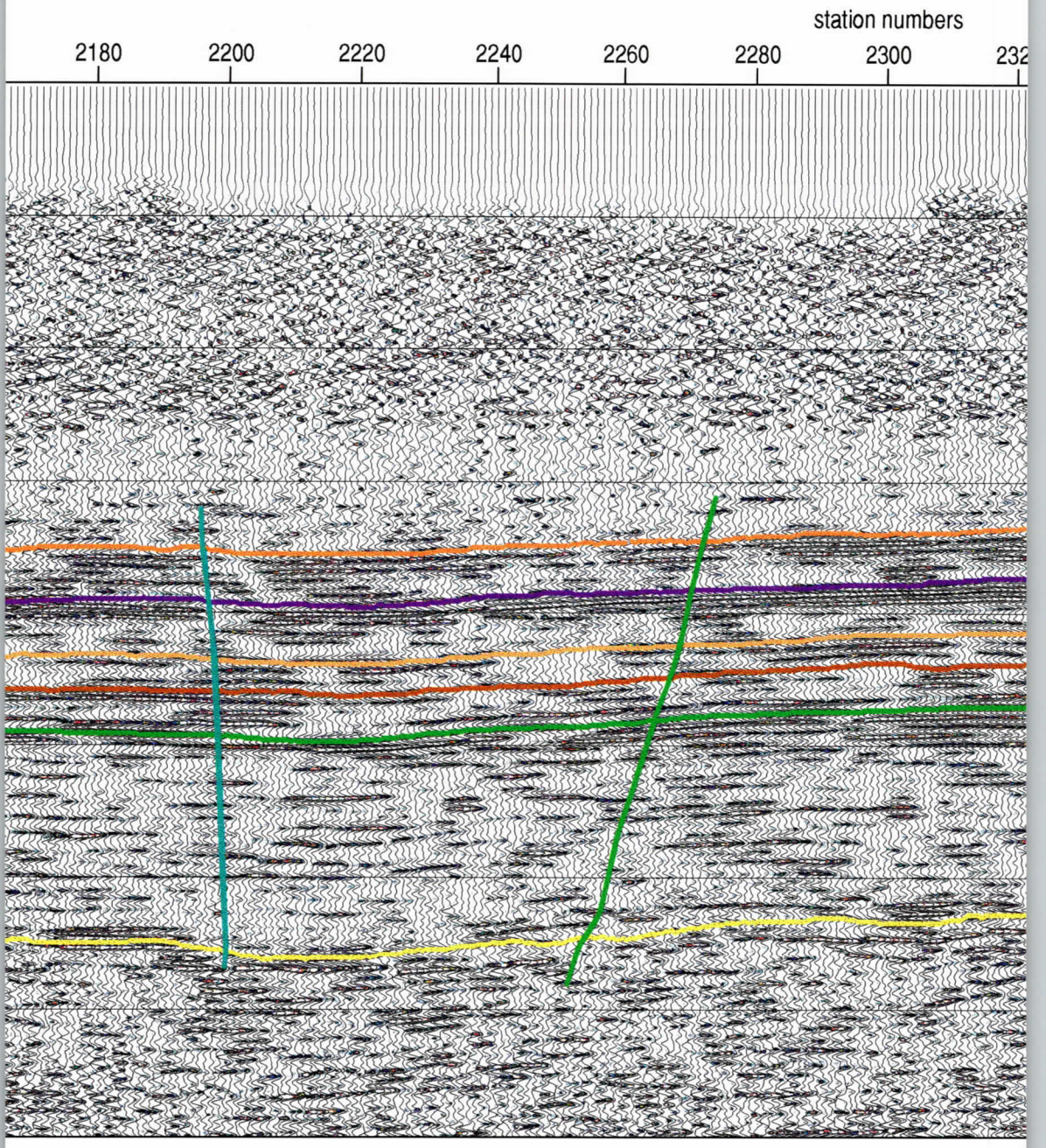

amplitude enhancement of the frequency mid-range (140 Hz to 180 Hz) and key sitewide coherent reflection e
ed as the sub-permafrost zones are very evident on this display format. Reflections within the coal and sub-co
quency content (useable in excess of 200 Hz in some places) and sitewide coherency. Faulting is interpreted i
the 391 m coal is likely indicative of changing thickness or changes in the physical characteristics of the coal a

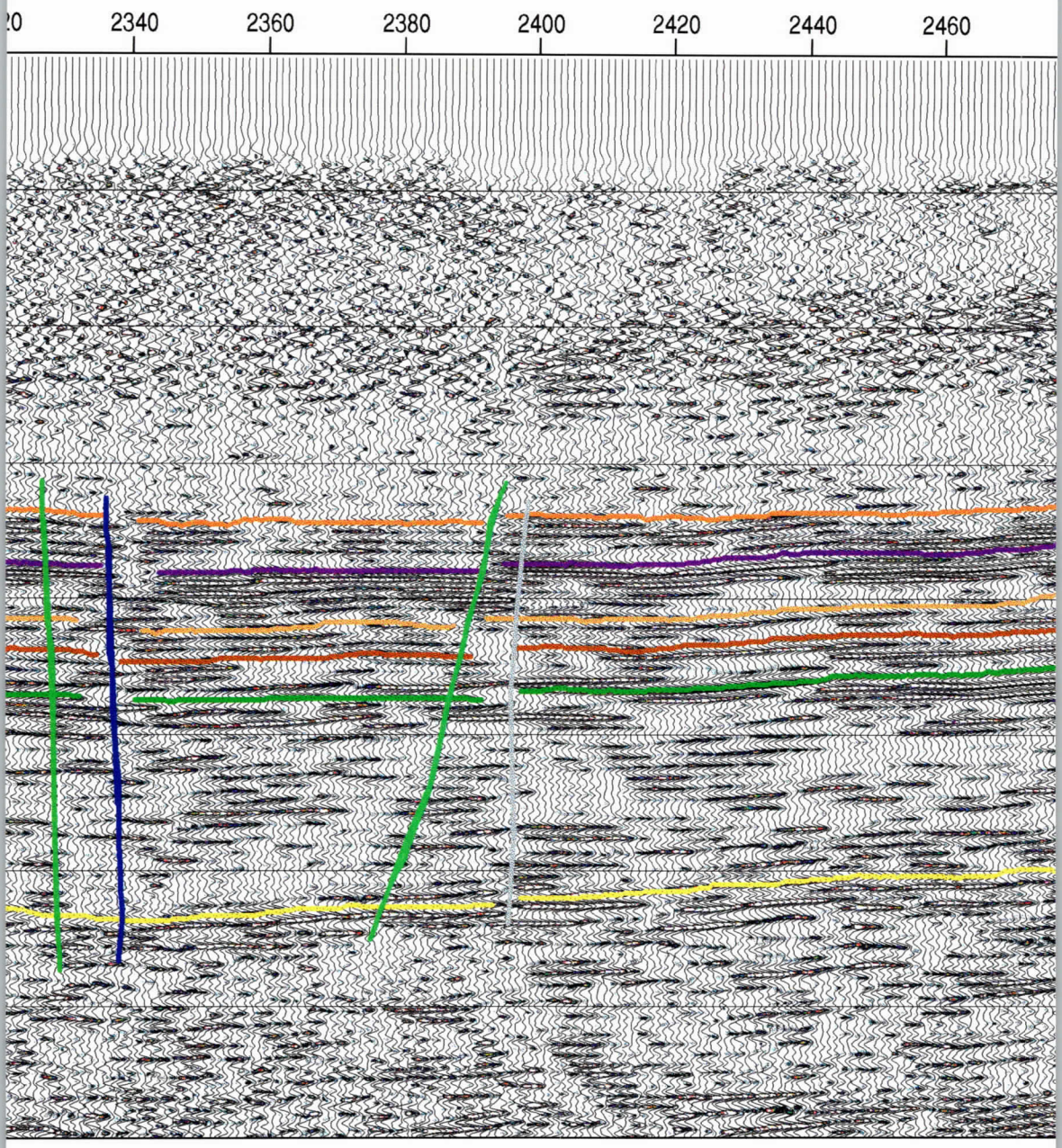

events interpreted using the color scheme consistent
al interval, extending from just above the 365 m coal
in several places along this profile. The color of the
and surrounding layers.

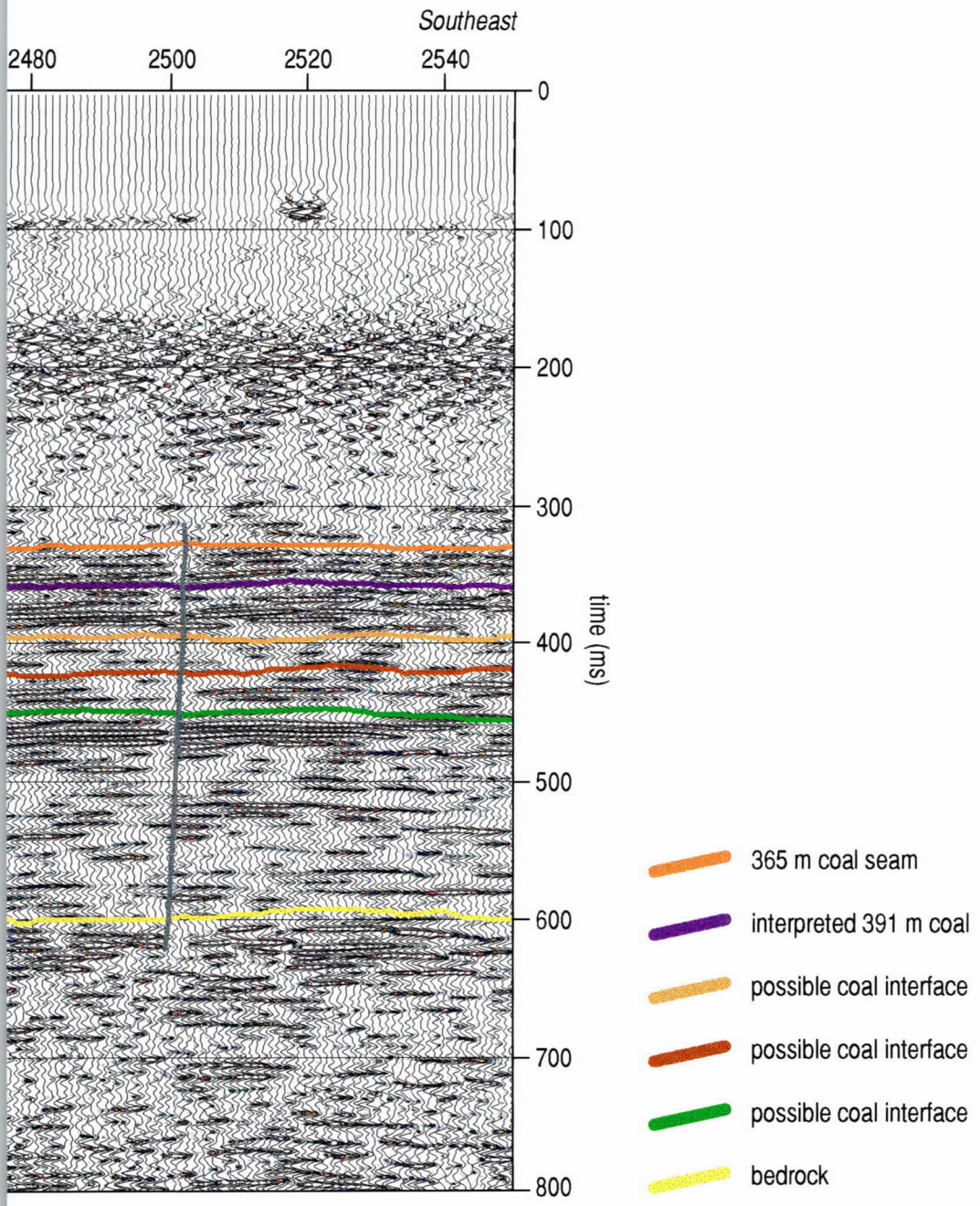
Southeast
2480
2500
2520
2540
0
100
200
300
400
500
600
700
800
time (ms)
365 m coal seam
interpreted 391 m coal
possible coal interface
possible coal interface
possible coal interface
bedrock

37d

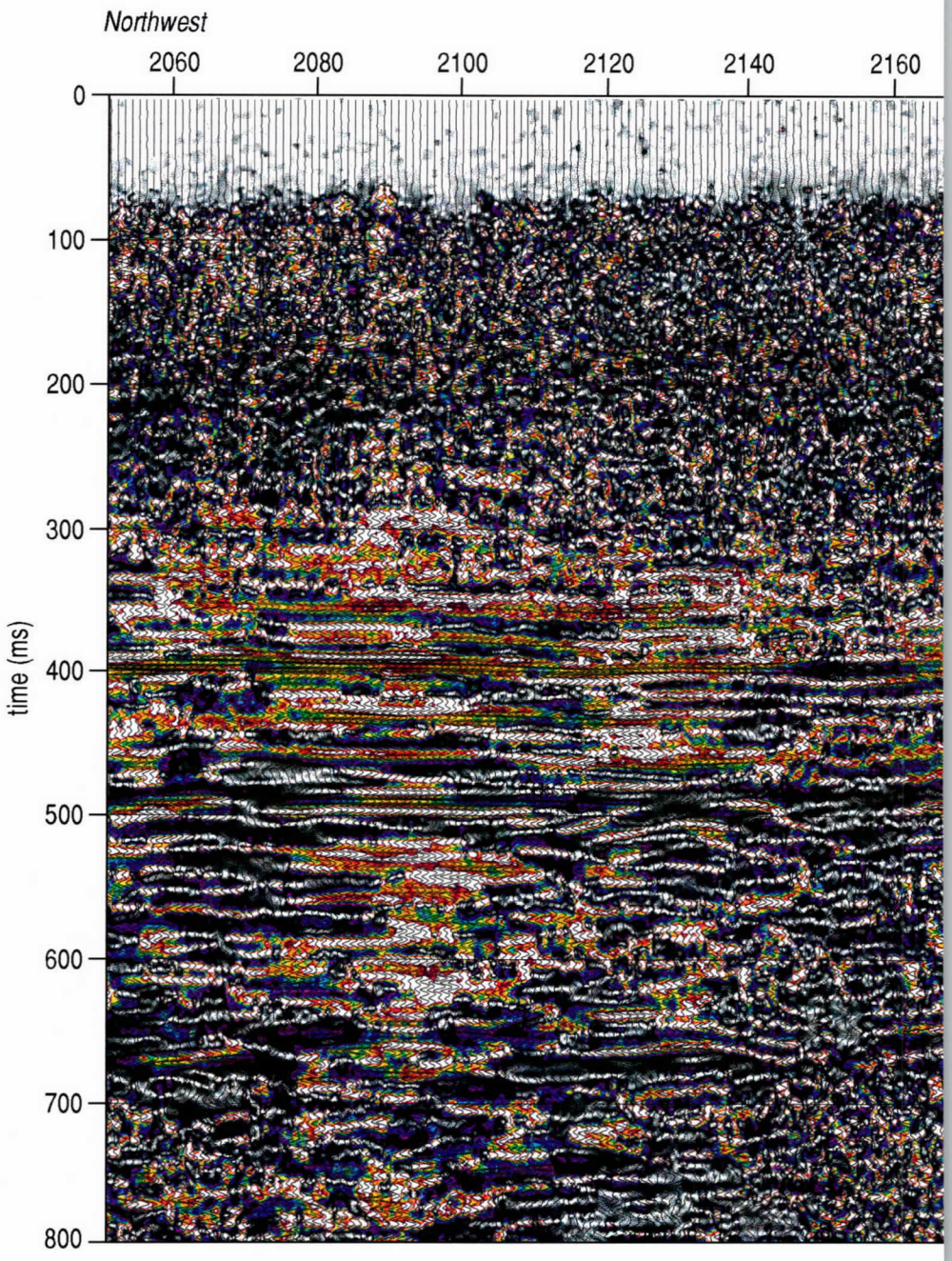

Figure 38. Line 2 CMP stacked section with instantaneous frequency overlain by wiggle trace
diffracted energy interpreted to be associated with faulting. Changes in reflection character, a
stations 2140, 2220, 2340, and 2380.

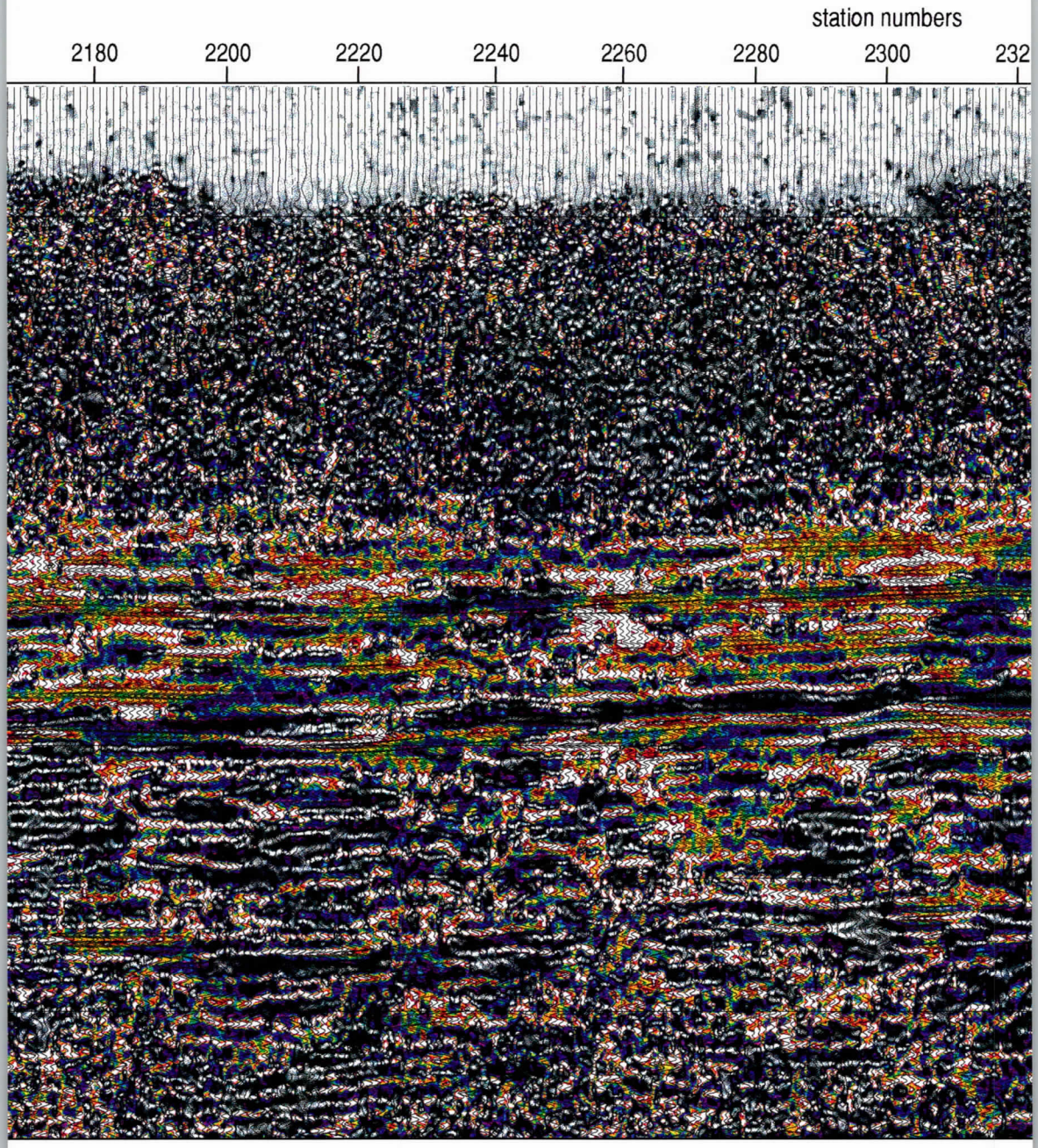

data focusing on the frequency range between 100 Hz and 150 Hz. This frequency range seems most sensiti
nd therefore geology, can be easily identified on frequency plots. The most dominant scatter patterns likely as

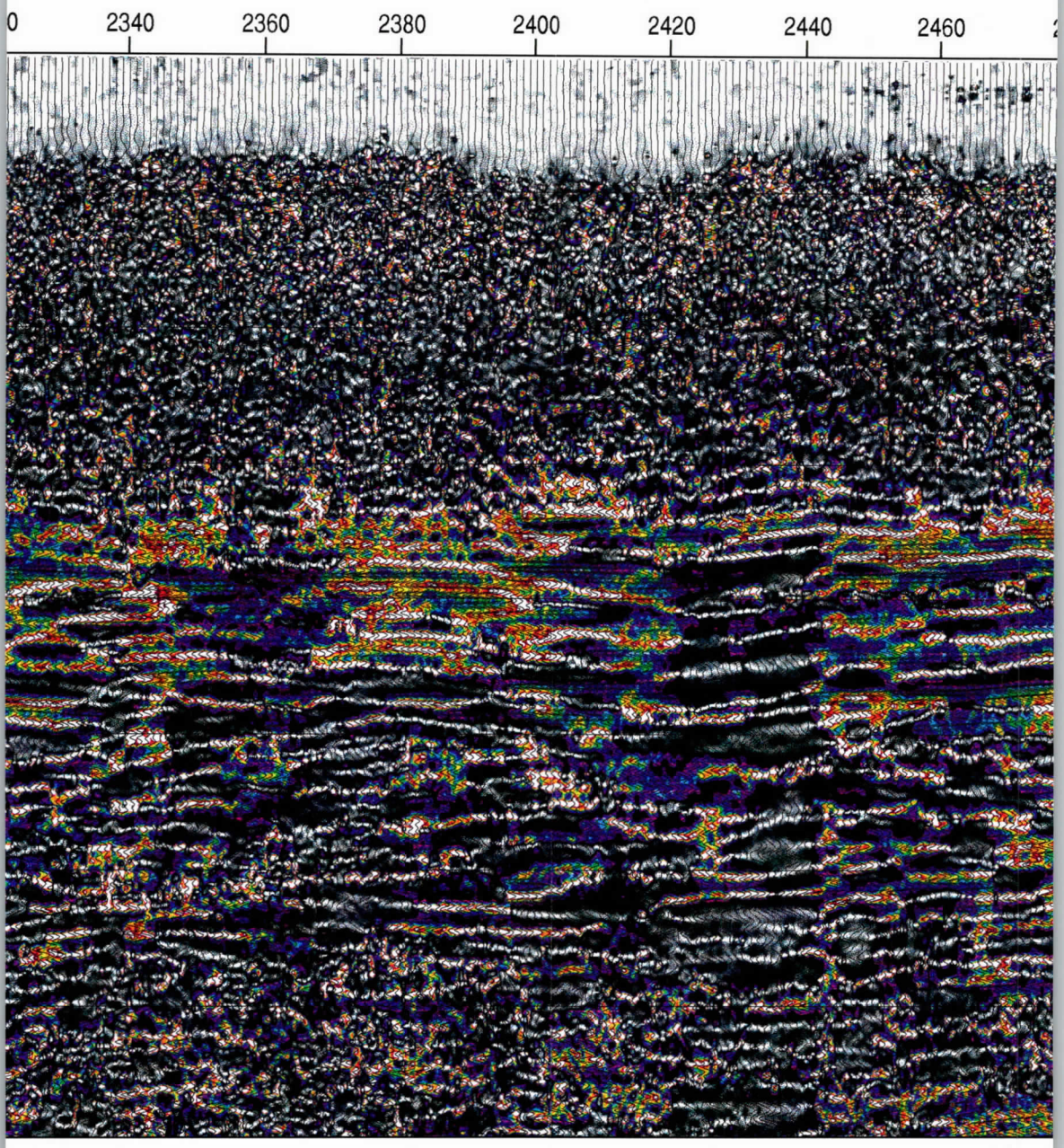

ive to bed terminations and the resulting
sociated with faulting are evident beneath

38c

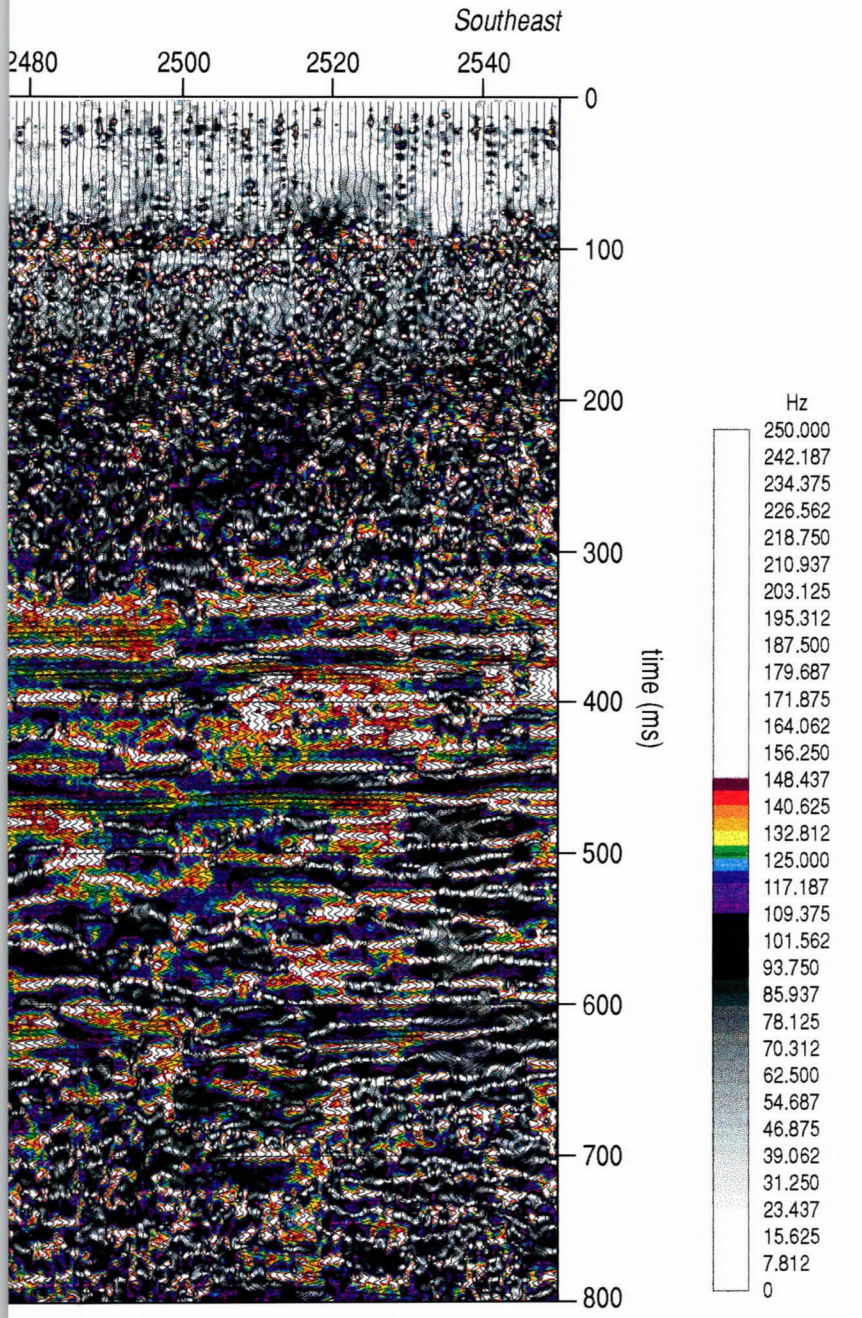
Southeast
2480
2500
2520
2540
0
100
200
300
400
500
600
700
800
time (ms)
Hz
250.000
242.187
234.375
226.562
218.750
210.937
203.125
195.312
187.500
179.687
171.875
164.062
156.250
148.437
140.625
132.812
125.000
117.187
109.375
101.562
93.750
85.937
78.125
70.312
62.500
54.687
46.875
39.062
31.250
23.437
15.625
7.812
0

38d

characteristics in the frequency domain. One is that these changes in frequency are related to gas concentrations or fractures, and therefore permeability. The diffractions are representative of point source re-radiation and are generally considered diagnostic of faulting. The dramatic drop in coherency on the frequency plots is also consistent with a fault zone. If we interpret the drop in coherency as a fault zone, using the calculated horizontal resolution, it is reasonable to suggest the fractured zone associated with this fault could be up to 50 m wide.

Distinctive attenuation characteristics on frequency spectra below the 391 m coal reflection near several interpreted structures could be related to changes in physical properties. Obvious drops in frequency content at diffraction apex and reduced reflection amplitudes below the 391 m coal reflection are consistent with the attenuation effects generally associated with changes in material properties, such as increasing percent gas or presence of fractures. On the opposite extreme from an amplitude perspective is an area beneath station 2425 where high frequencies experienced significant attenuation (Figure 38), but where little change is evident in the amplitude characteristics (Figure 37). Interesting are the two small monoclines in this area with contradictory attribute characteristics. The pronounced low frequency signature at station 2425 begins just below the 350 ms coal layer and is replicated between stations 2425 and 2445 throughout the lower portion of the section. With no apparent ties to a major structural feature or to changes in surface topography, this drop in frequency is likely related to a lateral change in material properties below the first coal layer. Identifying material characteristics or, more importantly, identifying changes in material characteristics using seismic attributes is possible here if specific measurable material properties that affect the seismic signal could be uniquely catalogued.

Amplitude analysis provides strong evidence supporting a higher percentage of coal in the northern portion of the survey area beneath line 2 (Figure 39) than on the southern side beneath line 1 (Figure 33). Using the same criteria on line 2 as on line 1, high amplitude events within the coal interval are classified as probable coal seams. Based on wavelet analysis, the 391 m coal appears to be the thickest of any in this interval. It is possible, yet unlikely, that this high amplitude event could be from interbedding within a large coal seam with its top and bottom defined by the 390 and 480 ms reflections, respectively. There is no drill evidence to support this thick coal scenario; there is strong evidence to support a cyclic coal setting as encountered between 350 and 400 m in the corehole. High amplitude events within this 150 m reflection interval (between 350 and 500 m) are likely indicative of coal layers.

Using changes in seismic attributes that appear characteristic of various structures and anomalies it is possible to correlate structures from line to line with some degree of confidence. Fault displacement and relative motion combined with diffraction patterns and fault inclinations were matched for faults interpreted between lines. Fold and/or graben/horst structures were correlated between lines using horizon topography and character, with the edges of the features defined by the bounding structures. In this fashion the small-scale structures interpreted on the 2-D profiles can be correlated into pseudo 3-D representations.

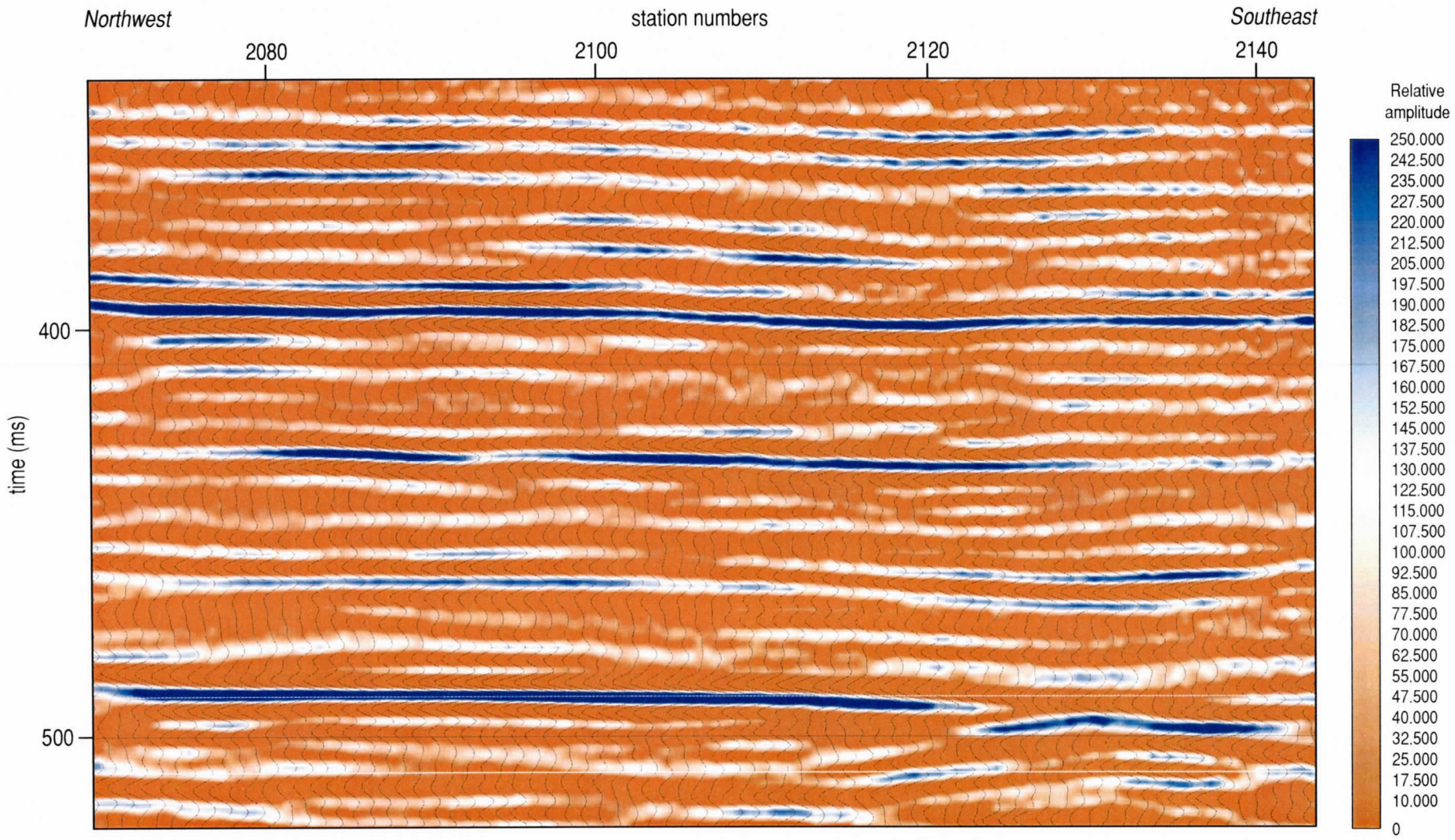

Figure 39. A zoomed-in portion of line 2 CMP stacked section focusing on the "coal interval" using color amplitude overlain by wiggle trace representation of the seismic reflection data. This display format highlights lateral amplitude variations. Several layers appear consistent across the length of this segment of the line with noteworthy variations in amplitude of the interpreted coal reflections. The apparent double that represents the 391 m coal seam loses significant amplitude of the first part of the wavelet between stations 2110 and 2135. This drop in amplitude is likely related to a thinning of the coal seam.

Line 3

Reflections on line 3 are of superior quality in comparison to the other six lines when considering the bandwidth and dominant frequency (Figure 40). Reflections from about 350 ms down to just over 480 ms define what is identified on this section and in this report as the "coal interval." An obvious lateral transition occurs near the center of this profile. This change appears to divide equivalent reflections possessing similar arrival sequences but slightly different wavelet characteristics. There are two likely scenarios that could explain this: deposition or faulting. Reflections from within the "coal interval" are higher amplitude than those observed within the same interval on line 1, but appear to have seismic characteristics consistent with the equivalent sequence near the west end of line 5 and the southwest end of line 2.

This transition zone near the center of the profile is somewhat unique to line 3. No other profile has such diversity in arrivals across a single small segment of the profile. One explanation is that this transition defines some kind of a depositional boundary that was active through a significant portion of Cenozoic sediment deposition. This does not seem likely considering the nature of shorelines to change and streams to meander over such a long period of time. A second explanation is faulting. With no obvious bed offset, two fault scenarios seem possible: one, a fault with predominantly strike/slip movement (this would explain the consistent reflection intervals but slightly different reflection wavelet characteristic on opposite sides of this section), and two, the 2-D seismic profile intersected a fault with vertical displacement at an oblique angle therefore spreading the fault zone out across a significant portion of the line 3 image. Considering the horizontal resolution of these data, the fault plane, if it exists, can be isolated to a 50 m wide zone centered on about station 3095. This transition zone (stations 3085 to 3110) appears wider on the seismic data than it actually is.

Reflection events are interpreted across the transition zone, demonstrating the consistency in reflection arrival sequences (bed patterns) across and on each side of the zone (Figure 41). Subtle channel-looking features that appear to truncate at the edges of this zone could be the result of wavelet interference. The blue channel feature at around 360 ms, interpreted on both sides of the zone, resembles a modern cut-and-fill feature indicative of high energy stream meanders. Throughout these data, broad channels can be interpreted within the "coal interval." The basement, indicated by the yellow band, clearly divides two uniquely different geologies. Directly above the basement reflection is a sequence of reflecting events with limited continuity and relatively low amplitude. This sequence of reflections resembles the shallowest interval (0-300 m) and is interpreted to be from geologic units consistent with those drilled through in the upper 300 m at this site. Below the basement reflection are clusters of reflection multiples from within the sedimentary section above.

The unique differences in reflection characteristics of the four different intervals between the ground surface and base of the Cenozoic are evident when color amplitude is overlain by the wiggle trace displays (Figure 42). Scattered low amplitude and minimally coherent reflections are present above about 300 ms. The "coal interval," loosely defined between about 350 ms and 500 ms, is characterized by its abundant high amplitude reflections with strong coherency across the entire section. A third interval above bedrock but below the coal interval contains a lower density of discontinuous reflecting events with lower amplitudes than present within the coal

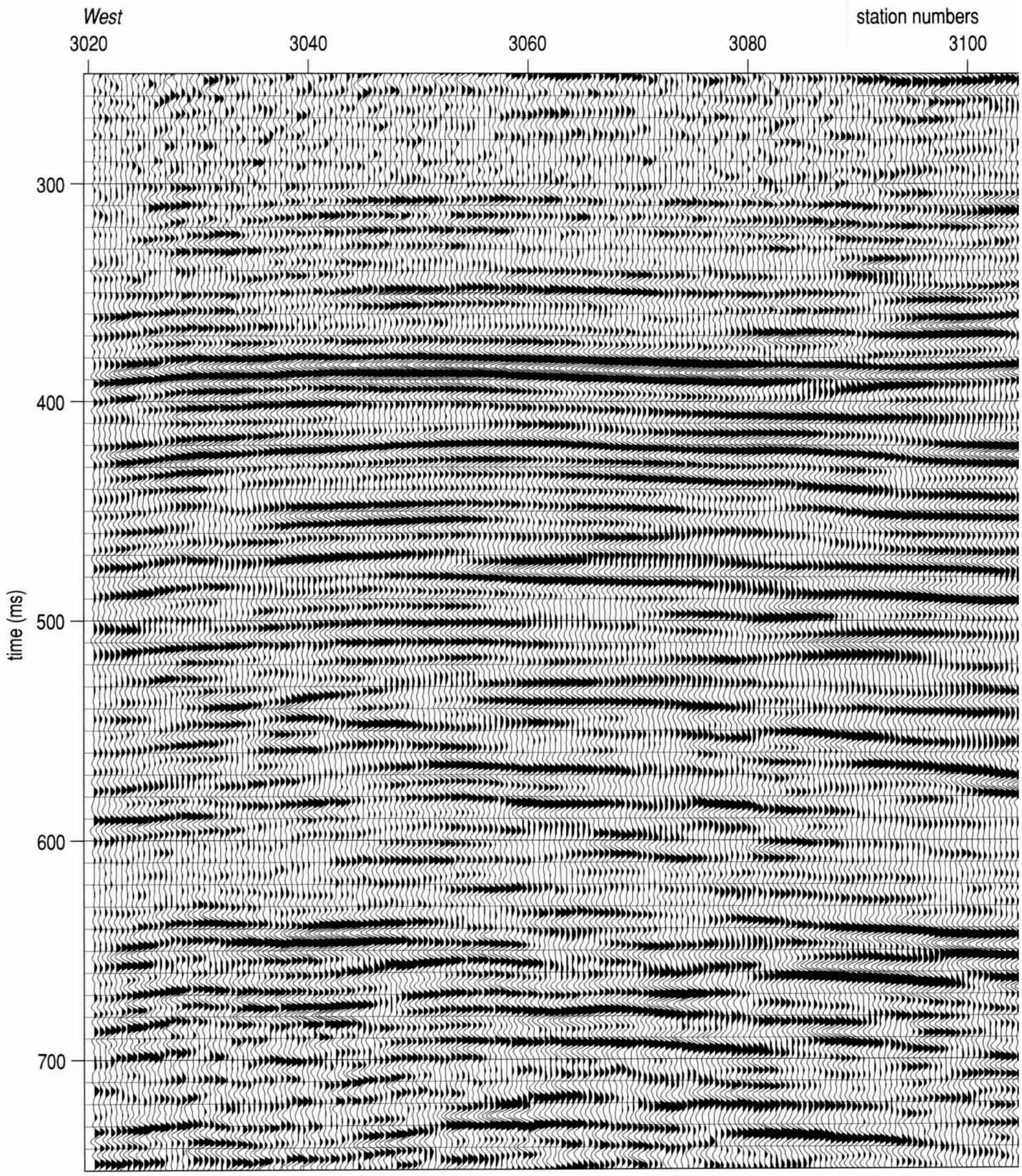

Figure 40.

40a

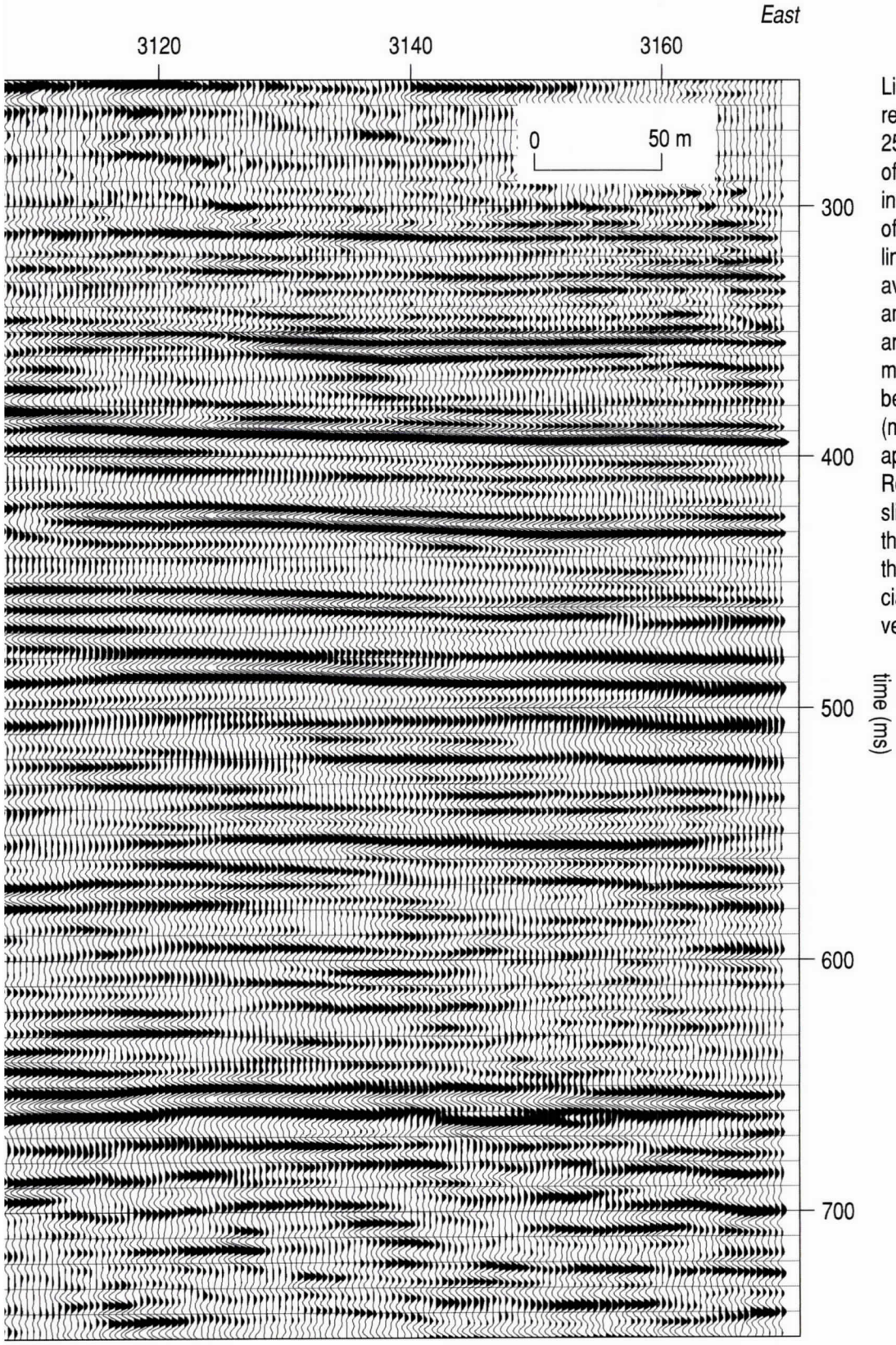

Line 3 CMP stacked seismic reflection section with upper 250 ms cropped. Several groups of coherent reflections can be interpreted across the length of this section and from line to line around the site. With the average velocity to the high amplitude coherent reflections around 2000 m/s, depth estimates are a 1-to-1 correlation between time (ms) and depth (meters) (e.g., 400 ms is approximately equal to 400 m). Reflection character changes slightly from west to east along this profile. Uniformity of events throughout the section, especially the 650 ms reflection, is very good.

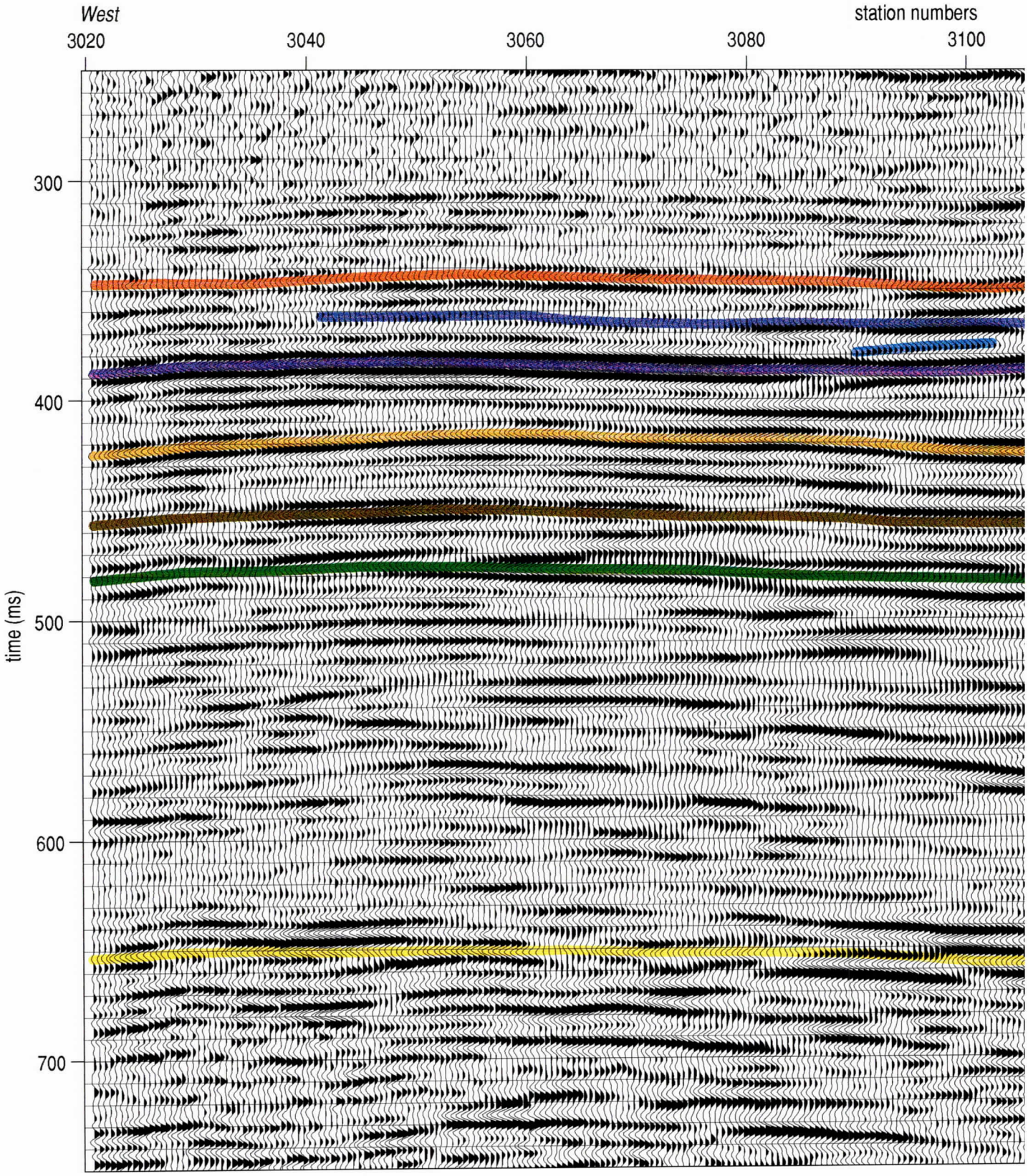

Figure 41.

41a

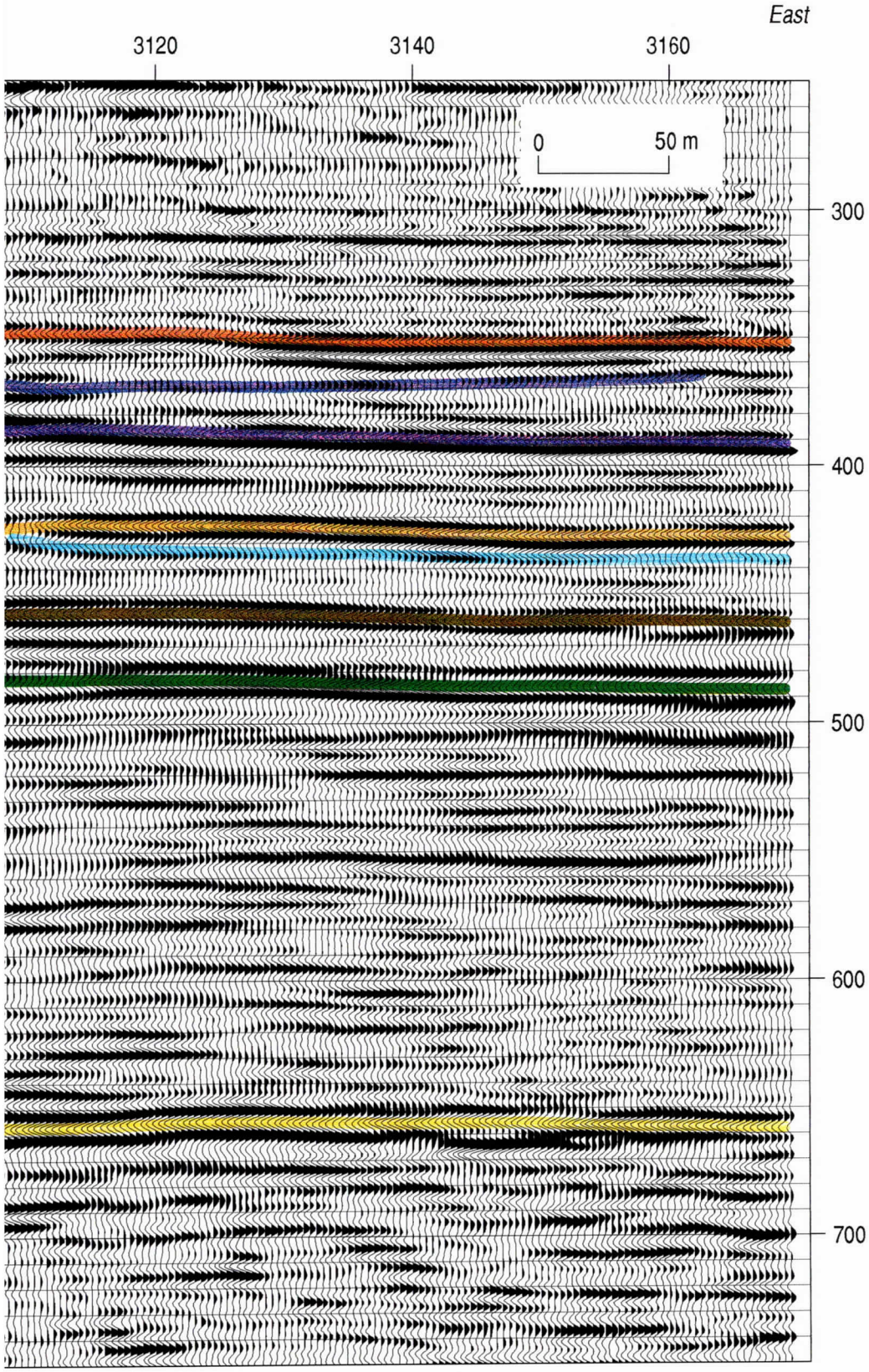

Line 3 CMP stacked seismic reflection section with upper 250 ms cropped and sitewide coherent and correlatable reflections interpreted with a sitewide consistent color sequence.The highest amplitude events are within the interval interpreted to be coal rich. Based on the only drill hole in the area, the orange event is the 365 m coal encountered in the corehole and the purple event is the 391 m coal that was penetrated about 9 m before drilling was curtailed. Several reflections with similar character are interpreted between the 391 m coal and about 500 ms and have been designated as the "coal interval." The yellow reflection possesses a broken, less trace-to-trace coherent appearance on the west side of the profile and is at a depth consistent with the top of the Mesozoic section. Unlike line 2, no fault and fold features are interpreted on this profile. Unique to this stacked section are several reflections with localized coherency and geometries consistent with channels cuts or lens type deposits. Reflections interpreted unique to this line are shown in blue.

- 365 m coal seam
- interpreted 391 m coal
- possible coal interface
- possible coal interface
- possible coal interface
- bedrock

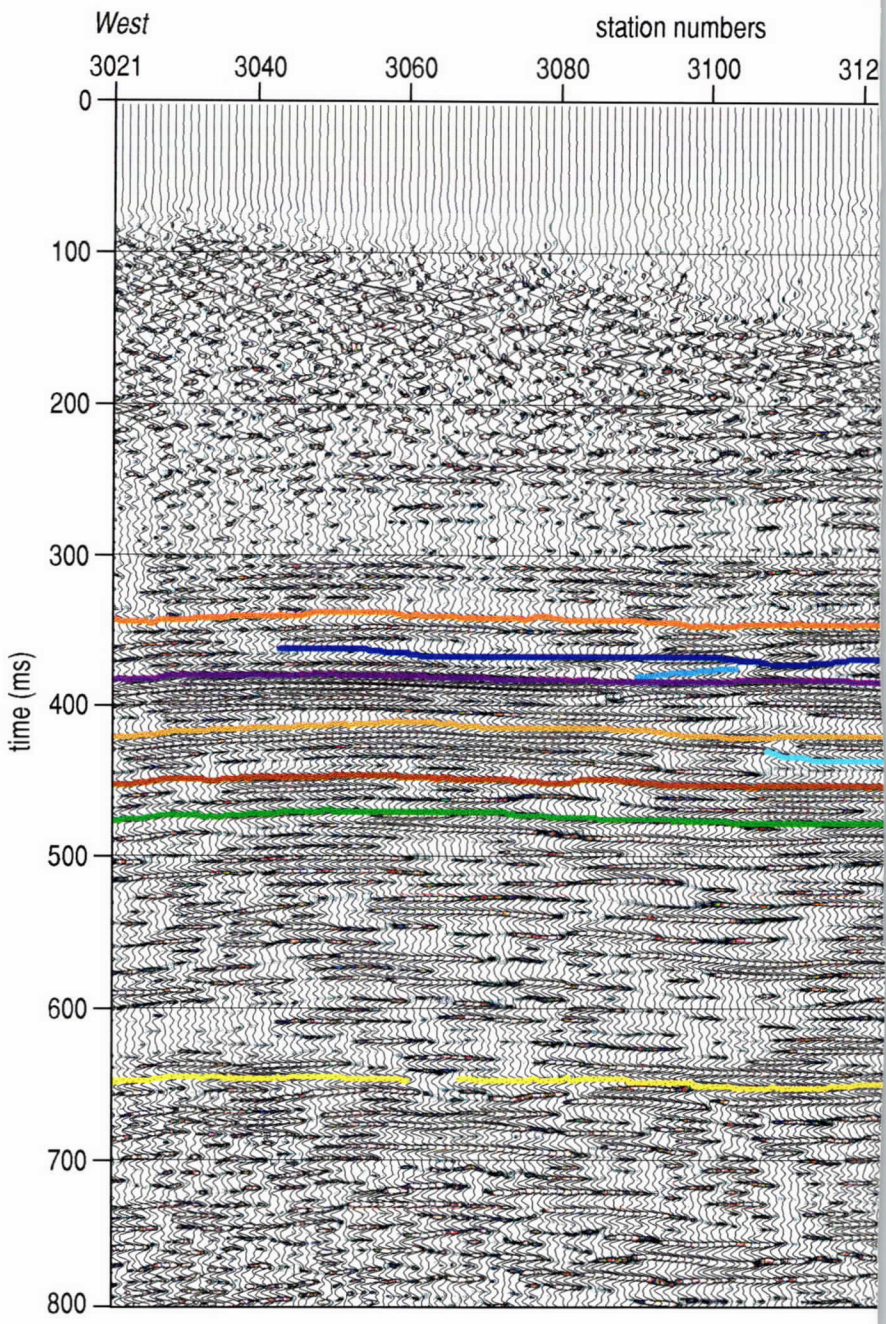

Figure 42. Line 3 CMP stacked seismic reflection section with wiggle traces overlai
180 Hz) and key sitewide coherent reflection events interpreted using the color sch
permafrost and what is identified as the sub-permafrost zones is very evident on th
evident below 200 ms. Reflections within the coal and sub-coal interval extend fron
begins at about 650 m. These reflections possess excellent frequency content (use
features interpreted in blue are consistent with lacustrine lakebed style deposition.
is likely indicative of changing thickness or changes in the physical characteristics

42a

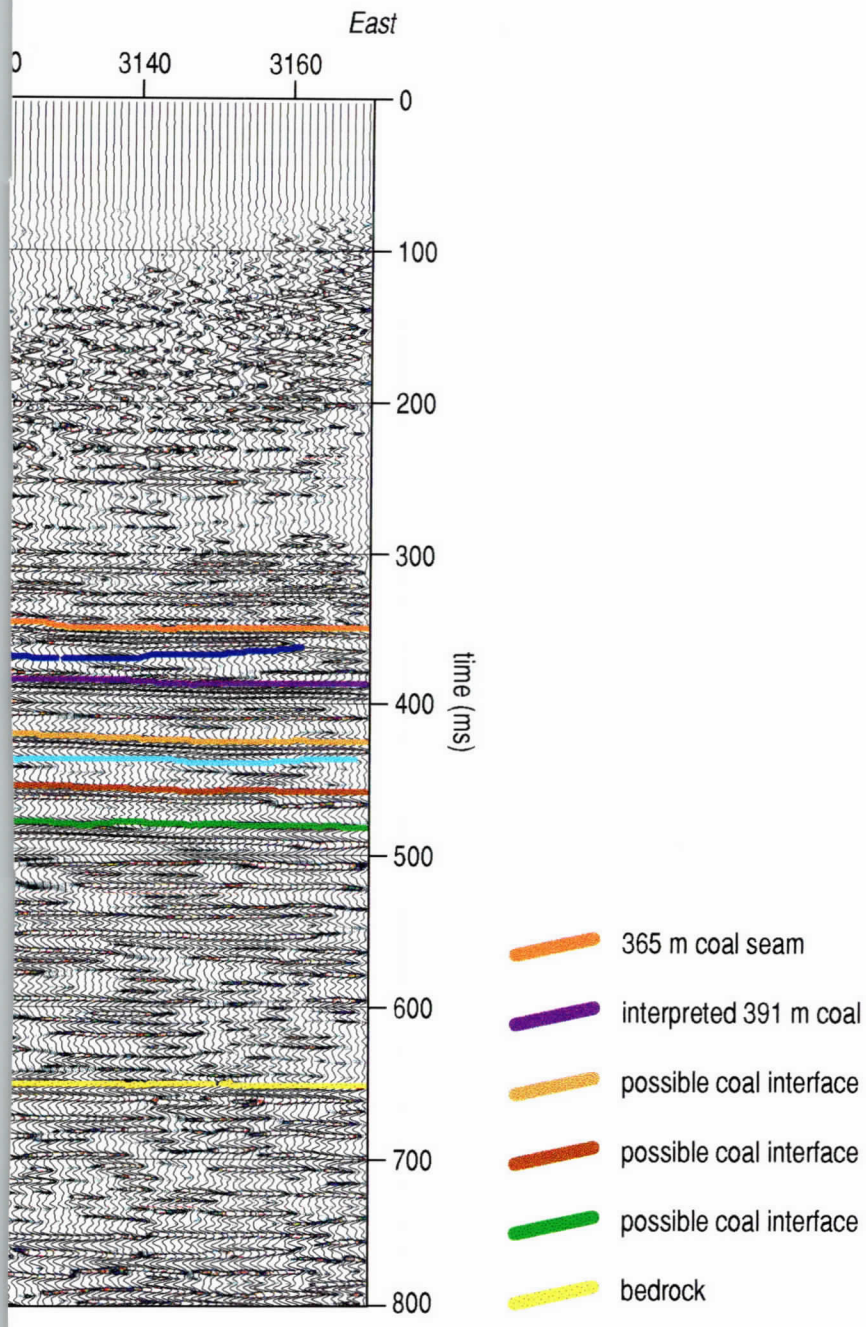

n by color amplitude enhancement of the frequency mid-range (140 Hz to
eme consistent throughout this report. The lack of coherent events within the
is display format. Subtle indications of reflections emerging from the noise are
n just above the 365 m coal down to the top of the Mesozoic section, which
eable in excess of 200 Hz in some places) and sitewide coherency. Channel-like
Variability in the reflection packet (about 20 to 30 ms) of the 391 m coal
of the coal and surrounding layers.

interval. Below basement, multiple reflections are widespread with extremely short stretches of lateral continuity and significant interference from energy scattered off the basement surface.

Spectral plots clearly separate the north and south ends of the profile (Figure 43). High frequency arrivals consistent with the reflections on profiles in proximity to this line (within a few hundred meters) dominate the southeast end of the profile. The transition zone is characterized by a low frequency energy band consistent with properties observed near station 2425 on line 2 (Figure 38). Besides being of slightly lower frequency, reflections on the northwest end of the profile are very similar in nature to those on the southeast.

Amplitude plots highlight the layers within the coal interval (Figure 44). Assuming the coal interval has been correctly distinguished, this interval on line 3 contains a higher percentage of within-coal stringers (1 to 20 m thick range) than the same interval on line 1. Depending on the lithology, interbedding within a coal sequence could produce relative high amplitude reflections; therefore, reflections within this "coal interval" could be widely-spaced, individual coal seams or thin clays interbedded in a massive coal seam.

Line 4

Coherency of the target reflections on line 4 is relatively good, with dominant reflection frequencies exceeding 180 Hz on some reflections (Figure 45). The 480 ms reflection is by far the highest amplitude, most coherent event on the stacked section. The variable amplitude and wavelet characteristics observed on secondary reflections within the coal interval are likely indicative of a very localized and specific depositional activity that occurred in this portion of the site. A reflection character change northwest of station 4080 is evident in arrival patterns and attributes in all but the 480 ms reflection.

The half-dozen reflections interpreted on line 4 are easily recognized and correlated from line to line (Figure 46). Basement reflections are easily distinguishable from Cenozoic reflections in the upper 600+ m of the section. The 390 ms coal reflection is clearly offset beneath station 4080. While the 480 ms event has equivalent total displacement manifested in the form of drape, which extends a distance of 100 to 150 m, the displacement on the 390 ms reflection occurs over a much shorter distance (less than 50 m). This difference implies the mechanism responsible for these elevation differences is different, the 480 ms layer is more pliable than the 390 ms unit, or the fault zone narrows upward. Also of interest along this profile are several what appear to be subtle depositional features within the "coal interval." Local changes in the layer geometry and complexity as defined by the reflection at around 370 ms could be indicative of a series of river channel meanders or changes in the shoreline of a shallow lake. Several other possible explanations can be conceived for this undulating reflection, but without physically defining this contact it is at best speculative to interpret subtle geology.

The southeastern three-quarters of line 4 has no obvious structures that can be clearly correlated to the other six profiles (Figure 47). Again, the unique reflection character of each of the four different intervals is obvious. In the compressed display of the line the general structural trends become more obvious and the reflection-specific detail becomes subdued. Clearly the structure beneath station 4080 is a dominant feature with an easily recognizable series of

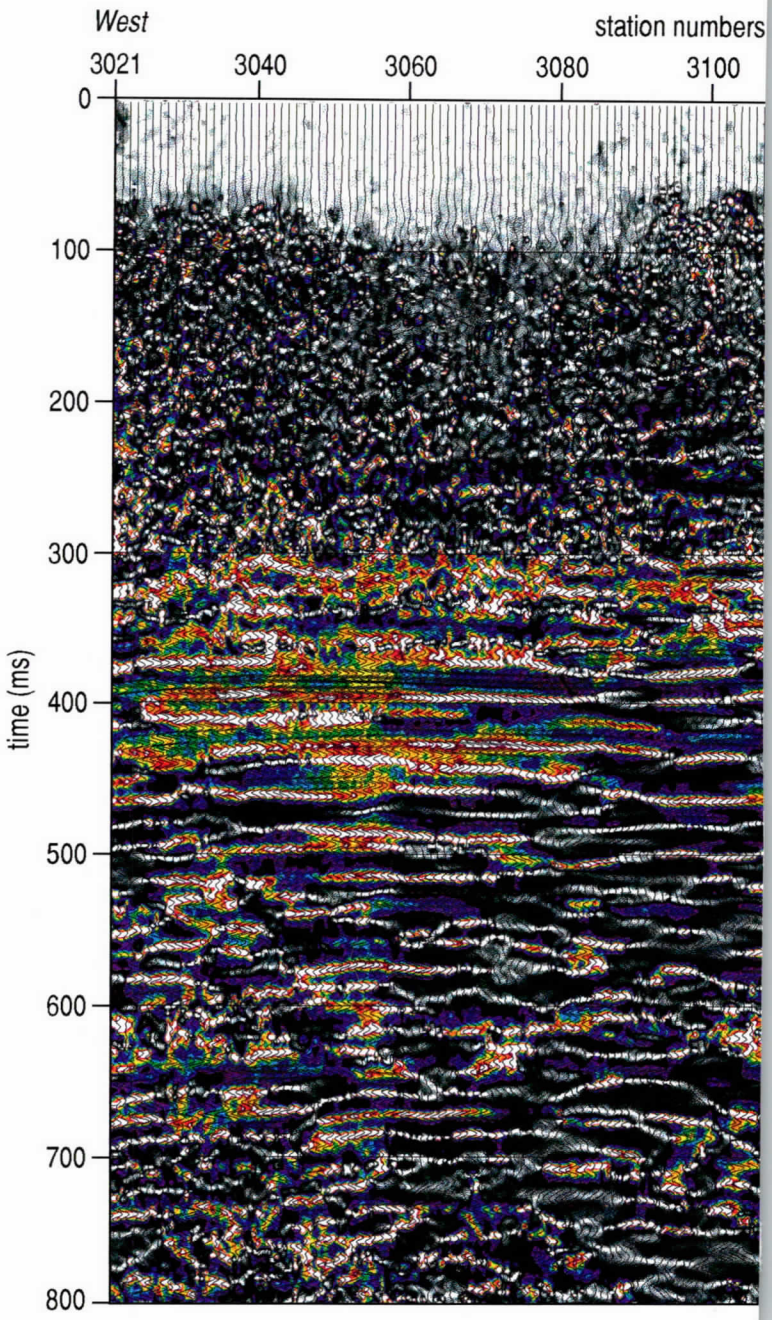

Figure 43. Line 3 CMP stacked section with instantaneous frequency o
100 Hz and 150 Hz. Changes in reflection character, and therefore geo
is the significant increase in dominant frequency on the east half of the
channel features interpreted on amplitude displays (Figures 40, 41, an

43a

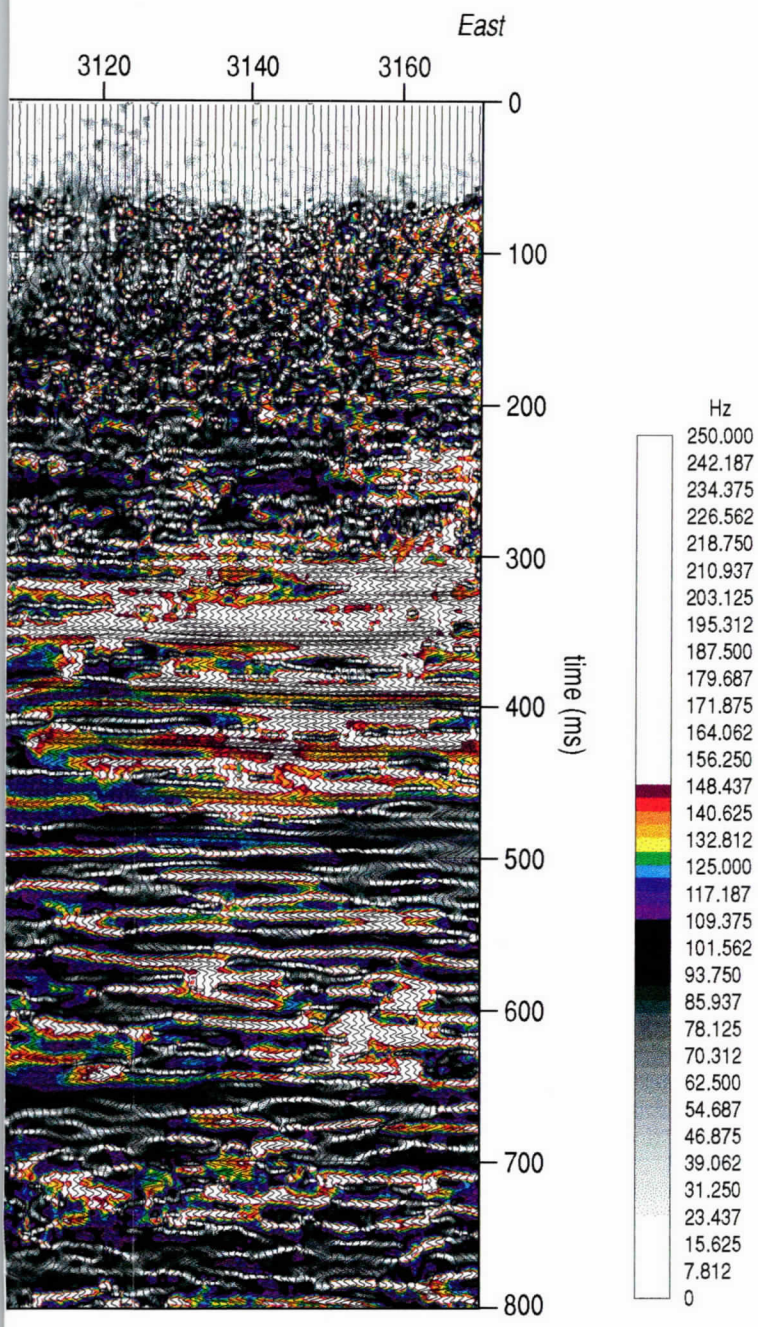

verlain by wiggle trace data focusing on the frequency range between
logy, can be easily identified on frequency plots. Evident on this display
profile. This increase in dominant frequency is coincident with the area
l 42).

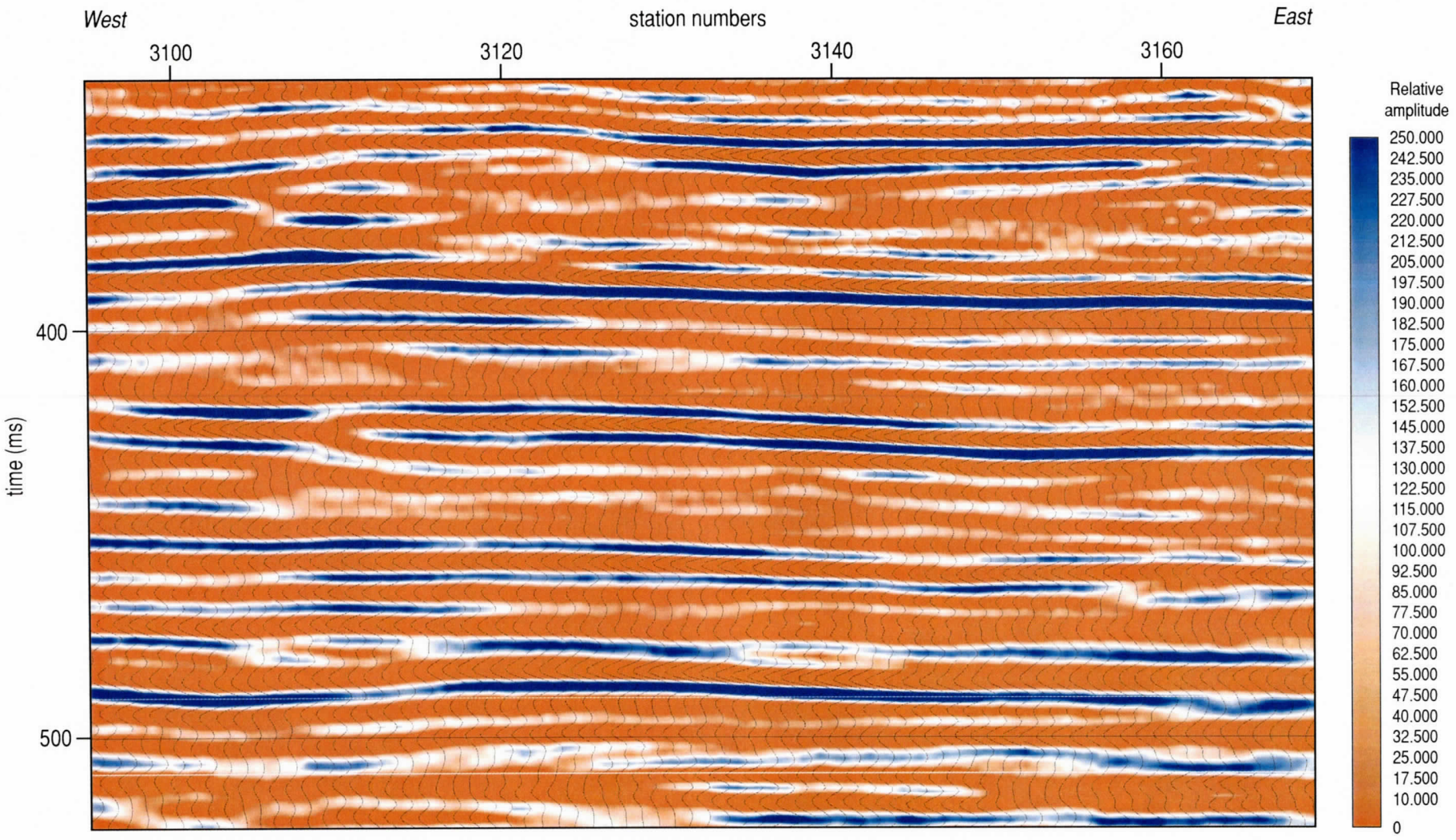

Figure 44. A zoomed-in portion of line 3 CMP stacked section focusing on the "coal interval" using color amplitude overlain by wiggle trace representation of the seismic reflection data. This display format highlights lateral amplitude variations. Several layers appear consistent across the length of this segment of the line with noteworthy variations in amplitude of the interpreted coal reflections. The characteristic doublet that represents the 391 m coal seam loses significant amplitude of the first part of the wavelet between 3110 and 3160. This drop in amplitude is likely related to a thinning of the coal seam. Most obvious on this section is the number of higher amplitude events that can be seen. Extending the drill-confirmed character of the 391 m coal through this interval, there could be as many as 5 significant coal seams (>7 m) along along this profile.

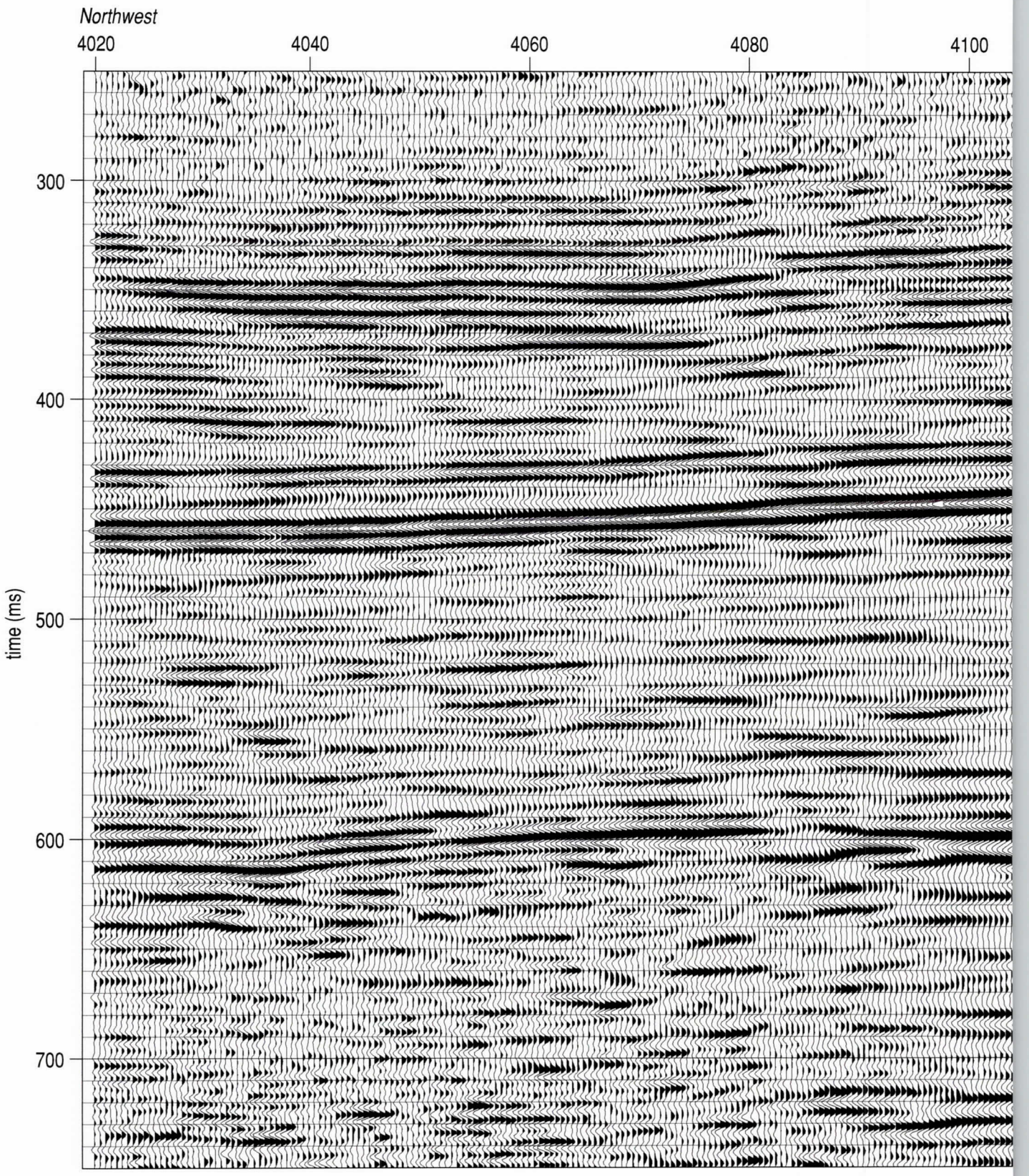

Figure 45.

45a

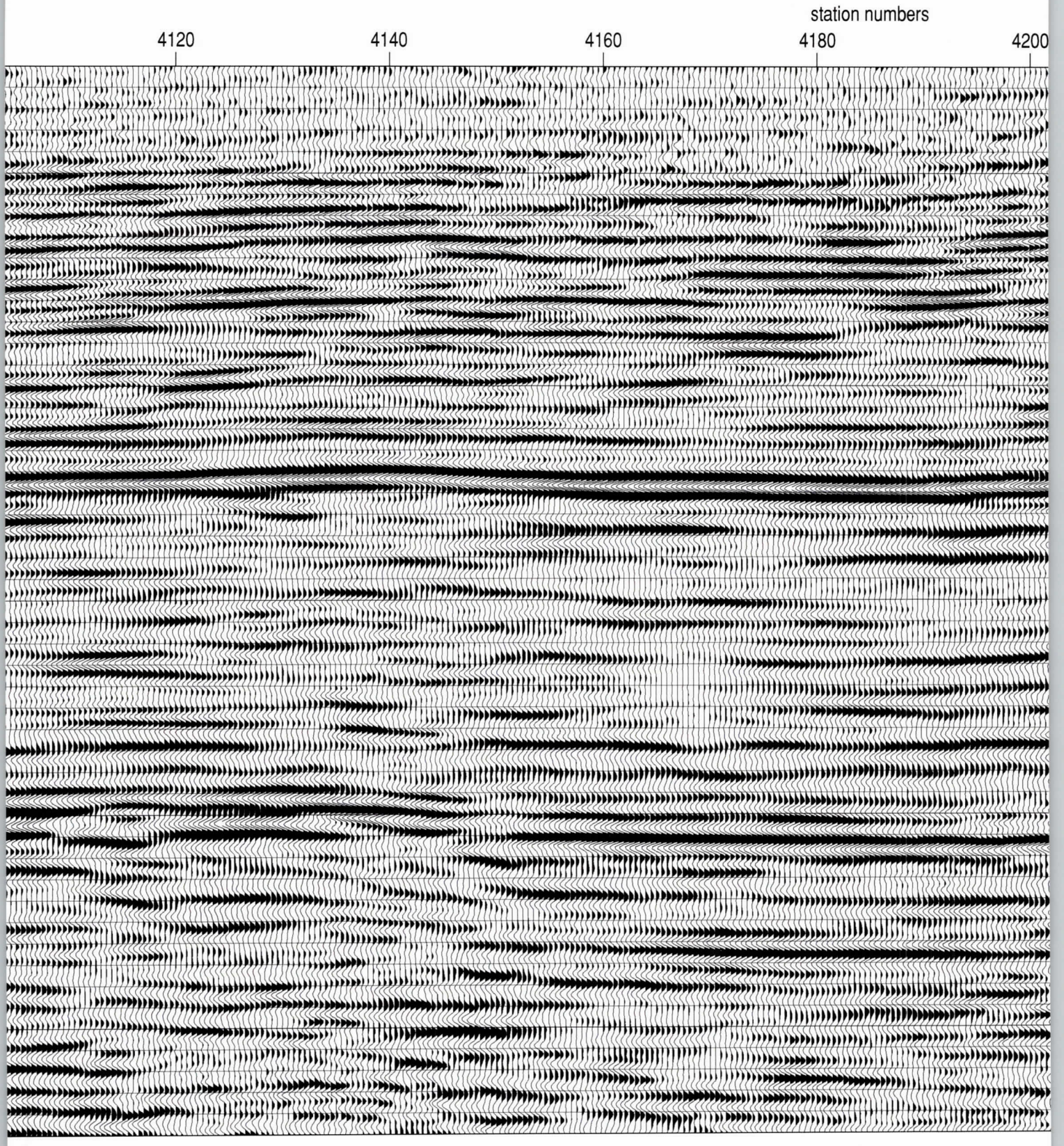
station numbers
4120
4140
4160
4180
4200

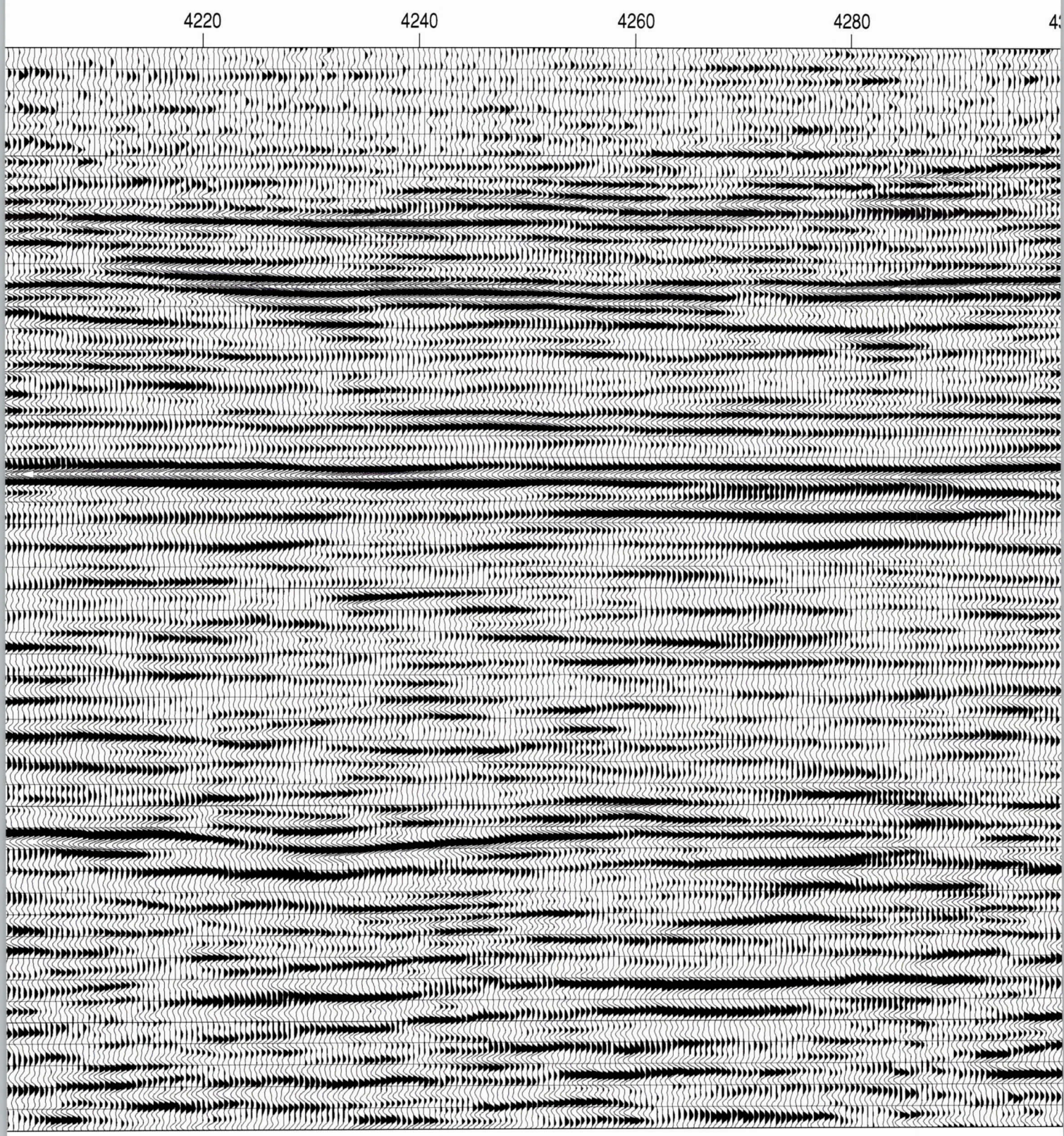

45c

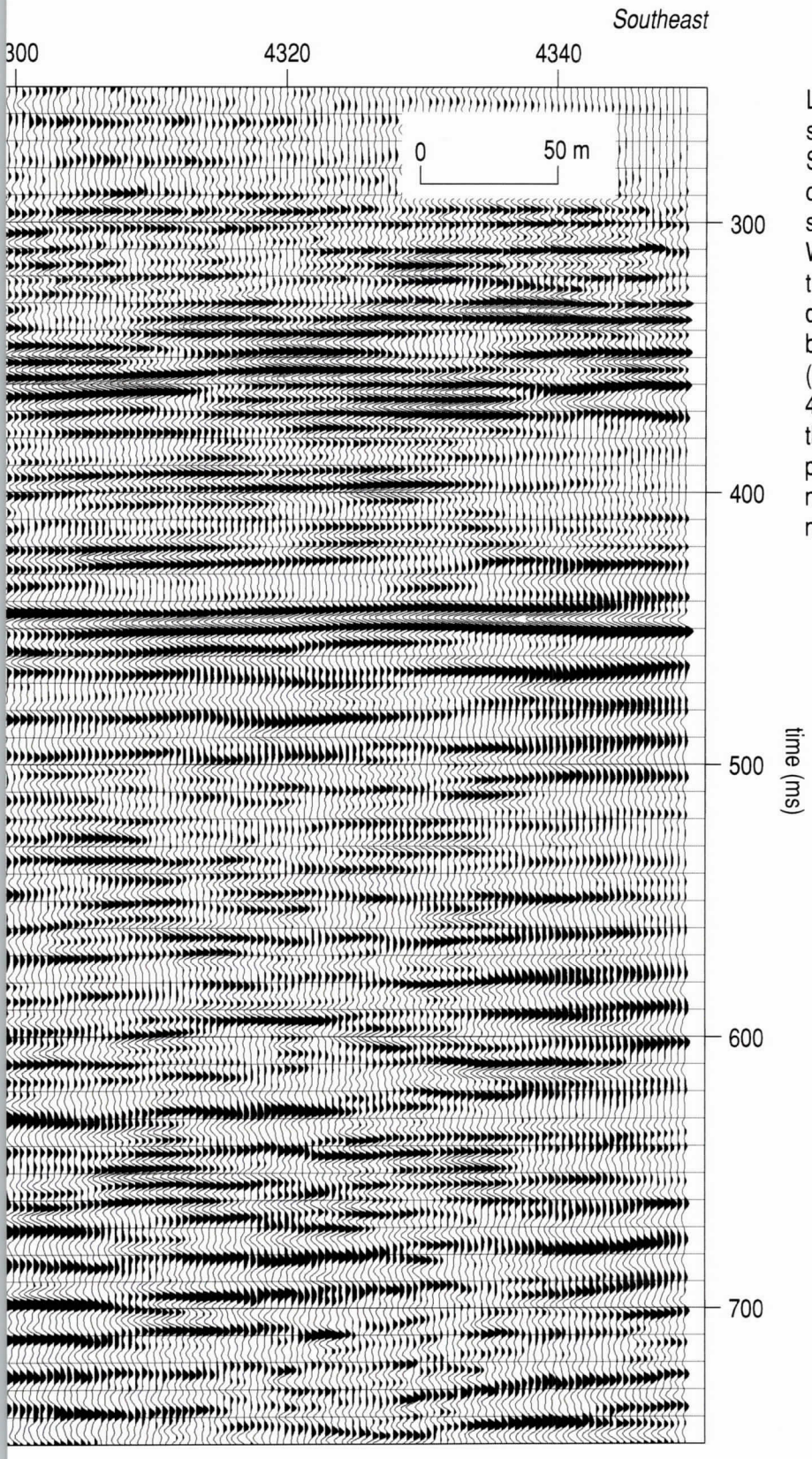

Line 4 CMP stacked seismic reflection section with upper 250 ms cropped. Several groups of coherent reflections can be interpreted across the length of this section and from line to line around the site. With the average velocity to the high amplitude coherent reflections around 2000 m/s, depth estimates are a 1-to-1 correlation between time (ms) and depth (meters) (e.g., 400 ms is approximately equal to 400 m). A drape or monocline feature on the northwest end of the profile is very pronounced and with its very non-vertical nature it cannot be an artifact of near-surface static.

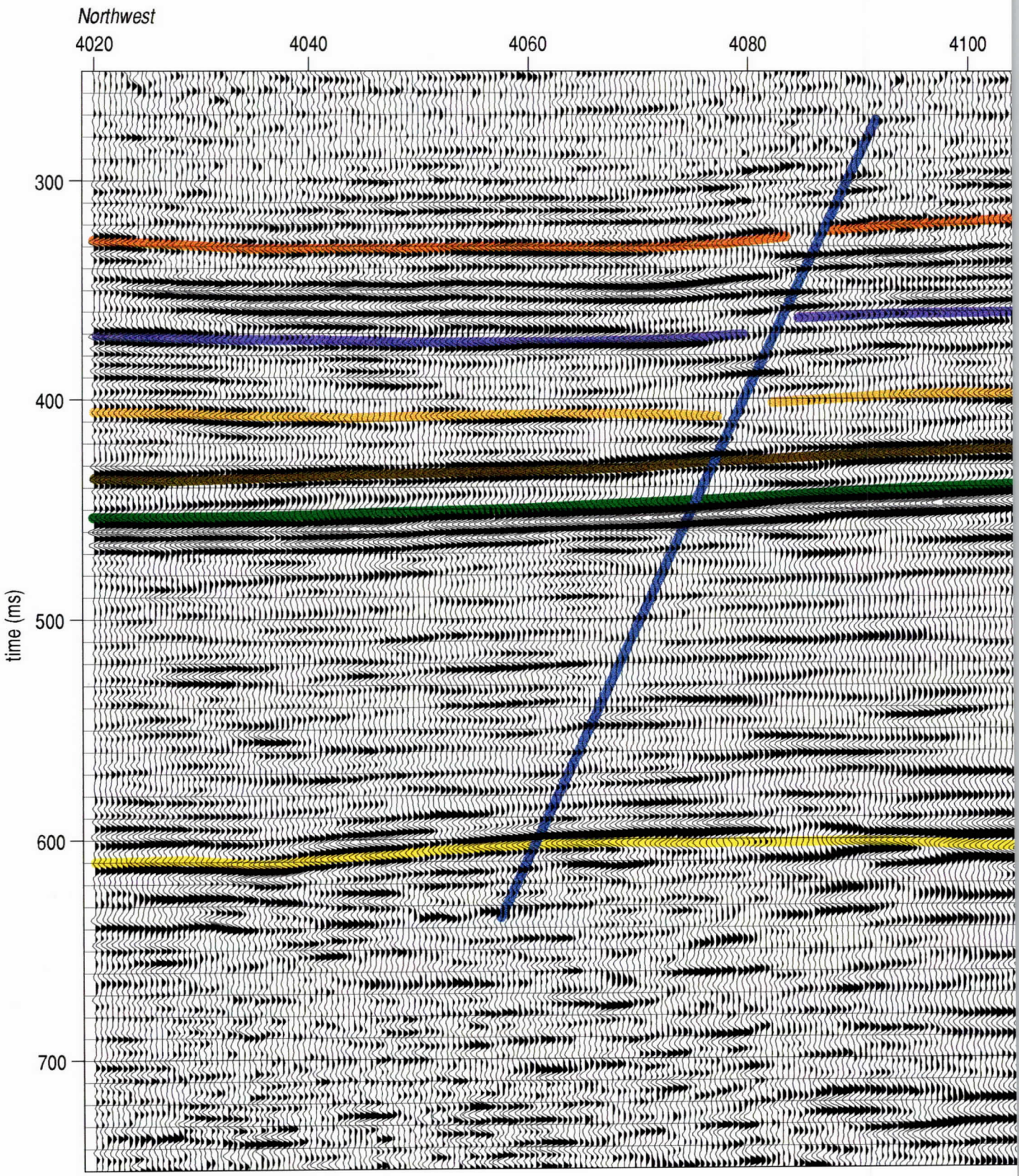

Figure 46.

46a

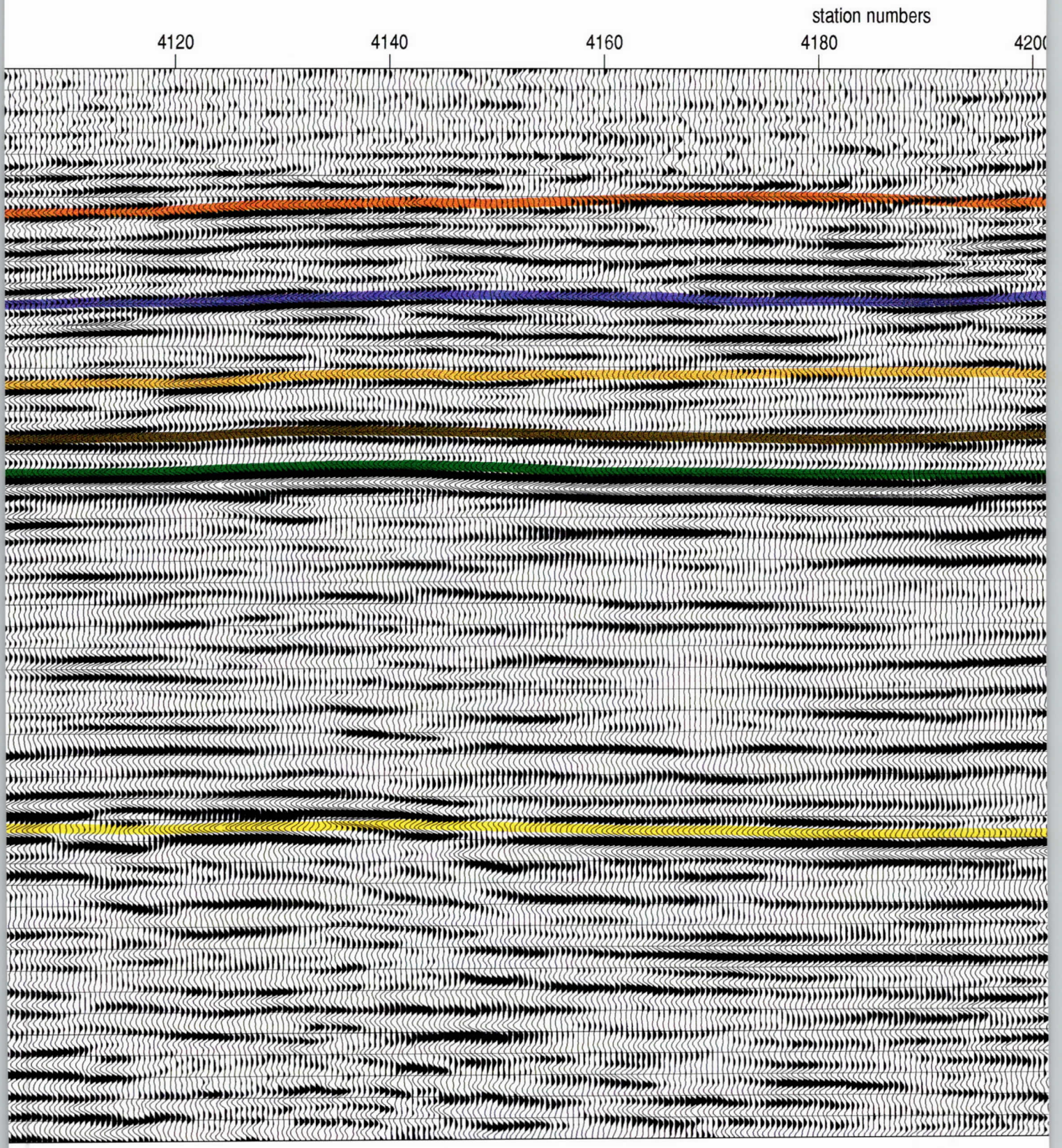
station numbers
4120
4140
4160
4180
4200

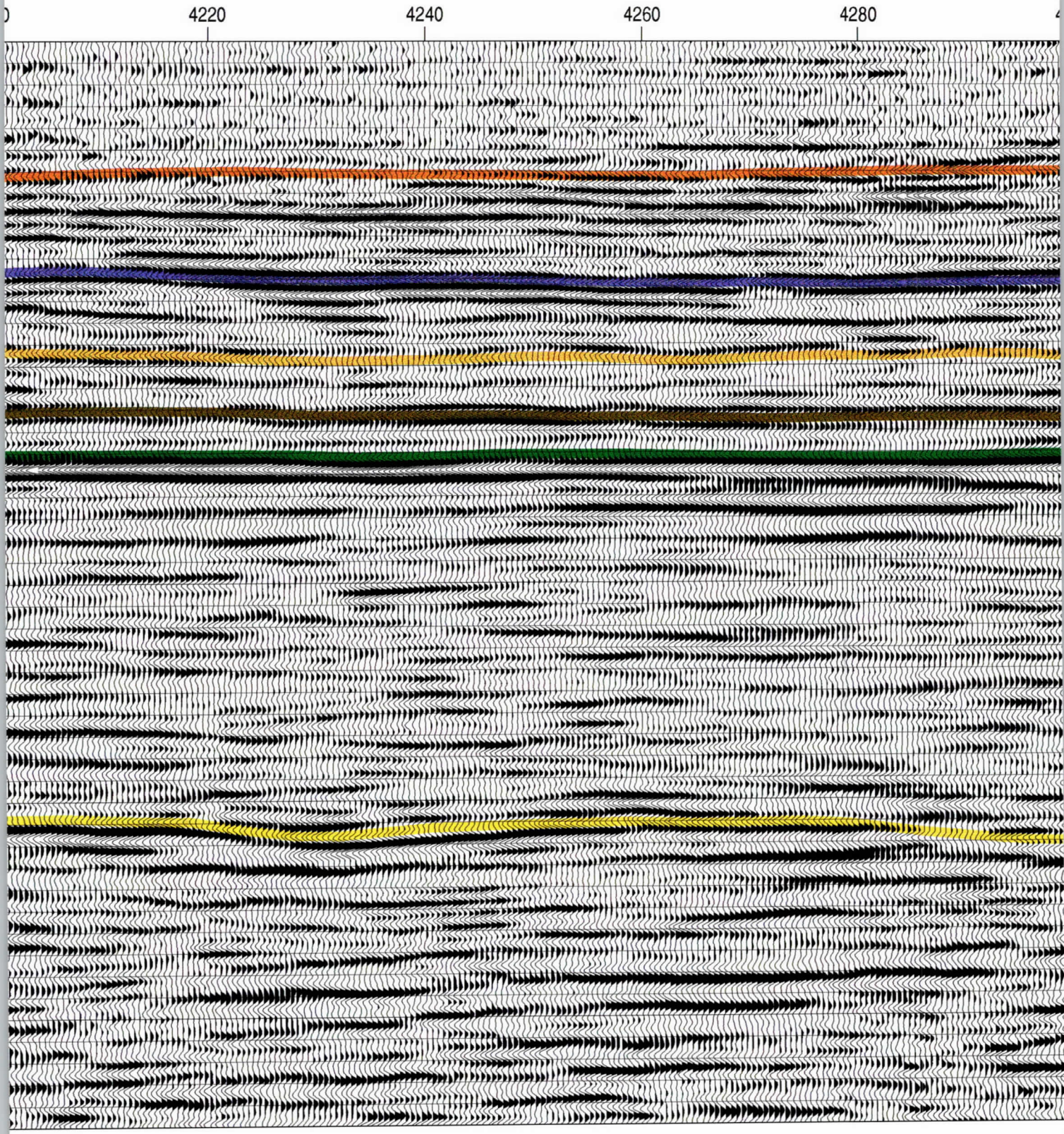

46c

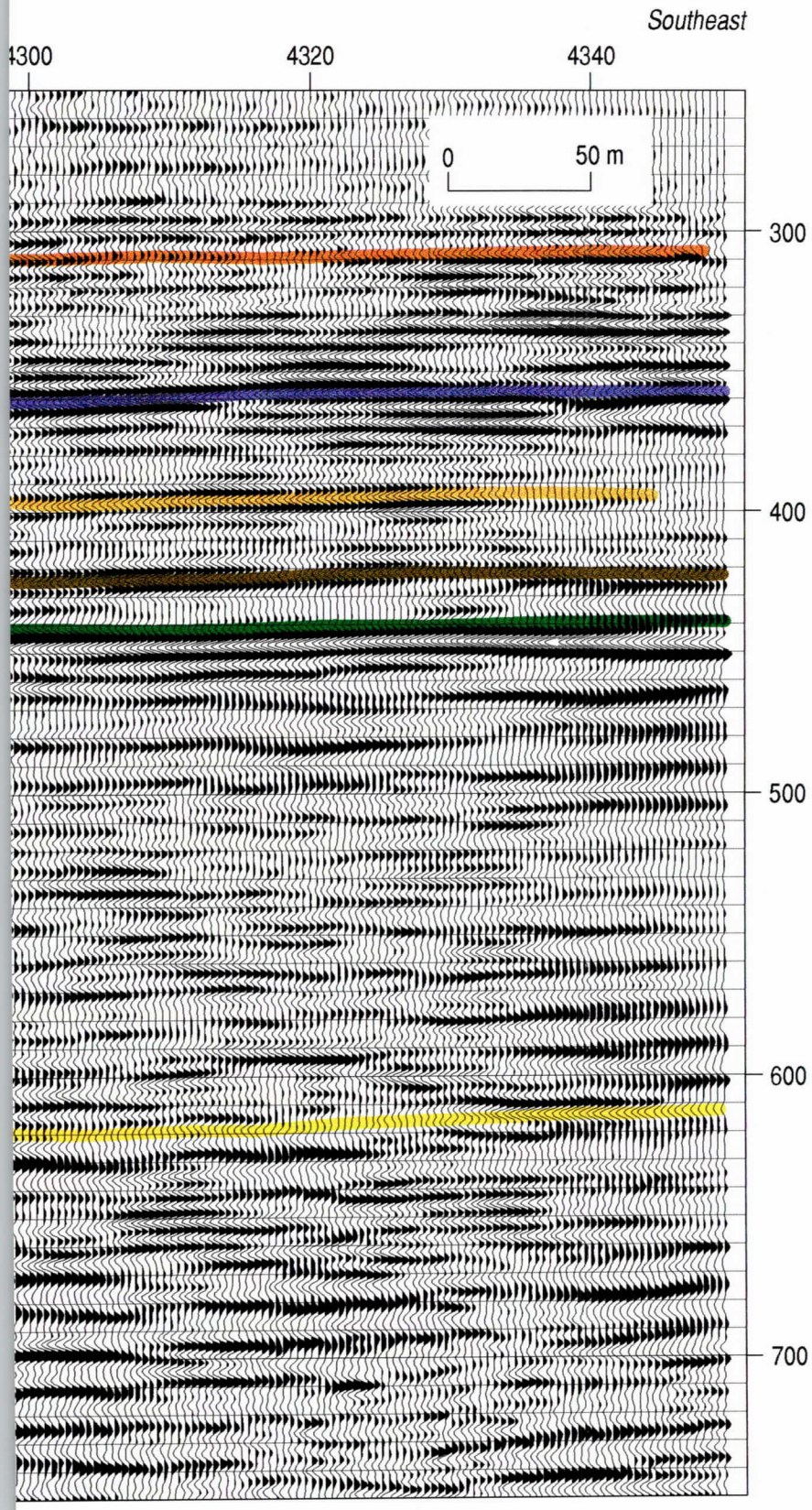

Line 4 CMP stacked seismic reflection section with upper 250 ms cropped and sitewide coherent and correlatable reflections interpreted with a sitewide consistent color sequence. The highest amplitude events are within the interval interpreted to be coal rich. Based on the only drill hole in the area, the orange event is the 365 m coal encountered in the corehole and the purple event is the 391 m coal that was penetrated about 9 m before drilling was curtailed. Several reflections with similar character are interpreted between the 391 m coal and about 500 ms and have been designated as the "coal interval." With the variability in the wavelet characteristics of the basement along line 4, the top of the Mesozoic section (yellow basement reflection) was interpreted based predominantly on amplitude. Unlike line 2 or line 3, only a single fault is interpreted on this profile. This fault is, however, a very pronounced local feature and one of the most significant imaged on any of the profiles.

- 365 m coal seam
- interpreted 391 m coal
- possible coal interface
- possible coal interface
- possible coal interface
- bedrock

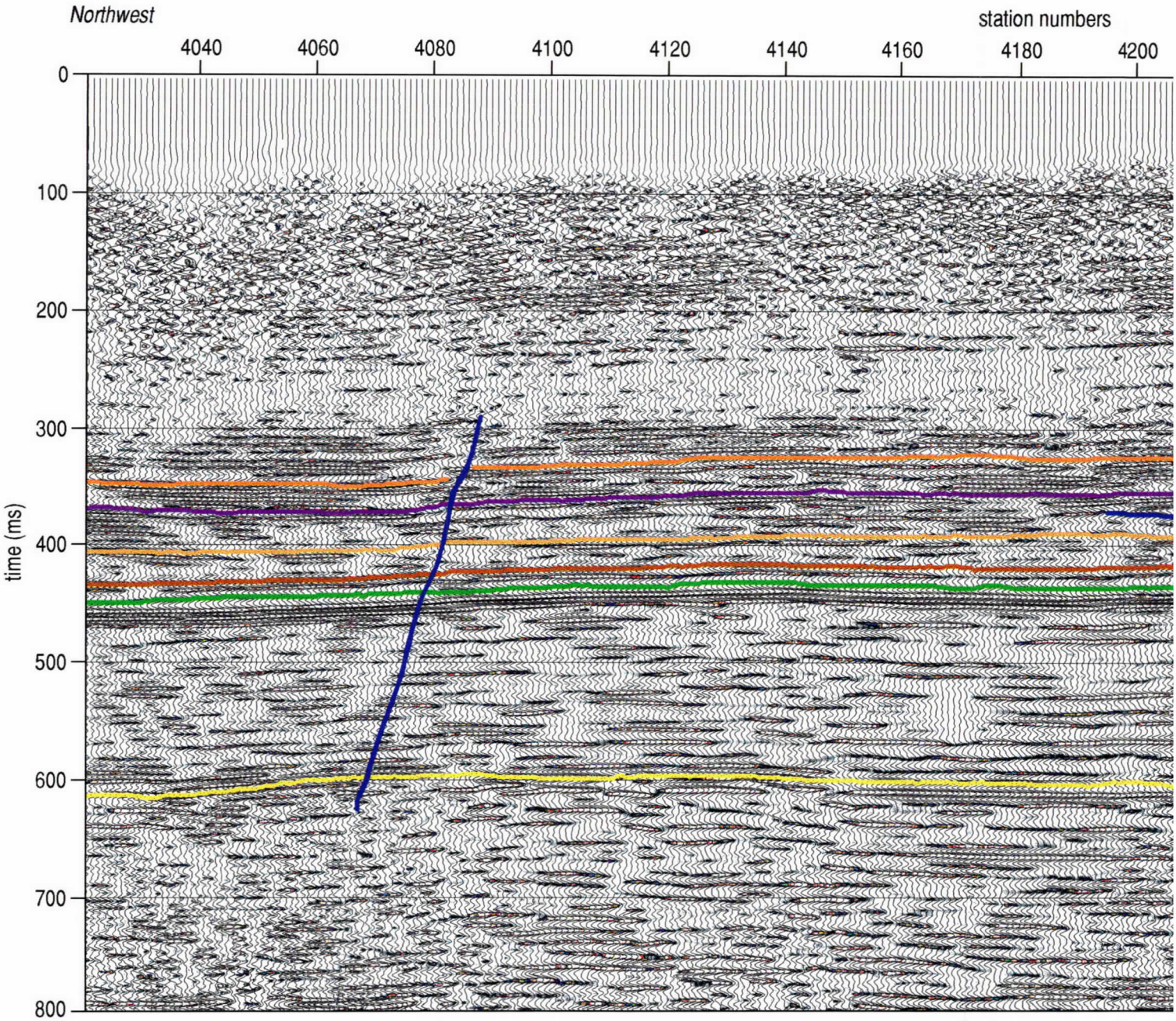

Figure 47. Line 4 CMP stacked seismic reflection section with wiggle traces overlain by color amplitude enhancement of the frequency mid-ran consistent throughout this report. The lack of coherent events within the permafrost and what is identified as the sub-permafrost zones is very below 100 ms, with a quiet zone (fewer reflections per unit time) between about 200 ms and first drill-confirmed coal at about 365 m. Reflectio Mesozoic section, which begins at about 650 m. These reflections possess excellent frequency content (useable in excess of 200 Hz in some consistent characteristic of all the seismic profiles collected in the Fort Yukon area.

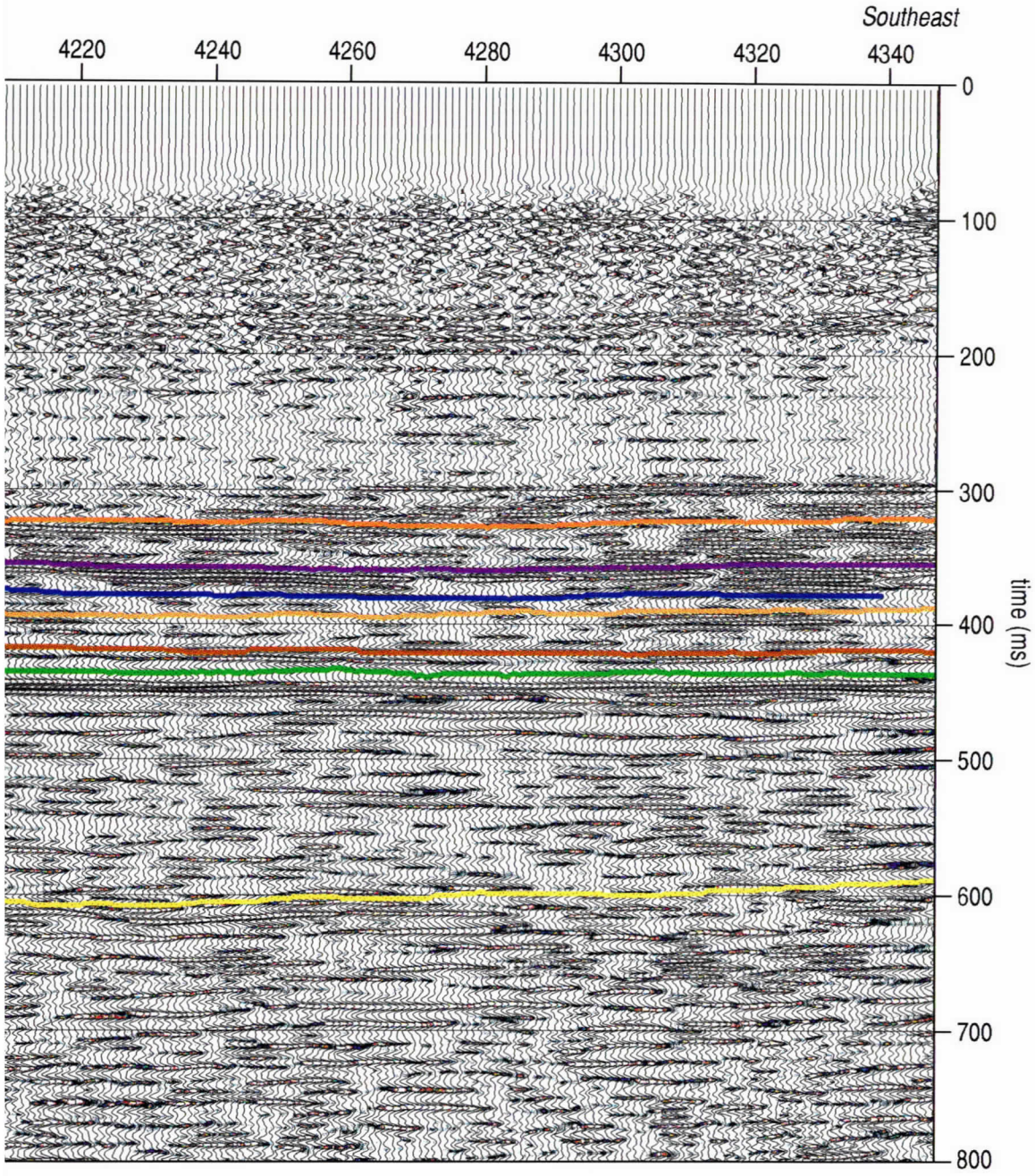

e (140 Hz to 180 Hz) and key sitewide coherent reflection events interpreted using the color scheme
vident on this display format. Subtle indications of reflections emerging from the noise are evident
s within the coal and sub-coal interval extend from just above the 365 m coal down to the top of the
aces) and sitewide coherency. This highly reflective time window interpreted as the "coal zone" is a

diffraction patterns beneath the basement reflection. The apex of the diffractions and a basement high seem to be centered around station 4120. This basement high is southeast of bed offset interpreted to be the result of faulting. It is not clear how these two features are related, but it is likely the basement feature predates the fault, considering the lack of uplift in the reflection above 480 ms. The "coal interval" seems to have reflection characteristics and bed thickness that vary quite dramatically across the site. Most variations appear depositional in nature.

Frequency-sensitive features beneath stations 4125 and 4180 are consistent in character but spatially out of phase with similar features on line 2 and line 3 (Figure 48). A near vertical frequency anomaly beneath station 4080 can be loosely correlated to the fault interpreted on the amplitude displays of line 4 (Figure 47). Pronounced diffraction patterns are associated with the basement high identified on the amplitude sections. A lower frequency energy band centered on about station 4180 cannot be correlated to amplitude wiggle trace displays. This low-frequency energy band evident on instantaneous frequency plots is similar to ones observed on lines 3 and 2. Spatially they don't correlate based purely on the relative location of each feature on their respective lines.

Lateral variations in reflection characteristics are extremely obvious on the amplitude displays of line 4 (Figure 49). Changes in amplitude and geometry of reflections within the "coal interval" above the 480 ms reflection are pronounced throughout the southeastern half of the line. These variations could be due to changes in material properties at a layer contact. It could also be related to changes within the coals that would be assumed to be present in this interval. If the coals within this unit (especially the 390 ms coal) are as discontinuous as a possible interpretation of these data would suggest, CBM production could be severely limited in this area. However, considering the overall continuity of the more compressed scale sections (Figure 47), it is more likely these changes in amplitude are related to changes in the physical properties of the coal units (i.e., gas concentration, thickness and changes in mineralogy of overclays, etc.).

Line 5

Line 5 crossed the most variable terrain and therefore is susceptible to the greatest degree of irregularities in reflection wavelet character and static across the profile. On the northeast side of the profile (Figures 50 and 51) the reflections are consistent and possess some of the highest coherency of any data collected at this site. The "coal interval" can be correlated directly with line 1 and the other profiles in proximity (a few hundred meters). As on the previously interpreted profiles, the upper Mesozoic and Cenozoic sediments can be vertically divided into four unique reflection intervals. The most significant for this study is the "coal interval," which on these data has a high number of reflections. Some of these reflections can be correlated all the way across the northeastern three-quarters of the stacked section. Data quality drops off noticeably on the southeastern end of the profile where the line passes between the slough and the USAF radar station. A highly irregular pulse of electrical (possibly RF) noise overpowered the seismic signals along portions of the profile immediately south of the radar station. Variability in the permafrost thickness and changes in near-surface material were the primary contributors to the observed decay in data at the low station number end of the profile.

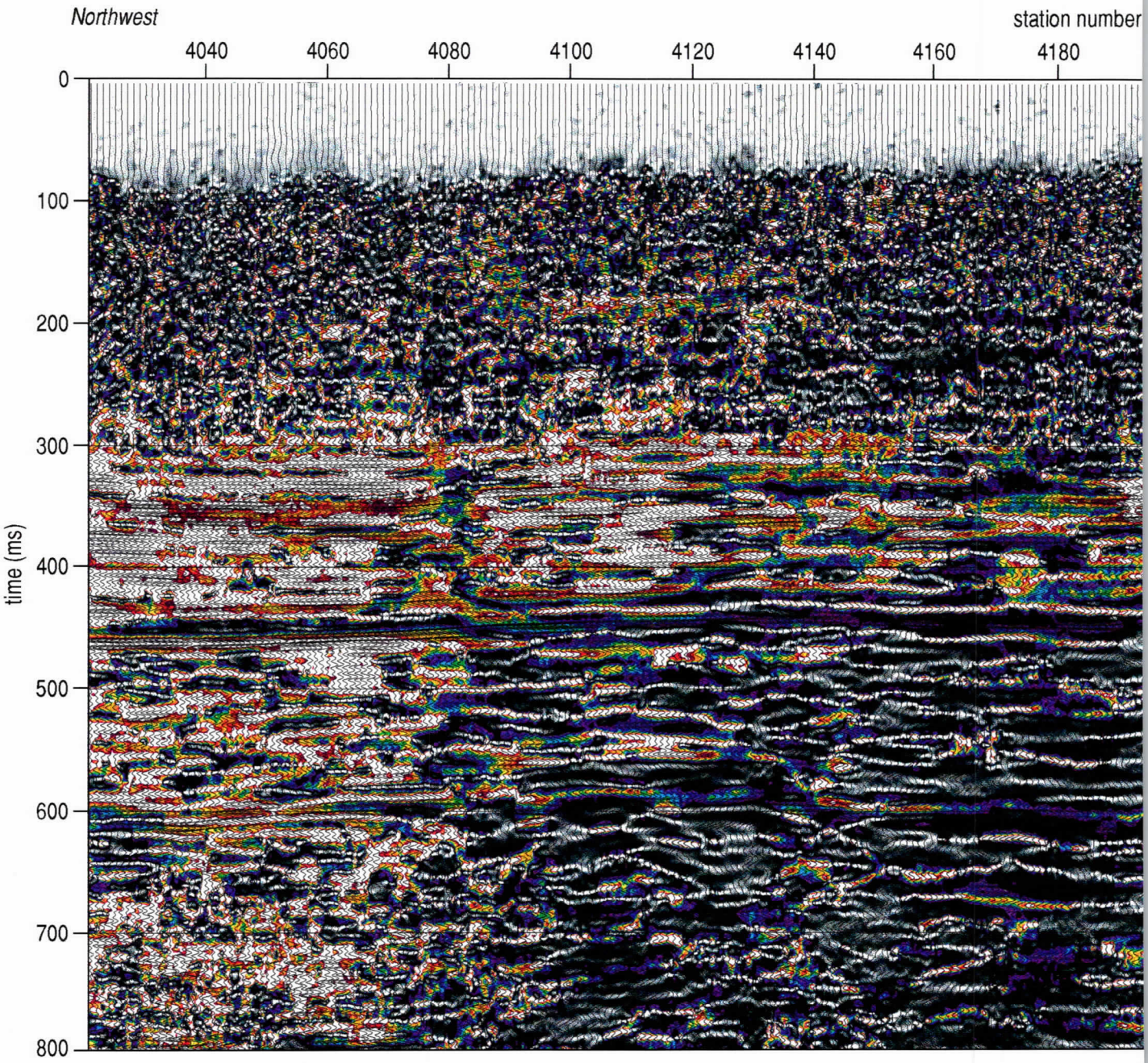

Figure 48. Line 4 CMP stacked section with instantaneous frequency overlain by wiggle trace data focusing on the frequency range b
frequency plots. Evident on this display is the significant increase in dominant frequency on the northwest quarter of the profile. This
to note is the frequency anomaly beneath station 4080 at about 300 ms that appears to dip to the southeast. Southeast of this freque

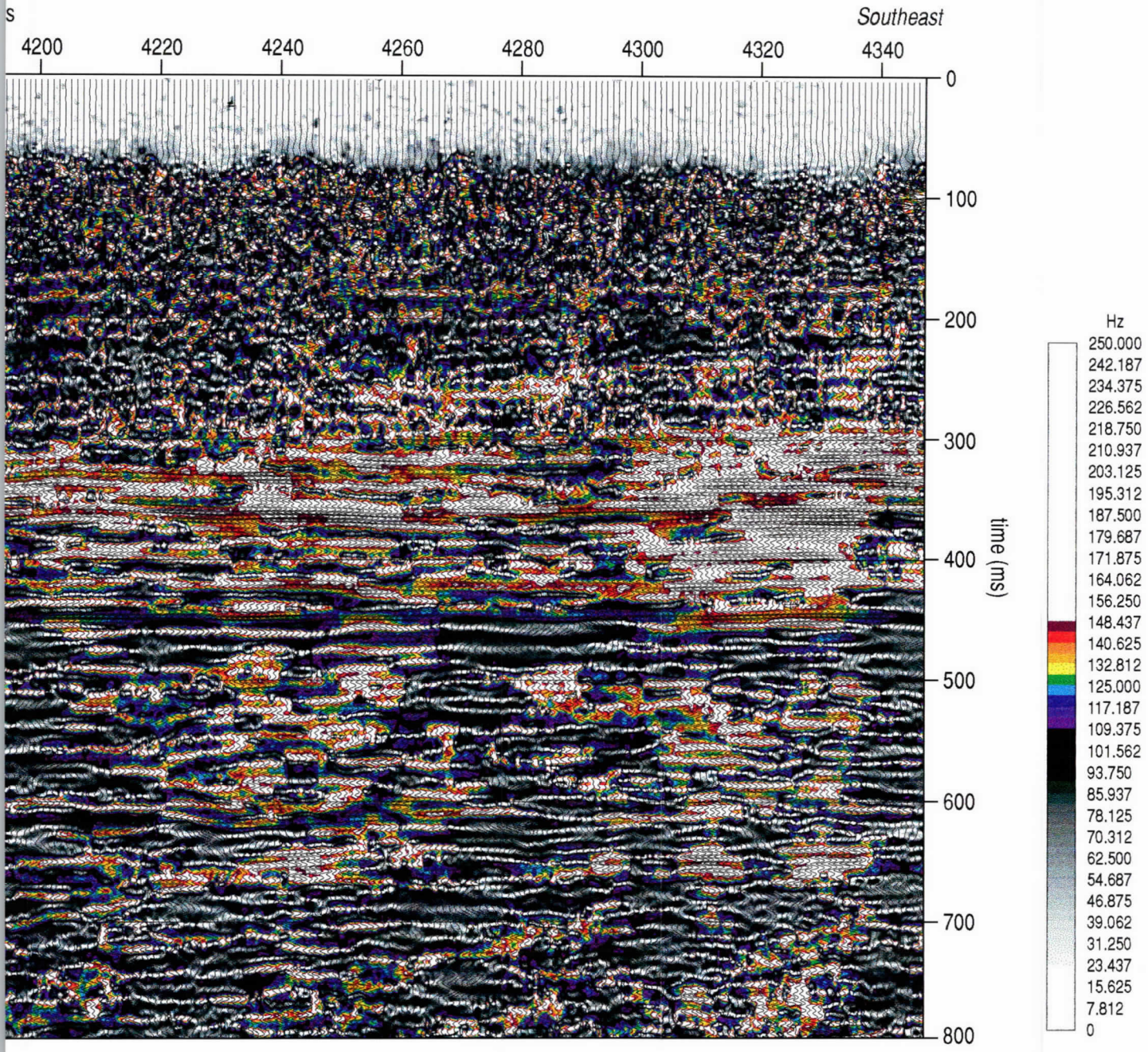

etween 100 Hz and 150 Hz. Changes in reflection character, and therefore geology, can be easily identified on
increase in dominant frequency marks a zone of diffractions and a fault interpreted on Figure 46. Interesting
ncy anomaly are lower frequency arrivals with diffraction or scattered energy readily interpretable.

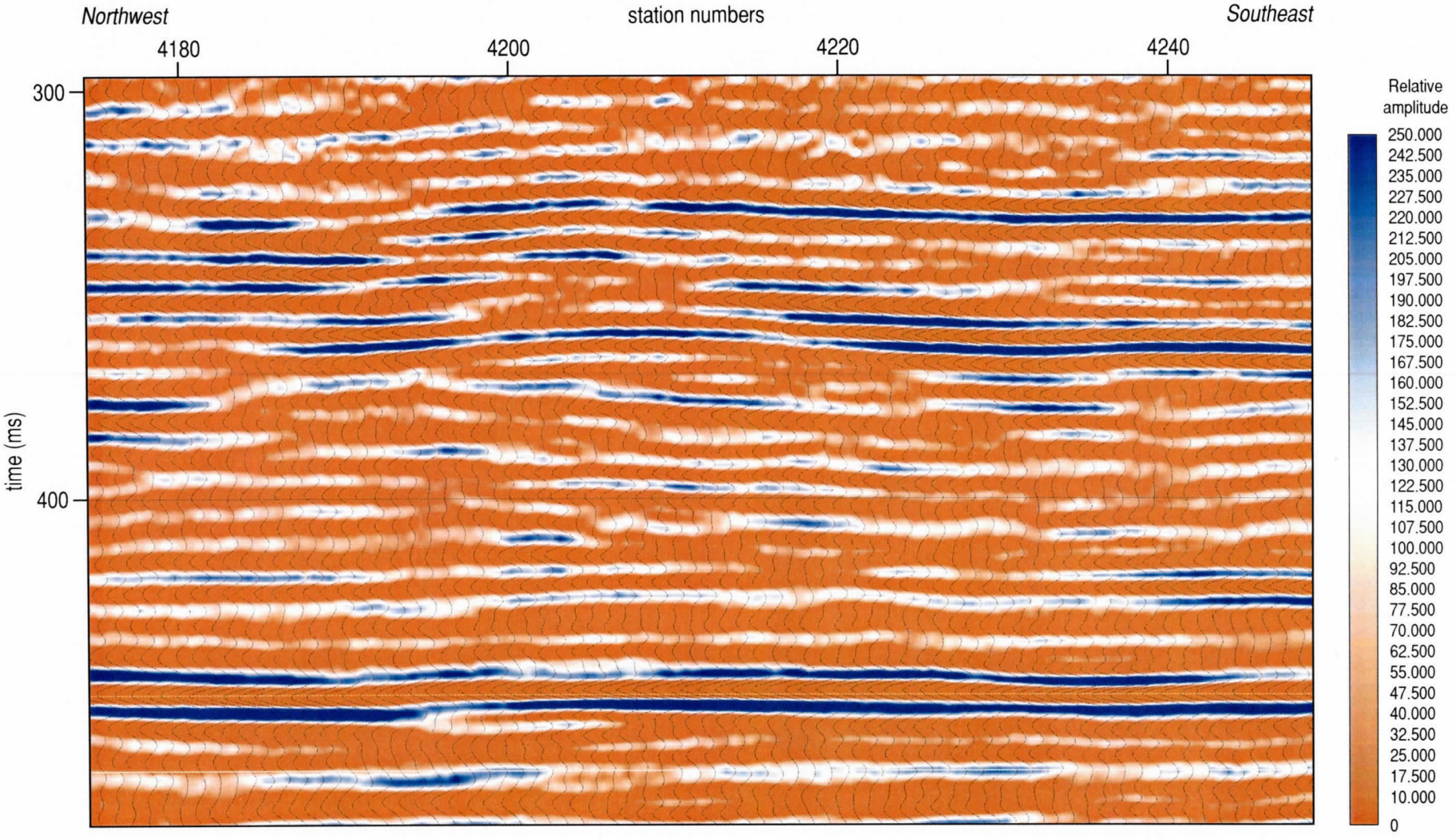

Figure 49. A zoomed-in portion of line 4 CMP stacked section focusing on the "coal interval" using color amplitude overlain by wiggle trace representation of the seismic reflection data. This display format highlights lateral amplitude variations. Several layers appear consistent across the length of this segment of the line with noteworthy variations in amplitude of the interpreted coal reflections. Unique to this portion of line 4 and the site in general is the change in reflection arrival patterns (apparent layer sequence and thickness) above 400 ms. This change likely indicates and is a measure of the amount of change in coal geometries and depositional subtleties.

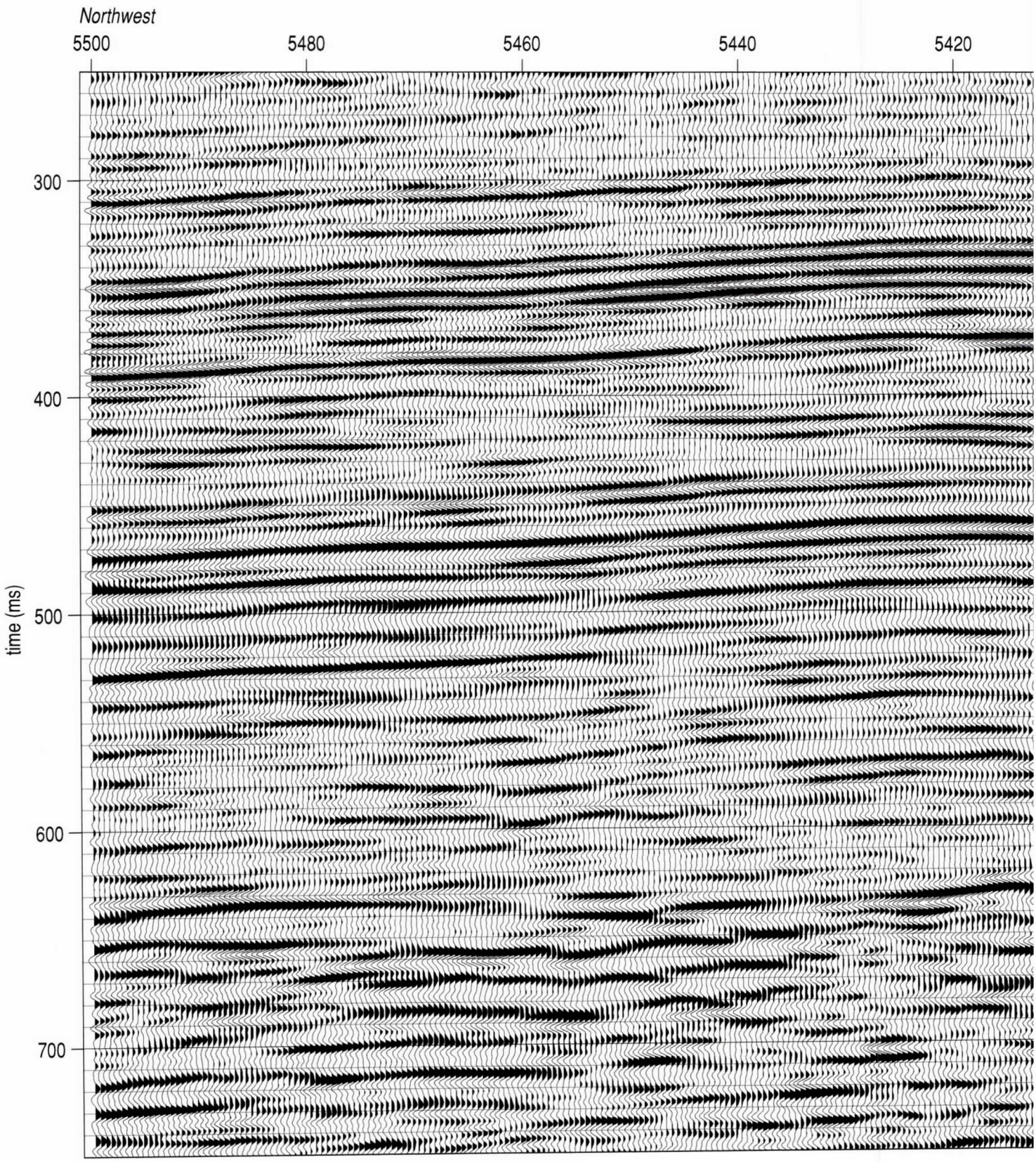

Figure 50.

50a

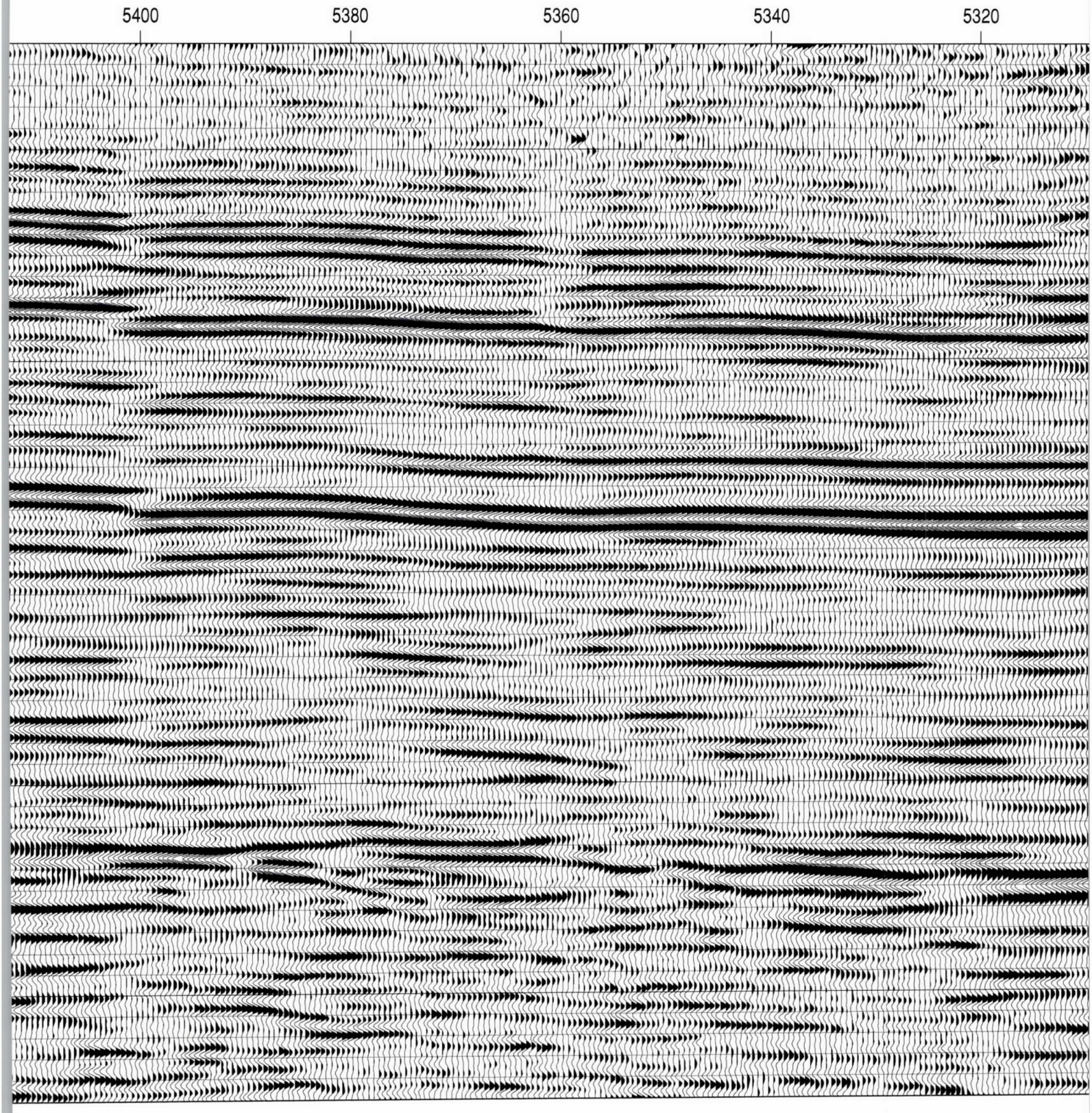
5400
5380
5360
5340
5320

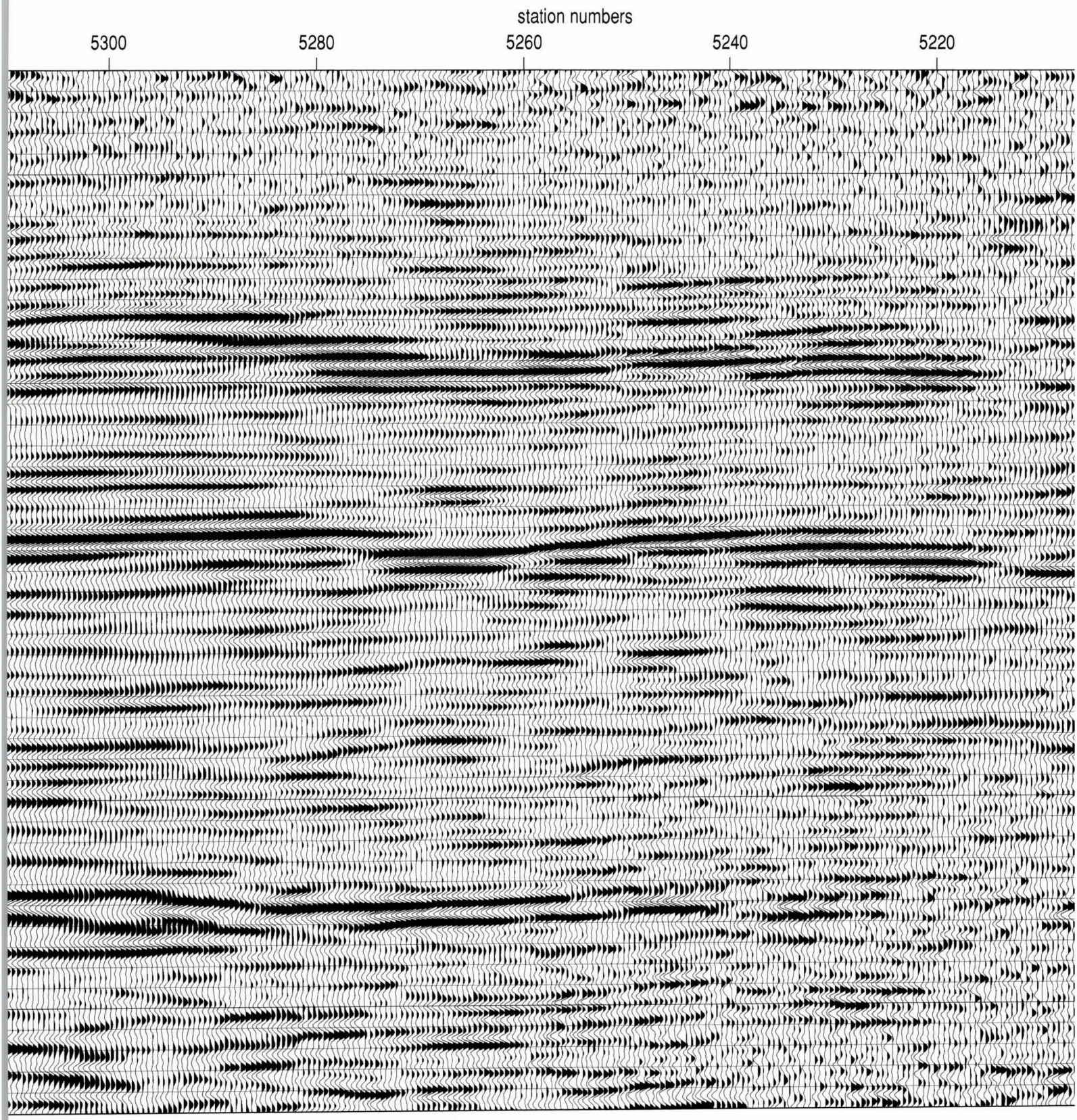

50c

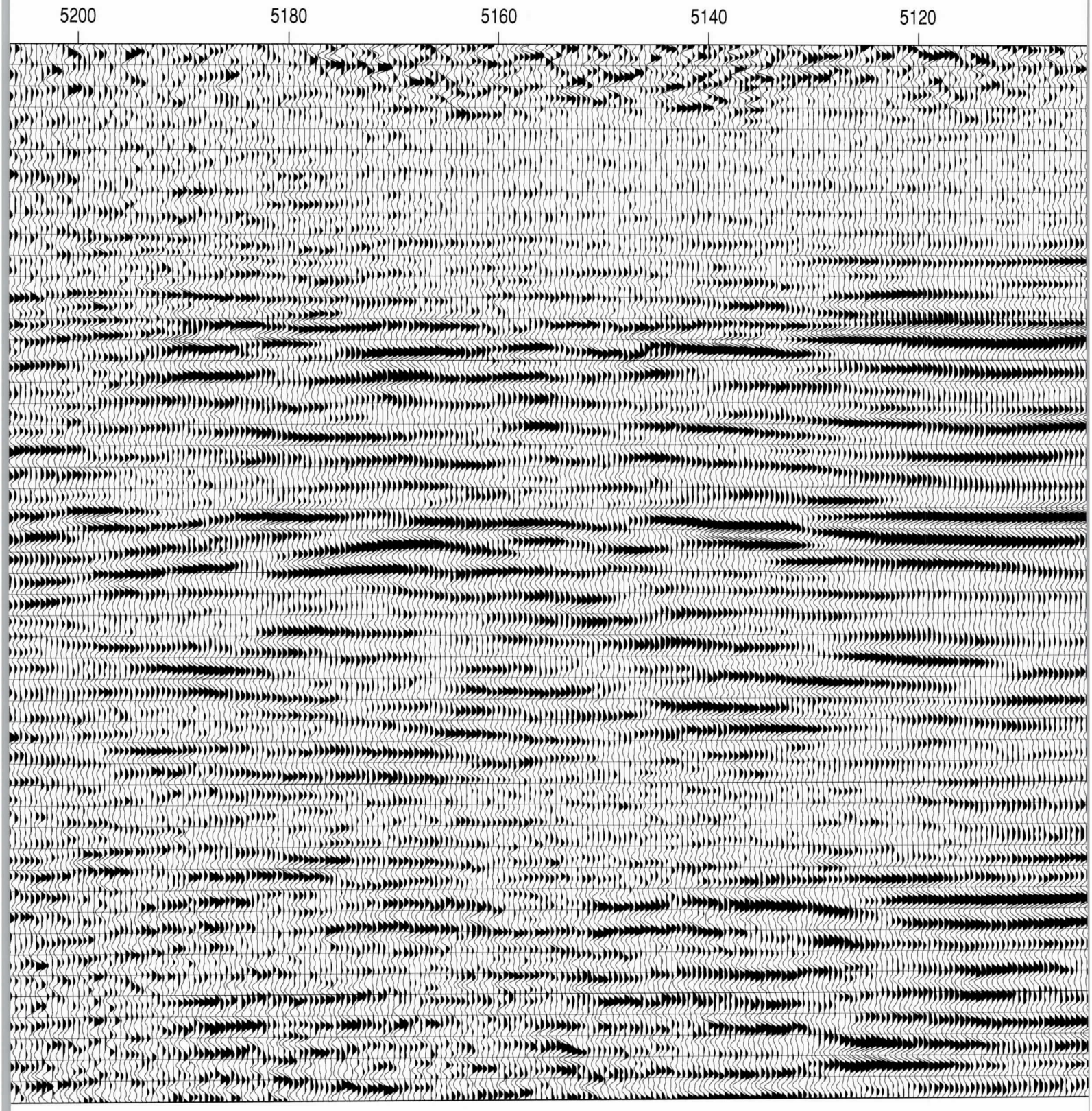

50d

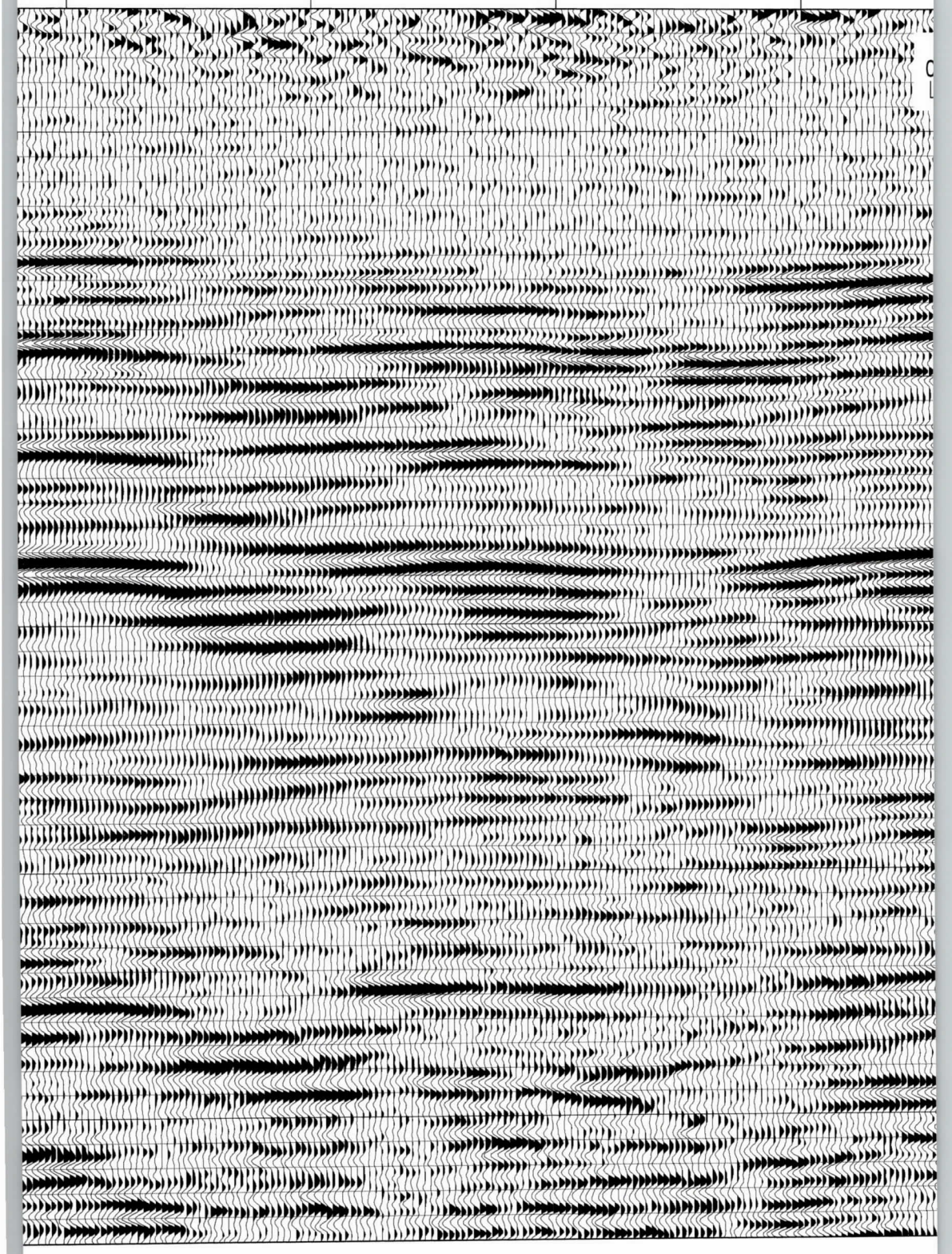

5e

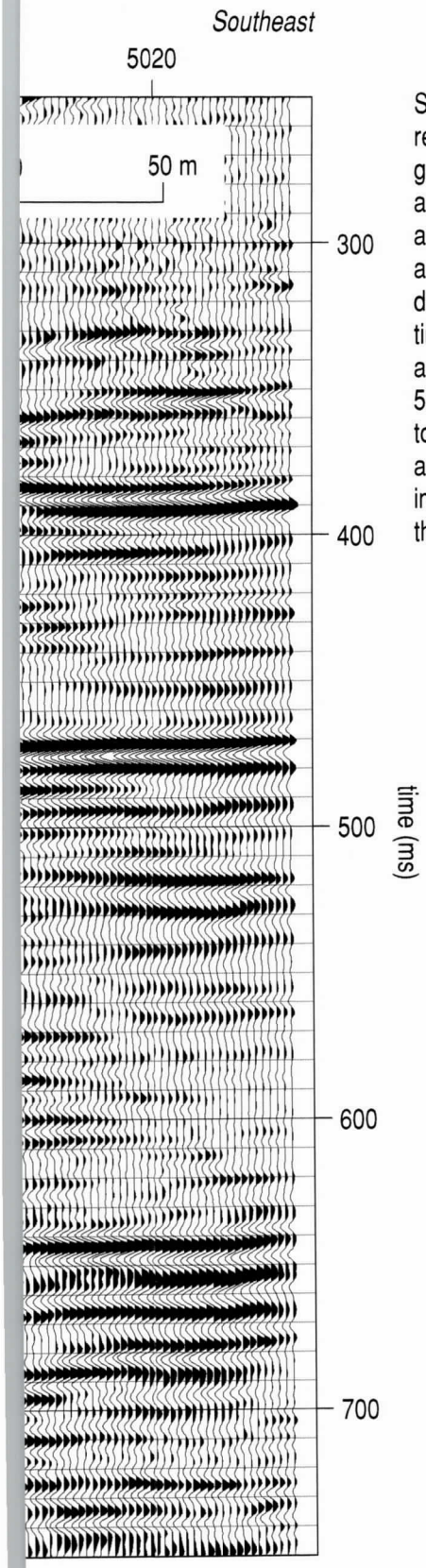

Southeast portion of line 5 CMP stacked seismic reflection section with upper 250 ms cropped. Several groups of coherent reflections can be interpreted across the length of this section and from line to line around the site. With the average velocity to the high amplitude coherent reflections around 2000 m/s, depth estimates are a 1-to-1 correlation between time (ms) and depth (meters) (e.g., 400 ms is approximately equal to 400 m). Southeast of station 5280 the general wavelet characteristics and signal-to-noise ratio changes, with much less consistency in amplitude and dominant frequency. The data quality improves southeast of station 5160 but not back to the level northwest of 5280.

5of

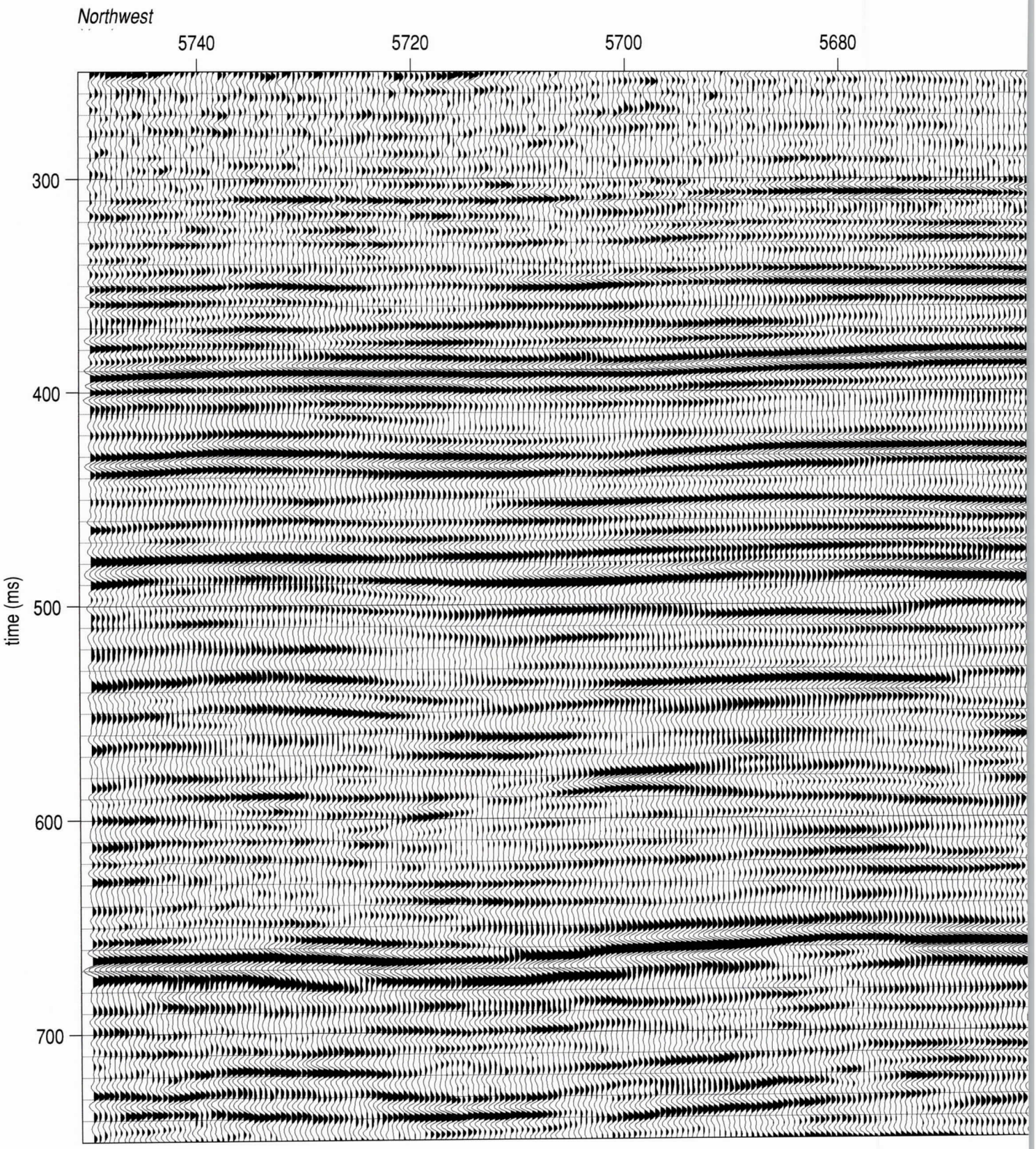

Figure 51.

5/a

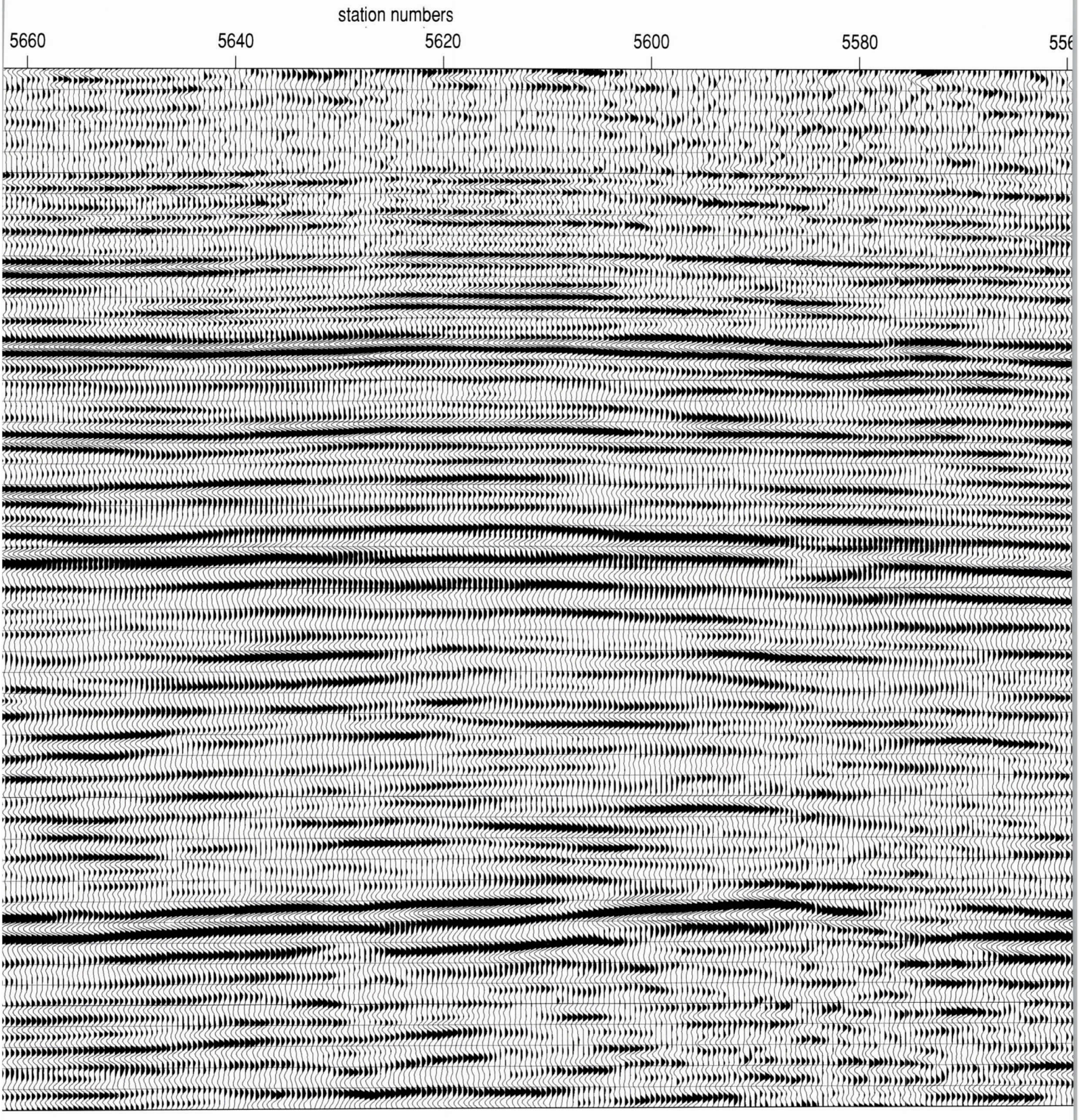
station numbers
5660
5640
5620
5600
5580
556

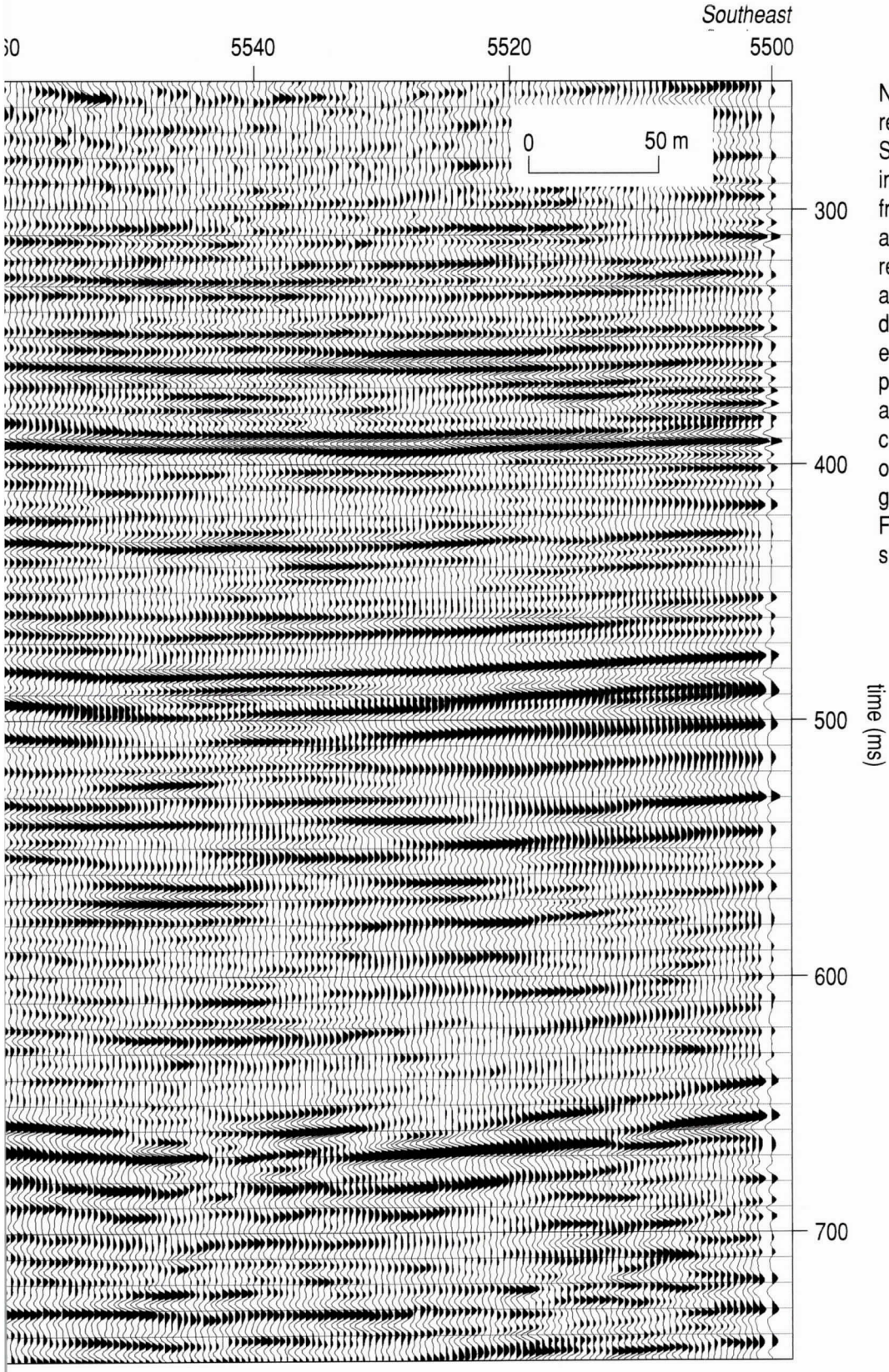

Northwest portion of line 5 CMP stacked seismic reflection section with upper 250 ms cropped. Several groups of coherent reflections can be interpreted across the length of this section and from line to line around the site. With the average velocity to the high amplitude coherent reflections around 2000 m/s, depth estimates are a 1-to-1 correlation between time (ms) and depth (meters) (e.g., 400 ms is approximately equal to 400 m). Overall data quality on this portion of the profile is as good or better than any other location surveyed. The surface conditions here were likely the worst in terms of cultural noise. This portion of the profile goes directly through the residential part of Fort Yukon and has several bends that require special compensation.

5/c

The same six reflections have been color correlated with equivalent reflections on the other stacked sections (Figures 52 and 53). The most pronounced and dramatic structure on line 5 is the fault beneath station 5400. This bed offset and its associated diffraction pattern (interpreted below the basement reflection in dark pink) provide the evidence for the fault interpretation and line-to-line correlations of this feature. Offset is estimated to be around 10 m along the fault. With almost 50 m horizontal resolution, some smearing of the fault plane is to be expected and is obvious adjacent to the fault beneath station 5280. The offset in reflections associated with this fault is obvious, but because of smearing due to the size of the Fresnel zone the interpreted fault plane appears to dissect coherent reflection events. The apparent sag in reflections between the top of the coal interval and basement between stations 5600 and 5480 forms a structure referred to here as a "synform." This synform structure and other similar features on interpreted seismic sections are bracketed by near-vertical lines (green). These synforms are in all cases in proximity to the major faults (blue). Both synforms and major faults were correlated between lines using displacement orientation and amount, general shape and unique physical characteristics, horizon contours, diffraction patterns, and relative positions of each. Amplitude and frequency data assisted these extrapolation and correlation methods, making unique determinations of connectivity between the structures as they appeared on different lines.

A higher density of coherent reflection is present on line 5 than on any other line (Figure 54). Unlike other profiles, reflections within the upper 300 ms can be interpreted through the noise on the northeastern end of line 5. Between stations 5400 and 5500 the coal interval seems to extend upward to include another set of high amplitude reflections between 300 and 350 ms. On other lines the orange event has been interpreted as being the 365 m deep coal stringer that was encountered during coring along line 1. Within the 500 m interval between stations 5400 and 5500 the 391 m stringer appears to have been joined by several reflective layers several meters thick or has thickened to as much as 30 m and now includes reflective interbedded clays. Either way, along this seismic line the percentage of coal in the sedimentary section has increased by possibly as much as 30%. Unlike observations on line 4, reflections within the coal interval appear very coherent, possessing consistent wavelet properties.

On frequency plots the "coal interval" can be identified by its characteristic higher dominant frequency (Figure 55). The reflection at 480 ms is significantly higher amplitude and lower frequency than reflections from within the "coal interval." This 480 ms reflection clearly defines a boundary between two markedly different sequences of materials. A major fault interpretable at station 5400 on these plots does not show up as a significant event on the amplitude wiggle trace plots. Data near the radar station and slough are of lower frequency and signal-to-noise ratio, likely due to near-surface and cultural effects. Beneath stations 5320 and 5580 data from the lower half of the sedimentary section are of notably lower frequency than other data arriving at equivalent times along the profile. At both locations these spectral anomalies are in close proximity to faults. Frequency might prove to be an important attribute in characterizing the CBM potential of these coals once representative physical samples can be correlated with spectral properties.

Amplitude data highlight the many individual reflection events presumably coal related within the "coal interval" (Figure 56). In some settings increased reflectivity with a uniform layer, as evidenced in higher amplitude reflection wavelets, is consistent with trapped gas (Miller et al., 2000). In coal settings the increased permeability created by faults can increase gas

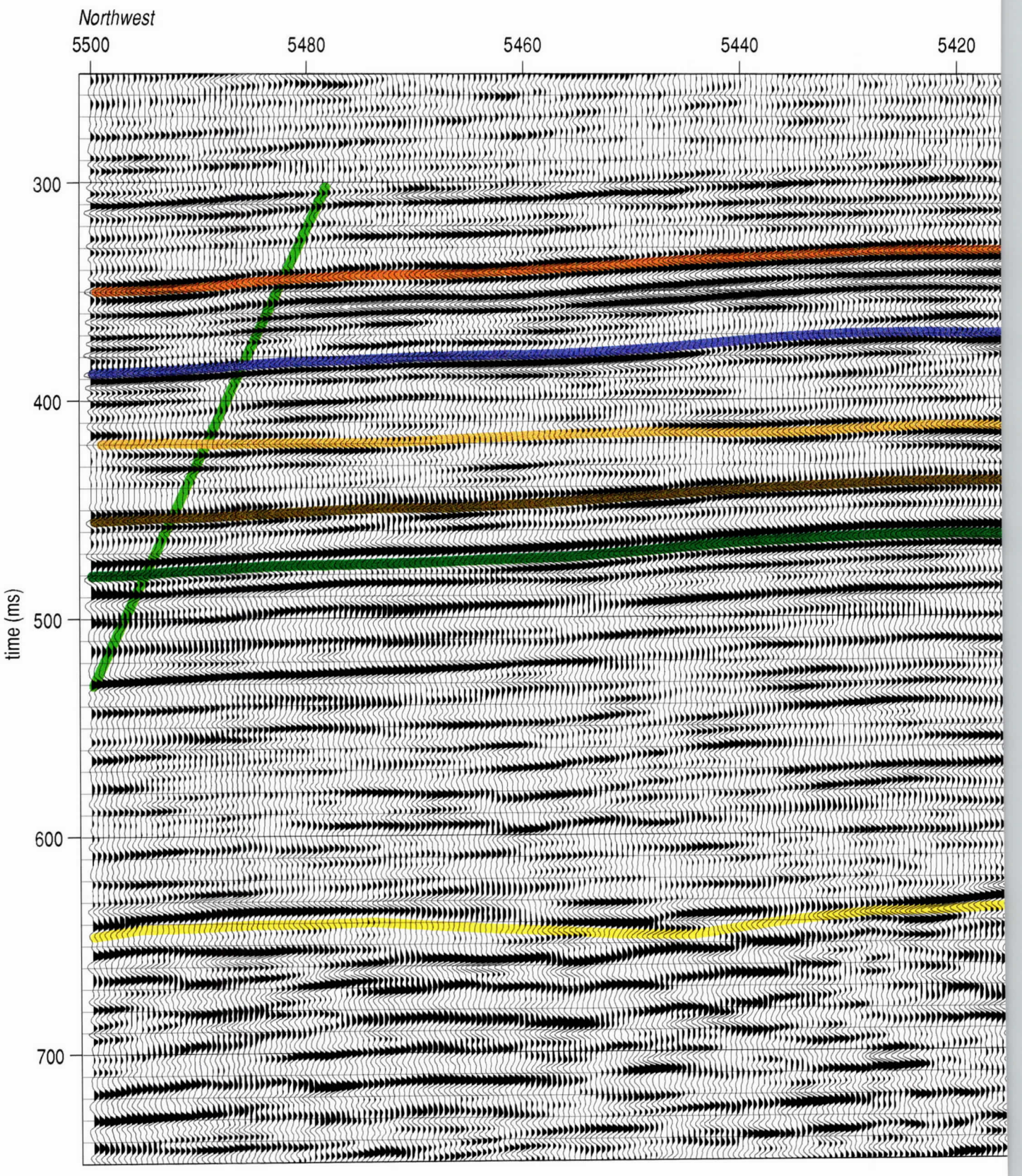

Figure 52.

52a

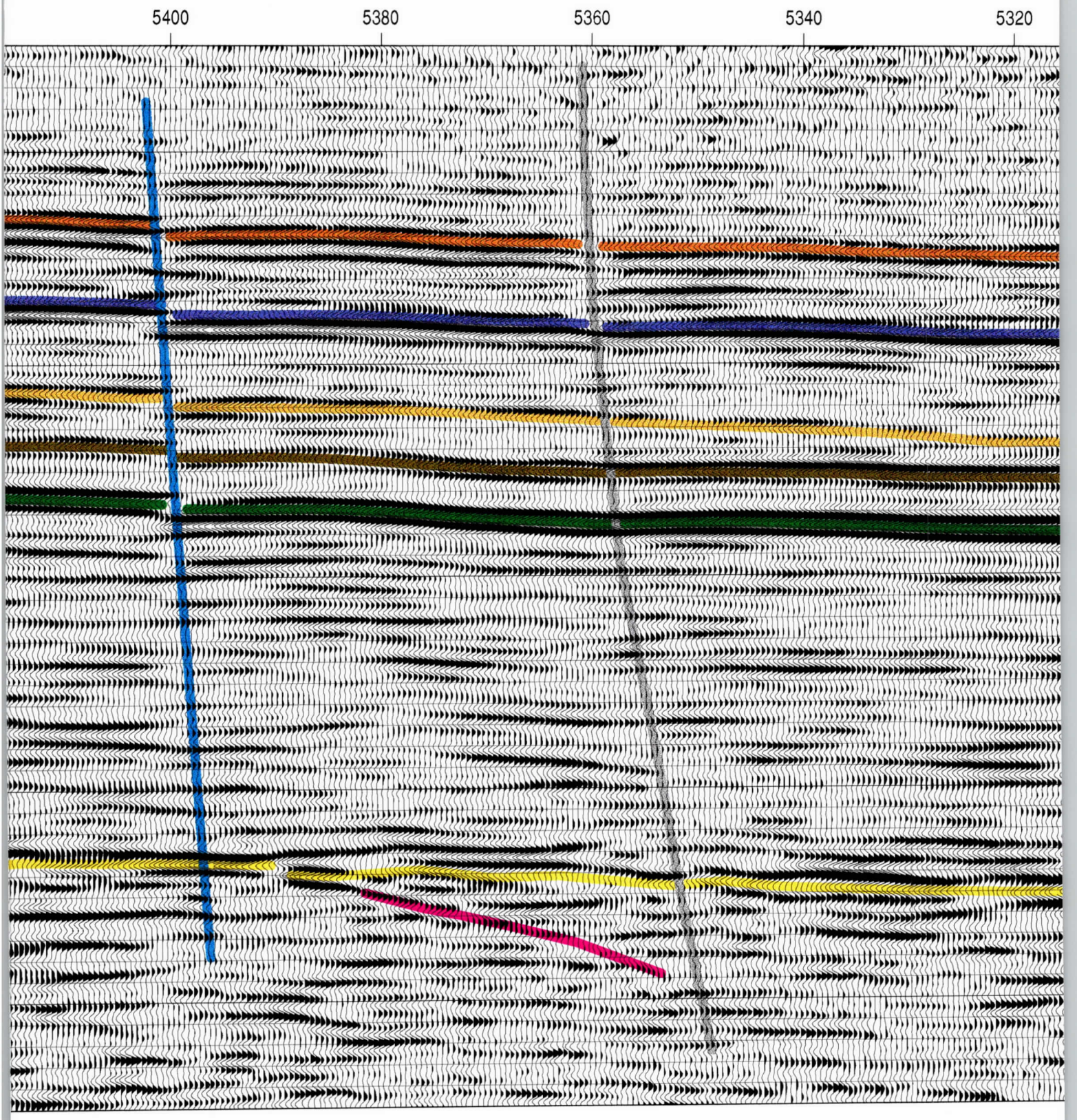
5400
5380
5360
5340
5320

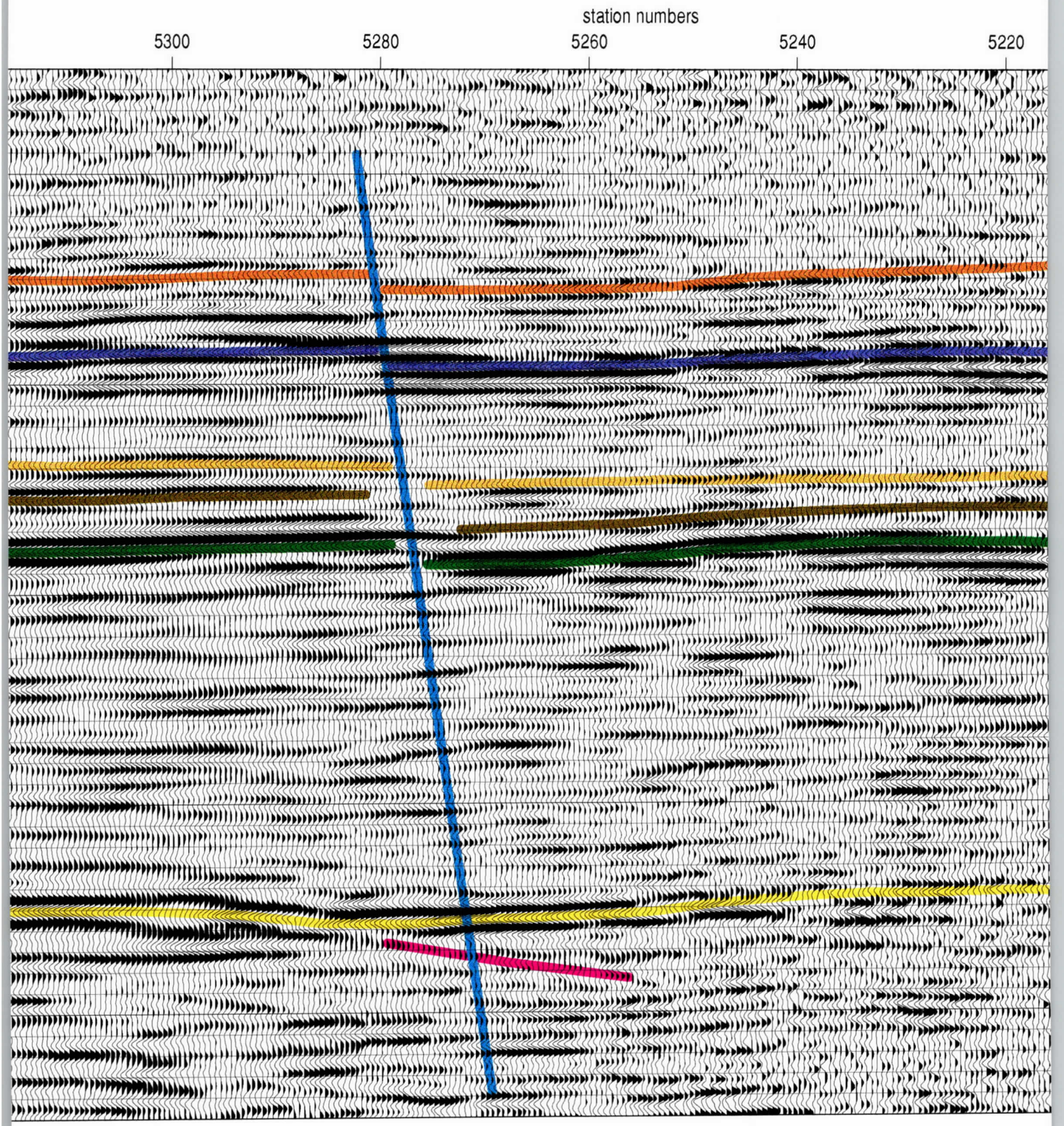

52c

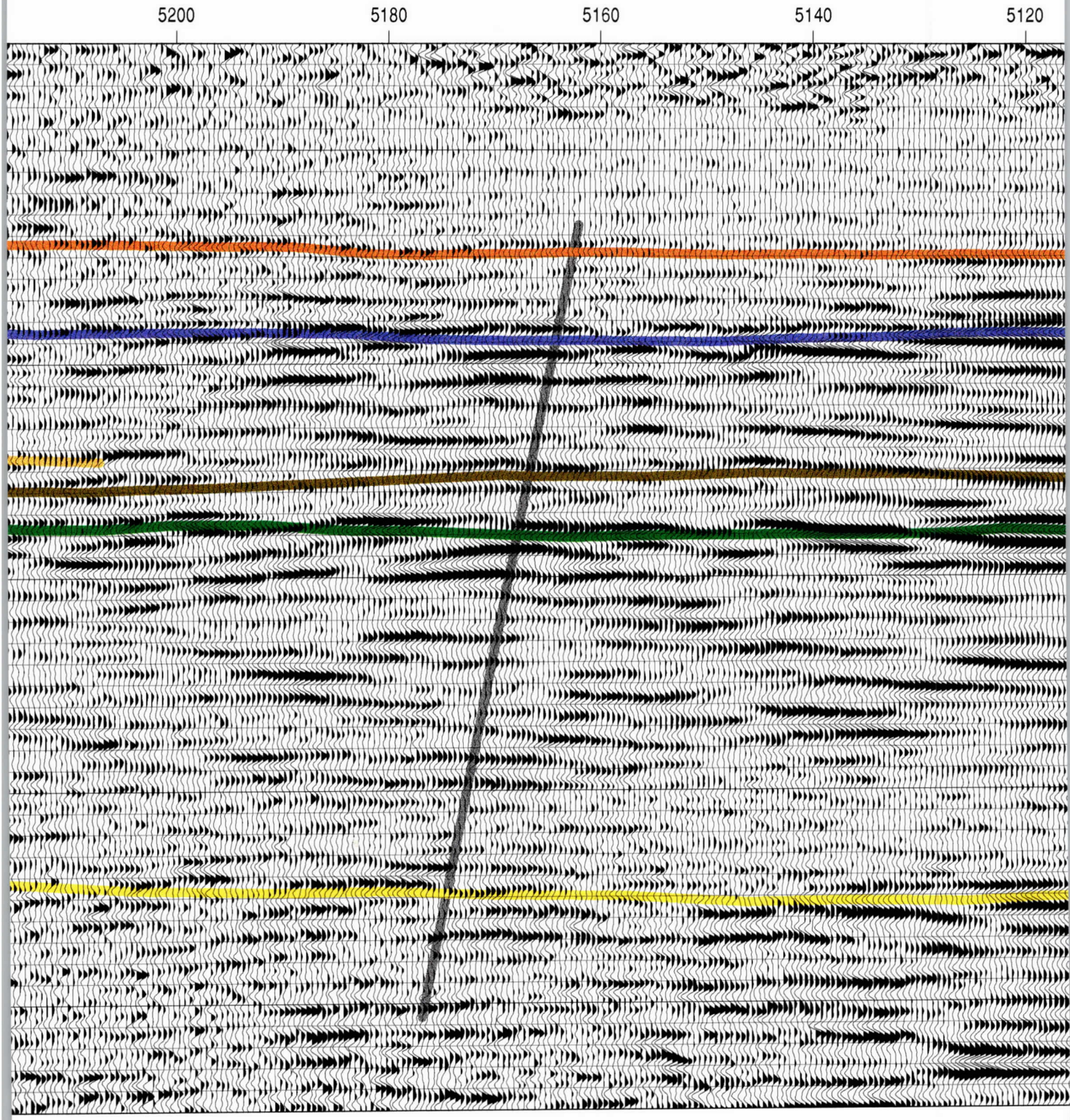

52d

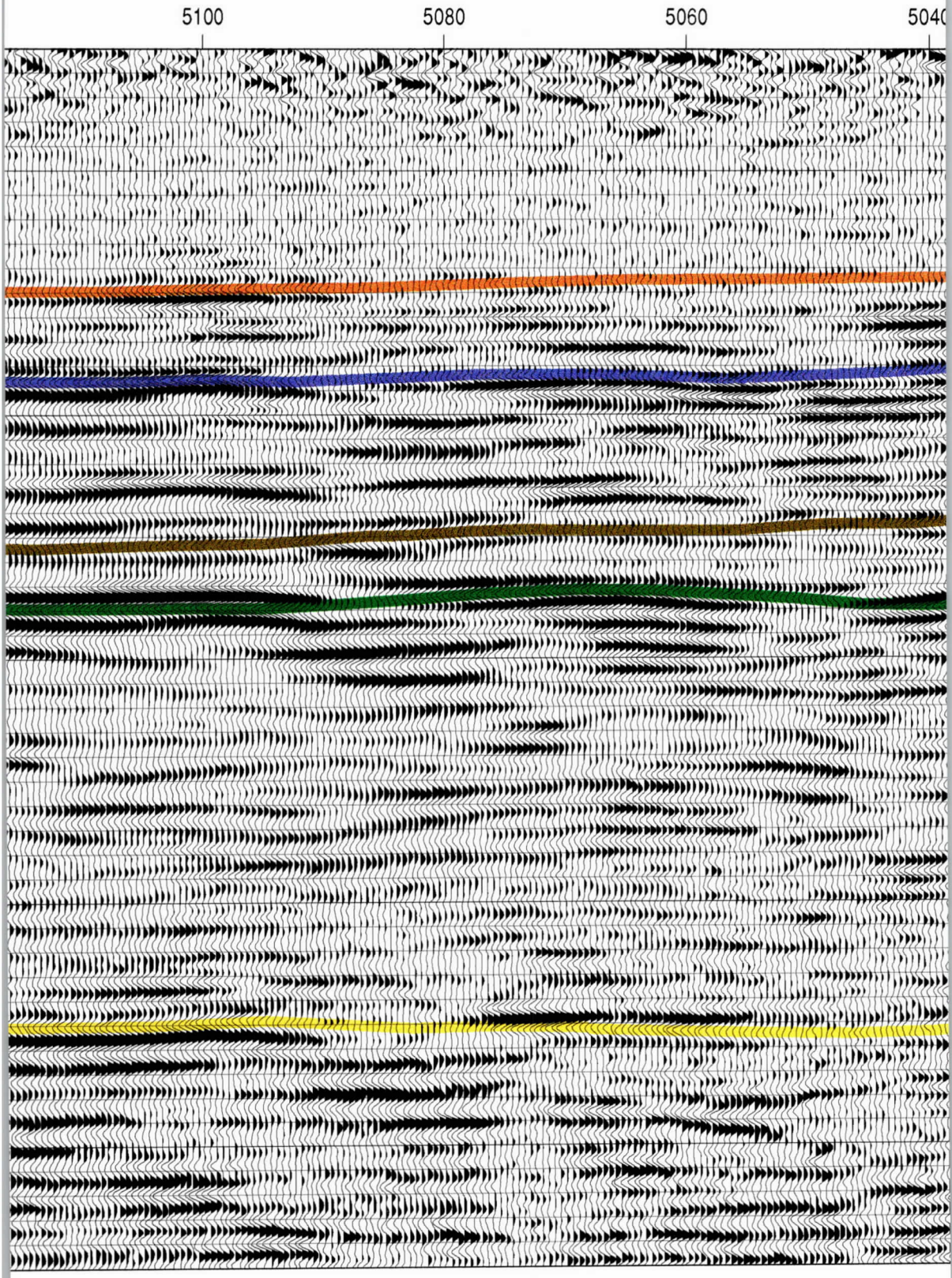

52e

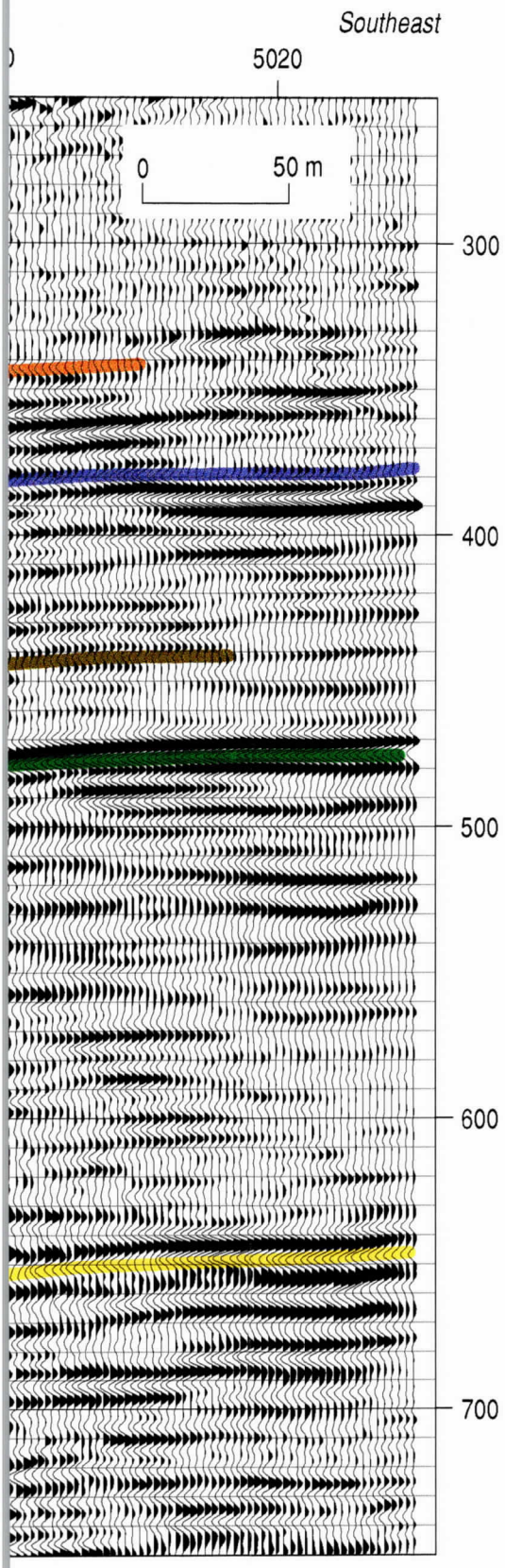

Southeast portion of line 5 CMP stacked seismic reflection section with upper 250 ms cropped and sitewide coherent and correlatable reflections interpreted with a sitewide consistent color sequence. The highest amplitude events are within the interval interpreted to be coal rich. Based on the only drill hole in the area, the orange event is the 365 m coal encountered in the corehole and the purple event is the 391 m coal that was penetrated about 9 m before drilling was curtailed. Several reflections with similar character are interpreted between the 391 m coal and about 500 ms and have been designated as the "coal interval." With the variability in the wavelet characteristics of the basement along line 5, the top of the Mesozoic section (yellow basement reflection) was interpreted based predominantly on amplitude and segmented coherency. Like line 2, several faults and fracture systems are interpreted on this profile. The most evident fault possessing classical diffraction patterns is beneath station 5400. Several of the synforms could actually be grabens, but the data does not possess the horizontal resolution to allow a confident and discernable interpretation.

- 365 m coal seam
- interpreted 391 m coal
- possible coal interface
- possible coal interface
- possible coal interface
- bedrock

52f

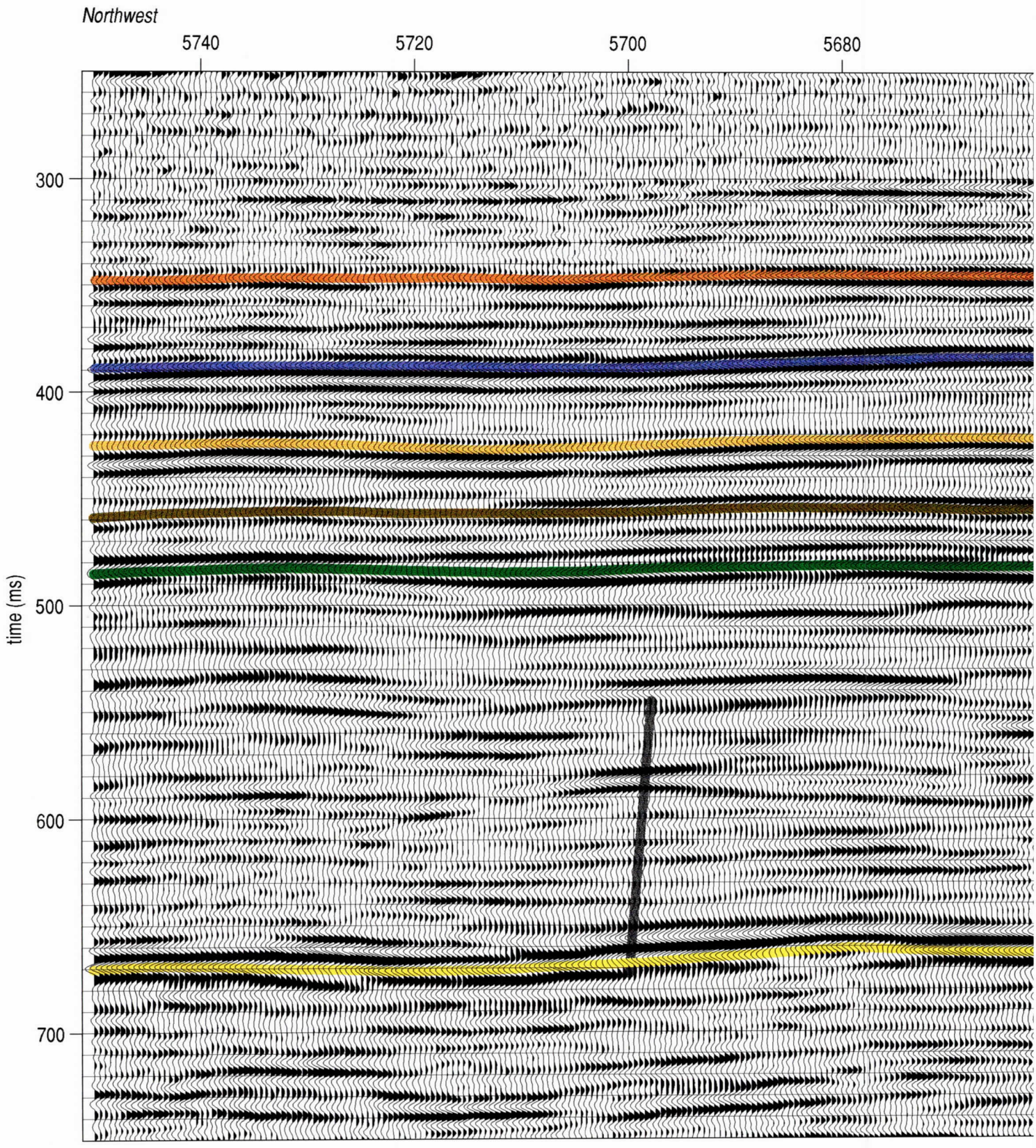

Figure 53.

53a

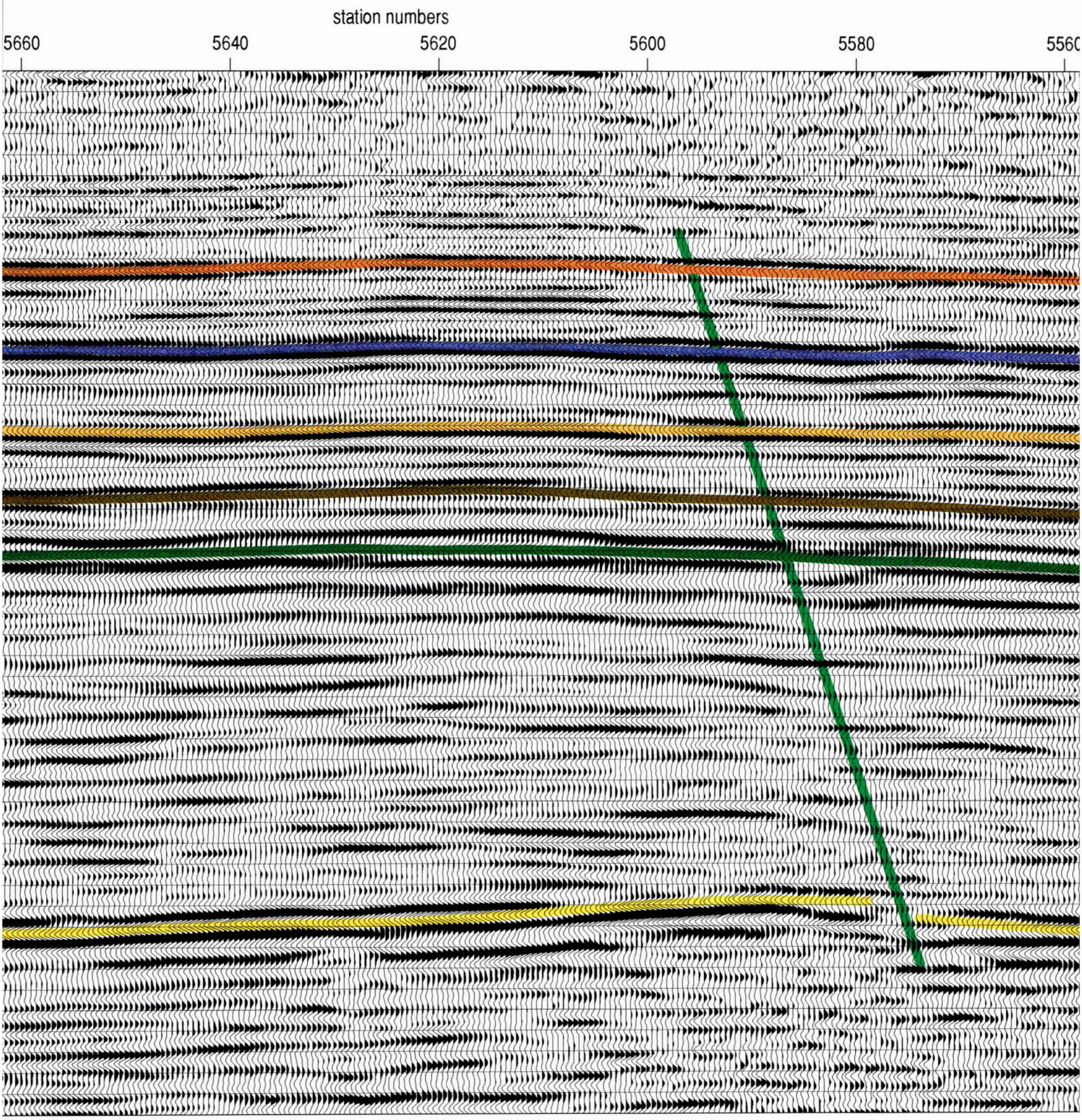
station numbers
5660
5640
5620
5600
5580
5560

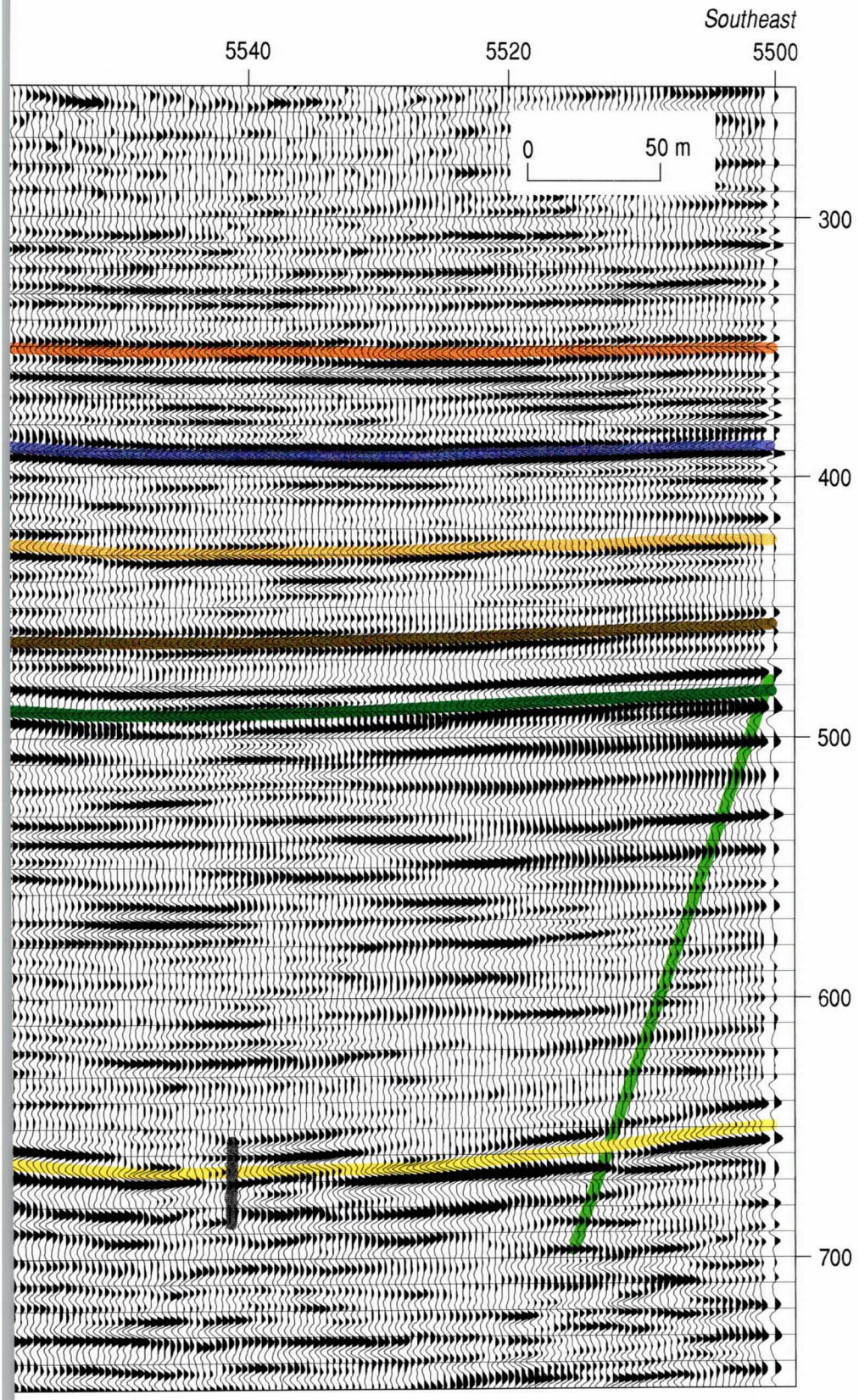

Southeast portion of line 5 CMP stacked seismic reflection section with upper 250 ms cropped and sitewide coherent and correlatable reflections interpreted with a sitewide consistent color sequence. The highest amplitude events are within the interval interpreted to be coal rich. Based on the only drill hole in the area, the orange event is the 365 m coal encountered in the corehole and the purple event is the 391 m coal that was penetrated about 9 m before drilling was curtailed. Several reflections with similar character are interpreted between the 391 m coal and about 500 ms and have been designated as the "coal interval." Consistency in the wavelet characteristics of the basement reflection along this portion of line 5 allows the top of the Mesozoic section (yellow basement reflection) to be interpreted based on several wavelet characteristics. The fault interpreted beneath station 5700 that does not penetrate the coal interval has a very pronounced diffraction pattern associated with it that clearly indicates some kind of bed termination.

- 365 m coal seam
- interpreted 391 m coal
- possible coal interface
- possible coal interface
- possible coal interface
- bedrock

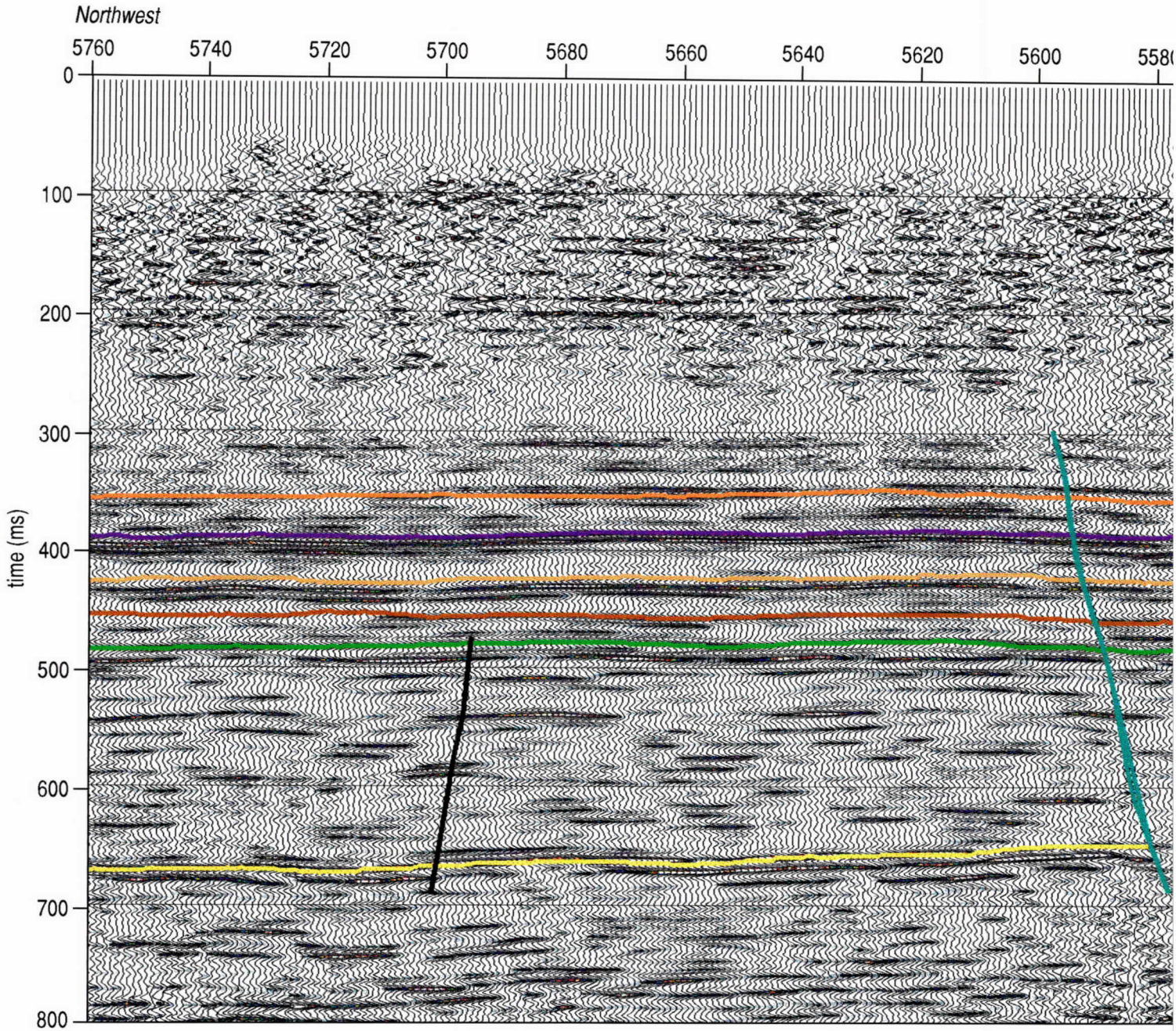

Figure 54. Line 5 CMP stacked seismic reflection section with wiggle traces overlain by color amplitude enhancement of the frequency mid-ra scheme consistent throughout this report. The lack of coherent events within the permafrost and what is identified as the sub-permafrost zon of reflections emerging from the noise are evident below 100 ms with a quiet zone (fewer reflections per unit time) between about 200 ms an extend from just above the 365 m coal down to the top of the Mesozoic section, which begins at about 650 m. These reflections possess exc This highly reflective time window interpreted as the "coal zone" is a consistent characteristic of all the seismic profiles collected in the Fort Y through 53) it is much easier to grasp the scale of the structures and layering and their dominance (or actually lack of) along the profile.

54a

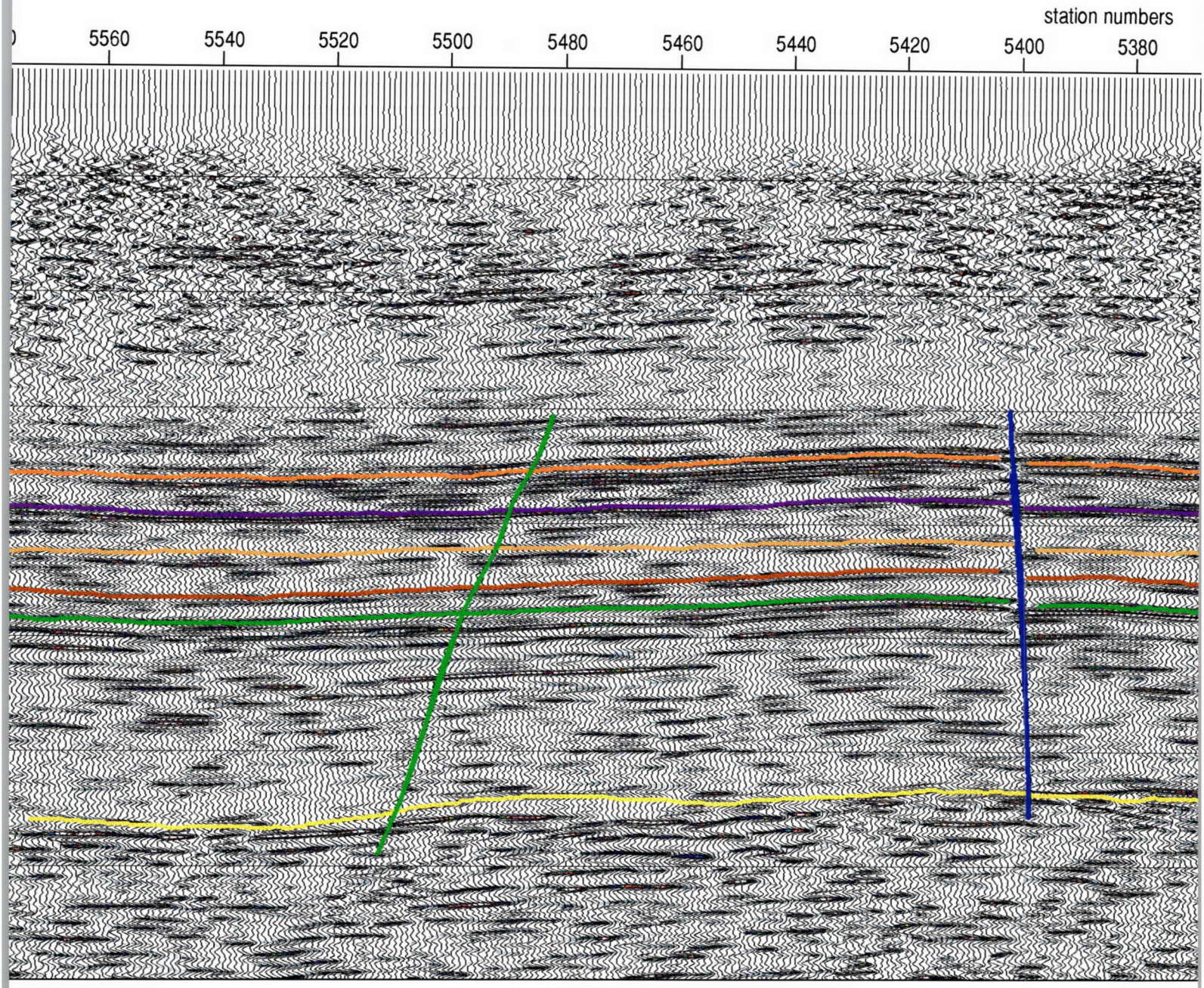

ange (140 Hz to 180 Hz) and key sitewide coherent reflection events interpreted using the color
es is very evident on this display format. Subtle indications, on the northwest end of this profile,
d the first drill-confirmed coal at about 365 m. Reflections within the coal and sub-coal interval
cellent frequency content (useable in excess of 200 Hz in some places) and sitewide coherency.
ukon area. In this vertically and horizontally compressed format (in comparison to Figures 50

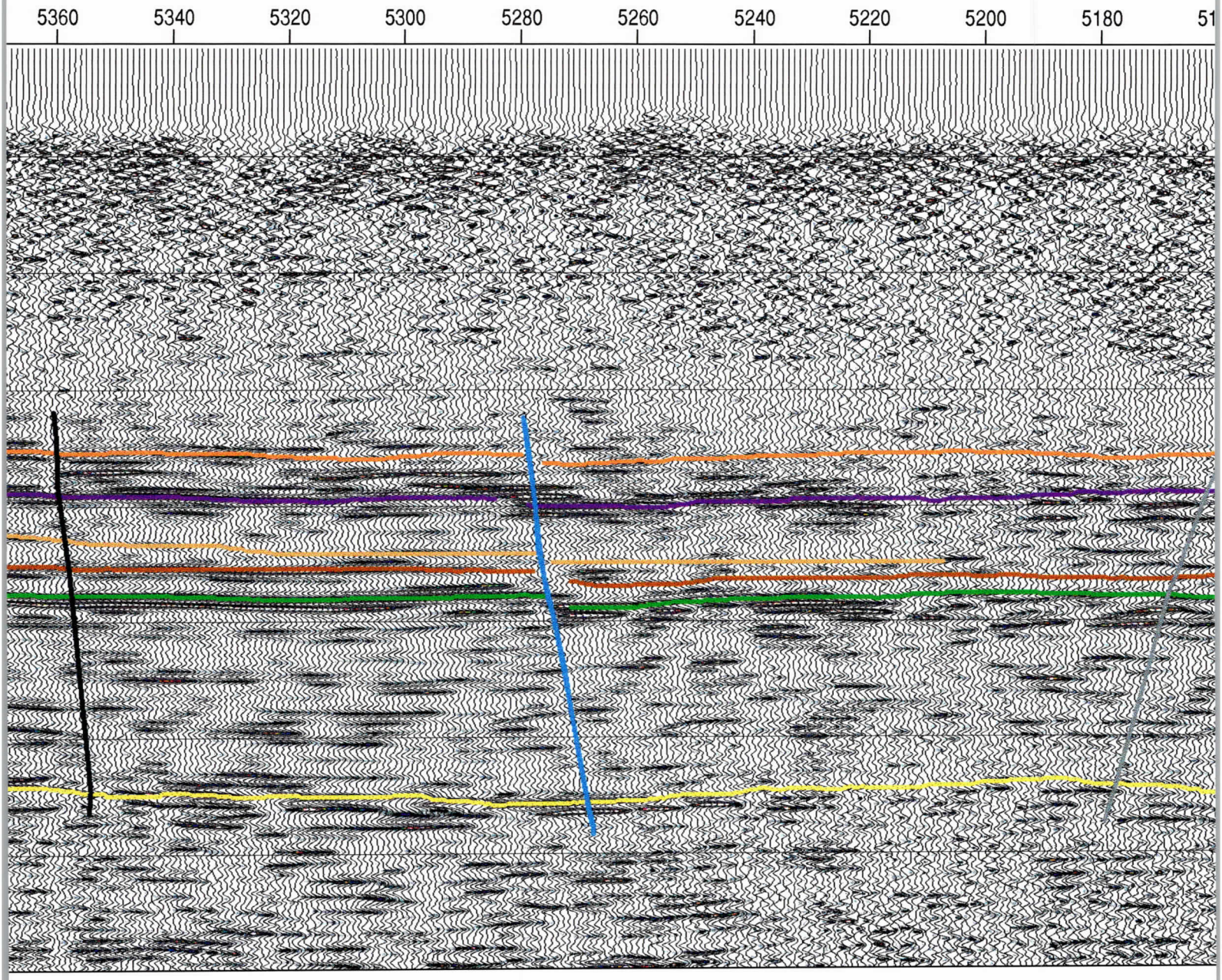

54c

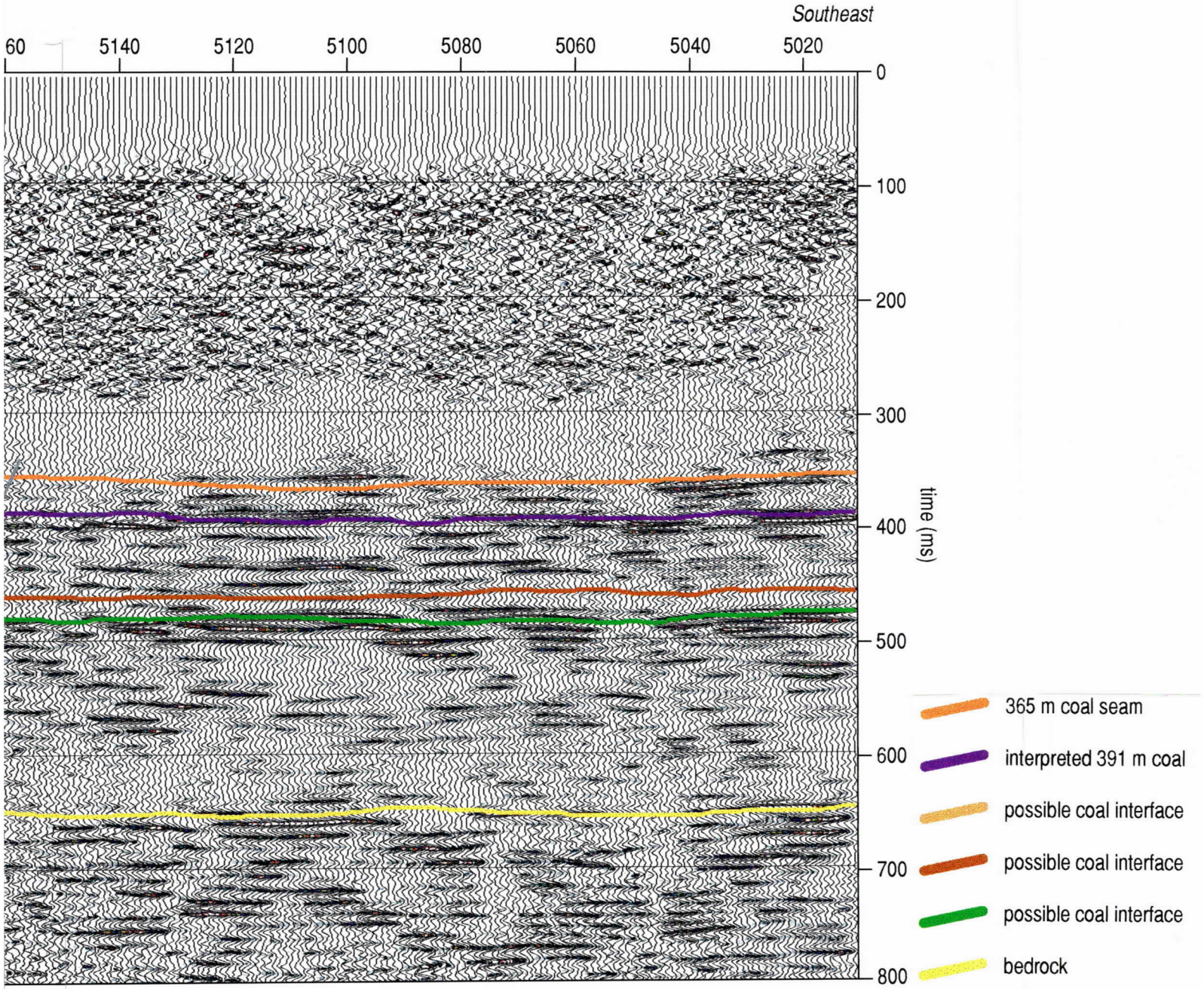
Southeast
60
5140
5120
5100
5080
5060
5040
5020
0
100
200
300
400
500
600
700
800
time (ms)
365 m coal seam
interpreted 391 m coal
possible coal interface
possible coal interface
possible coal interface
bedrock

54d

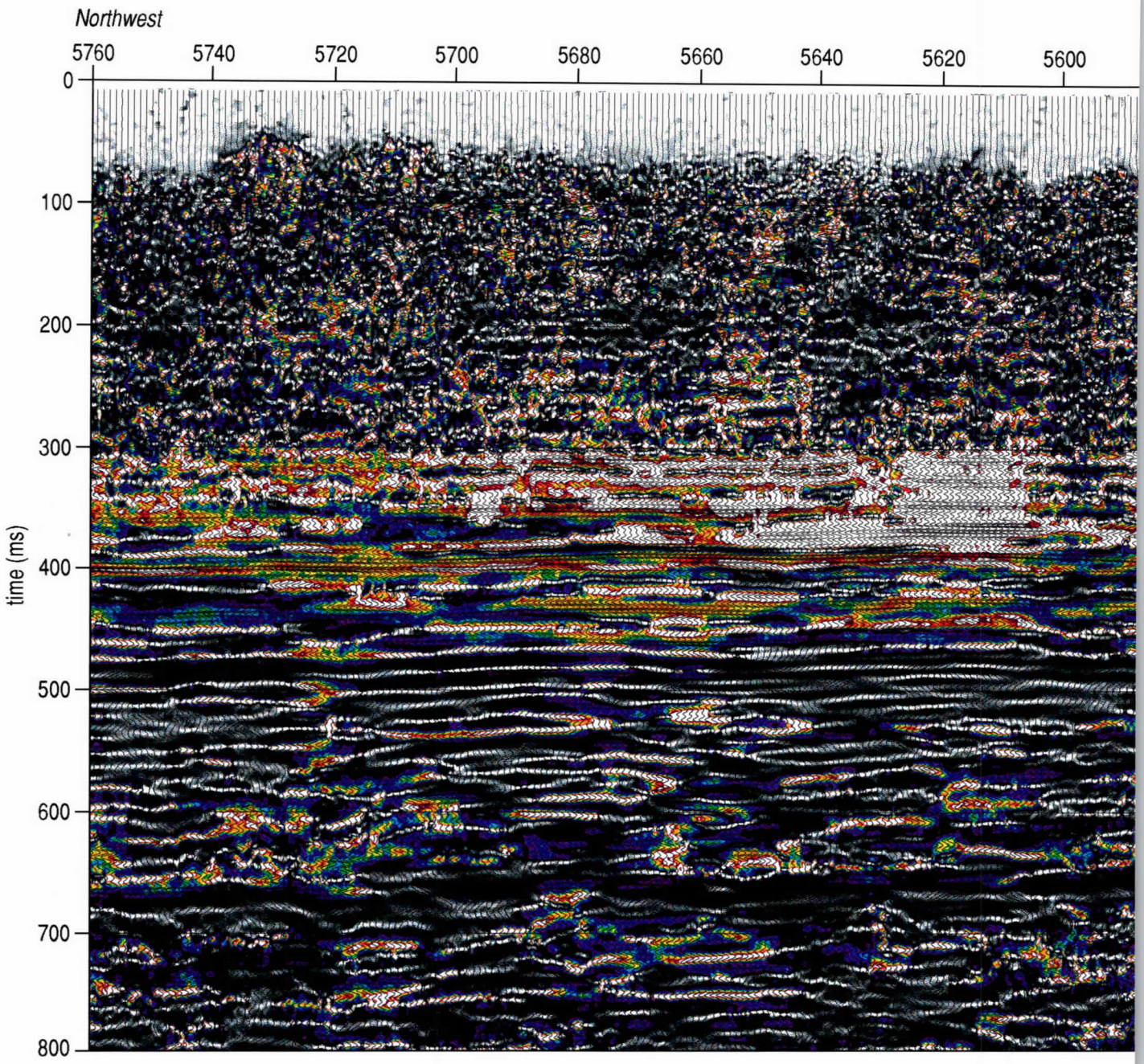

Figure 55. Line 5 CMP stacked section with instantaneous frequency overlain by wiggle trace data focusing on the frequency range b identified on frequency plots. Evident on this display is the significant increase in dominant frequency on the northwest three-quarter displays, the diffraction and unique geologic/seismic intervals are more pronounce than conventional wiggle trace displays.

55a

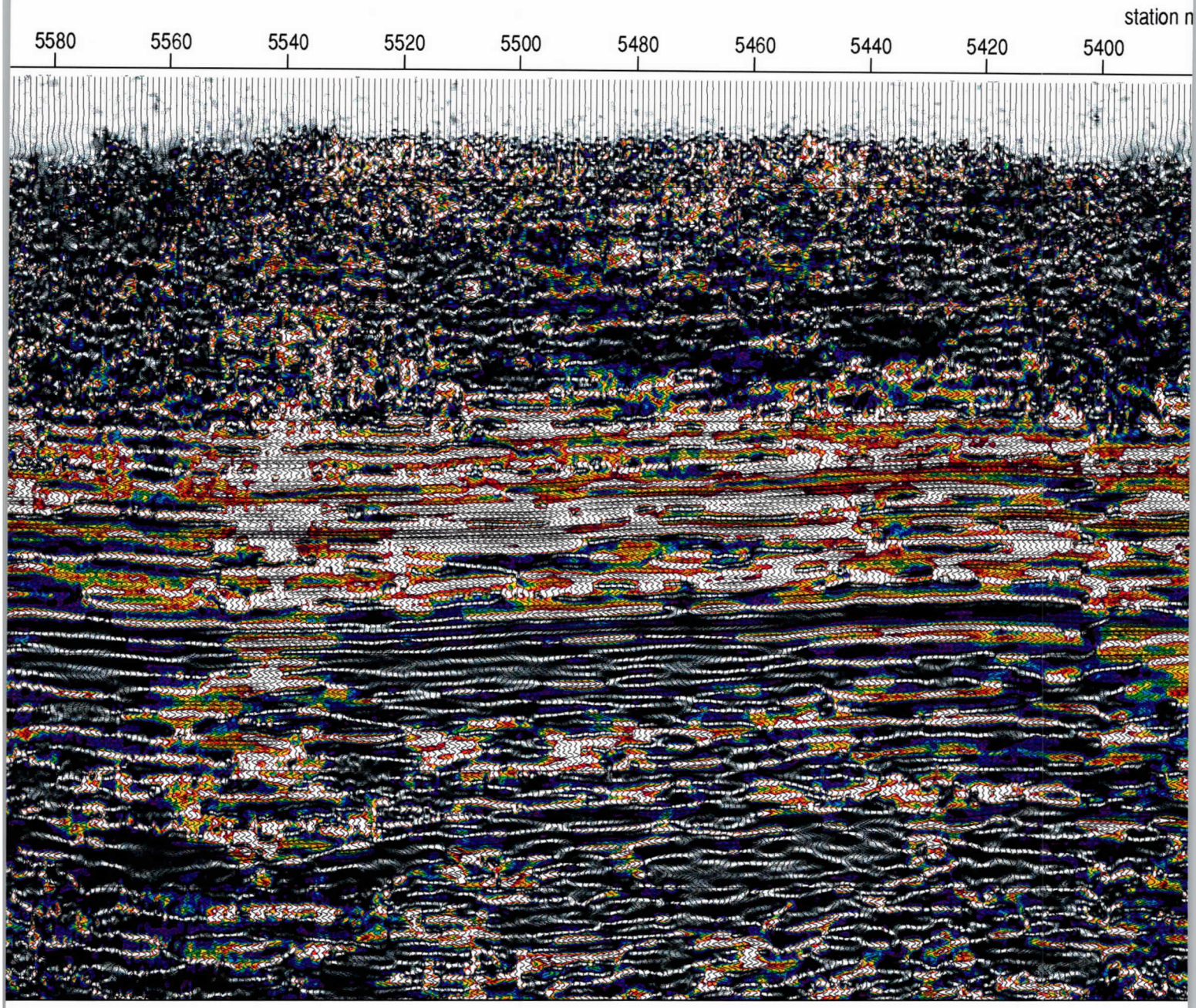

between 100 Hz and 150 Hz. Changes in reflection character, and therefore geology, can be easily
s of the profile and within the coal interval (350 ms to 500 ms). As on other instantaneous frequency

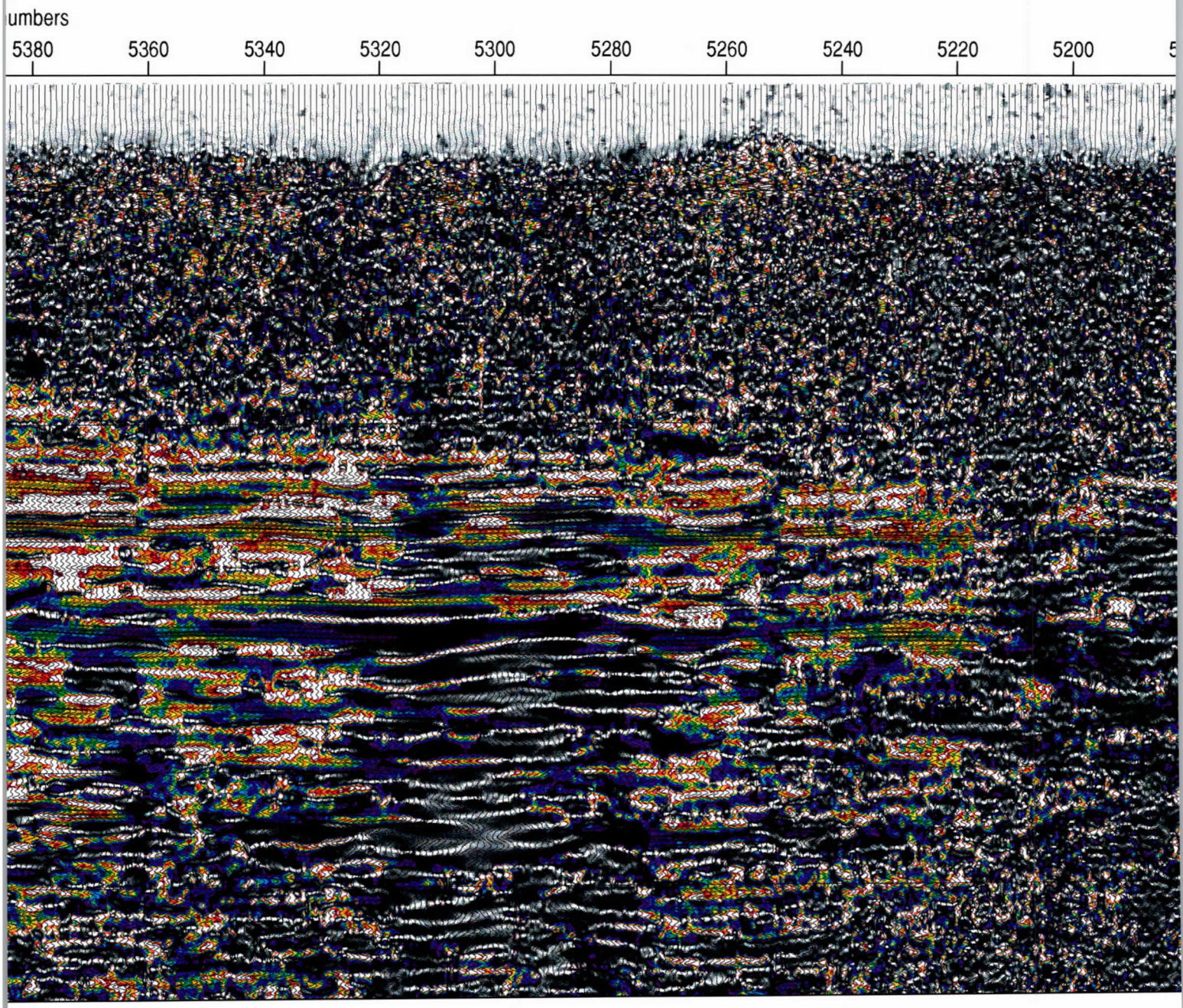

55C

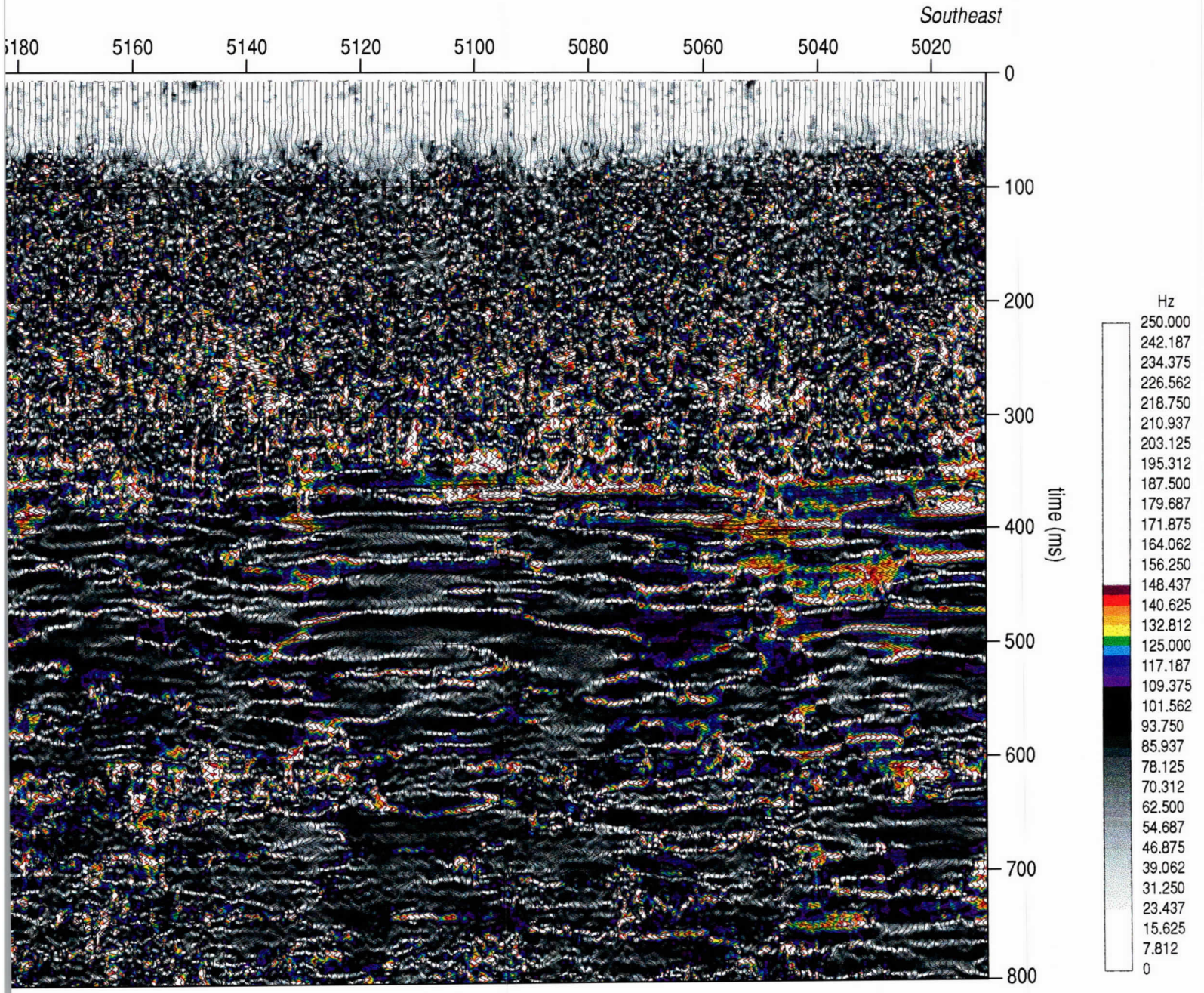
Southeast
5180
5160
5140
5120
5100
5080
5060
5040
5020
0
100
200
300
400
500
600
700
800
time (ms)
Hz
250.000
242.187
234.375
226.562
218.750
210.937
203.125
195.312
187.500
179.687
171.875
164.062
156.250
148.437
140.625
132.812
125.000
117.187
109.375
101.562
93.750
85.937
78.125
70.312
62.500
54.687
46.875
39.062
31.250
23.437
15.625
7.812
0

55d

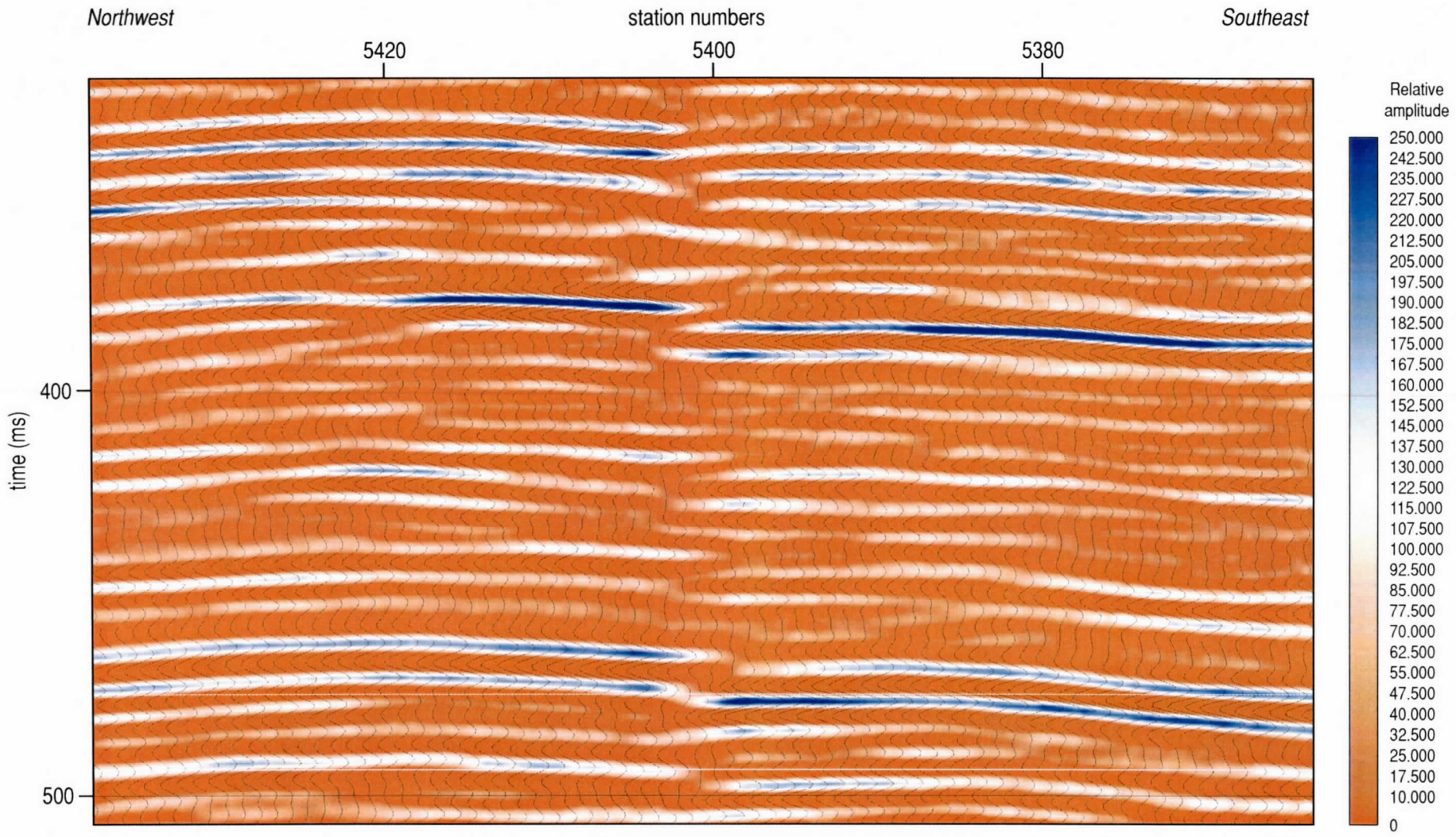

Figure 56. A zoomed-in portion of line 5 CMP stacked section focusing on the "coal interval" using color amplitude overlain by wiggle trace representation of the seismic reflection data. This display format highlights lateral amplitude variations. This portion of the profile focuses on the most pronounced fault interpreted on all profiles. Of particular interest is the apparent increase in amplitude near the fault itself. Based on the method of gas desorption from coal, faults or fractures provide the exposed surface necessary and therefore one would expect higher gas concentrations near faults and fractures. Bright spots or localized high amplitude reflections are indicative of increased gas content. If drilling bears out this interpretation, then bright spot technology might be a key component of any seismic program targeting coal bed methane.

concentrations and therefore production in proximity to those faults. This interpretation is, of course, speculative since ground truth correlations between materials, material properties, and seismic attributes have not been confidently established. Lateral changes in amplitude from 25% to 50% were measured in both the 390 ms and 480 ms reflection events across distances less than 100 m. Considering the horizontal resolution of these data, physical changes occurring over distances of less than 50 m cannot be uniquely located.

Line 6

Reflection arrival patterns, amplitudes, and frequency characteristics are reasonably consistent across the entire line 6 profile (Figure 57). The east end of line 6 comes within a few hundred meters of line 1 and the corehole. Vertical discontinuities in reflections seem to define blocks of reflectors with rotational components, making the interpretations along this line somewhat unique in comparison to the other six profiles. Interpreting abrupt, small relative displacement bed offsets that are near vertical as faulting is a bit presumptuous. Near-vertical disturbances in bedding that translate throughout a reflection section can be diagnostic of near-surface variability related to signal-to-noise or static rather than true geologic features. Obvious drops in amplitude along a near-vertical offset plane beneath stations 6055 and 6065 are consistent with near-surface effects, such as ice lakes or variable permafrost, but amplitude drops here associated with the change in reflection dip appear to be consistent with the synforms synonymous with small offset faulting interpreted on other lines in this area.

Faulting is prevalent along line 6 (Figure 58). Overall displacement as measured across the entire profile is minimal, and considering the orientation of the profile and its location on the eastern extreme of the survey area, correlating this area of high density faulting with other profiles has not been possible. The strike of this fault zone cannot be established through either shape or orientation matching with other lines or from the horizon topography. A small synform is consistent with one interpreted on lines 2 and 7 and defined by the green lines on the west end of the profile. The trend of this structure is relatively consistent with the contours of the reflecting horizons (Figures 67-72). Interpreting these disturbances in reflections as faulting is supported by the obvious abrupt dip changes each block experiences as defined by these near-vertical anomalies. Considering the abrupt nature and high signal-to-noise along the identified fault surface it is reasonable to suggest line 6 intersected these faults at nearly right angles. Faults are interpreted in red along line 6 and do not have a strike that can be clearly determined with these data.

Compressing the scale of the wiggle trace display and overlaying the color amplitude data emphasizes the lateral continuity of the “coal interval” and improves segregation of the four unique reflecting intervals (Figure 59). Within the coal interval there is a minimum of five distinguishable events that, with the exception of where the apparent faults interrupt their coherency, are easily traced across the section. The shape of the synform interpreted near the north end and the bounding faults all match with synforms interpreted on lines 2, 5, and 7.

Little unique information can be extracted from the frequency representation of these data (Figure 60). The coal interval has its characteristic higher frequency nature, consistent with

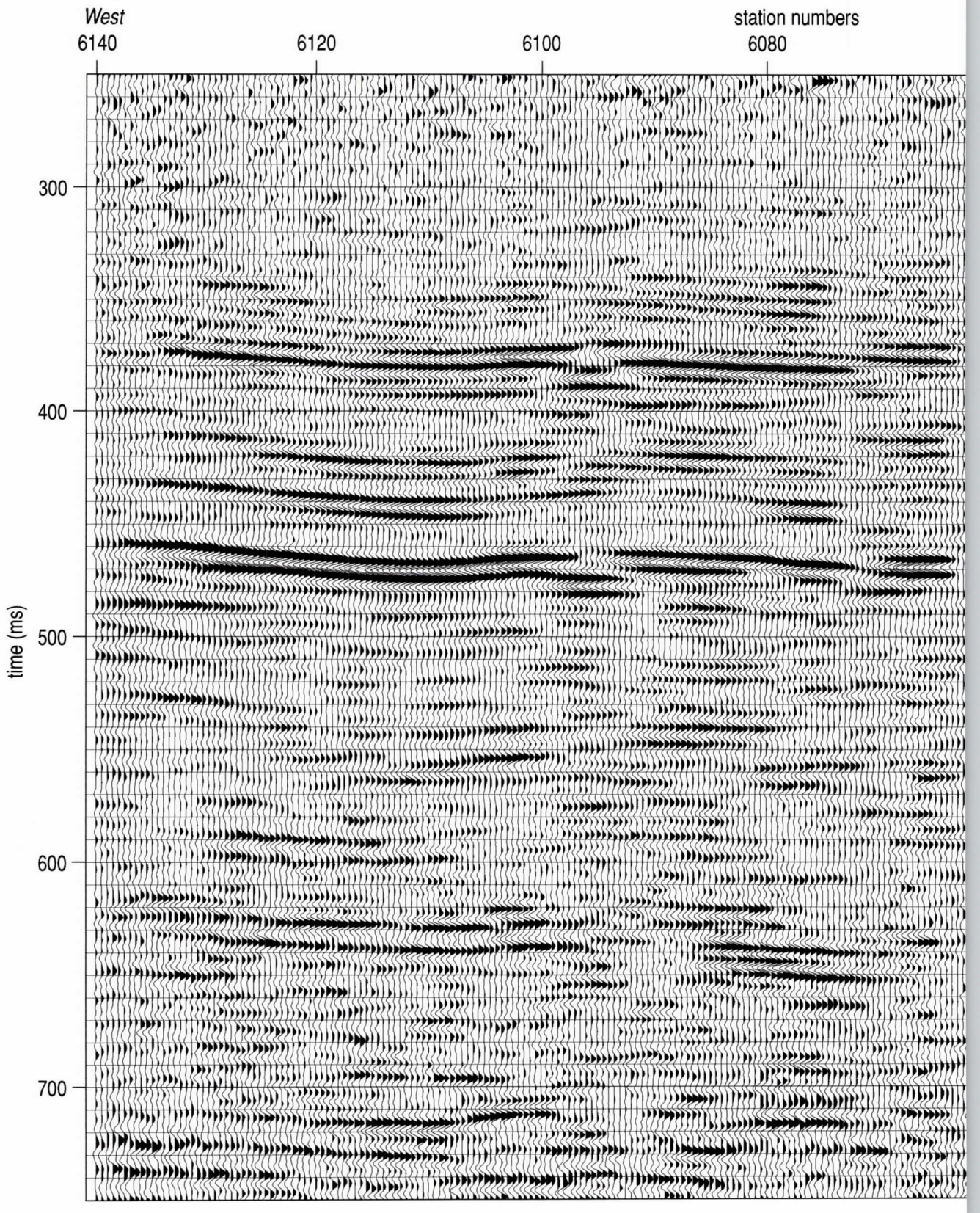

Figure 57.

57a

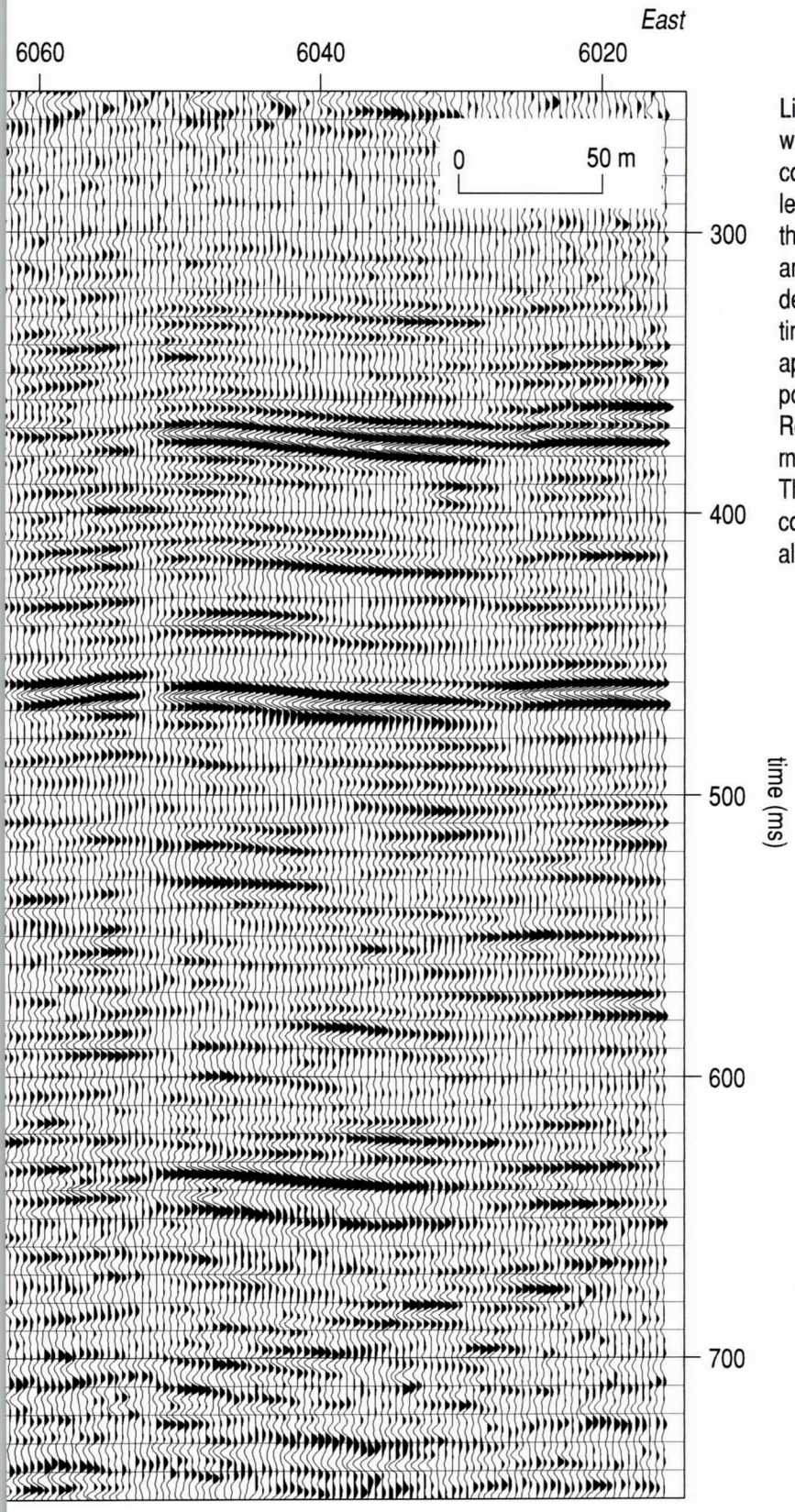

Line 6 CMP stacked seismic reflection section with upper 250 ms cropped. Several groups of coherent reflections can be interpreted across the length of this section and from line to line around the site. With the average velocity to the high amplitude coherent reflections around 2000 m/s, depth estimates are a 1-to-1 correlation between time (ms) and depth (meters) (e.g., 400 ms is approximately equal to 400 m). Data from line 6 possess the least distinctive coal interval. Reflections that can be correlated sitewide are more difficult to confidently interpret on this line. This difference was likely related to the thawing conditions along this path through the timber along the U.S. Air Force property boundary.

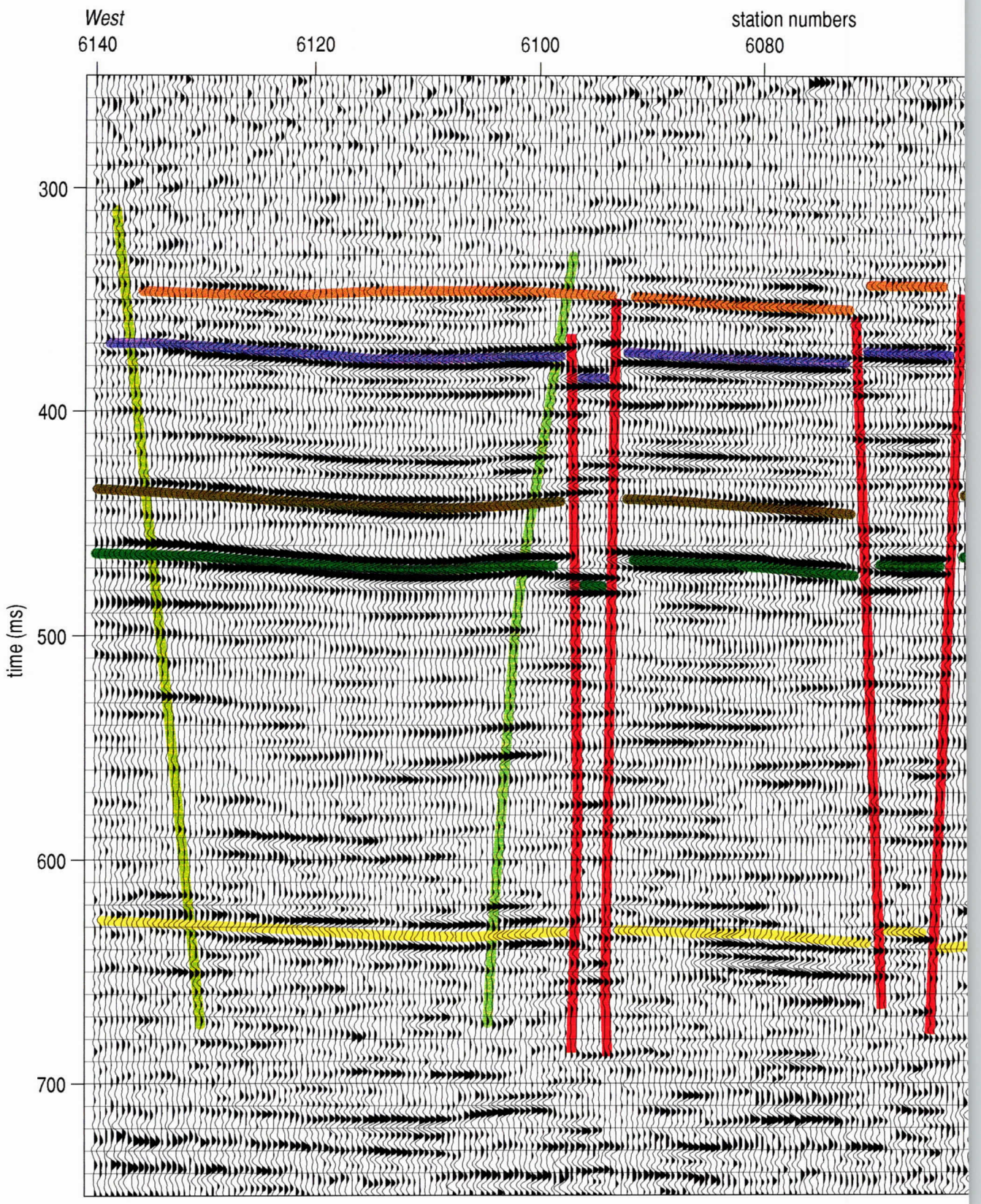

Figure 58.

58a

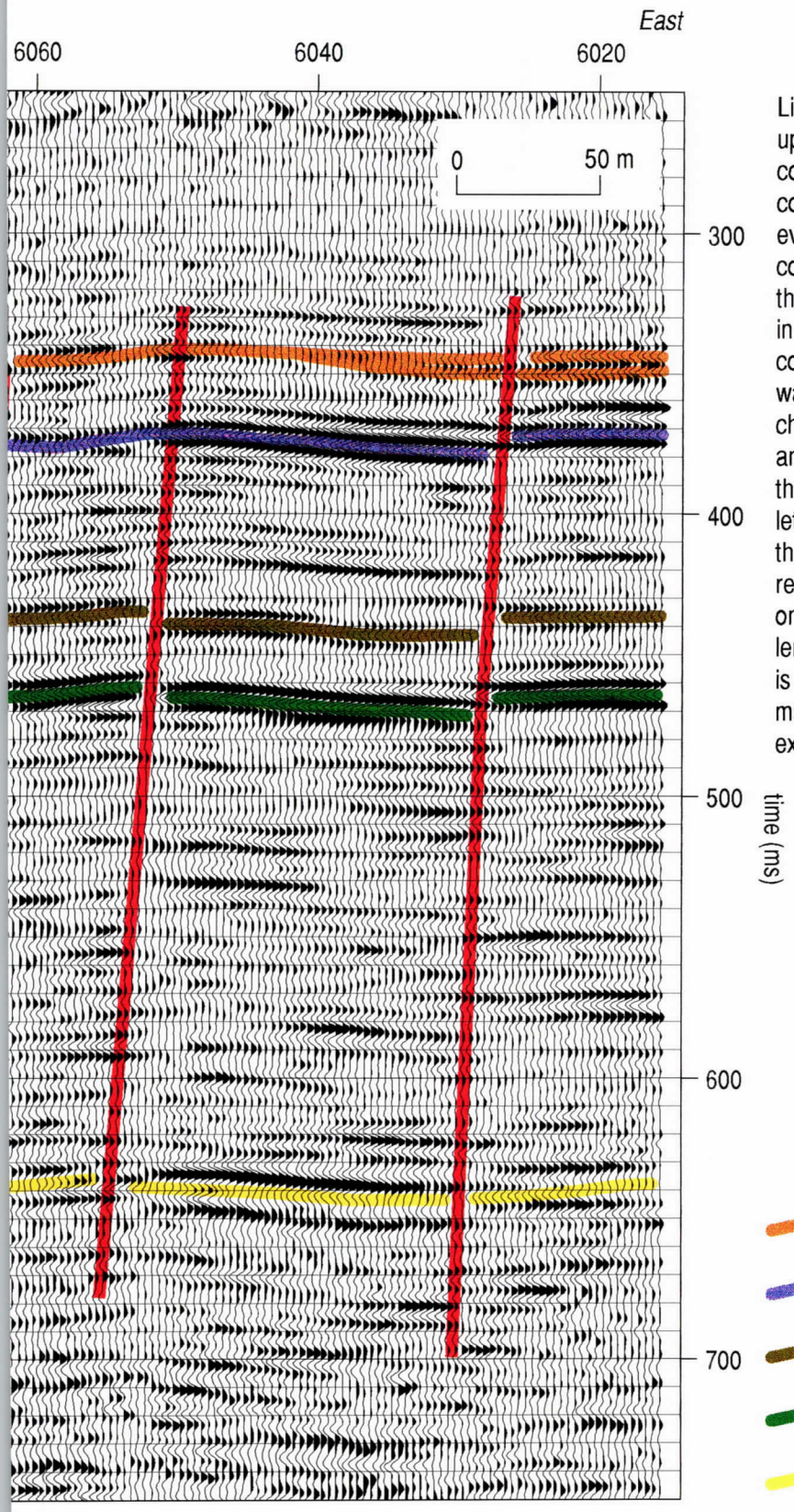

Line 6 CMP stacked seismic reflection section with upper 250 ms cropped and sitewide coherent and correlatable reflections interpreted with a sitewide consistent color sequence. The highest amplitude events are within the interval interpreted to be coal rich. Based on the only drill hole in the area, the orange event is the 365 m coal encountered in the corehole and the purple event is the 391 m coal that was penetrated about 9 m before drilling was curtailed. Several reflections with similar character are interpreted between the 391 m coal and about 500 ms and have been designated as the "coal interval." With the variability in the wavelet characteristics of the basement along line 6, the top of the Mesozoic section (yellow basement reflection) was interpreted based predominantly on amplitude. Like lines 2 and 5, faults are prevalent along this profile. The nature of the faulting is somewhat unique along this profile, which lacks many interpretable diffractions that would be expected to originate from the fault plane.

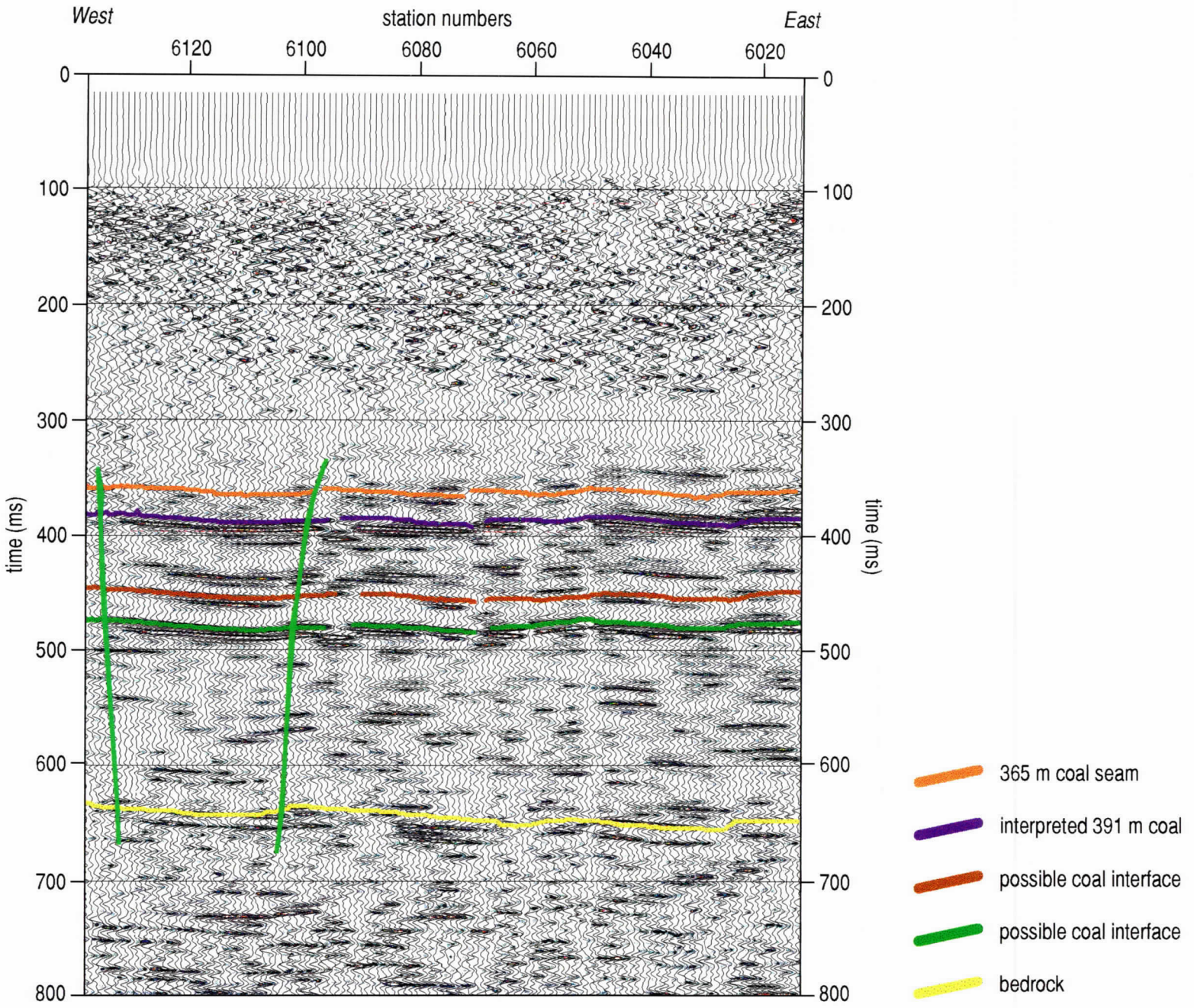

Figure 59. Line 6 CMP stacked seismic reflection section with wiggle traces overlain by color amplitude enhancement of the frequency mid-range (140 Hz to 180 Hz) and key sitewide coherent reflection events interpreted using the color scheme consistent throughout this report. The lack of coherent events within the permafrost and what is identified as the sub-permafrost zones is very evident on this display format. Reflections within the coal and sub-coal interval extend from just above the 365 m coal down to the top of the Mesozoic section, which begins at about 650 m. These reflections possess excellent frequency content (useable in excess of 200 Hz in some places) and sitewide coherency. This highly reflective time window interpreted as the "coal zone" is a consistent characteristic of all the seismic profiles collected in the Fort Yukon area.

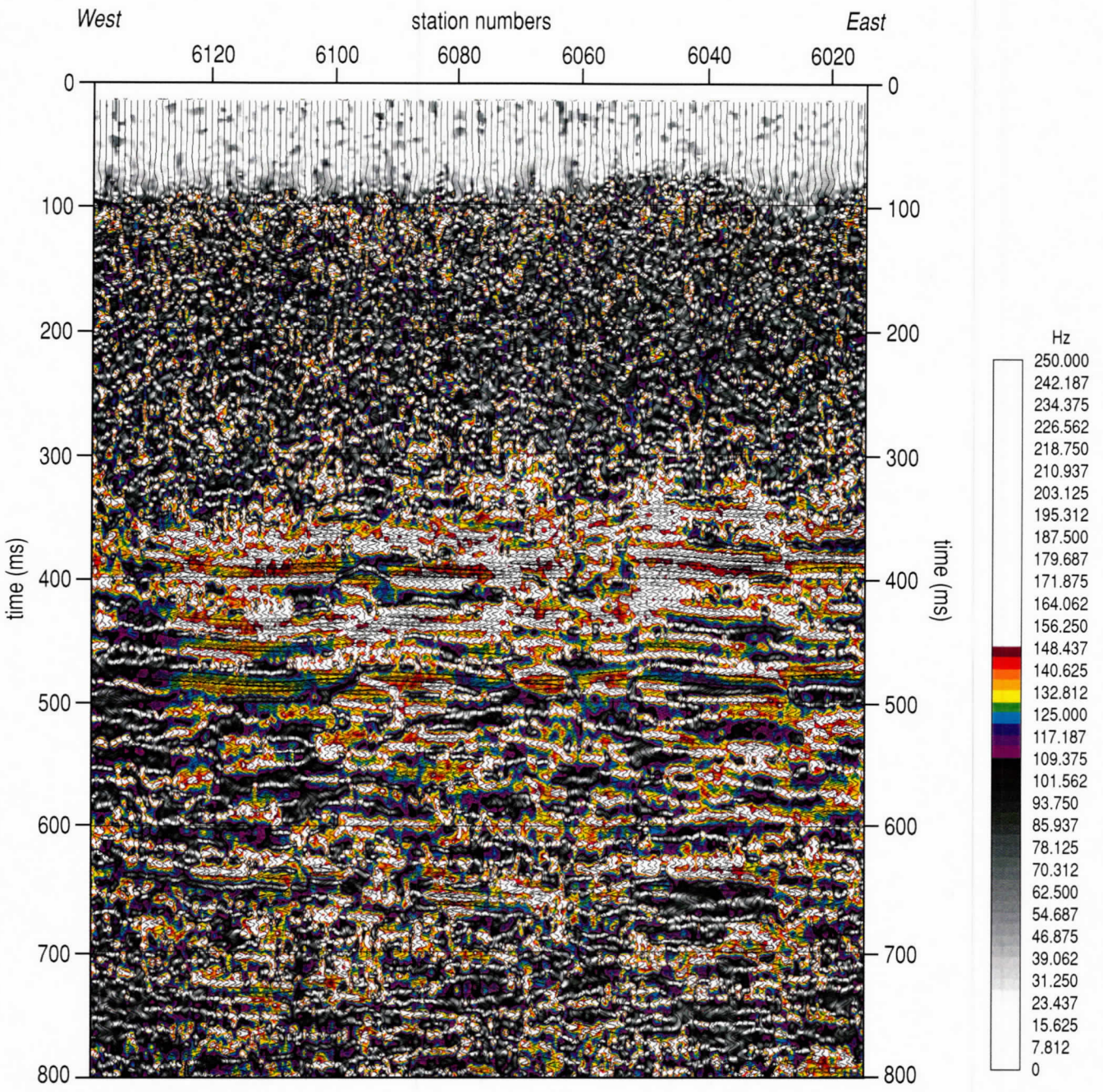

Figure 60. Line 6 CMP stacked section with instantaneous frequency overlain by wiggle trace data focusing on the frequency range between 100 Hz and 150 Hz. Changes in reflection character, and therefore geology, can be easily identified on frequency plots. Evident on this display is the significant increase in dominant frequency within the coal interval consistent with observations on other CMP stacked sections. A series of small diffraction events are evident beneath station 6100, which is indicative of faulting.

other profiles. A localized diffraction or scatter event can be seen beneath station 6100 and correlates to the very small down-drop block defining the edge of the synform.

Amplitude analysis focusing on the "coal interval" again highlights the extreme variations of the reflections within the coal interval (Figure 61). The drill-confirmed coal at 390 ms has a high amplitude segment bounded by the fault on the north and an apparent fault on the south. In a conventional petroleum seismic environment this apparent "bright spot" would be interpreted as a potential indicator of the presence of gas. With the degree of faulting and fracturing observed on these profiles it is not unreasonable to suggest enough surface area has been exposed to allow gas to escape from the coal and be subsequently trapped by the overclay. Confirming or refuting this scenario is only possible through drilling.

Line 7

Considering the variable terrain line 7 was acquired over, reflections have very consistent wavelet characteristics (Figure 62). Coherent reflection arrivals within the "coal interval" near the northwest end of the line have some of the highest amplitudes observed anywhere around this site. The 480 ms reflection clearly marks the bottom of the sequence of higher frequency, more coherent reflections previously classified as the "coal interval." It is likely the variability evident in wavelet character of individual reflections is related to changes in material properties at the reflector contact or immediately above the contact.

Interpretation of the six reflections identified on stacked sections has relied on arrival time, wavelet characteristics, and vertical consistency (Figure 63). Line 7 was a key profile for establishing structure orientation. Spatial separation between seismic lines along the perimeter was great enough that any one or set of structures could have been correlated to any one or variety of different features on adjacent profiles. Line 7 forced compliance with the three-point problem for any major feature crossing both lines 5 and 7. These two lines were close enough in proximity that similarity in geometries as well as seismic character was necessary to correlate. The major fault identified on line 5 at 5400 matches reasonably well with the fault interpreted at stations 7240 and 7100 on line 7. Considering relative displacement, seismic characteristics, strike of the fault plane, and vertical declination, the fault at 5400 on line 5 matches with the fault at 7240 on line 7 as well as one at station 2340 on line 2. As with all structures correlated across the site, line-to-line matches involved comparisons of not only the specific feature being correlated but also the structures and seismic characteristics of surrounding features.

Studying the line 7 section on a larger scale provides an improved perspective of line-to-line correlations of apparent structures (Figure 64). For the most part, the northwestern end of the profile is rich with high-amplitude coherent reflections and closely resembles the section of line 5 between stations 5400 and 5500 previously discussed. With this observation and shape matching, the fault at station 5400 matches up quite nicely with the fault interpreted at station 7240 on line 7. A synform indicated by the green lines matches in shape reasonably well to one on line 6 and another on line 2. This feature is consistent with the horizon contours of all six sitewide interpreted reflecting events. As on other lines, faults without unique characteristics are interpreted in either gray or red. This color indicates there were no obvious correlations to the other lines.

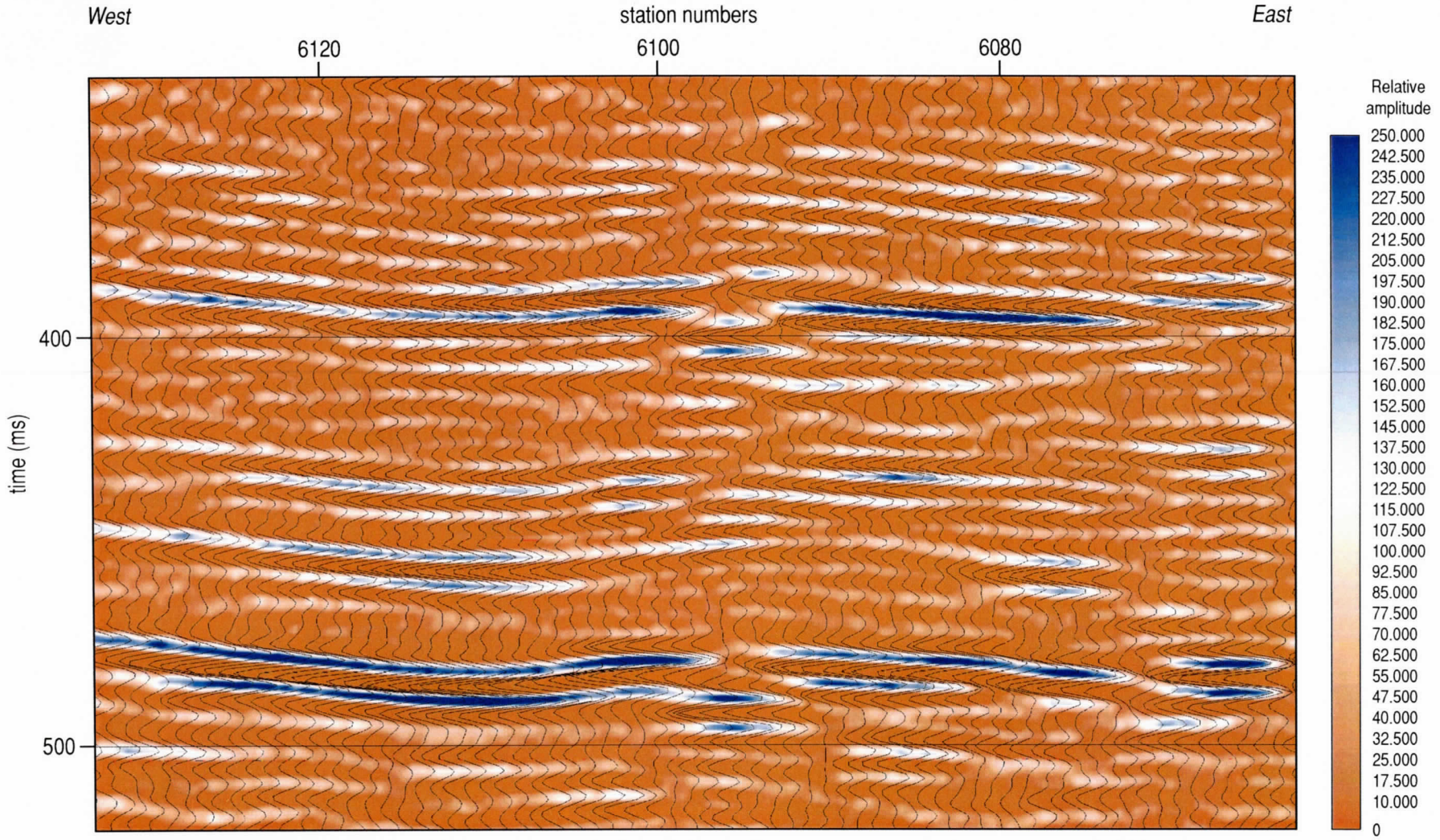

Figure 61. A zoomed-in portion of line 6 CMP stacked section focusing on the "coal interval" using color amplitude overlain by wiggle trace representation of the seismic reflection data. This display format highlights lateral amplitude variations. The two most dominant sitewide layers appear consistent across the length of this segment of the line with noteworthy variations in amplitude beneath station 6100. This disturbance is near vertical from layer to layer suggesting a possible association with static, but with the diffraction patterns observed in Figure 60 faulting becomes the most likely explanation for this discontinuity.

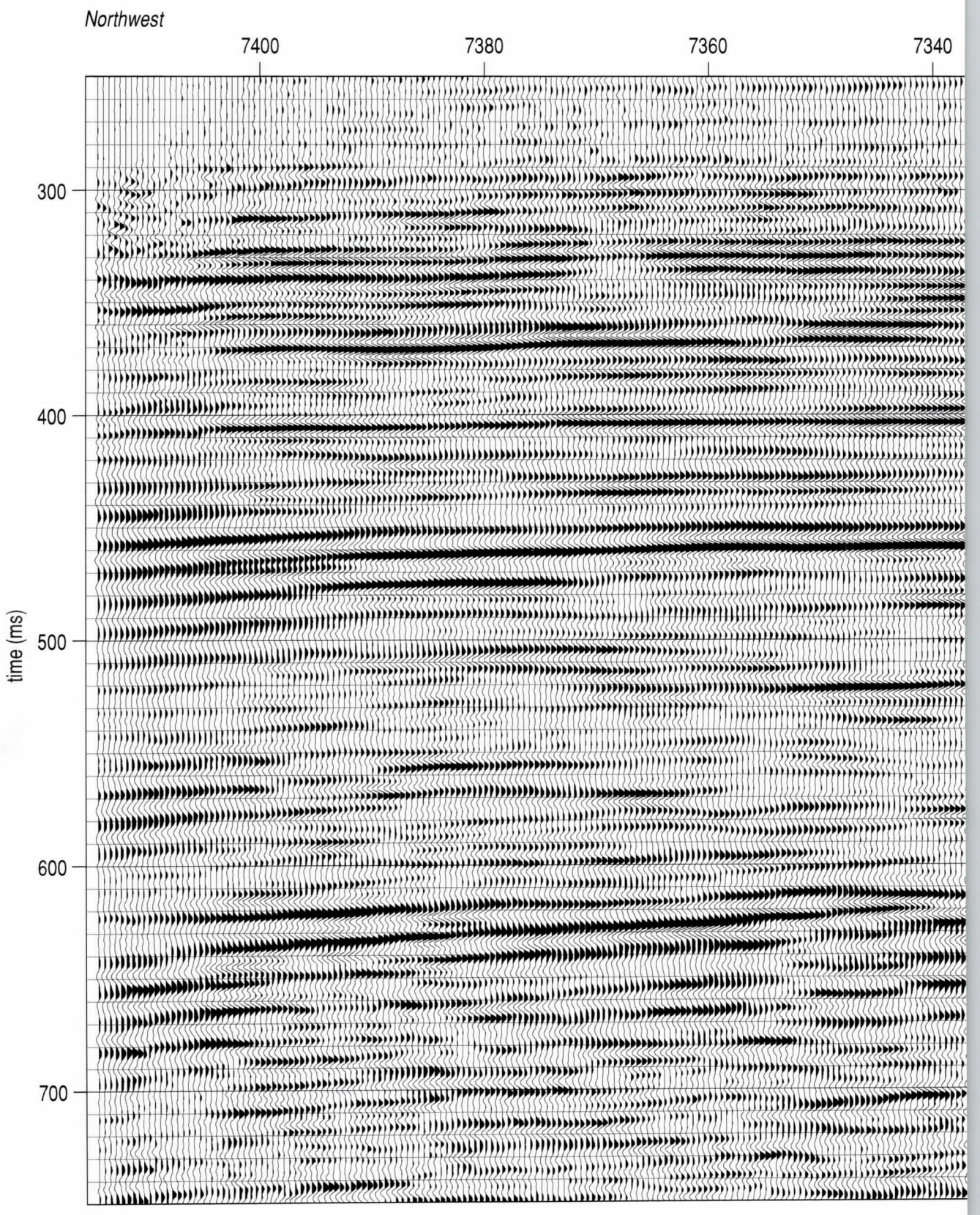

Figure 62.

62a

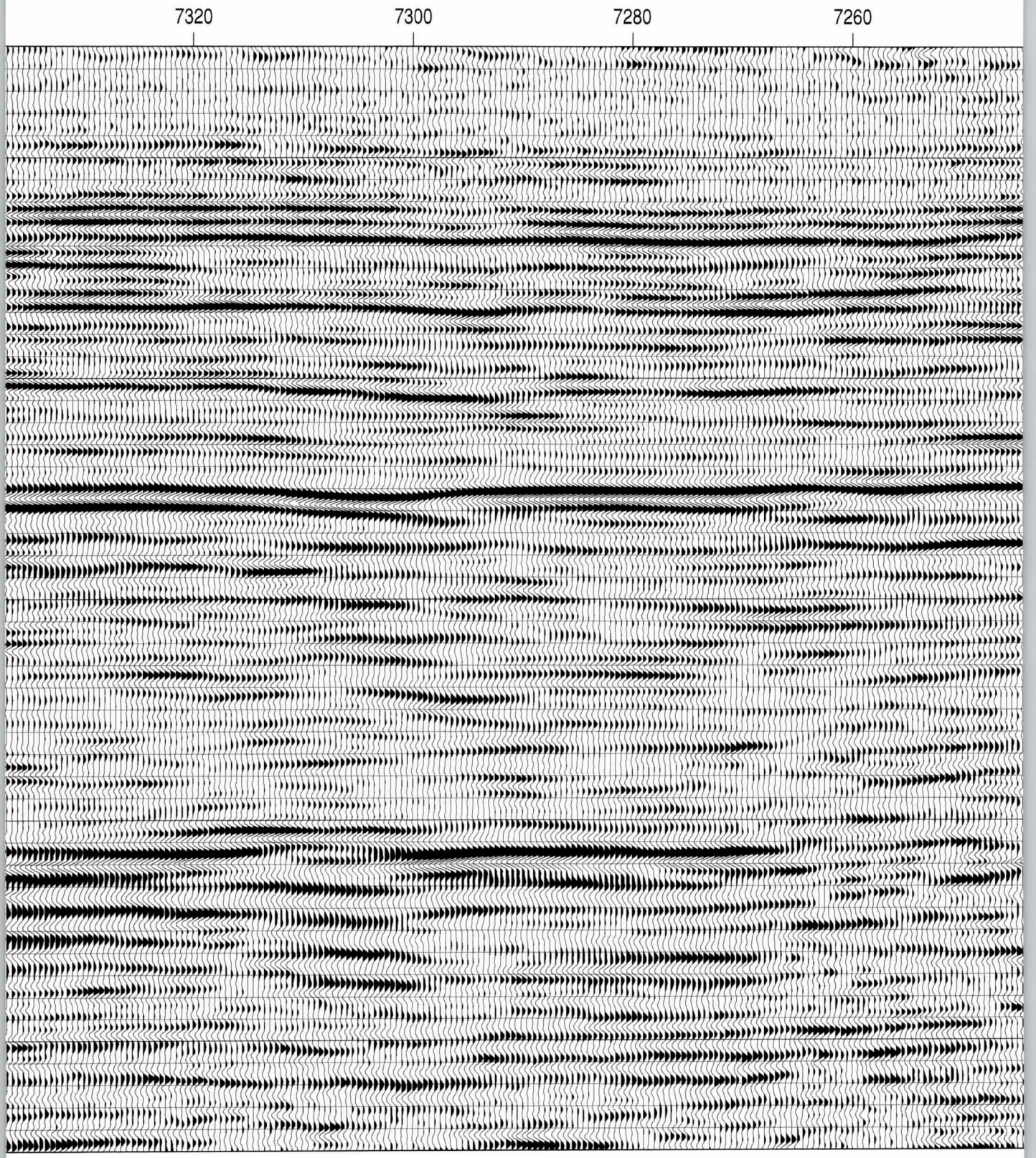
7320
7300
7280
7260

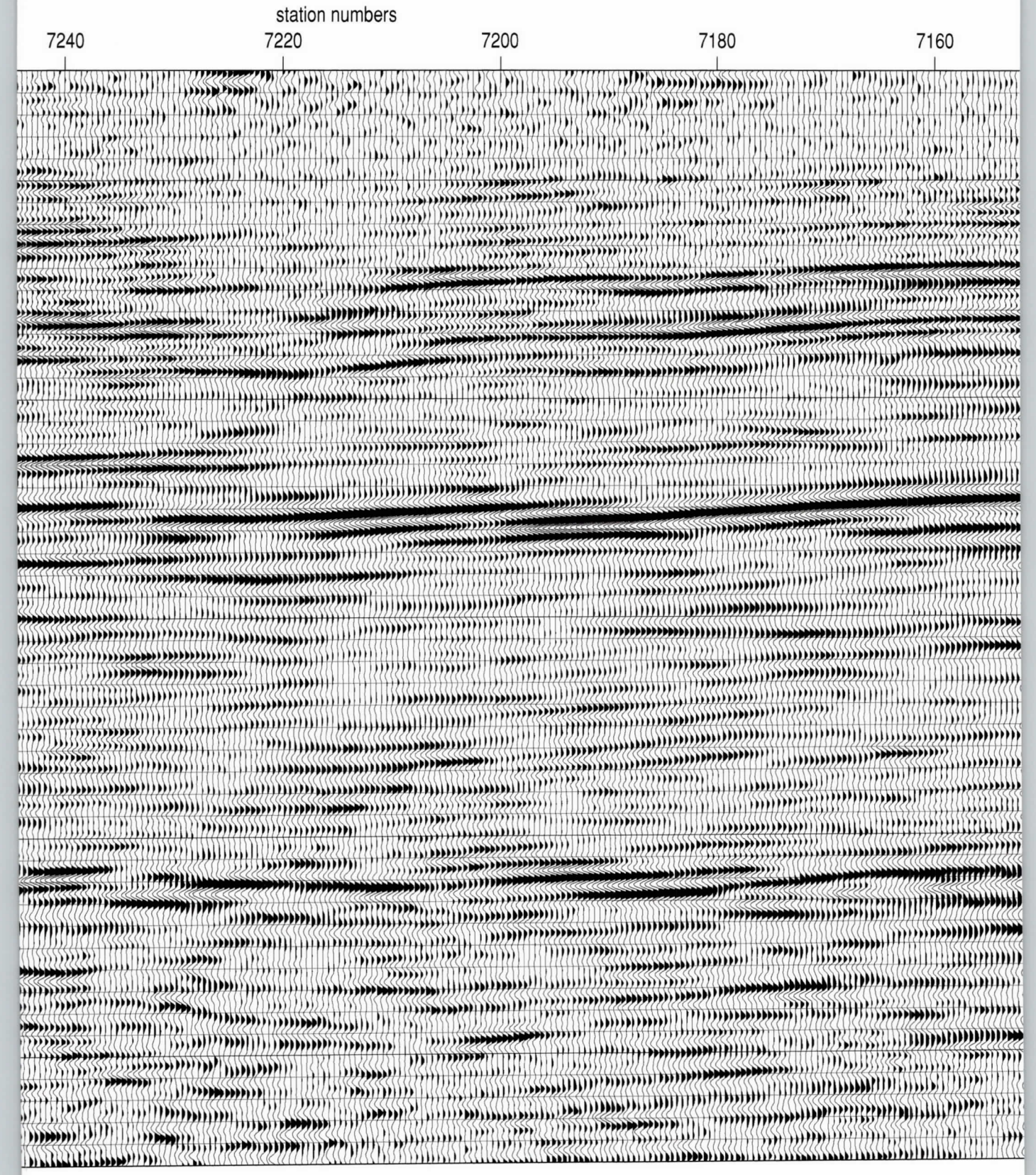

62c

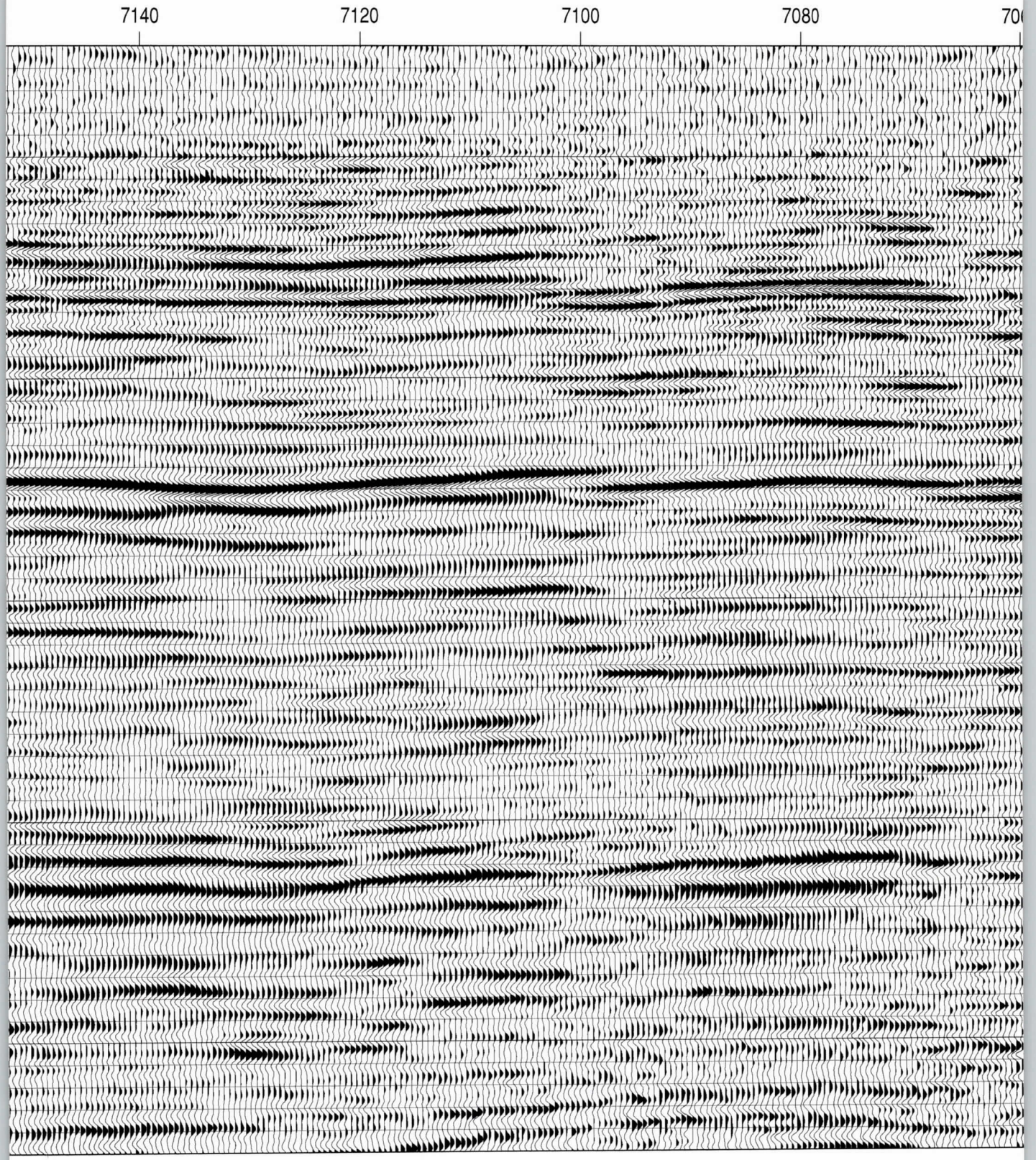

62d

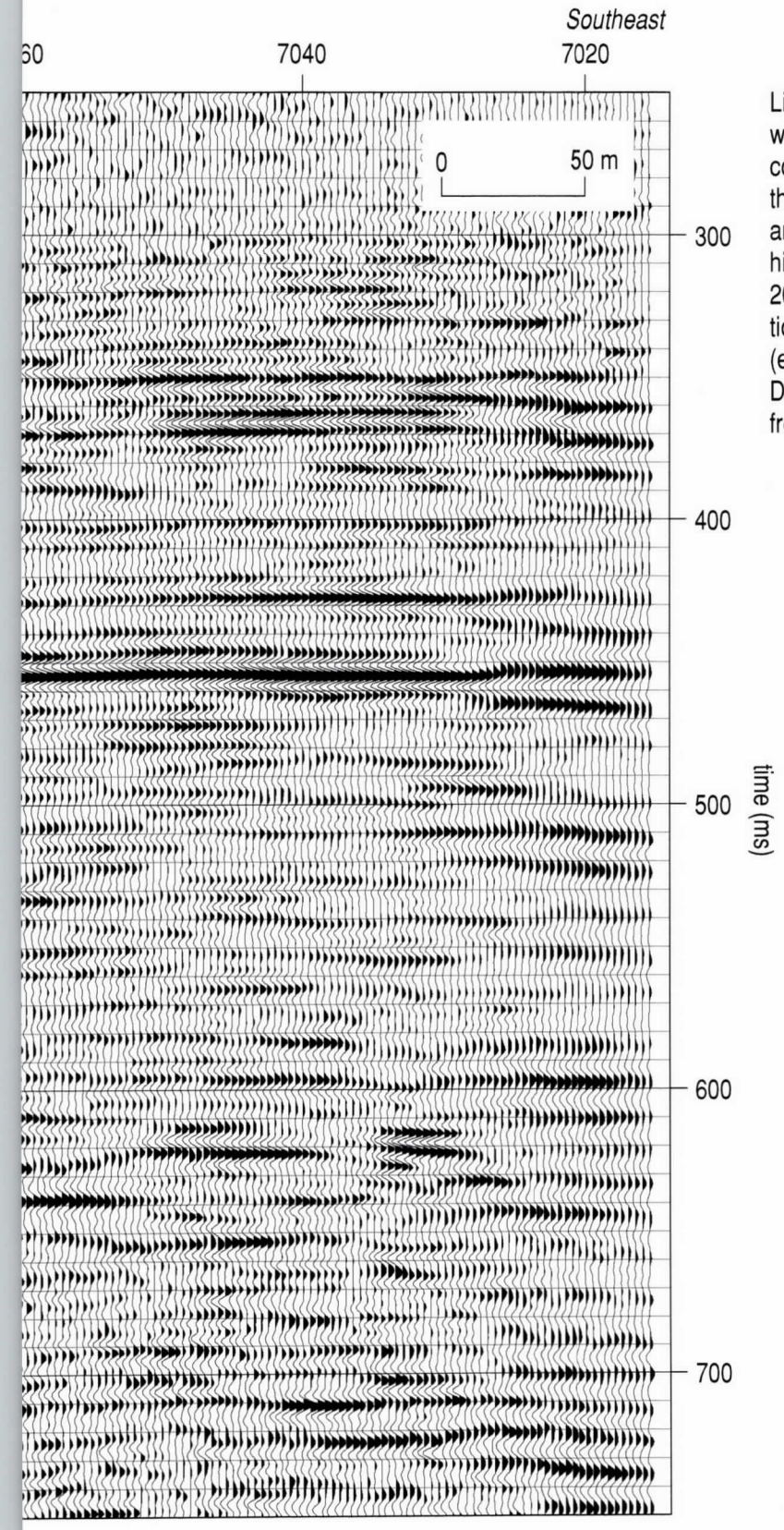

Line 7 CMP stacked seismic reflection section with upper 250 ms cropped. Several groups of coherent reflections can be interpreted across the length of this section and from line to line around the site. With the average velocity to the high amplitude coherent reflections around 2000 m/s, depth estimates are a 1-to-1 correlation between time (ms) and depth (meters) (e.g., 400 ms is approximately equal to 400 m). Data quality on this profile is consistent with that from the other six lines.

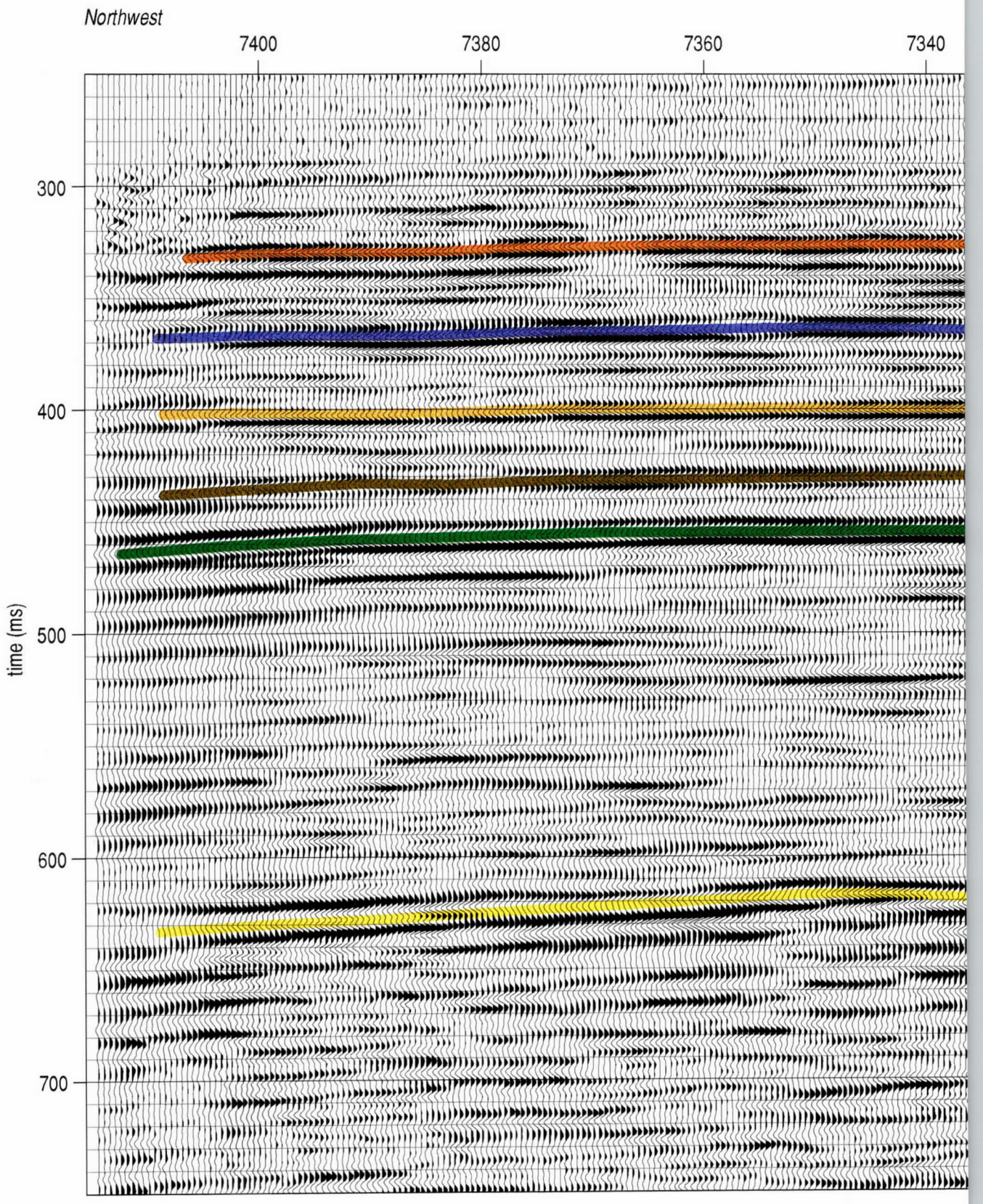

Figure 63.

63a

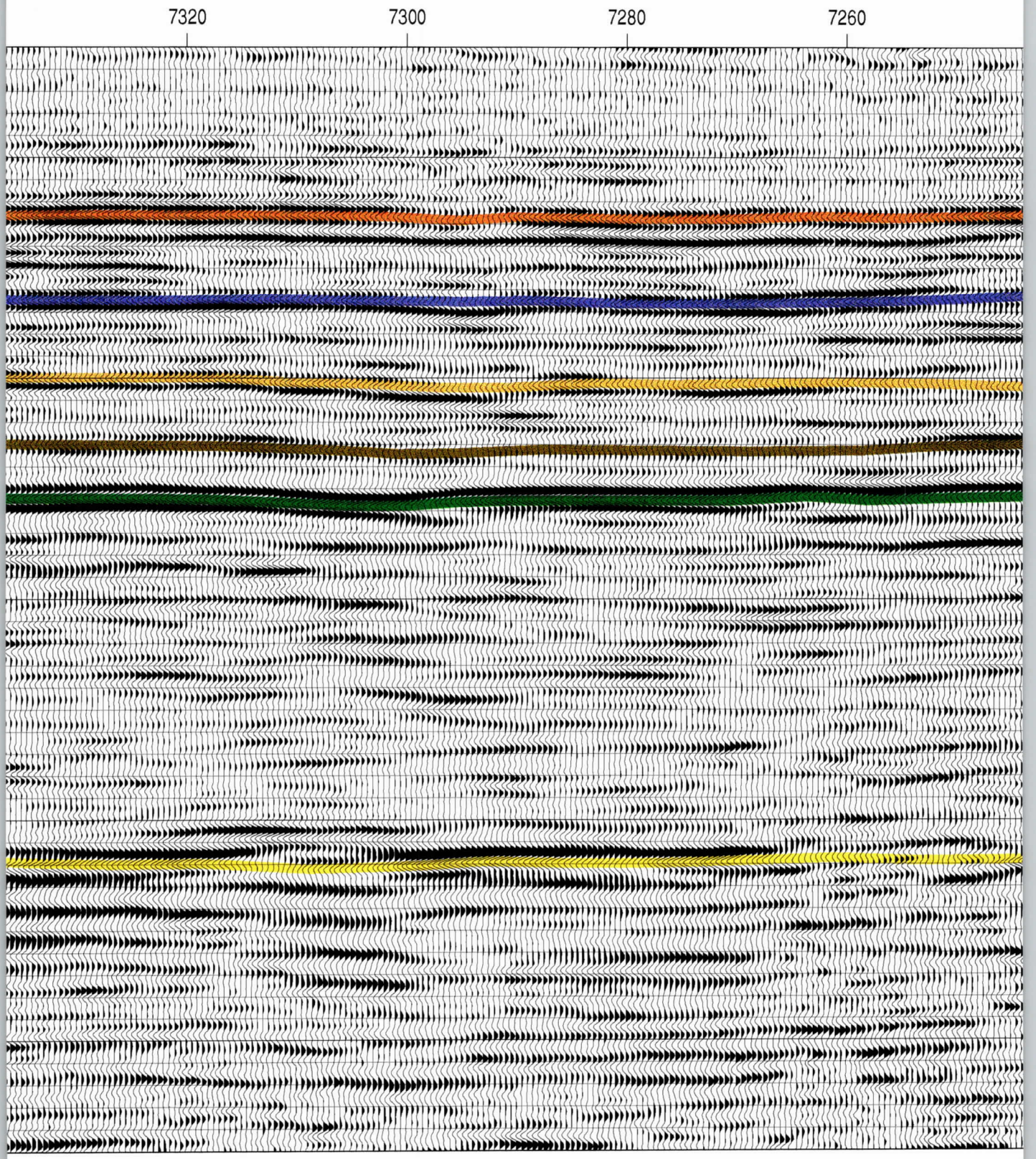

63b

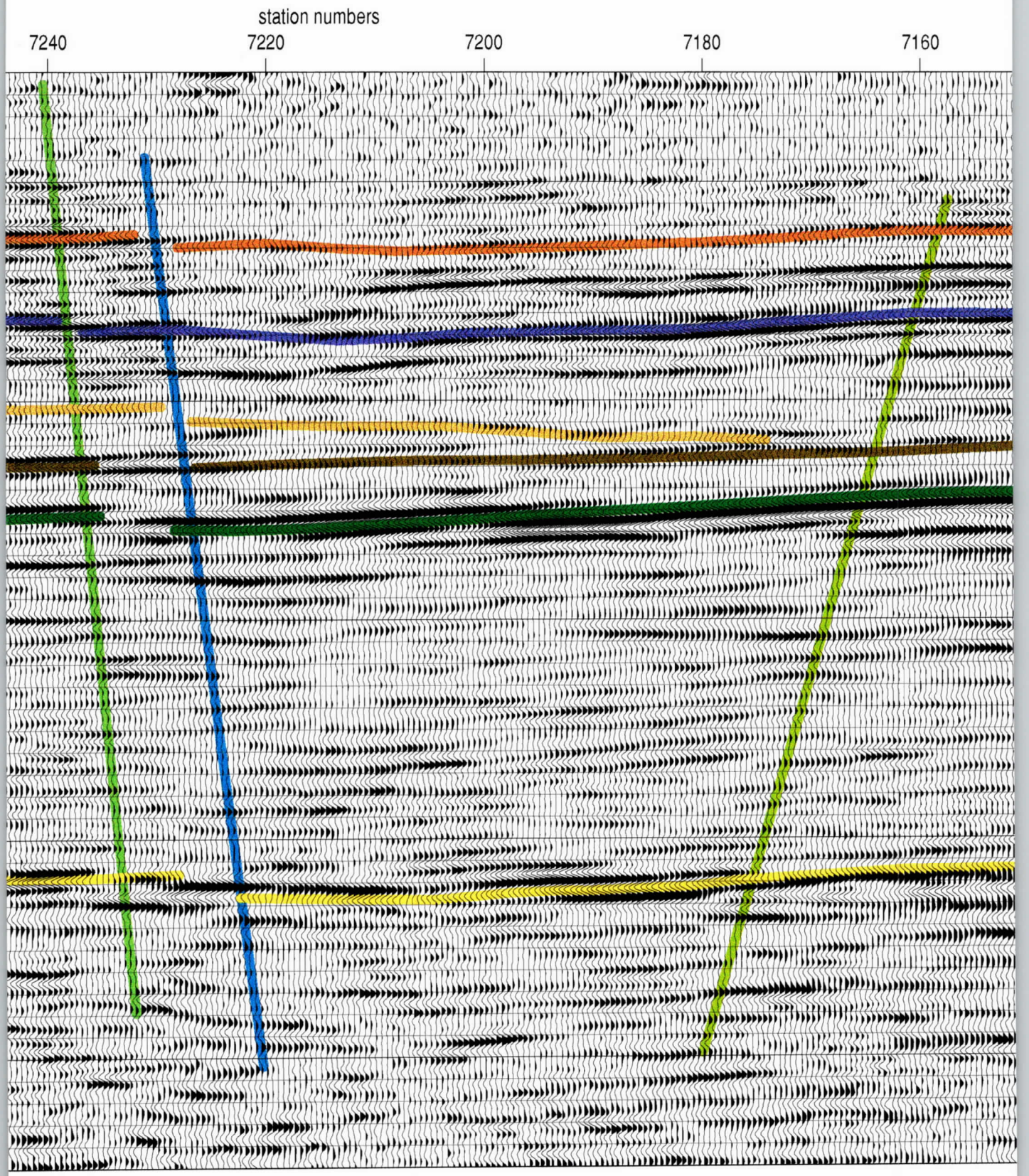

63c

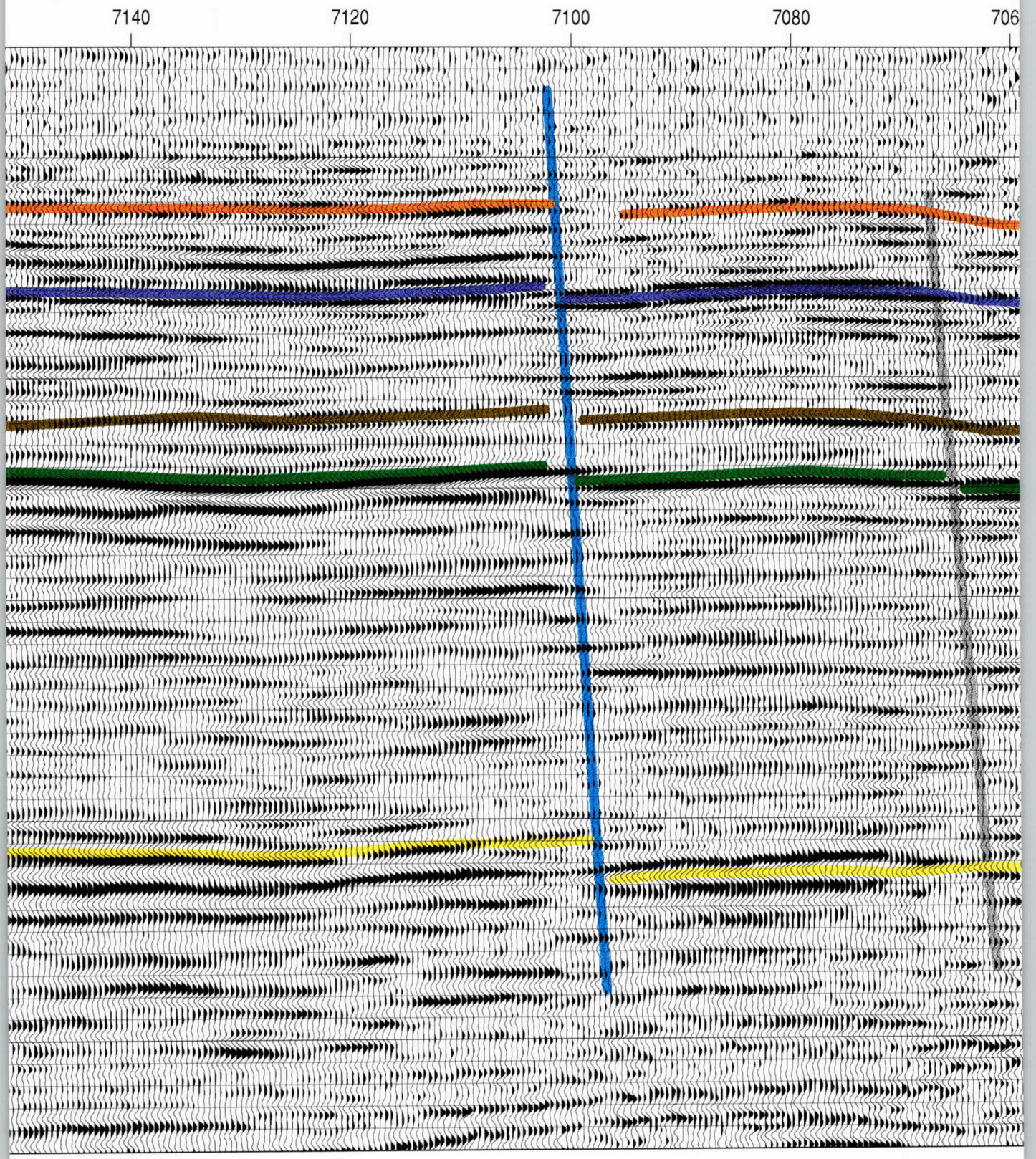

63d

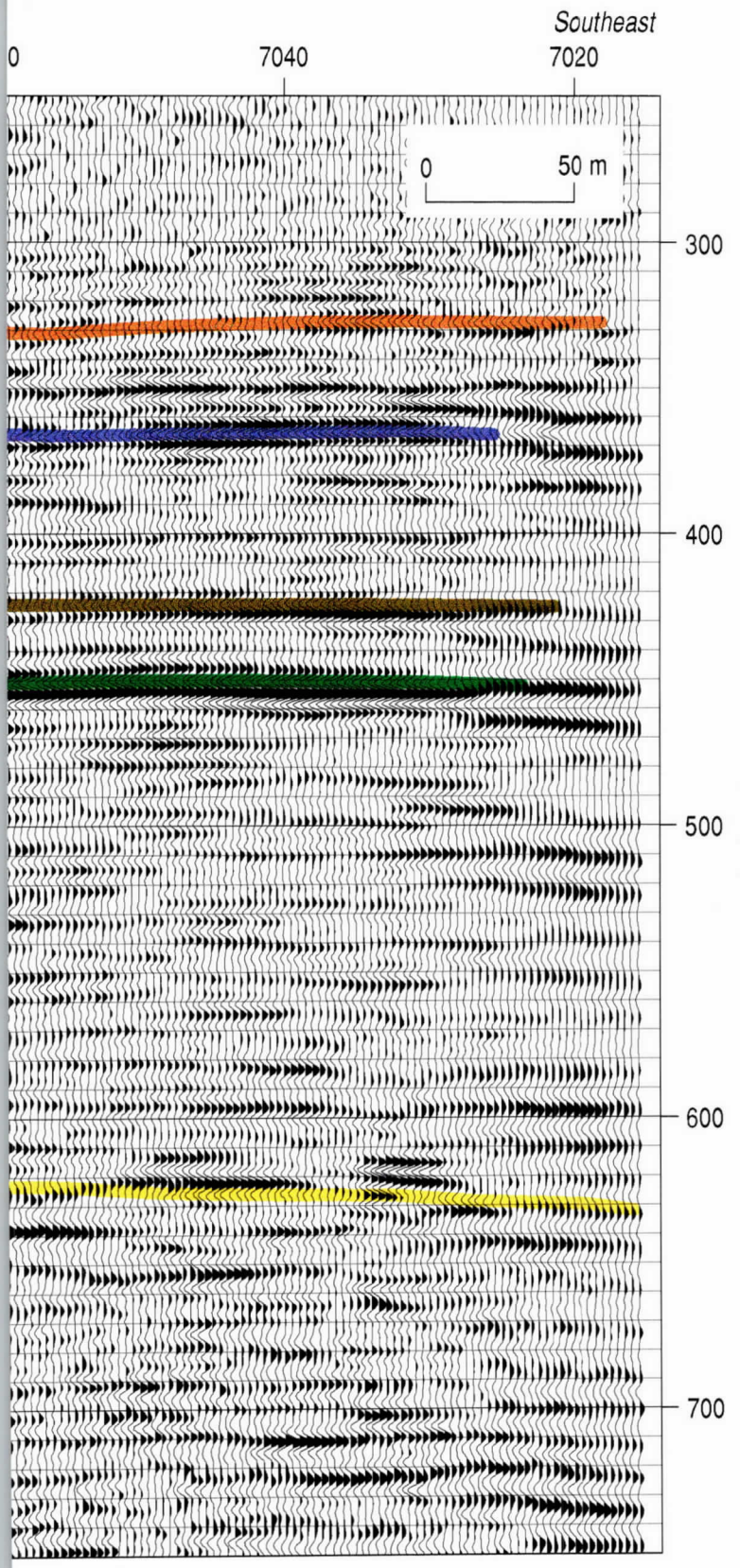

Line 7 CMP stacked seismic reflection section with upper 250 ms cropped and sitewide coherent and correlatable reflections interpreted with a sitewide consistent color sequence. The highest amplitude events are within the interval interpreted to be coal rich. Based on the only drill hole in the area, the orange event is the 365 m coal encountered in the corehole and the purple event is the 391 m coal that was penetrated about 9 m before drilling was curtailed. Several reflections with similar character are interpreted between the 391 m coal and about 500 ms and have been designated as the "coal interval." With the variability in the wavelet characteristics of the basement along line 7, the top of the Mesozoic section (yellow basement reflection) was interpreted based predominantly on amplitude. Two areas with faults have been interpreted on the southeast end of the profile and correlated to lines 2 and 5.

63e

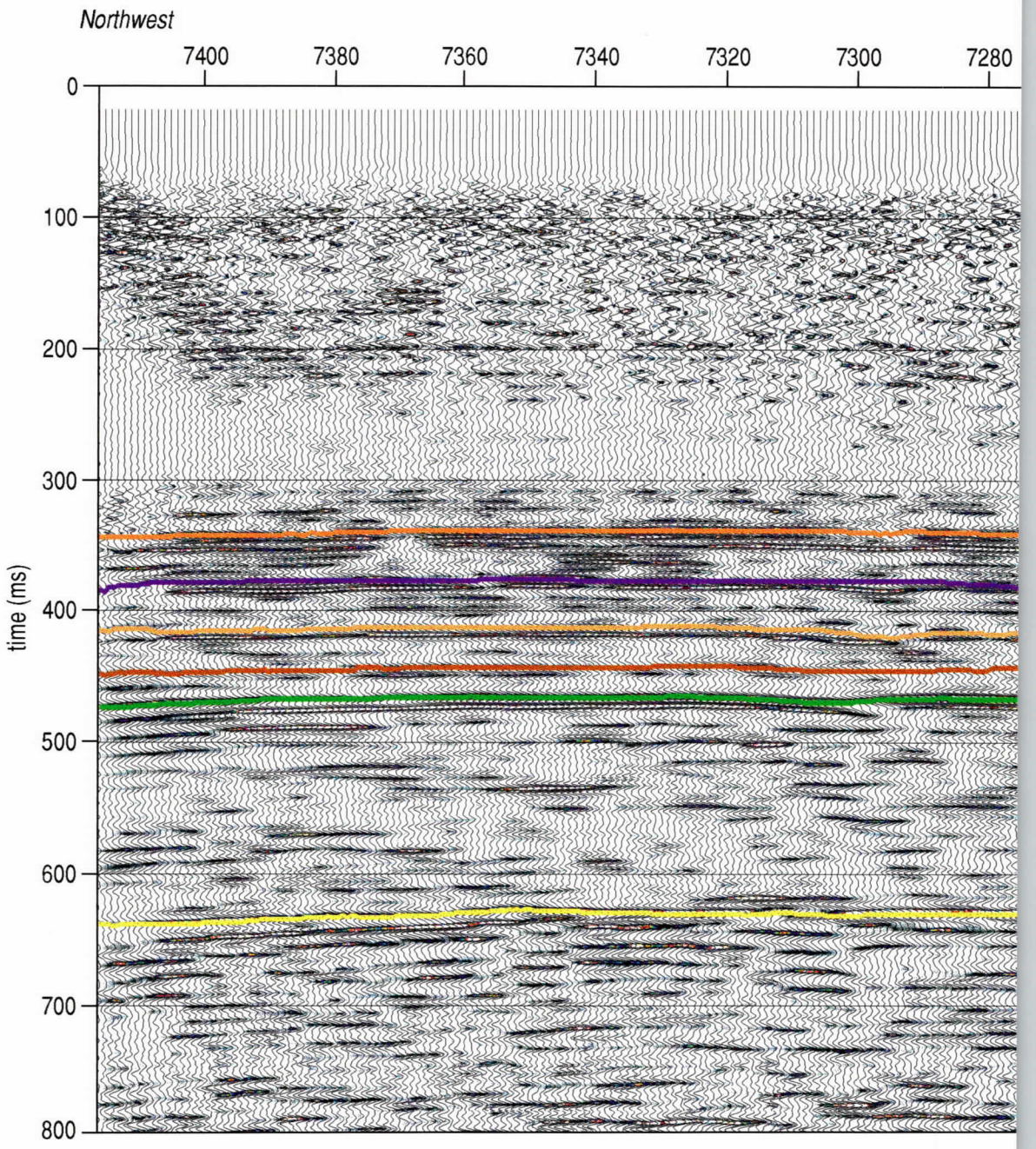

Figure 64. Line 7 CMP stacked seismic reflection section with wiggle traces overlain by color amplitude enhan
scheme consistent throughout this report. The lack of coherent events within the permafrost and what is ident
noise are evident below 100 ms with a quiet zone (fewer reflections per unit time) between about 200 ms and
down to the top of the Mesozoic section, which begins at about 650 m. These reflections possess excellent fr
interpreted as the "coal zone" is a consistent characteristic of all the seismic profiles collected in the Fort Yuko

64a

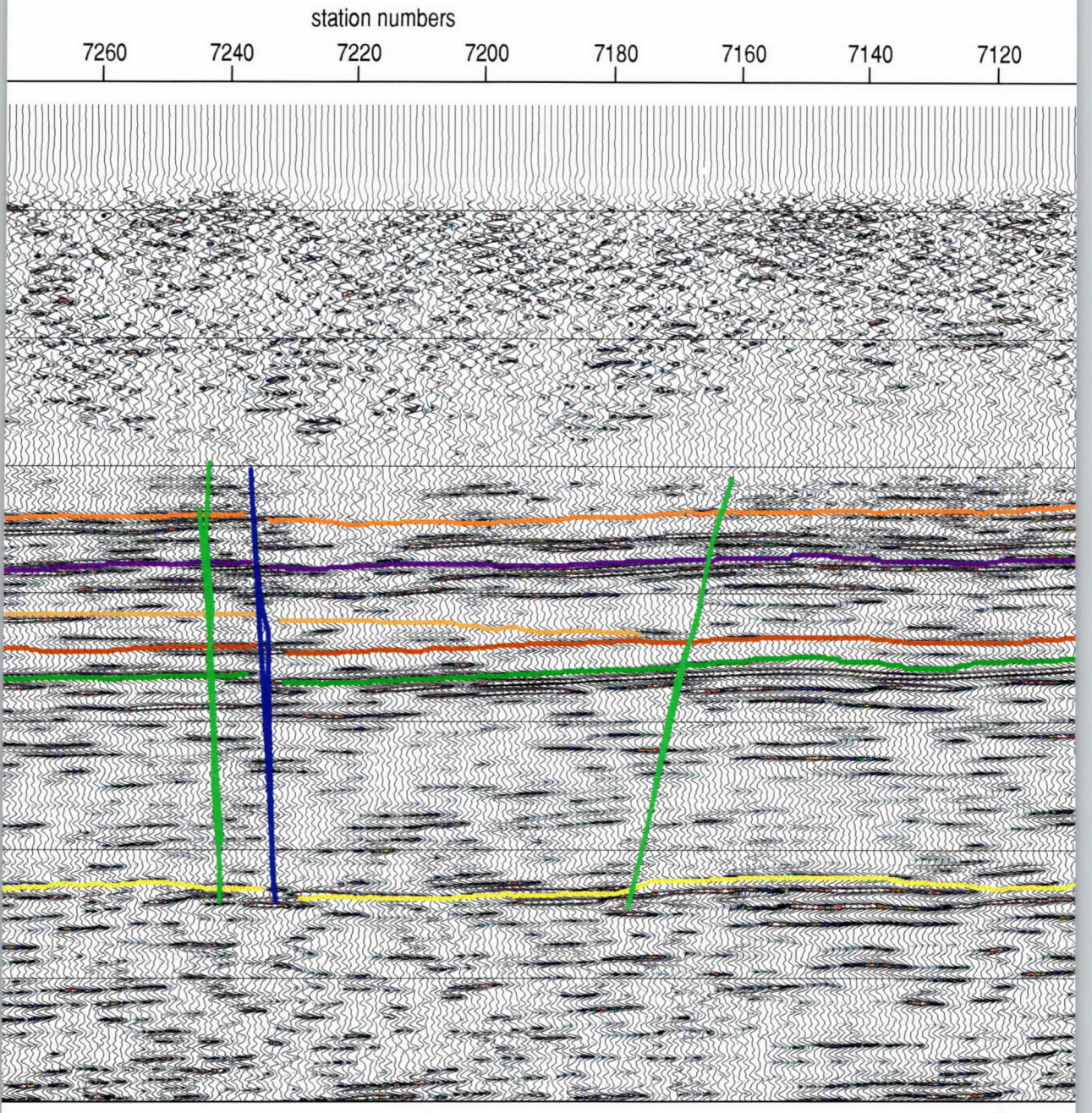

cement of the frequency mid-range (140 Hz to 180 Hz) and key sitewide coherent reflection events interpreted using the
ified as the sub-permafrost zones are very evident on this display format. Subtle indications of reflections emerging fron
first drill-confirmed coal at about 365 m. Reflections within the coal and sub-coal interval extend from just above the 365
equency content (useable in excess of 200 Hz in some places) and sitewide coherency. This highly reflective time windo
n area. Faulting is very easy to interpret based on frequency and coherency.

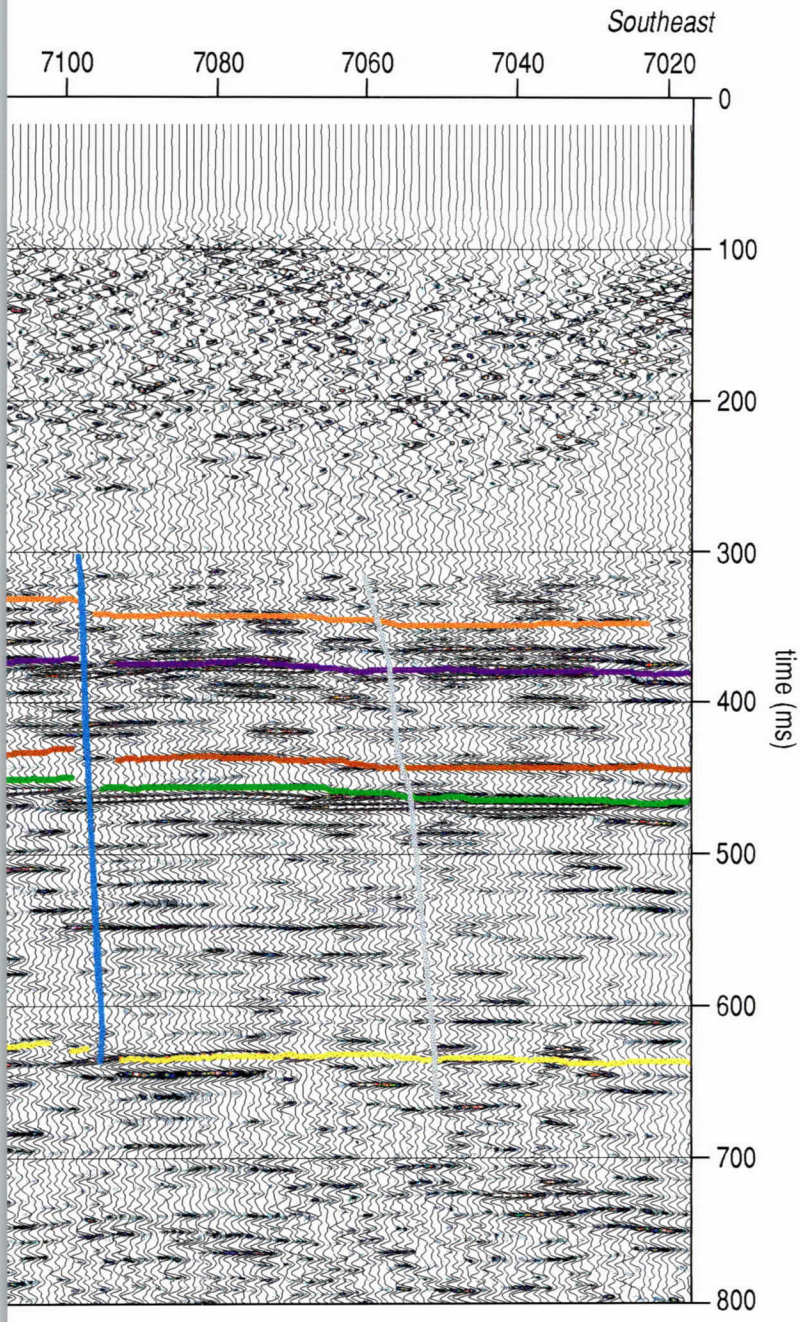

e color
n the
5 m coal
ow

64c

Frequency mapping again has emphasized an area that is relatively bland on the amplitude and wiggle trace displays but has experienced significant attenuation of high frequencies and seems to be the apex for scatter (Figure 65). As on previous lines, the base of the "coal interval" is defined by a high-amplitude, lower-frequency reflection that fully crosses the profile. The unique spectral properties as well as coherency and amplitude characteristics of this reflection suggest it would be a significant marker bed, possibly indicating it is a geologic contact with regional significance. Also on this frequency display is an anomalous zone immediately northwest of the fault at station 7100. This notable frequency drop at and just below the 390 ms coal reflection is not obvious on the wiggle trace or amplitude displays. As this program progresses, unique changes in material properties as suggested by anomalously low frequency areas such as this one can be correlated to material properties and quantified for use as indicators on future CBM exploration programs.

Amplitude displays of a segment of line 7 highlight coherent reflections within the coal interval and, as on other profiles from this site, possess unique characteristics likely related to material properties (Figure 66). Determining the geologic significance and therefore the relationship of these characteristics to CBM will require physical sampling and associated analysis. Clearly the basal contact of the "coal interval" has lower frequency and higher amplitude characteristics than shallower reflections within the coal interval. From this display scale and highlighted attributes the subtle channel-looking feature on the 480 ms reflection beneath about station 7300 is not replicated in the units directly above. The non-vertical nature of this feature dramatically reduces the possibility that it is an artifact of near-surface statics (such as a variable permafrost thickness). Moving up in time, the bowl-shaped feature trends to the southeast and is beneath station 7295 at the 350 ms reflection.

Horizon Contours

Six horizons were interpreted and correlated around the site based on event coherency, wavelet characteristics, and arrival time. By taking these six seismically interpreted 2-D horizons and incorporating geostatistical analysis it was possible to not only extend the 2-D interpretations into the unsampled space between the profiles, but quantify the confidence or certainty of those extrapolations. Production of geostatistical maps included the following basic steps:

1. Preparation of a data set free of errors. These data must contain the geographic coordinates of each measurement for the attribute of interest;
2. Analysis to determine possible existence of a trend and the average size of anomalies, analysis that is summarized in the form of a semivariogram model;
3. Generation of two sets of values at regular intervals, values that are weighted averages of the data. The weights come from systems of equations taking into account relative location of data and the semivariogram of the previous step;
4. Finally, any contouring software can be employed to display these two sets of values. One set produces the areal variations of the attribute, the other map can be used to assess the reliability of the attribute map.

Color used to enhance the horizon topography does not correlate to the colors used to interpret the seismic data.

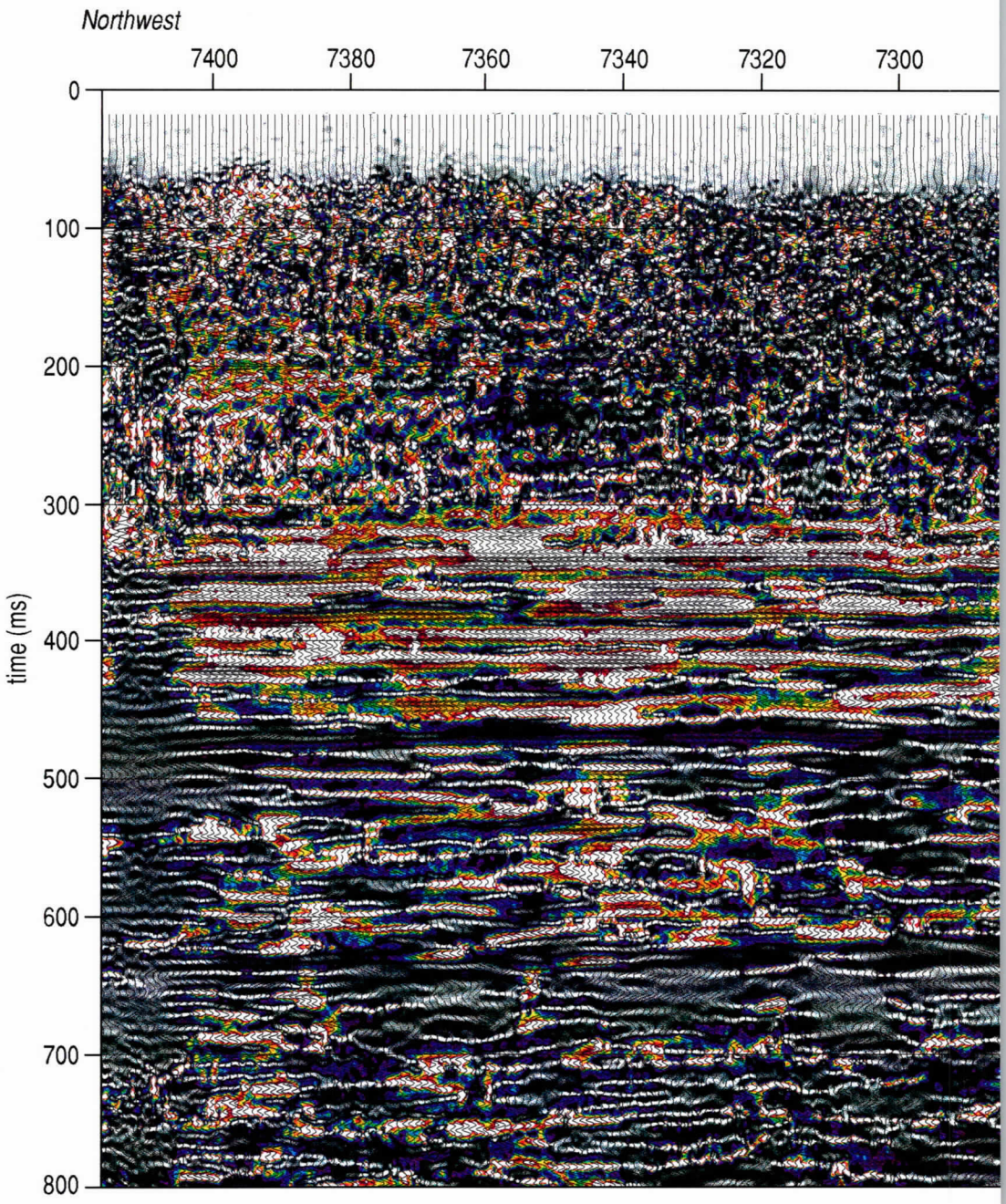

Figure 65. Line 7 CMP stacked section with instantaneous frequency overlain by wiggle trace data focu
identified on frequency plots. A dramatic change in dominant frequency marks a zone of diffractions an

65a

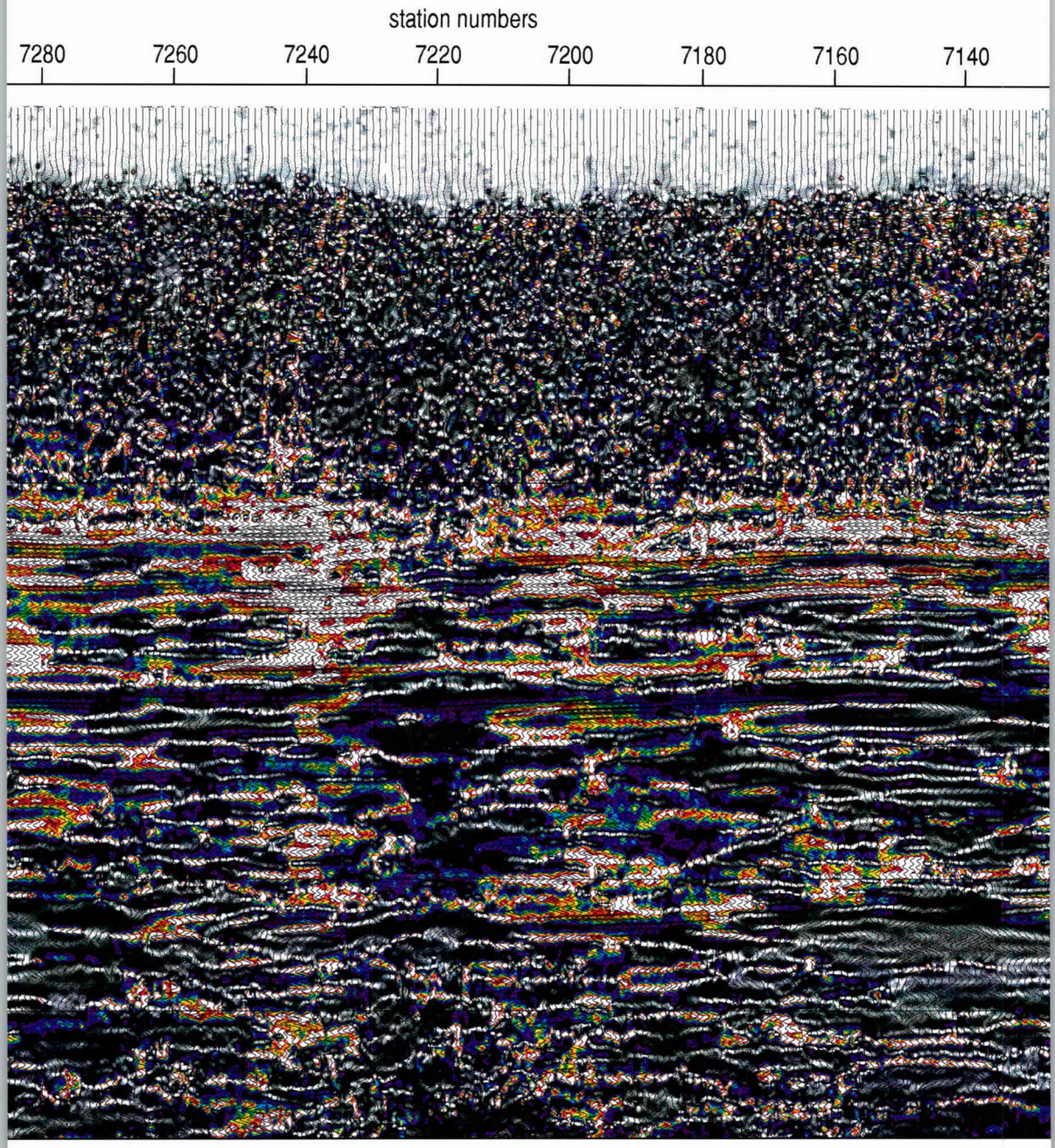

sing on the frequency range between 100 Hz and 150 Hz. Changes in reflection character, and therefore geolog
d a fault interpreted beneath station 7220 at about 470 ms and correlates to the fault interpreted on Figures 63 a

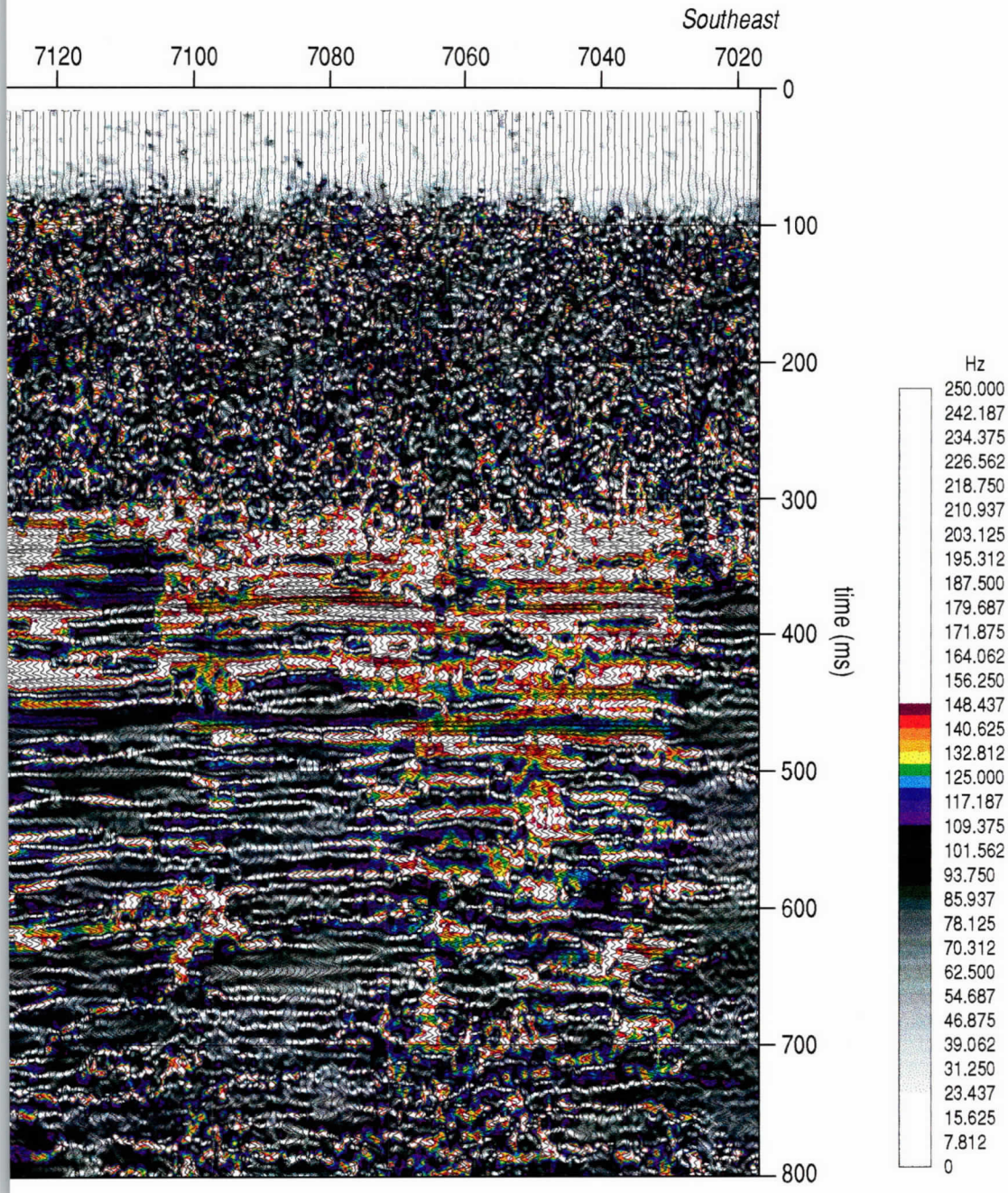

y, can be easily
nd 64.

65c

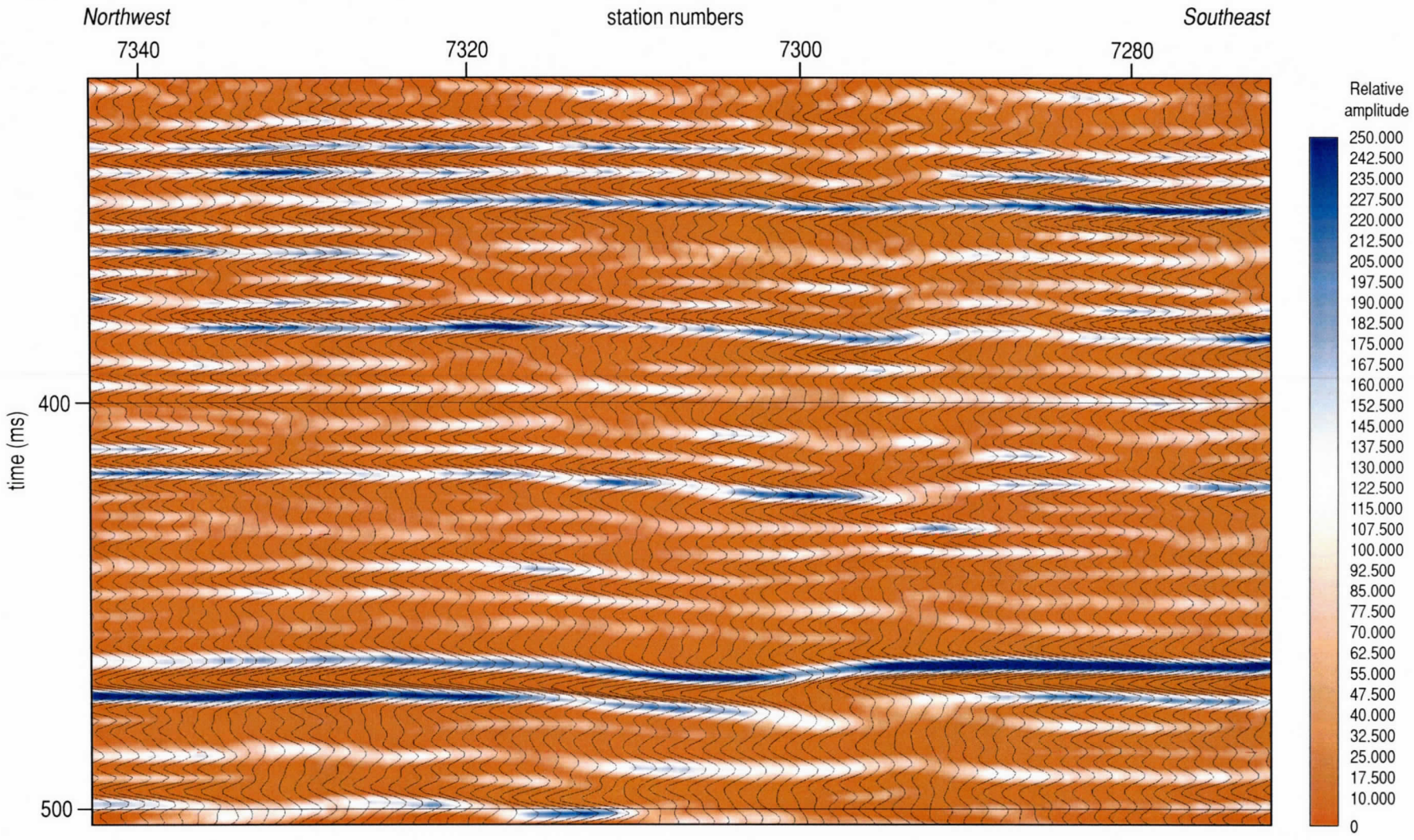

Figure 66. A zoomed-in portion of line 7 CMP stacked section focusing on the "coal interval" using color amplitude overlain by wiggle trace representation of the seismic reflection data. This display format highlights lateral amplitude variations. Several layers appear consistent across the length of this segment of the line with noteworthy variations in amplitude of the interpreted coal reflections. Unique to this portion of line 7 is the very subtle monocline beneath station 7290. This feature is interpreted on the CMP stacked wiggle trace display (Figure 63) and is most pronounced at this amplitude.

All six sitewide reflections dip locally to the southwest (Figures 67 through 73). Even though the data were acquired and processed as separate lines with no hard ties between them, all the interpreted horizons on the seven lines are consistent in relative time. The low on the western end of line 4 that is missing at the northeastern end of line 2 is the only feature that lacks continuity between adjacent lines.

The seismically inferred surface of the 391 m coal seam appears relatively smooth and dips to the southwest, resulting in about 30 m change in elevation across the site (Figure 68). The surface topography of the coal horizon is remarkably consistent with conceptual geologic models and developments for the Yukon Flats Basin. The dip of the coal horizon along line 2 is very uniform and parallel to the line. Details of the seismic interpretations are evident on the horizon contour lines. Assuming the approach used to interpret the 391 m deep coal seam is valid, the coal is continuous around the site and possesses a structure consistent with the regional geology.

Reflections below the drill-confirmed coals and within the "coal interval" all possess a very uniform 1° dip to the southwest (Figures 69, 70, and 71). Subtle differences in the topography of the different horizons are in large part controlled by and related to the active subsidence of this basin. The basal contact of the coal interval is marked by a high amplitude reflection at about 480 ms, which is interpreted as the green horizon (Figure 69). The dip on the green horizon is obviously greater than that observed on the top of coal and more consistent with the dip on the basement horizon in all locations with the exception of the northeastern end of line 2 (Figure 68). Deposition of these sediments was likely in a shallow water environment where mounds and channels formed through the influence of water level changes and variable currents.

Basement time contour trends are consistent with overlying layers and possess a dip of just over 2° (Figure 72). The surface topography of the basement strongly influenced line-to-line extrapolation of the synforms interpreted on lines 2, 4, 5, and 7. Basement configuration interpreted here is consistent with the documented regional dip to the southwest toward the center of this 3000+ m deep basin (Figure 72). The basement is 650 m or so deep at the barge landing on the Yukon River, near the northwest end of line 3, and less than 600 m deep near the eastern end of line 4.

The isotime of the interval between the coal and basement clearly demonstrates the growth characteristics of the basin (Figure 73). Throughout the Cenozoic when sediments currently present in this basin were being deposited, the basin was deepening to the southwest (predominantly to the west). Geologic processes responsible for the formation of the Yukon Flats Basin have been suggested to be currently active. Isotime maps of the coal and basement reinforce that suggestion with an apparent deepening of the bedrock about 50 m since the start of the Cenozoic.

High gradient areas (steep surface topography) are generally consistent between all contoured horizons. Using these horizon data in association with attribute analysis and stacked seismic sections, the relative throw of the faults and fault plane orientations can be designated with reasonable confidence. The target coal seam is at a depth of around 390 to 400 m near the southern end of the survey area, rising to around 350 to 360 m at the northeastern extreme of this site.

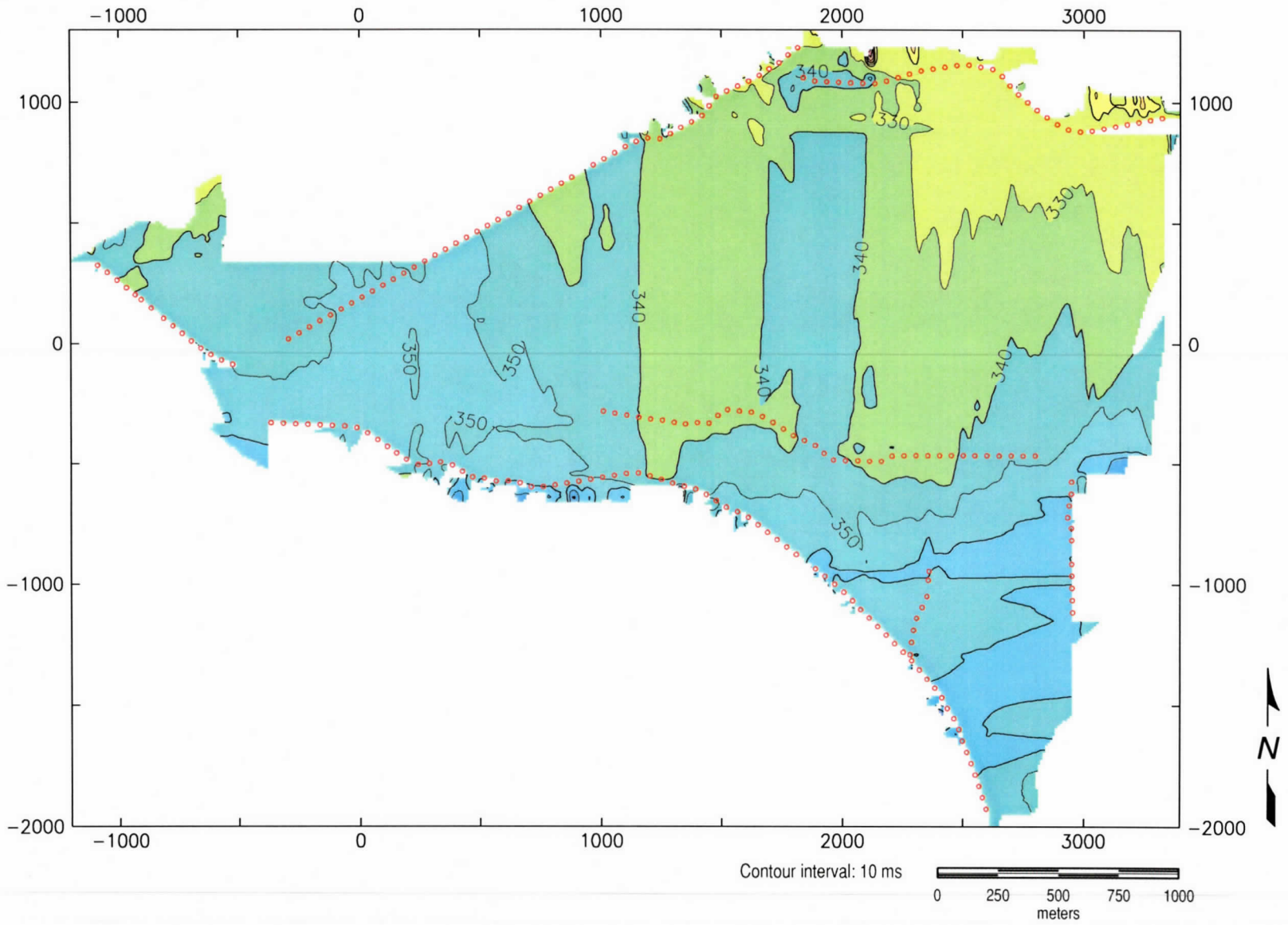

Figure 67. Reflection time to the top of the 365 m coal seam.

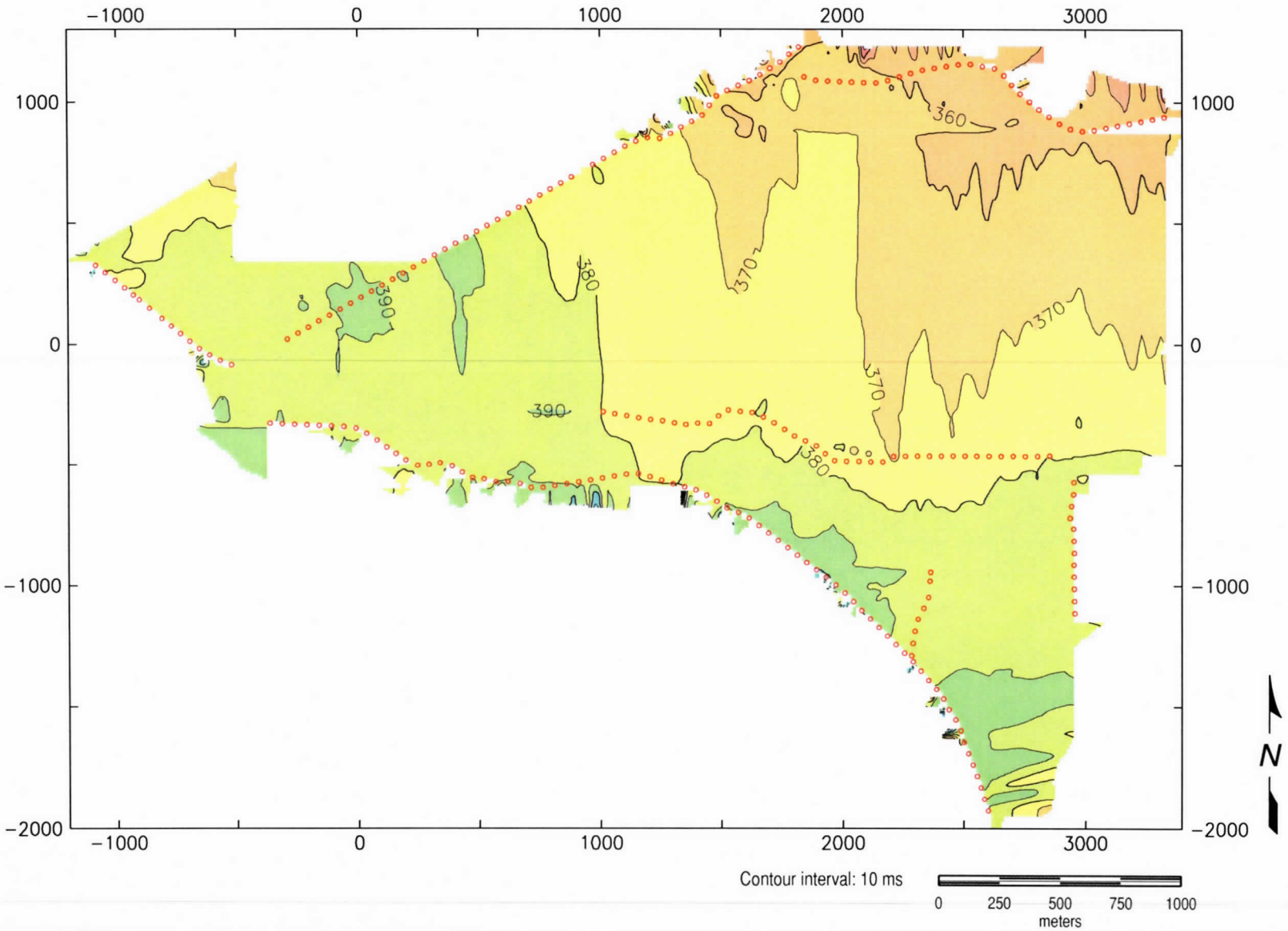

Figure 68. Reflection time to the top of the 391 m coal seam.

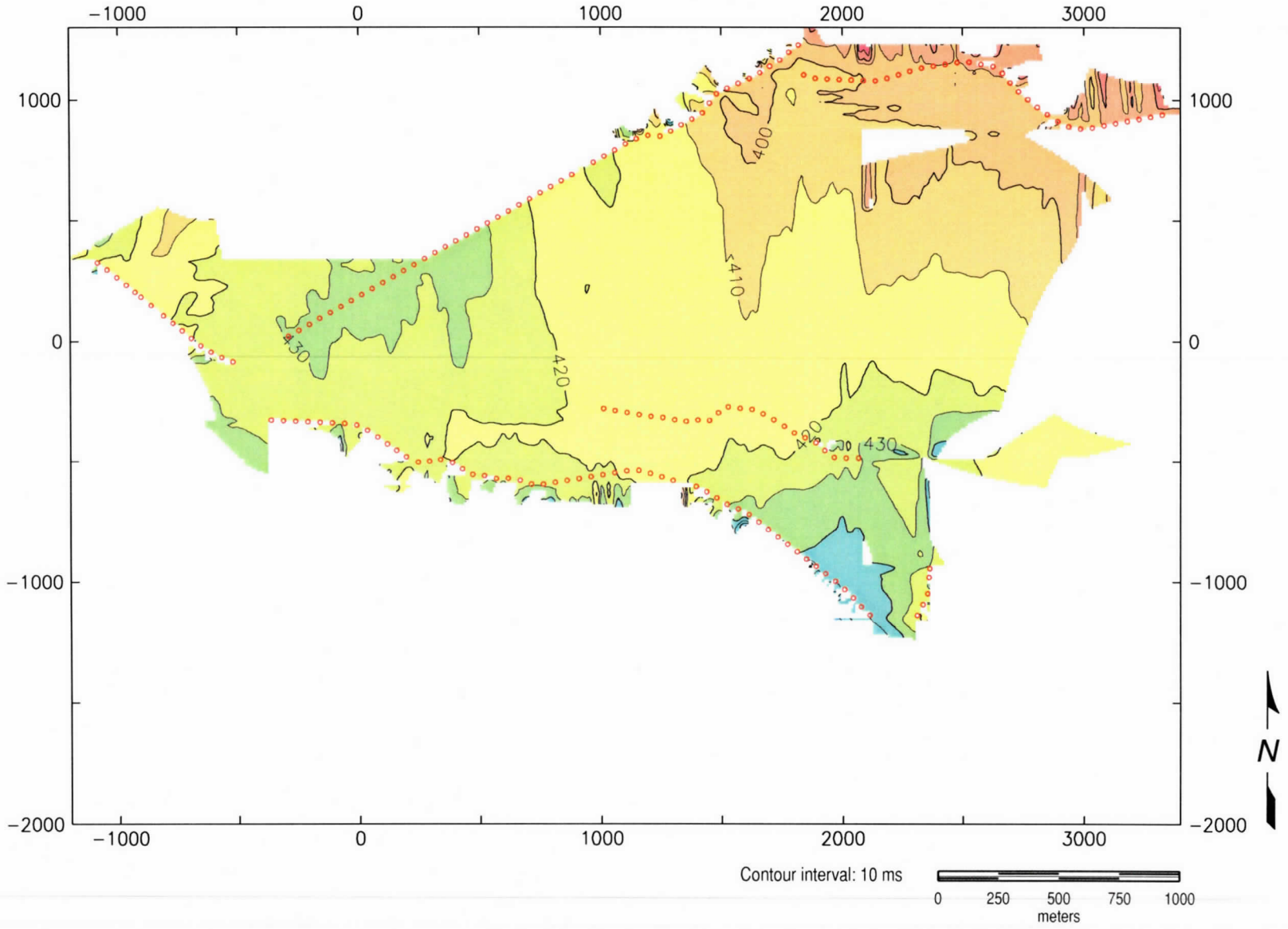

Figure 69. Reflection time to the top of the shallowest of the possible coal interfaces.

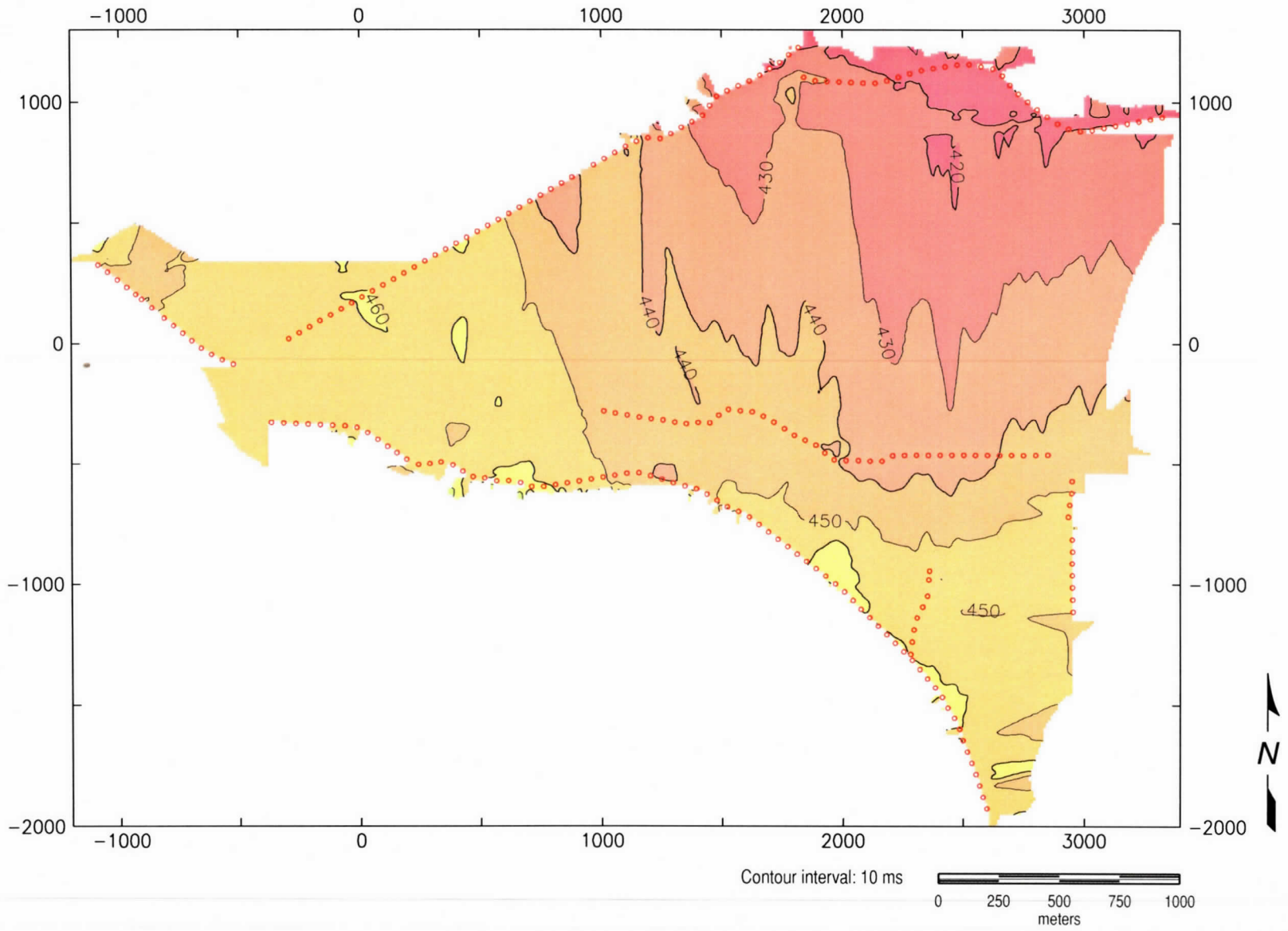

Figure 70. Reflection time to the top of the intermediate of the possible coal interfaces.

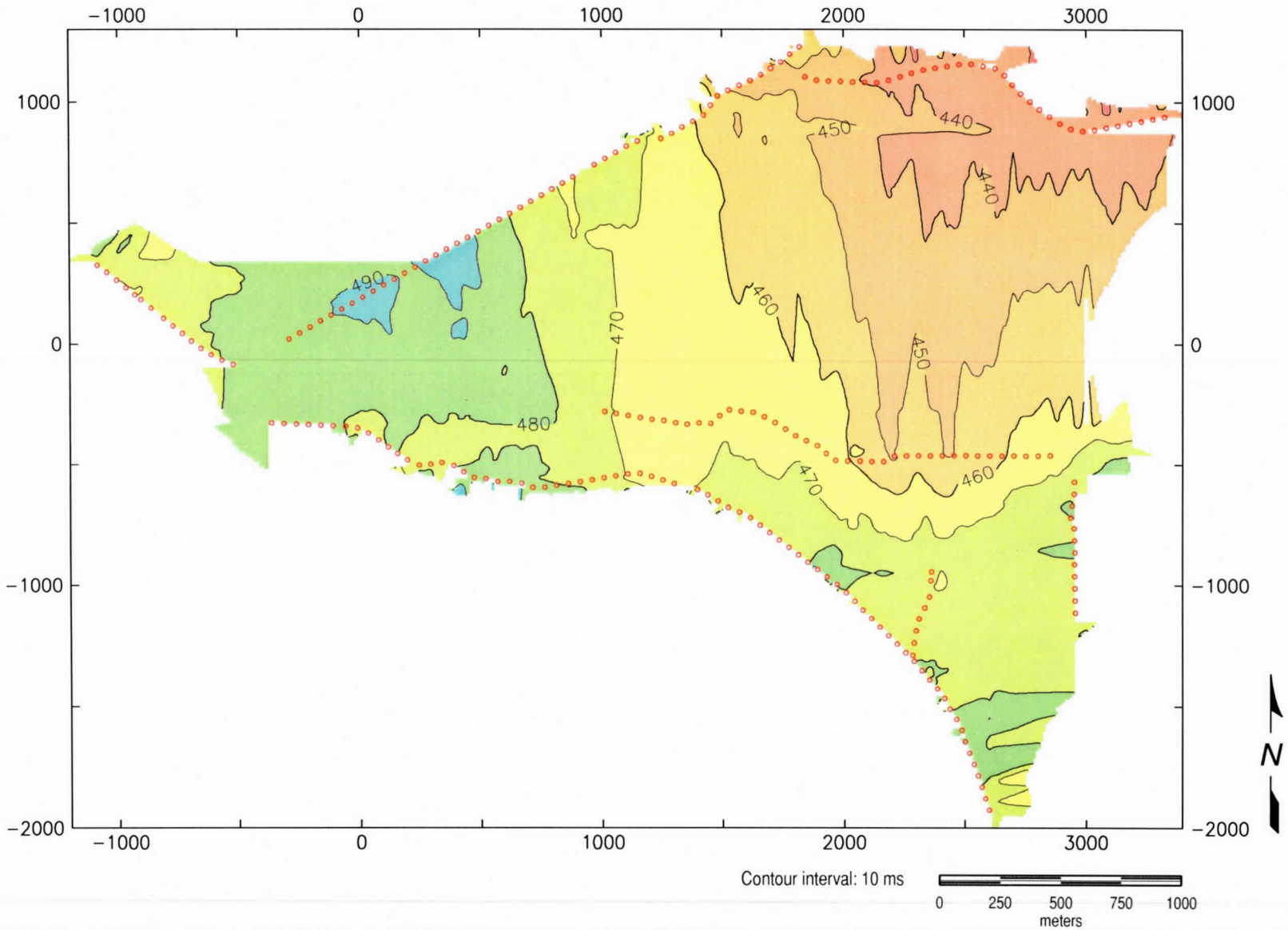

Figure 71. Reflection time to the top of the deepest of the possible coal interfaces.

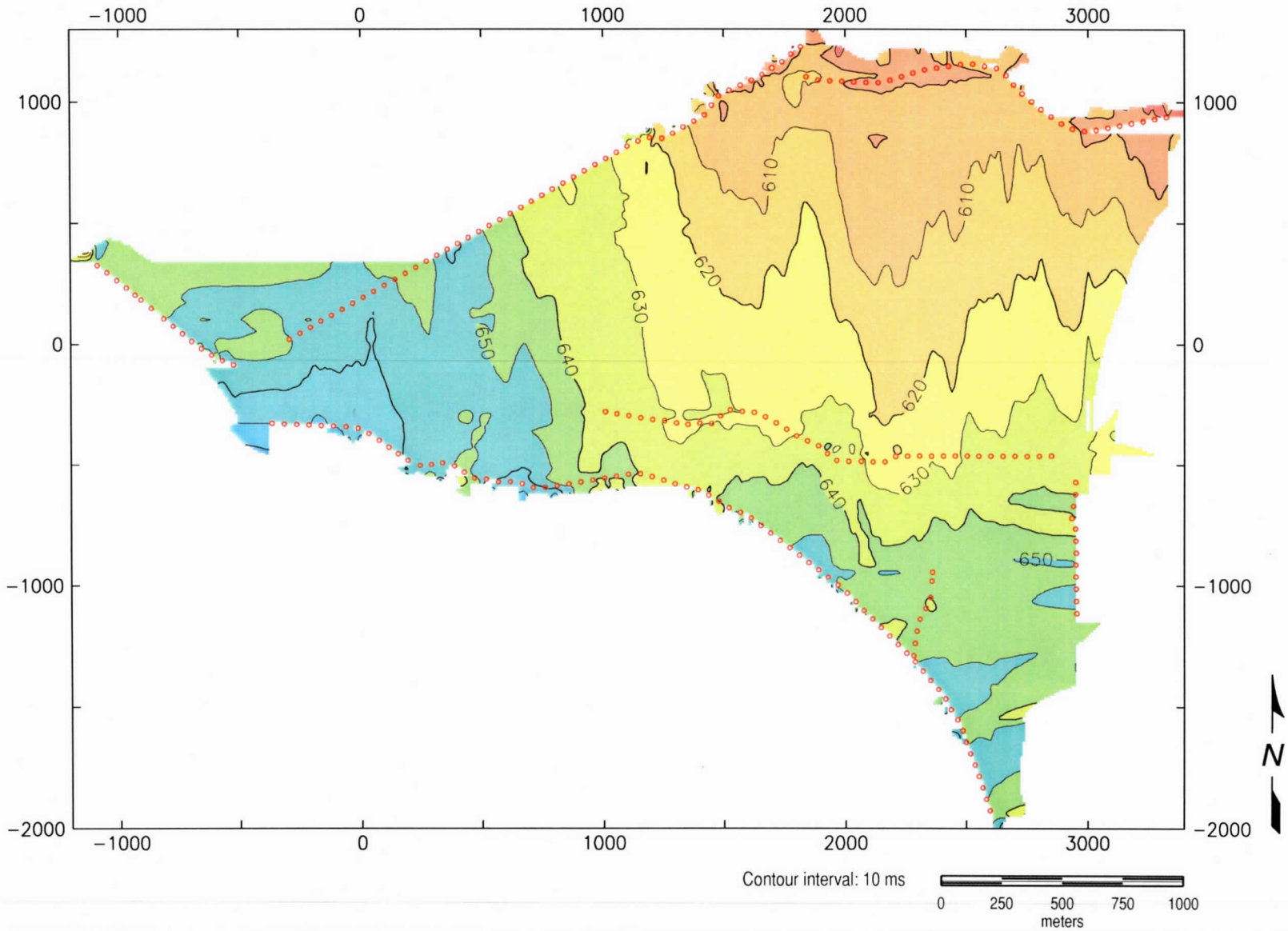

Figure 72. Reflection time to bedrock.

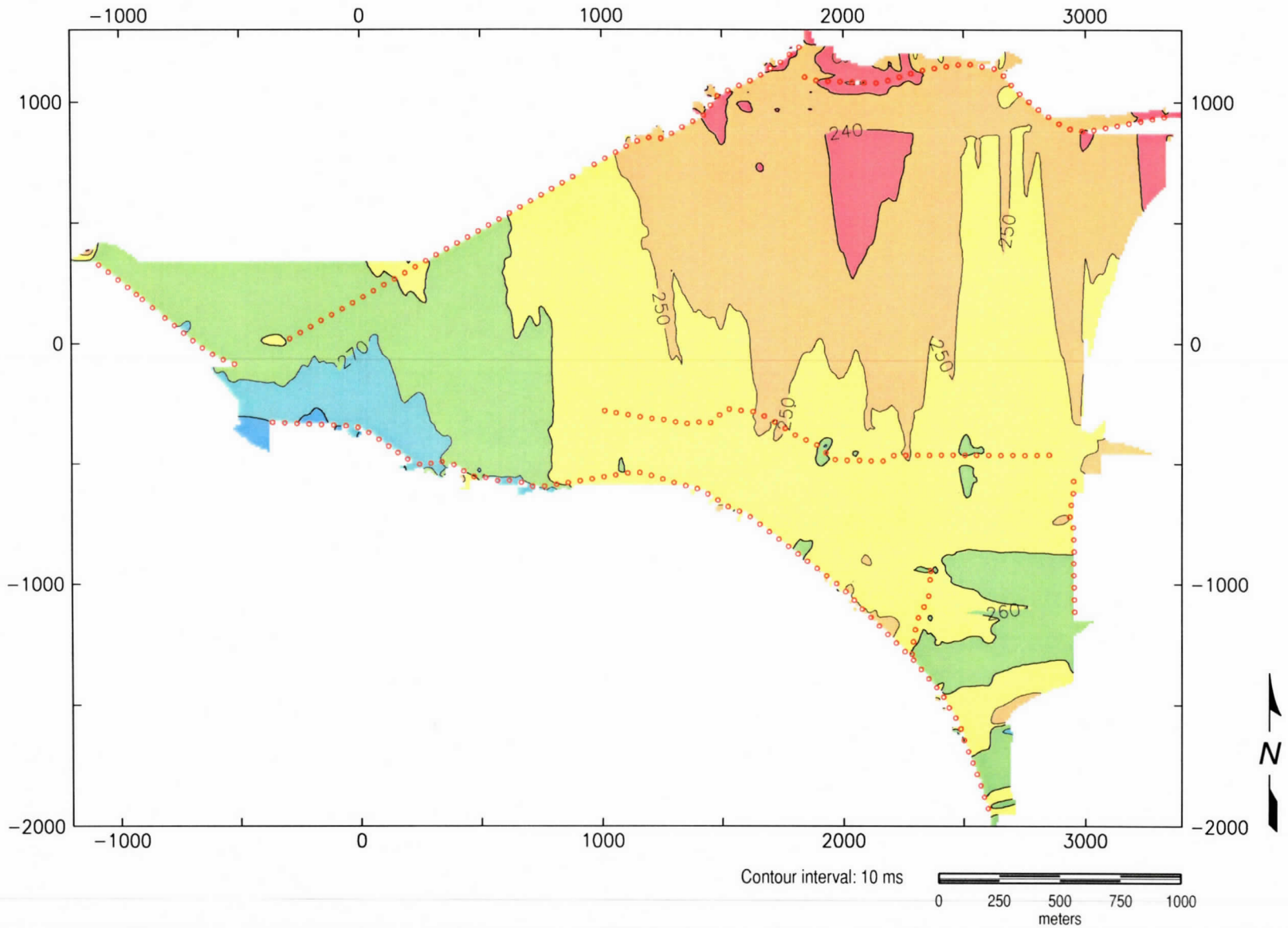

Figure 73. Isopach map for the interval from the top of the 391 m coal to bedrock.

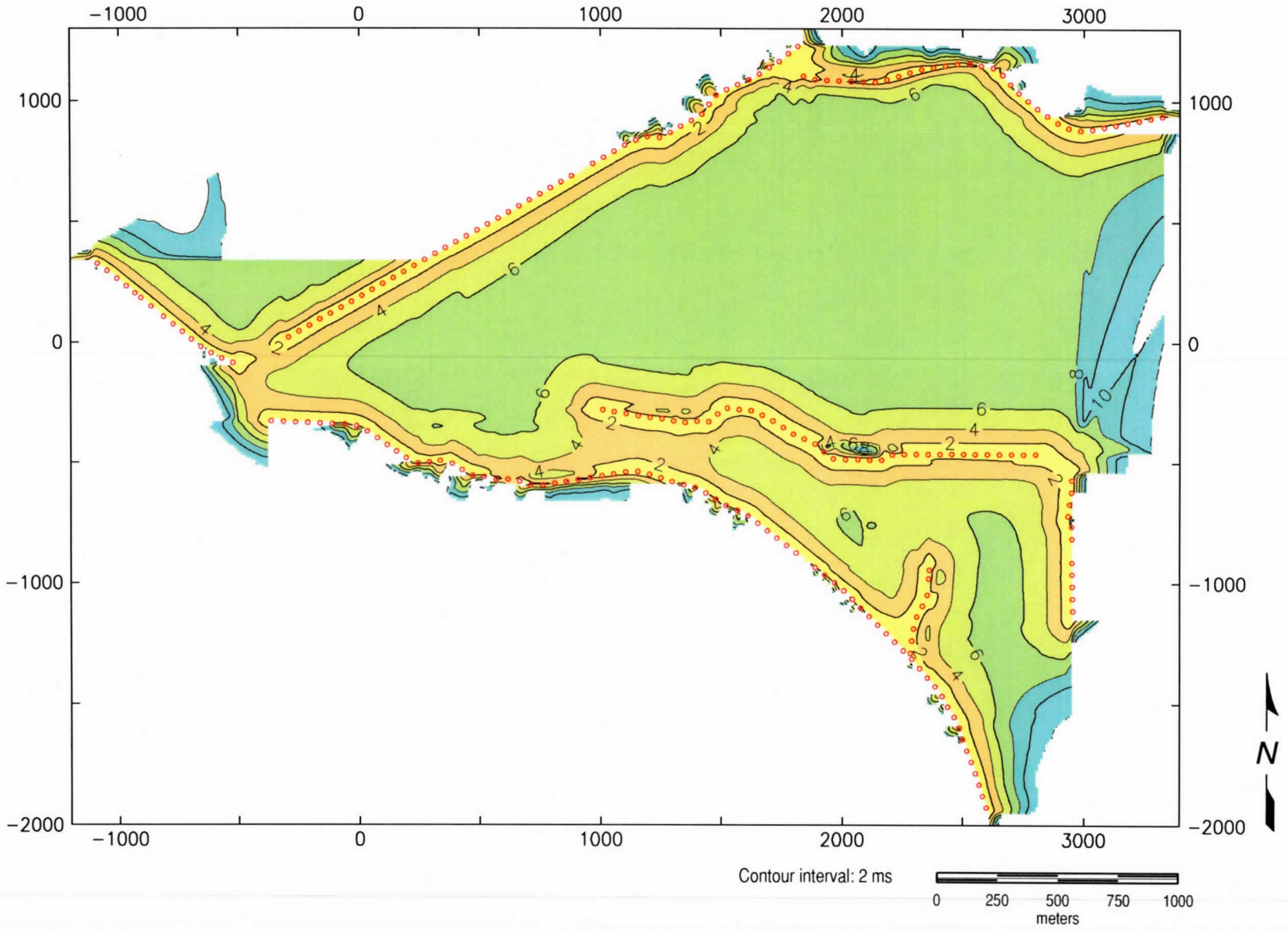

Figure 74. Standard error map for the 365 m coal seam (Figure 67).

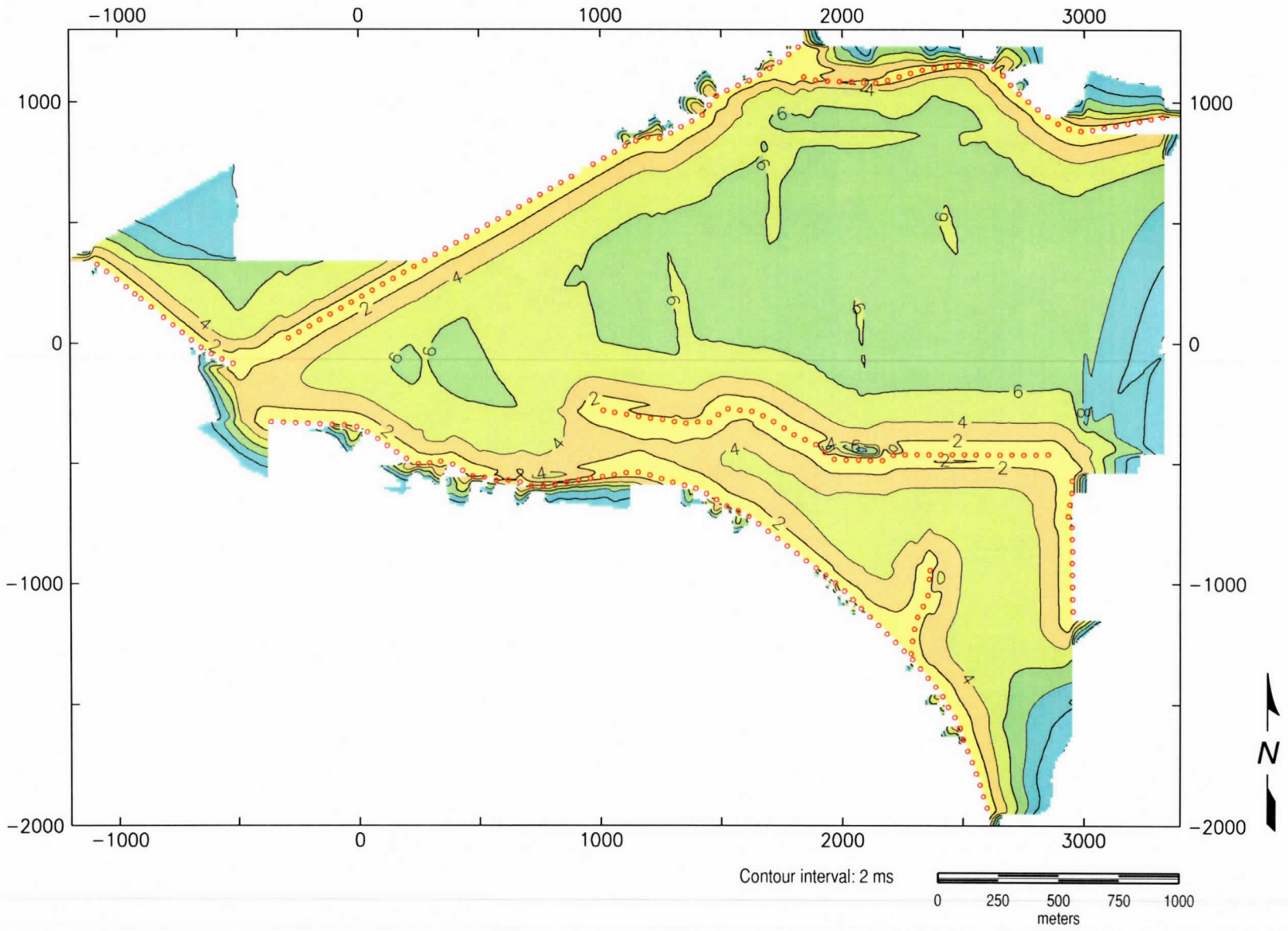

Figure 75. Standard error map for the 391 m coal seam (Figure 68).

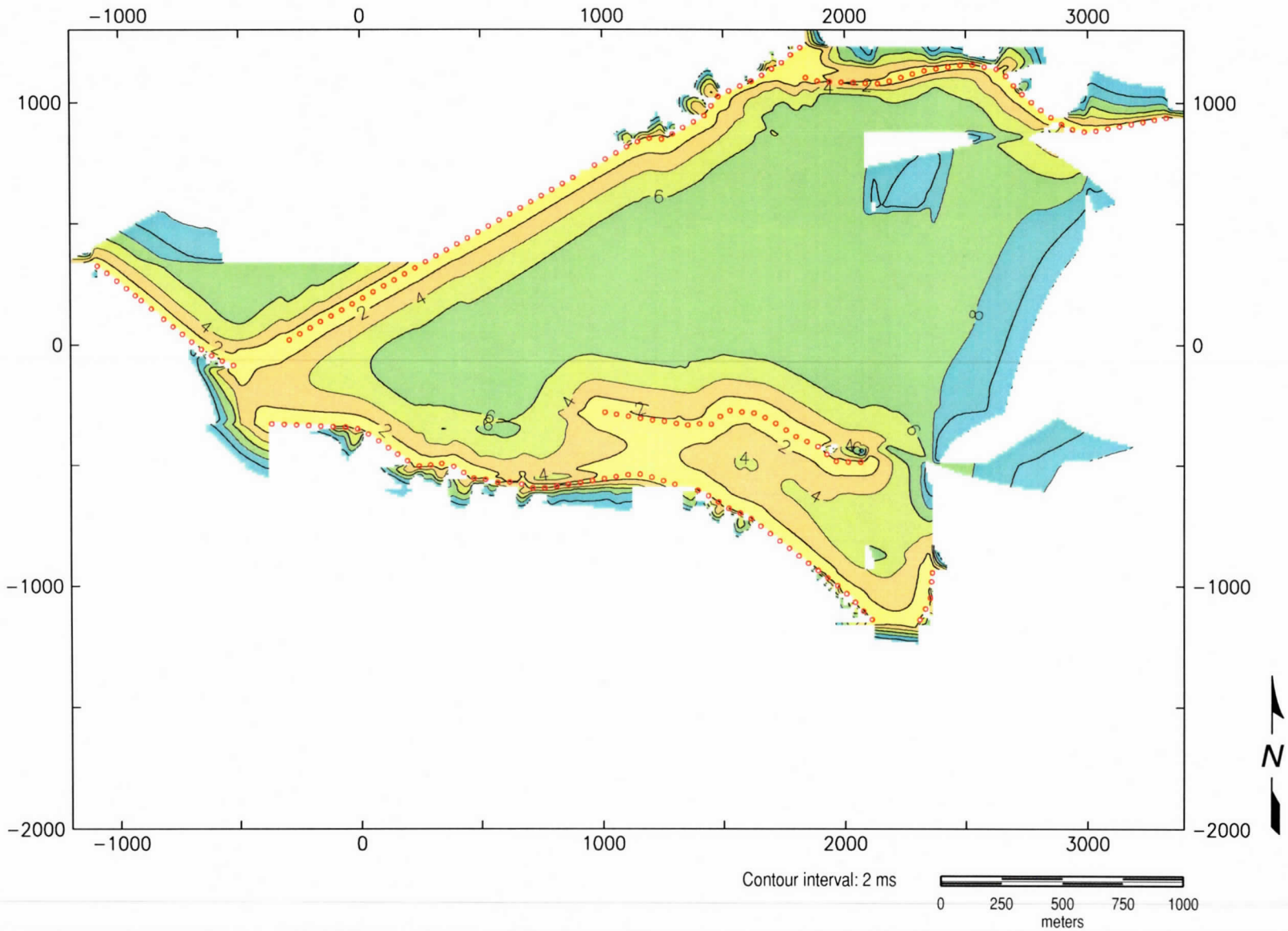

Figure 76. Standard error map for the shallowest possible coal interface (Figure 69).

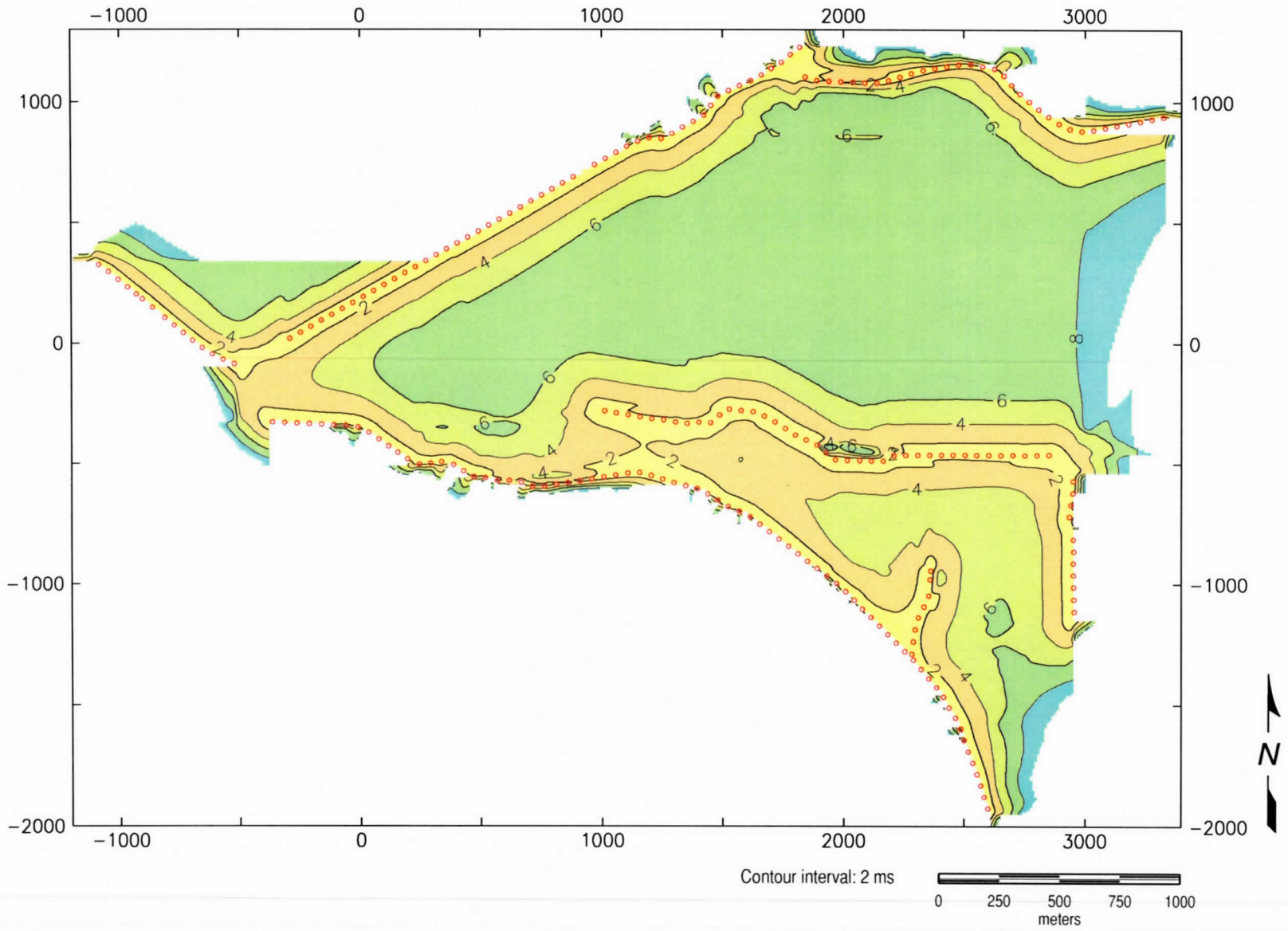

Figure 77. Standard error map for the intermediate possible coal interface (Figure 70).

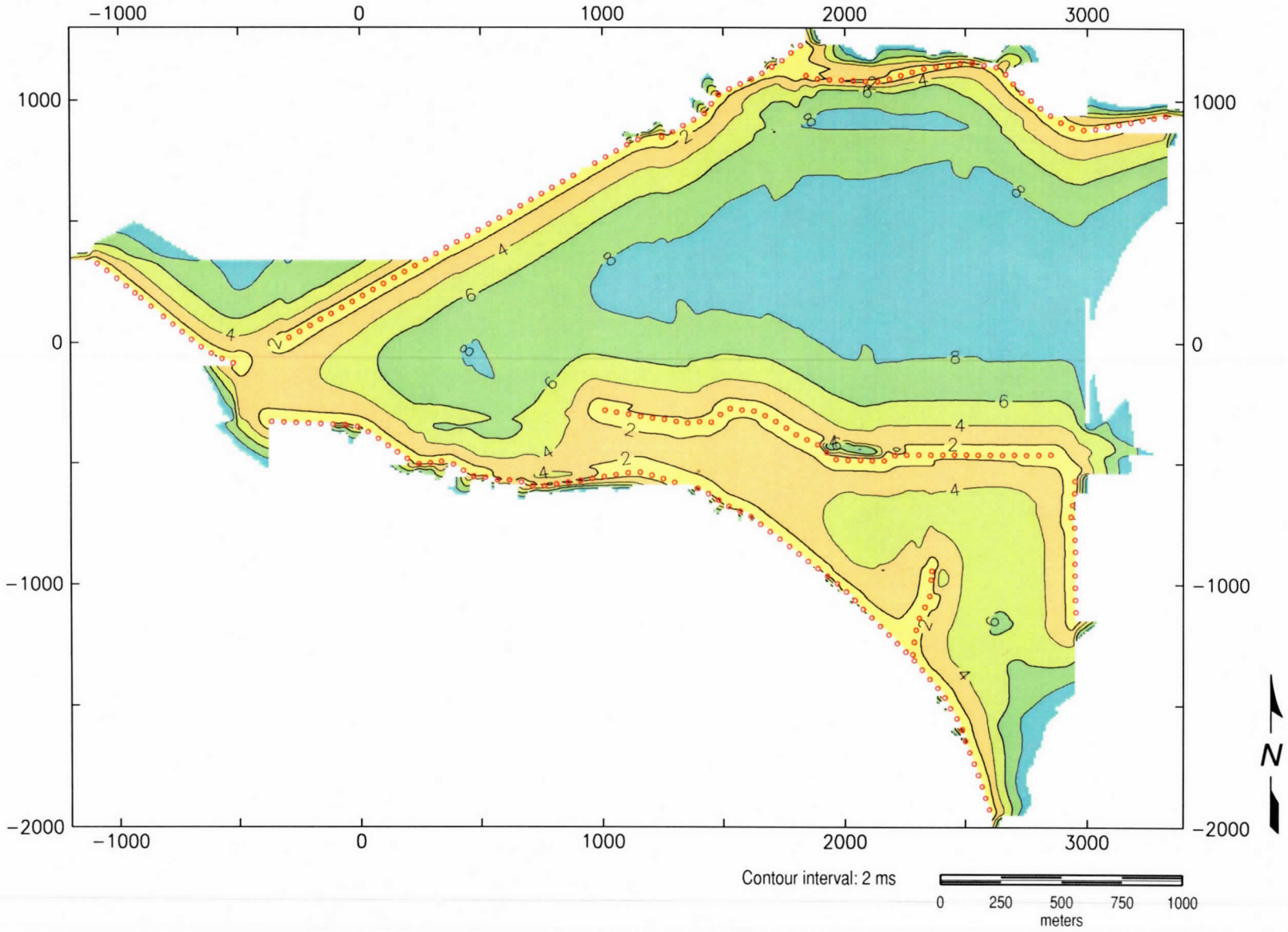

Figure 78. Standard error map for the deepest possible coal interface (Figure 71).

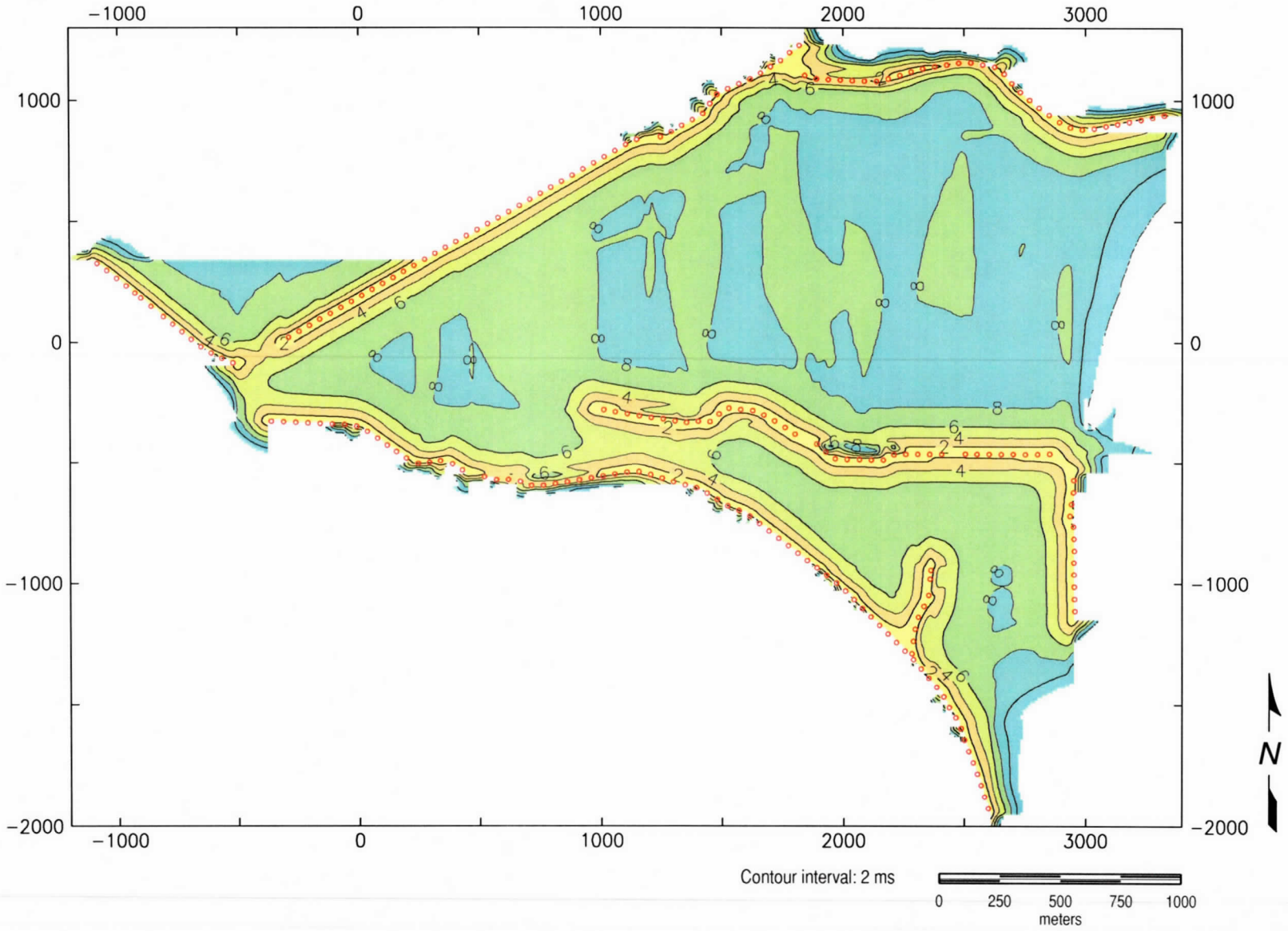

Figure 79. Standard error map for the bedrock (Figure 72).

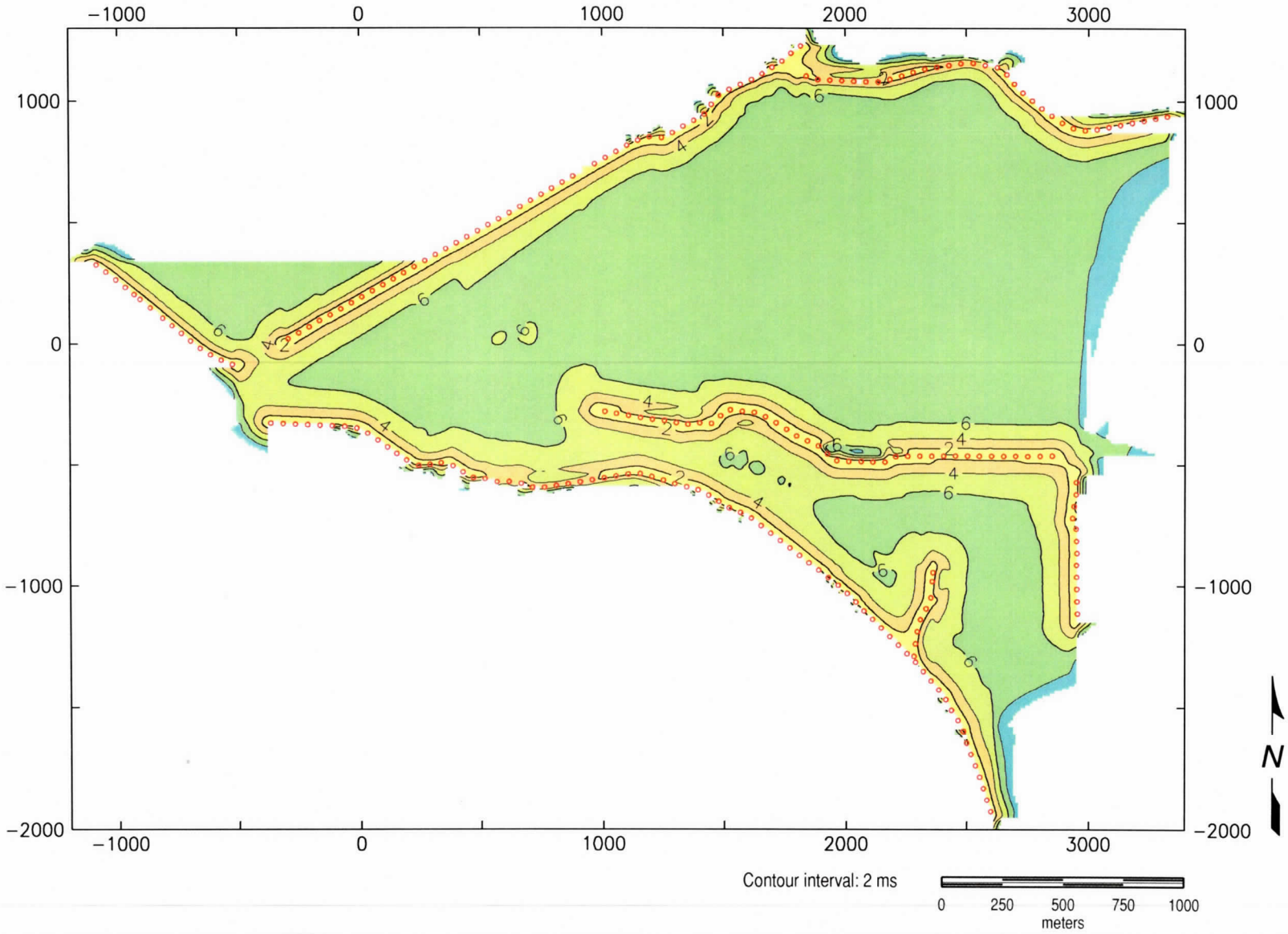

Figure 80. Standard error map for the interval from the top of the 391 m coal to bedrock (Figure 73).

Standard error estimates of the mapped horizon topography provide a sense of relative accuracy of interpolations between sample points (Figures 74 through 80). Within 50 m or so of the profile lines the error is 2 ms. Inside the triangle defined by lines 2, 4, and 7 the error reaches over 8 ms on some horizons. This relative measure of error is based on the separation in sample points and consistency in change of data values for those sample points.

Structures

Combining the attribute analysis, reflection offset estimates, and contouring of the key horizon tops permitted structures to be mapped across the site with a high degree of confidence. Faulting as interpreted is consistent not only with these data but also with inferred basement faults that control the deep basin to the south (Figure 81). Block faults dropped downward to the south and southwest control the structure of the basement and thickness of overlying sediments in this area. Faults are mapped so that displacement and layer configurations are consistent.

Confidence is good in the location of faults on the 2-D profiles. A lot can happen across the 4 or 5 km^2 that make up this site. With structures as small and as subtle as interpreted on these data, changes in strike and splaying are always a real possibility and a concern.

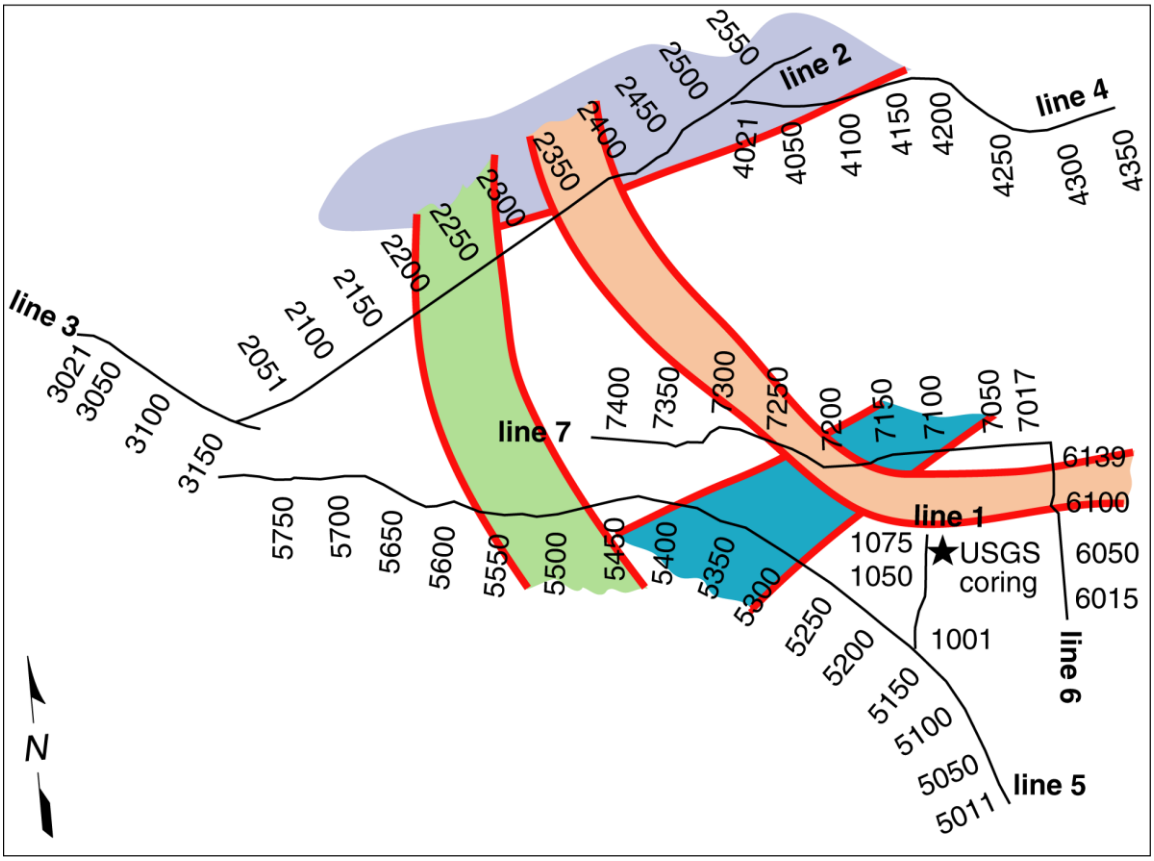

Figure 81. This map shows the seismic profiles overlain by a possible sitewide interpretation of the structural features interpreted on each individual profile. Several possible orientations of the faults, fracture systems, and folds are possible; this representation is one of the more likely possibilities.

Extrapolating the faults into three dimensions with no more control than available at this time is very speculative. The current interpretation is one of many possible structural scenarios.

The 390 ms coal reflection is present on all lines. Waveform attributes suggest the coal layer is over half a wavelength thick. Uniform, relatively undisturbed reflections indicate areas with very consistent stratigraphy and limited or no structural features. The characteristics of individual events can easily be correlated with and between the seismic lines.

Reflections from the western side of the survey area are uniform with little or no indication of faulting or fracturing. Several subtle depositional features can be interpreted within the coal interval. These features resemble channels and could be areas that have experienced cut-and-fill processes.

Synforms or graben structures with movement along high-angle faults extend throughout the Cenozoic section at several locations and clearly penetrate the basement on lines 2, 5, 6, and 7. Using the relative displacement and a variety of seismic characteristics and wavefield attributes, the synforms or grabens seem to be consistent with the predominant dip on the reflecting horizons.

The coal reflection and "coal interval" is consistent with a high degree of similarity across all faults mapped on this survey. The east end of both lines 5 and 7 are highly disturbed, likely indicative of significant fracturing of the rock layers. Line 1 is void of any faults or apparent fractures. This geometry suggests there is no single dominant fault/fractures orientation, but that the orientation of these small offset faults and associated fracture systems has changed over time consistent with the tectonics and sediment loading of Yukon Flats.

With the increased ground truth that will be provided by future drilling at this site, subtle channel features directly beneath the coal reflection interpreted in blue on lines 3 and 4 should be correlatable to specific stratigraphic units. If these blue events represent the base of the coal along these lines, in places the coal could be over 25 m thick. In this depositional environment, thick sequences of coal could come and go based on ancient river meanders and changes in lake shorelines.

CONCLUSIONS

This seismic reflection program successfully extended the geologic information obtained from the 1994 USGS corehole about the coal seam at 400 m depth across the Fort Yukon study area. It was designed to optimize signal-to-noise and resolution of the data and therefore enhance the eventual usefulness of the data through incorporation into geologic models designed to evaluate the potential of coalbed methane as a municipal resource. Several objectives and goals were identified at the onset of this project. Each objective was successfully accomplished and in some cases expectations were significantly exceeded.

Looking sitewide, the drill-encountered 391 m deep coal appears continuous around the site (Figure 82). There appears to be at least two major coal seams and several locally discontinuous beds on the order of 0.25 km^2 in areal extent. Structures are small and prevalent across

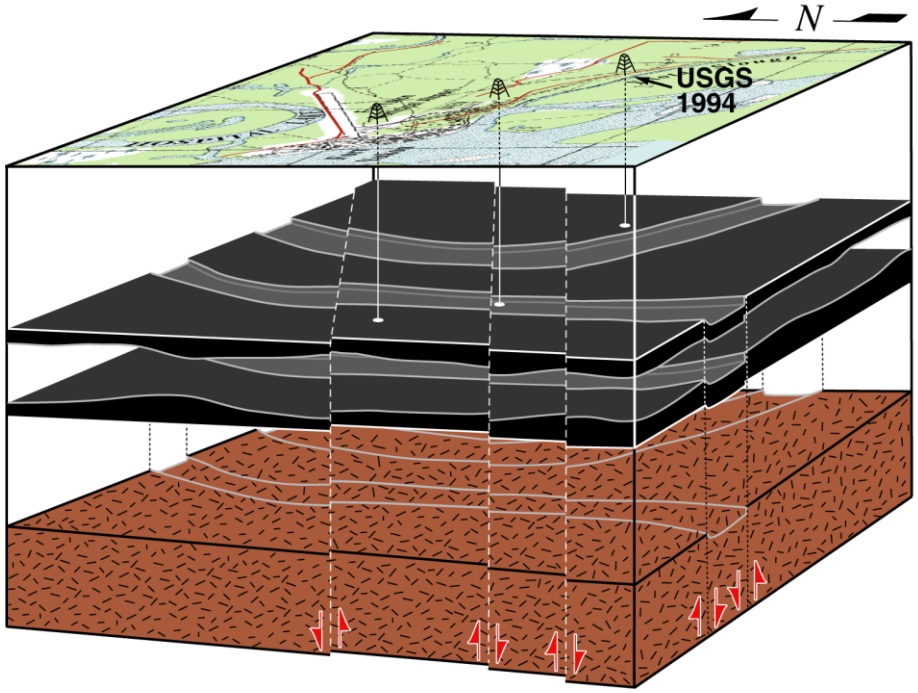

Figure 82. Cartoon of a geologic cross-section that fits the data, but lacks sufficient controls to allow much confidence. This figure demonstrates the overall continuity of the major coal layers across the site and to some extent the degree of fractures and fault features.

the site. The coal intervals are well fractured with significant variability in seismic attributes that in other settings have been indicative of the presence of gas. These faults are parallel to the gradient of dip and the graben or synforms interpreted around the site are parallel to the topography of the interpreted subsurface horizons.

Goals and *Accomplishments*

1) Generate high resolution (>120 Hz) signals with sufficient sitewide coherency, resolution, and signal-to-noise ratio to allow the top and basal contact of the lignite coal encountered at around 400 m to be mapped;

Reflections with upper corner frequencies over 200 Hz and dominant frequencies over 150 Hz were generated and recorded sitewide. Over a dozen uniquely distinguishable reflections are interpreted within the depth range of interest. Practical minimum resolution limits are around 5 m, allowing both top and bottom of the 400 m coal seam to be imaged.

2) Optimize acquisition for 2½-D imaging for line-to-line extrapolations;

Reflection wavelets possessed sufficient consistency and uniqueness that individual reflection events can be tied from line to line across distances as great as 2 km. Resolution was high enough that subtle stratigraphic features, varying over hundreds of meters, were observed. Drilling will be required to confirm their geologic significance.

3) Evaluate and optimize equipment and parameters to maximize signal-to-noise ratio and resolution potential, including offset sensitivity due to permafrost;

The permafrost setting presented unique challenges to achieving optimum offset. These were met by using an asymmetric, split-spread geometry recorded into a fixed oversized receiver spread. A high output value proved critical to pushing the dominant frequencies above 120 Hz.

4) Correlate reflections with units seen in borehole data;

The top of the coal at around 391 m matches perfectly with the borehole lithologic log.

5) Processing flows modified and optimized for extending the upper corner frequency;

Precorrelation and offset-sensitive processing was customized for this project and its special data characteristics.

6) Evaluate and adapt source and receiver coupling to exceed any previous high-frequency signal recorded in a land setting at depths greater than 400 m;

Drill emplaced geophone spikes and hard surface source pad coupling matched with a computer controlled optimized drive signal helped push the previous high of around 120 Hz dominant at 400 m to over 150 Hz at depths over 500 m.

7) Map the 391 m coal seam and any significant structural features above the basement;

A series of very small offset faults were imaged with trends consistent with basement faults to the south and with the general topography of the basement and multiple layers mapped above basement. Top and bottom of the coal seam will be mappable with additional ground truth.

8) Image below the 391 m coal seam for more potential coal horizons.

Speculation based on geology and reflection characteristics suggests that events between about 350 and 500 m producing strong reflection returns may be coal layers.

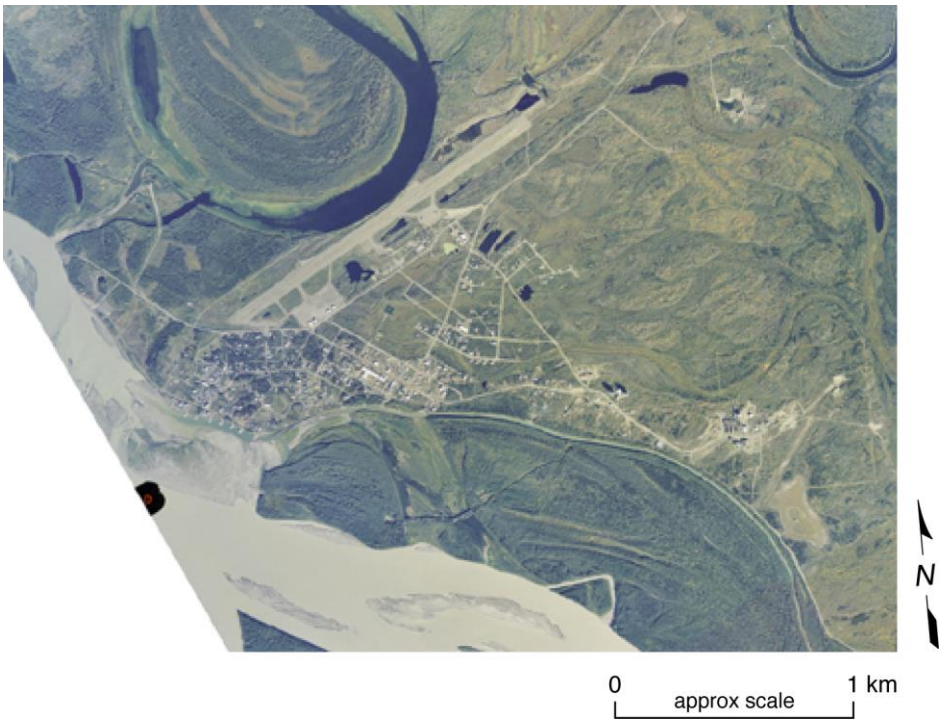

Figure 83. Aerial photo of the Village of Fort Yukon, Alaska.

Acknowledgements

Thanks to Jim Clough (Alaska Division of Geological & Geophysical Surveys—ADGGS) for long hours of hard work and relentless enthusiasm directed at providing the State of Alaska and its citizens a quality product. Charley Barker (USGS) provided extensive time and knowledge that have been the basis for many of the interpretations and conclusions in this report.

A great deal of thanks goes to Dave Thomas from the Village of Fort Yukon who provided invaluable assistance with site logistics (Figure 83). Assistance in planning, logistics, and field work from the Native Village of Fort Yukon, City of Fort Yukon, Gwitchyaa Zhee Corporation, State of Alaska Dept. of Transportation, and the U.S. Air Force was greatly appreciated! We would like to acknowledge all the help and the gracious reception from the people of Fort Yukon, especially Bonnie Thomas (city manager), Rocky James (former city manager), and Mayor Richard Carroll. We would like to express a great deal of appreciation for Elmo Christenson (Industrial Vehicles International—IVI), Chad Gratton (Kansas Geological Survey), Valerie Webb (ADGGS), and Paige Peapples (ADGGS), for their relentless assistance during data acquisition. Thanks to Mary Brohammer who helped produce the formatted copy and Brett Bennett for assisting with computer and hardware activities. The State of Alaska provided funding, with additional funding by the U.S. Dept. of Energy.

Appendix A
Summary of Processing Parameters

All Lines

Data format and gather into 240 channel shot gathers
AGC scale (1.5 seconds pre-correlation)
Correlate with synthetic sweep (25 Hz to 250 Hz linear up sweep)
Hum filter (predictive filter targeting 60 Hz, 120 Hz, and 180 Hz powerline hum)
Body Wave Analysis (velocity, frequency, amplitude, etc.)
Define source and receiver geometry
Offset edit (remove all traces with offset > 500 m)
Noisy trace edit (remove when S/N < 1 within depth of interest)
Datum statics correction (correction velocity 3750 m/s, floating datum)
Spherical divergence correction (24 dB/second)
Spectral balance (band limited spiking decon—25 Hz – 50 Hz – 200 Hz – 250 Hz)
Vertically stack, 3 individually recorded sweeps per station
Fk filter, targeting ground roll w/ linear phase velocities range: 1800 m/s to 2200 m/s
First Arrival Mute, remove everything above 3rd zero crossing of first arrival
Offset edit (remove all traces with offset < 50 m and > 250 m)
AGC scale, 500 msec window
Band pass filter (40 Hz – 80 Hz – 200 Hz – 250 Hz)
Noise cone mute (trace specific and limited to near-source noise)
CMP sort
Velocity analysis (100 m/sec velocity intervals, defined every 125 m)
Auto-surface consistent statics (400 ms window, 500 ms center, 10 ms max shift, 9 trace pilot)

Velocity Function:

Line 1

CMP	time/velocity	time/velocity	time/velocity
1998	350/1800	460/1850	664/1900
2048	357/1800	587/1850	
2098	365/1750	483/1800	
2148	400/1750	495/1800	

Line 2

CMP	time/velocity	time/velocity	time/velocity	time/velocity
4000	402/1850	643/1900		
4050	399/1900	499/1950	672/2000	
4100	336/1950	651/2000		
4150	393/1900	487/1950	651/2000	
4200	395/1900	488/1950	678/2000	
4250	397/1900	673/2000		
4300	401/1950	494/2000		
4350	395/1950	509/2000		
4400	353/1900	400/1950	503/2000	665/2050
4450	432/1950	492/2000	672/2050	

Line 2 (continued)

4500	390/1850	475/1900	667/1950
4550	383/1850	499/1950	
4600	369/1850	515/1900	624/1950
4650	382/1800	488/1850	636/1900
4700	386/1900	470/2000	630/2050
4750	380/1950	462/2000	615/2050
4800	387/1950	467/2000	629/2050
4850	364/1950	451/2000	
4900	351/1950	437/2000	
4950	356/1950	616/2000	

Line 3

CMP	time/velocity	time/velocity	time/velocity
6005	366/1950	512/2000	588/2050
6055	309/2000	396/1900	469/1950
6105	421/1950	585/1900	
6155	383/2000	407/2050	476/2050
6205	356/1950	455/2000	
6255	310/2000	426/2050	
6305	355/2000	428/2050	511/2100

Line 4

CMP	time/velocity	time/velocity	time/velocity
8005	371/1900	459/1950	597/2000
8055	350/1850	458/1950	608/2000
8105	351/1900	597/2000	
8155	444/1900	518/1950	
8205	424/1900	552/1950	594/2000
8255	356/1900	441/1950	590/2000
8305	377/2050	446/2100	
8355	346/2150	617/2200	
8405	360/2000	449/2050	
8455	356/1950	573/2000	
8505	363/2050	556/2100	
8555	365/2100	628/2150	
8605	393/2000	629/2050	
8655	331/2000	454/2050	

Line 5

CMP	time/velocity	time/velocity	time/velocity
10050	387/2050	539/2100	
10100	473/2050	580/2100	
10150	491/2100	597/2150	
10200	445/2000	577/2100	
10250	424/2000	563/2100	

Line 5 (continued)

10300	387/2000	483/2100	
10350	483/2100	620/2150	
10400	391/1950	547/2050	
10450	382/2000	485/2050	
10500	452/1950	550/2100	
10550	404/1950	653/2000	
10600	389/1950	576/2000	
10650	388/2000	543/2050	
10700	352/2000	628/2100	
10750	333/2000	631/2050	
10800	444/2000	580/2050	
10850	459/1900	613/2000	
10900	467/1950	660/2000	
10950	367/1900	653/1950	
11000	331/1900	401/1950	
11050	332/2000	665/2050	
11100	389/2050	510/2100	
11150	382/2000	605/2050	
11200	339/2050	569/2100	
11250	368/2000	653/2050	
11300	385/2050	658/2100	
11350	347/2050	649/2100	
11400	395/2000	535/2050	658/2100
11450	351/2050	549/2100	
11500	430/2100	624/2150	

Line 6

CMP	time/velocity	time/velocity
12005	492/1950	651/2000
12055	378/1950	461/1900
12105	467/1900	634/1950
12155	381/2000	624/2050
12205	379/2150	630/2200
12255	461/2050	603/2150

Line 7

CMP	time/velocity	time/velocity	time/velocity
14050	351/1900	538/1950	
14100	361/1900	456/2000	
14150	320/2000	448/2050	619/2100
14200	331/2050	491/2100	
14250	339/2050	476/2100	
14300	340/1950	471/2000	
14350	345/2000	497/2050	609/2100
14400	348/2100	621/2150	

Line 7 (continued)

14450	326/2000	423/2050	527/2100
14500	320/1950	433/2000	
14550	338/2100	448/2150	611/2200
14600	301/2100	400/2150	604/2200
14650	295/2050	446/2100	610/2150
14700	300/2050	452/2100	627/2150
14750	296/2000	452/2050	620/2100
14800	481/2000	621/2100	

Residual statics (300 ms window, 450 ms center, 5 ms max shift, 13 trace pilot)
CMP stack (fold range from 1 to 30, w/ average center fold ~18)
Fk migration filter (velocity 2000 m/s)
Trace mix (three consecutive trace contribution—15%, 100%, 15%)
Attribute analysis (Kingdom Suites)

REFERENCES

Barker, C., 2001, personal communication.

Barnes, F.F., 1967, Coal resources of Alaska: *U.S. Geological Survey Bulletin* 1242-B, p. B1-B36, plate 1.

Brühl, M., G.J.O Vermeer, and M. Kiehn, 1996, Fresnel zones for broadband data: *Geophsyics*, v. 61, p. 600-604.

Doll, W.E., and C. Çoruh, 1995, Spectral whitening of impulsive and swept-source shallow seismic data [Exp. Abs.]: Ann. Mtg. of Soc. Explor. Geophys., p. 398-401.

Ebrom, D.A., S.A. Markley, and J.A. McDonald, 1996, Horizontal resolution before migration for broadband data [Exp. Abs.]: Ann. Mtg. of Soc. Explor. Geophys., p. 1403-1433.

Garland, G.D., 1979, Introduction to geophysics–Mantle, Core, and Crust: Philadelphia, Pa., W.B. Saunders Co., 494 p.

Gochioco, L.M., 1992, Modeling studies of interference reflections in thin-layered media bounded by coal seams: *Geophysics*, v. 57, p. 1209-1216.

Hite, D.M., and E.M. Nakayama, 1980, Present and potential petroleum basins of Alaska: In Landwehr, M.L., ed., *New Ideas, New Methods, New Developments: Exploration and Economics of the Petroleum Industry*, v. 18, p. 511-560.

Hunter, J.A., R.D. Miller, W.E. Doll, B.J. Carr, R.A. Burns, R.L. Good, D.R. Laflen, and M. Douma, 1999, Feasibility of high resolution P- and S-wave seismic reflection to detect methane hydrate: Geological Survey of Canada Open-file Report 3850.

Hunter, J.A., S.E. Pullan, R.A. Burns, R.M. Gagne, R.S. Good, 1984, Shallow seismic-reflection mapping of the overburden-bedrock interface with the engineering seismograph—Some simple techniques: *Geophysics*, v. 49, p. 1381-1385.

Kaiser, W.R., D.S. Hamilton, A.R. Scott, and R. Tyler, 1994, Geological and hydrological controls on the producibility of coalbed methane: *Journal of Geology*, v. 151, p. 417-420.

Kallweit, R.S., and L.C. Wood, 1982, The limits of resolution of zero-phase wavelets: *Geophysics*, v. 47, p. 1035-1046.

Kirschner, C.E., 1994, Interior basins of Alaska: In G. Plafker and H.C. Berg, eds., *The Geology of Alaska*: Boulder, Colorado, Geological Society of America, *The Geology of North America*, v. G-1, p. 469-493.

Mayne, W.H., 1962, Horizontal data stacking techniques: Supplement to *Geophysics*, v. 27, p. 927-938.

Miller, R.D., N.L. Anderson, H.R. Feldman, and E.K. Franseen, 1995, Vertical resolution of a seismic survey in stratigraphic sequences less than 100 m deep in Southeastern Kansas: *Geophysics*, v. 60, p. 423-430.

Miller, R.D., V. Saenz, and R. Huggins, 1992, Feasibility of CDP seismic reflection to image structures in a 220-m deep, 3-m thick coal seam near Palau, Coahuila, Mexico: *Geophysics*, v. 57, p. 1373-1380.

Miller, R.D., W.L. Watney, D.K. Begay, and J. Xia, 2000, High-resolution seismic reflection to delineate shallow gas in eastern Kansas: *Compass*, v. 75, n. 2/3, p. 134-145.

Montgomery, Scott L., 1999, Powder River Basin, Wyoming: An expanding coalbed methane (CBM) play: *AAPG Bulletin*, v. 83, n. 8, p. 1207-1222.

Murray, D.K., 1991, Coalbed methane: Natural gas resources from coal seams: In D.C. Peters, ed., *Geology in Coal Resource Utilization*, Fairfax, Virginia, TechBooks, p. 97-103.

Palmore, D.R., 1984, Permafrost effects on geophysics exploration (special workshop): Soc. Expl. Geophys., p. 855.

Poley, D.F. and D.C. Lawton, 1991, A model study of multichannel reflection seismic imaging over shallow permafrost in the Beaufort Sea continental shelf: J. Can. Soc. Expl. Geophys., v. 27, no. 1, p. 34-42.

Pullan, S.E., and J.A. Hunter, 1990, Delineation of buried bedrock valleys using the optimum offset shallow seismic reflection technique: Soc. Explor. Geophys. *Investigations in Geophysics, Investigations in Geophysics no. 5*, Stan H. Ward, ed., *Volume 3: Geotechnical*, p. 75-87.

Rightmire, C.T., 1984, Coalbed methane resource: In *Coalbed Methane Resources of the United States*, ed. C.T. Rightmore, G.E. Eddy, and J.N. Kirr, *AAPG Studies in Geology Series #17*, p. 1-3.

Sheriff, R.E., 2002, *Encyclopedic dictionary of exploration geophysics, 4th ed.*: Soc. Exp. Geophys., Tulsa.

Steeples, D.W., and R.D. Miller, 1990, Seismic reflection methods applied to engineering, environmental, and groundwater problems: Soc. Explor. Geophys. *Investigations in Geophysics no. 5*, Stan H. Ward, ed., *Volume 1: Review and Tutorial*, p. 1-30.

Tyler, R., A.R. Scott, and J.G. Clough, 2000, Coalbed methane potential and exploration targets for rural Alaska communities: Alaska Division of Geological & Geophysical Surveys, Preliminary Interpretative Report 2000-2, 169 p., 1 sheet.

Wahrhaftig, C., S. Bartsch-Winkler, and G.D. Stricker, 1994, Coal in Alaska: In G. Plafker and H.C. Berg, eds., *The Geology of Alaska*: Boulder, Colorado, Geological Society of America, *The Geology of North America*, v. G-1, p. 937-978.

Widess, M.D., 1973, How thin is a thin bed: *Geophysics*, v. 38, p. 1176-1180.

Zuber, M.D., 1996, Basic Reservoir Engineering for Coal, in Saulsberry, J.L., Schafer, P.S., and Schraufnagel, R.A., eds.: *A Guide to Coalbed Methane Reservoir Engineering*: Chicago, Gas Research Institute, p. 3.1-3.33.